NEUROINFORMATICS APPROACHES TO UNDERSTANDING AFFECTIVE DISORDERS

Dina Michaela Kronhaus

PhD

2004

I declare that this thesis was composed by me and all the work contained herein is my own, unless otherwise indicated.

Edinburgh, October 2004

Dina M Kronhaus

Contents

Figures

Acknowledgements

First and foremost, I would like to thank my first supervisor, David Willshaw, for giving me this opportunity and for his ongoing support. I could not have wished for a better mentor. I thank Klaus Ebmeier, my second supervisor, for teaching me Psychiatry. At the IOP, I am grateful to Mary Phillips for a wonderful collaboration and to Nat Lawrence, for her patience and eagle eyes. In St. Louis, my thanks go to Rachel Wong and Tim Holy for welcoming me in among their lab-children and of course to Dennis Oakley, for all his help. In Jerusalem, I thank Udi Zohary and Idan Segev for their hospitality. In Toronto, I thank Randy McIntosh for his data and encouragement.

I thank my office mates, Becca Smith and Kit Longden, for their companionship and I am also grateful to my former office mate Al Reid, for introducing me to this subject and for unleashing my imagination. I would like to thank people at ANC and the Department of Psychiatry, for making this an interesting and enjoyable experience. Thanks to Andrew Gillies, for supervising my MSc project and encouraging me to try; Amos Storkey and Heather Sibley for useful discussions; Emma Rose for use of her data and Enrico Simonotto for his help and programming skills. I thank Emma Black for her smile and Fiona Jamieson for her wisdom and her kindness. Thank you Fiona for helping me push.

Goldilocks Babycakes and Dorothy deserve my thanks for warmth, fun and fro(li)cks. I also thank Scotty for his relentless support; Jaime for speaking his mind; Tamar for encouraging my curiosity; Darren and especially Mike for keeping their door open and for their friendship. I am grateful to Brigid and Paul from the BMPS for propping me up and for the laughter; and to Charlotte for knowing me better than I would like to admit. Of course, I would like to thank Stephen, for more than I could ever express. Thank you for keeping me on my (not so perfectly punctuated) toes, helping me see the light along some very dark tunnels and for the journey.

To the Medical Research Council, the European Commission, the Marine Biological Laboratory, ICNC, HBM and the BNA, I am extremely grateful for financial support.

Finally, I thank my Mum for her compassion, and my Dad for giving up his chance to get this far in order to create a better future for us all. I thank you both for your love, understanding and for all the sacrifices that you have made along the way. This thesis is dedicated to you.

Abstract

Neural activity in major depressive disorder and bipolar disorder has been the subject of much debate. Conflicting findings show that cognitive deficits associated with affective disorders can persist beyond remission, and the neural activity associated with such deficits is often inconsistent across different studies. Analytical and theoretical neuroinformatics-based methods (time-series analysis and neural-network modelling) have been used in this thesis to study neural activity associated with depressive illness.

My aim was to test whether there are specific structures or networks that are associated with the cognitive function in depression. Further, since depressed patients are often unimpaired during performance of cognitive tasks, I wanted to investigate the neural activity which may underpin compensatory strategies. Three approaches were used to investigate the underlying computational deficit in affective disorders. These can be described as the segregational, integrational and neural-network modelling paradigms.

In the first study, I analysed data from mildly-depressed bipolar patients and healthy control subjects performing the Stroop task. I found potential dysfunctional loci, such as the orbito-medial prefrontal cortex, which appears to be vulnerable in bipolar patients and may be normalised when these patients are depressed.

Functional connectivity methods were used in the second study to compare task-independent fluctuations between unipolar patients and healthy controls. These methods evinced a putative compensatory strategy in unipolar patients, who showed stronger connectivity between visual and parietal cortices during performance of a memory task.

Finally, I used a neural-network approach to study the internal dynamics of an effective connectivity network and subsequently to test different hypotheses regarding both global and localised deficits in depression. These suggested further ways in which networks that involve matching stimuli differ from networks that support working-memory paradigms.

The studies in this thesis suggest that depressive illness may be associated with vulnerable links in neuronal-networks associated with cognition and mood. The combination of different paradigms and approaches used highlight the wealth of possibilities that different computational approaches can offer both to data analysis, and to the representation and investigation of this data through theoretical modelling.

Abbreviations

BA	Brodmann area
BDI	Beck depression inventory
BOLD	blood oxygenation level dependent
DCM	dynamic causal modelling
DLPFC	dorsolateral prefrontal cortex
DSM	diagnostic and statistical manual
EEG	electro-encephalography
EPI	echo-planar imaging
FDR	false discovery rate
fMRI	functional magnetic resonance imaging
GABA	γ - aminobutyric acid
GLM	general linear model
GH	hippocampus
HD	Huntington's disease
MDD	major depressive disorder
MEG	magneto-encephalography
OCD	obsessive-compulsive disorder
OFC	orbitofrontal cortex
OMPFC	orbito-medial prefrontal cortex
PET	positron emission tomography
PFC	prefrontal cortex
rCBF	regional cerebral blood flow
RCM	reverse Cuthill-McKee (algorithm)
RF	radio frequency
ROI	region of interest
RT	reaction-time
SEM	structural equation modelling
SNR	signal to noise ratio
SPECT	single photon emission computed tomography
SPM	statistical parametric mapping
SSQ	sum of squares quotient
TE	time to echo
TMS	transcranial magnetic stimulation
TR	repetition time

Chapter 1

Introduction

"..Becoming depressed is like going blind, the darkness at first gradual, then encompassing; it is like going deaf, hearing less and less until a terrible silence is all around you, until you cannot make any sound of your own to penetrate the quiet..."

The Noonday Demon (Solomon, 2001)

1.1 Overview

Could our darkest daemons be an emergent property of faulty wiring in the brain?

Mental disorders, which have probably existed throughout human history, have carried a mysterious or even shameful stigma for generations. Even though evolutionary theories in psychiatry consider changes of mental states to be necessary transitional states responding to an environment which can sometimes be hostile (Stevens and Price, 2000), these disorders are still perceived as frightening by the general public. In the last few decades precise classification and better control of these disorders has been achieved with the help of psychotrophic medications. Raised public awareness to mental disorders generally and disorders of mood in particular, by outlining the physiological causes of these ailments, help integrate patients back into society. Neuroimaging has played an important role in this process, by uncovering altered patterns of neural activity in patients and proving that changes in brain activity, brain chemistry and subsequently pharmacological intervention, are likely to have a positive effect on alleviating symptoms. Thus, mental disorders could be argued to have become more understandable, in a physical sense, since they can now be perceived as physical illnesses rather than unknown entities of the human mind. However, we do not clearly understand the interaction between emotional, physiological and cognitive aspects of mental illness nor have we managed to establish a direct mapping between neurobiological abnormalities and behaviour.

This thesis will focus on affective disorders, or mood disorders, including Major Depressive Disorder (MDD; also known as unipolar depression) and Bipolar Disorder (manic depression). Both syndromes are characterised by changes of mood, perception and behaviour, with a general negative shift in the depressive state and a hyper-active state in the manic phase of bipolar illness. Both local and global neuropathology have been reported in patients suffering from these disorders. Namely, specific structures such as prefrontal cortical areas show abnormal activity during the clinical phase of the illness or even through remission.

Furthermore, global changes in cortical excitability, as a measure of hyperactivity or hypoactivity have also been found. These suggest that global neuropathology may account for some of the behavioural symptoms, particularly in depression.

Specific neuropsychological deficits, such as memory and attentional impairment, along with emotional lability and mood fluctuations, are shared by unipolar and bipolar patients. Furthermore, these clinical groups may share a neurobiological vulnerability (Drevets et al., 1997) that affects the activity of analogous neuronal networks. I wished to examine neural activity in both patient groups, to reflect on the effects that damage to different structures may have on global activity in the brain and on specific neuronal networks therein. The following sections provide a brief overview of the issues and questions addressed in this thesis. A somewhat dualistic approach to the subject matter, involving both clinical and computational investigations is reflected in this document. My aim throughout this project was to investigate brain abnormality in mental illness, focusing on both neuropsychology and neurobiology of mental disorders, from a computational perspective. Thus, analysis of neuroimaging experiments is combined with theoretical models, addressing specific questions that have been raised by the experimental work.

1.2 Emotion, cognition and the associated neural circuitry

The scientific exploration of affective disorders spans many fields, including psychology, physiology, neurobiology and neuroanatomy. Despite the rich sources of knowledge in these fields, we are struggling to agree on the precise nature of the abnormality as regards brain dysfunction in affective disorders. Clinical studies may produce conflicting results due to two main factors. First, the unique personal and environmental circumstances in individual cases can render experimental results

spurious. Second, patients with a heterogeneous aetiology (symptoms, number of previous episodes, medication and family history) may be grouped together in experimental studies. The differences in patient profiles, which may bias results, can be confounded by small subject numbers in clinical trials.

Although affective disorders are typically characterised by changes in mood and emotional regulation (Phillips et al., 2003), cognitive function is often affected in symptomatic (Elliott et al., 1997) or even euthymic (Paradiso et al., 1997; Zubieta et al., 2001) clinical groups. Since impairment appears to be positively correlated with illness duration and number of clinical episodes (Strakowski et al., 1999), or with a family history of mental illness (Drevets et al., 1997), it may be argued that psychiatric morbidity in unipolar and bipolar disorders may have a neurodegenerative course, deteriorating over time, with a possible genetic underpinning.

My work will focus on the putative links between neural deficits associated with cognitive dysfunction in mood disorders, described in the neuroimaging literature and observed through experimental studies. Approaching this subject from a computational perspective, I was interested in four principal questions. First, I wished to examine the task-oriented activity in patients and compare this activity to control subjects, examining both groups' performance and the associated neural response. Second, different brain areas cooperate to solve or perform specific tasks. Therefore, I wished to evaluate the functional connectivity representing the interaction between different brain areas in patients and in healthy control subjects. Third, I wished to examine a task-oriented neuronal-network from a modelling perspective, to see how vulnerable its activity may be to disruption in both global and local parameters representing structural and functional deficits in affective disorders. Finally, I wished to see whether gradual decline was an inevitable

consequence of these deficits and could worsen as a function of time or whether compensatory strategies are possible.

1.3 Why modelling is potentially useful

At first glance, it may seem strange to use theoretical models to study such a human experience. Theoretical models can address divergent findings in the experimental literature by representing what are believed to be the important elements and the relationships between them, in mathematical terms. Computational models can complement or supplement experimental paradigms capturing various aspects of brain activity in different subject groups. Models can be used both to test existing hypotheses and to generate new hypotheses regarding the dynamic interactions within and between networks. Thereafter, the activity of different units can be altered to represent state or trait related pathology. The generative properties of computational models allow a direct and rigorous examination of interactions between suggested cause (e.g. reduced activity in the prefrontal cortex, termed hypofrontalitiy) and effect (e.g. the ability of a network to solve a task, or subsequent activity changes of units representing remote brain areas). Furthermore, to provide an insight into a putative neurodegenerative course in affective disorders, suggested by the association between illness duration and cognitive dysfunction, the effects of discrete deficits on neural activity may be tested over time.

1.4 Aims of the thesis

This thesis studies different aspects of neural activity in unipolar and bipolar patients with an emphasis on the neural response to cognitive challenges. The approach is both experimental and theoretical with the aim of discovering whether activity patterns observed in neuroimaging studies can be examined in a systematic fashion, in order to identify potential loci of dysfunction and to tease apart global from localised abnormalities.

Using different computational methods to analyse and model neuroimaging data, I wished to associate brain activity and structural deficits in unipolar and bipolar patients to behavioural and neuropsychological deficits reported in these groups. For this purpose, neural response in healthy subjects was compared to the neural response of patients by identifying task-related and task-independent neural activity in these subjects. My modelling endeavours include a dynamical characterisation of task-related network activity in the delayed match to sample task, using an effective connectivity network suggested by McIntosh et al. (1996). The characteristic activity patterns of two simulated networks were then perturbed, altering both global activity and the output from specific structures associated with unipolar and bipolar disorders. These simulations were intended to test the functional implications of illness-related abnormalities on a memory-related functional network in affective disorders under different task-related constraints.

1.5 Thesis outline

The topics introducing the background to my research are divided into two chapters. First, neurobiological aspects of affective disorders and technical issues involved with delineating the neurobiology associated with these disorders are discussed in chapter 2. Chapter 3 follows by discussing different methods for modelling both the symptoms and neurobiology of these disorders; looking at animal models and then the analytical methods for studying the activity of networks of neurons (in humans), such as functional and effective connectivity methods. The latter part of chapter 3 is an introduction to neural-network modelling techniques, describing several models which used these techniques to study either mental illness or brain activity.

The neuroimaging components of the thesis start with an investigation of brain activity in a group of bipolar patients and healthy control subjects performing the Stroop task (chapter 4). This is followed by a study of functional connectivity, comparing depressed patients and healthy controls performing the N-back task (chapter 5). Both the Stroop and the N-back are common tests to investigate cognitive capacity, namely selective-attention and working-memory. The computational modelling component of the thesis first characterises qualitative differences between activity patterns in a perceptual-matching and a long-delay network by simulating systems-level networks representing brain activity in a working-memory study (chapter 6). This is followed by an investigation of the discrete effects of global and local neurobiological deficits in depression (such as decreased excitability or structural vulnerability), and specific interactions between different brain areas (chapter 7). Finally, chapter 8 suggests future studies and discusses different implications of my findings.

Chapter 2

The Neurobiology of affective disorders

2.1 Introduction

With the aim of giving a general overview of the subject, this chapter will first describe the diagnostic criteria for unipolar and bipolar depression (sections 2.2.1-2.2.3). The experimental chapters in the thesis (chapters 4-7) are based on neuroimaging data. Therefore, I review neuroimaging modalities focusing on functional Magnetic Resonance Imaging (fMRI) to investigate *in vivo* brain activity in healthy subjects and in patients (section 2.3). An outline of potential culprit areas or networks underlying depression and therapeutic strategies forms the latter half of

this chapter, highlighting specific areas and networks. The rationale for focusing on the computational parameters underlying affective illness, rather than providing an overview of findings from the neuroimaging literature for example, is based on the potential application of these findings to modelling frameworks. In sections 2.4-2.5 I make the distinction between deficits of formation (neuroanatomy and genetics) and deficits of function (neuropsychology), which are both prevalent in affective disorders.

Structural abnormalities may bring about changes in behaviour, mood and neuropsychological performance. These changes can be divided into cognitive and emotional domains, producing specific impairment associated with the corresponding modes of processing. Neuroimaging methods, such as Positron Emission Tomorgraphy (PET) or fMRI, can reveal brain activity associated with specific tasks or search for metabolic markers at rest. These studies can identify localised changes in function, comparing the averaged brain activity of clinical groups with healthy control subjects. A review of neuroimaging findings in mood disorders, was published elsewhere (Ebmeier and Kronhaus, 2001); attached to this thesis as Appendix A). There we progressed from a molecular (neurotransmitter) hypothesis of dysfunction, looking at pharmacotherapy and related therapeutic strategies, through to a systems approach to neurobiological dysfunction in affective disorders. The following sections therefore present mainly seminal findings in the field of neuroimaging, as an introduction to the ideas developed further in the experimental chapters. Specific neuropsychological abnormalities associated with bipolar and unipolar illness are reviewed in the relevant chapters (chapters 4 and 5 respectively).

To introduce the computational problems that may arise as a consequence of the neurobiological correlates of unipolar and bipolar illness, I examine the anatomical

framework of neuropsychological deficits in affective disorders. This includes the rationale for focusing on specific culprit areas for modelling and analysis (sections 2.5.1-2.5.4), the anatomical connections of these areas (section 2.5.5) and the link between structural deficits and affective disorders (section 2.4). Finally, the experimental projects in this thesis will be set in the context of the two prevailing approaches to understanding brain activity (section 2.6), namely the segregation and integration of brain function (Friston and Price, 2001b).

2.2 Background and specification of symptoms

Affective disorders, namely unipolar and bipolar depression (manic-depression), are expressed through changes in mood, thought and behaviour patterns. This thesis will focus mainly on depressive symptoms and the neural activity associated with them. Investigating the neurobiological markers of the depressed state, both in unipolar and bipolar disorders, may provide an insight into the shared and divergent aspects of depression in these disorders. Therefore, the symptoms associated with mania will be mentioned only briefly. During the clinical phase of depressive illness, motor activity is altered, physiological (vegetative) processes, such as sleep and appetite, are compromised and even physical strength can decrease (Shajahan et al., 1999). These changes appear to be periodic and reversible with appropriate treatment such as psychotrophic medication. Formal diagnosis of depressive and manic episodes, defined in the Diagnostic and Statistical Manual of Mental Disorders, the DSM-IV (American Psychiatric Association, 1994), is based on episode length, recurrence, severity and relative disruption to normal functioning. Diagnosis of depressive or bipolar disorders can be described as a collection of ubiquitous clinical episodes. The following section will present some of the formal

diagnostic criteria for unipolar and bipolar depression. The purpose of presenting these here is to highlight the main physiological and behavioural changes, which may account for the characteristic brain activity patterns and neuropsychological changes, forming the basis of this thesis.

2.2.1 Major Depressive Disorder

The diagnosis of a Major Depressive Episode according to DSM-IV is based on the presentation of symptoms related to mood, (e.g. continuously depressed mood, anhedonia) cognition (e.g. suicidal thoughts, excessive guilt, lack of concentration) or somatosensory changes (e.g. changes in sleeping or feeding patterns) for at least a fortnight. Major Depressive Disorder (MDD) is subject to diagnosis of one or more Major Depressive Episodes.

A staggering 9.5% (NIMH statistics; www.nimh.nih.gov/publicat/numbers.cfm) of the US population is afflicted with depression every year, causing severe disruption to the individual and to their working and social environment. Episodes can be triggered by diverse internal and external factors, such as traumatic life-events (bereavement, redundancy, as well as other changes in personal or professional circumstances). Stressful circumstances are mostly associated with the onset of the first-episode (Lewinsohn et al., 1999), while chronic illness has been linked with with developmental factors, pre-morbid personality and continuous stress (Riso et al., 2002). Furthermore, response to treatment, which is sometimes taken as an indicator for an underlying pathology (Frederick et al., 1990), can fluctuate during the illness.

2.2.2 Bipolar Disorder

Bipolar illness is characterized by an oscillation between hyperactivity and hypoactivity. This illness is of particular interest due to its association with artistic temperament and the process of creativity and the relatively high intellectual ability of sufferers (Jamieson, 1996). The prevalence rate of bipolar disorder is approximately 1.2% (NIMH statistics), with a considerable genetic component. Monozygotic twin studies have indicated 40% heritability in unipolar depression compared to 80% heritability in bipolar illness (Karkowski and Kendler, 1997). A gender bias towards the female population is more pronounced in unipolar depression than in bipolar illness (NIMH statistics).

The main diagnostic criteria for mania, listed in the DSM-IV, include cognitive (e.g. an inflated perception of self, flight of ideas), somatic (e.g. decreased need for sleep) and psychomotor (e.g. pressure of speech, agitation) symptoms.

2.2.3 Psychomotor symptoms associated with MDD and bipolar illness

Two different motor output states may be associated with depressed mood and cognition. First, psychomotor slowing has often been associated with depressive illness, especially with melancholic depression (Rogers et al., 2002) and may be linked to basal ganglia dysfunction (Caligiuri and Ellwanger, 2000). Psychomotor symptoms correlate with the severity of depressive illness in MDD but not in depressed bipolar subjects (Swann et al., 1999). Second, psychomotor agitation, which has also been associated with depression (Koukopoulos, 1999), is more pronounced in melancholic bipolar patients, while psychomotor slowing was more common among MDD subjects (Benazzi, 2004). Nonetheless, some behavioural symptoms associated with depressive illness, such as psychomotor slowing and

disturbed sleep, may be interpreted as adaptive and may conserve valuable resources (Ebert and Berger, 1998).

Evidently, this method of classification is qualitative rather than explanatory, since the fundamental cause of illness development or the neurobiological basis of its progression remains unexplained. This symptom-based system of diagnosis can be highly variable, since it essentially relies on personal views of the diagnosing clinician. Furthermore, it seems unsatisfactory to ascribe a label on the cumulative basis of specific symptoms, since failing to accumulate a sufficient number of symptoms at any one time will preclude a formal diagnosis of these disorders. Therefore new developments in the fields of genetics, neuroscience and neuroimaging in particular will become essential to improve classification and hence treatment (Helmuth, 2003).

2.3 Neuroimaging

The association of discrete brain regions with specific functions has become possible with the invention of modern neuroimaging methods that indirectly infer brain activity from the electrical, magnetic or radioactive labelling of various neurophysiological properties. With the development of new and more powerful imaging tools and data analysis techniques, our grasp of the functional neuroanatomy associated with mood disorders is constantly improving. We are able to measure electrical activity of neuronal assemblies in the living human brain using techniques such as electro-encephalography (EEG) and magneto-encephalography (MEG). Functional imaging methods such as PET, Single Photon Emission Computed Tomography (SPECT) and fMRI measure blood flow (haemodynamic response) and glucose metabolism, believed to be coupled with neuronal firing,

through different states of brain activity. The temporal and spatial resolution of these different imaging methods are compared in Figure 2.1, spanning the sub-neuronal to the systems level, in animal and human studies. The relative merits and disadvantages of fMRI are briefly summarised below, after discussing the underlying assumption: coupling of neuronal activity with blood flow in the brain.

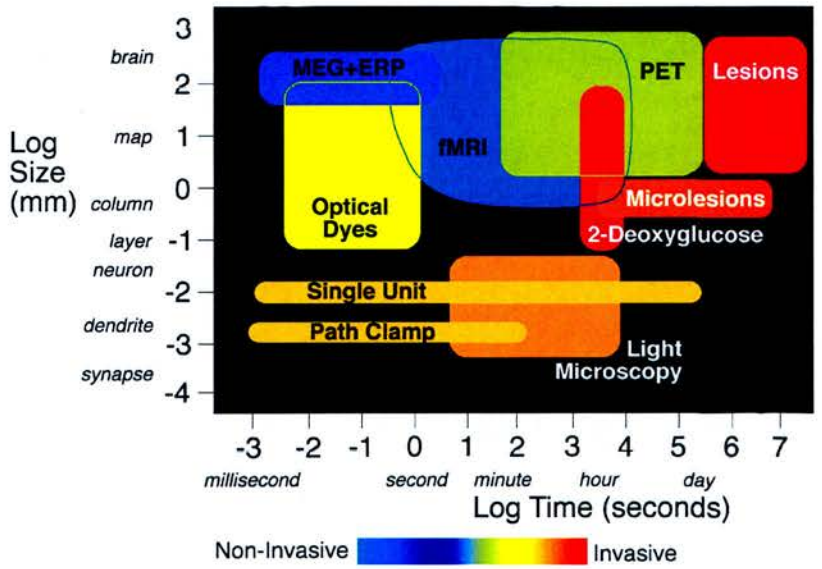

Figure 2.1: Spatio-temporal resolution of different techniques for recording brain activity in humans and animals. Although fMRI improves the spatio-temporal resolution of PET, it cannot achieve the same resolution as methods measuring electrical activity such as EEG (not shown) and ERP. Image from Cohen and Bookheimer (1994).

A crucial assumption in imaging blood flow is that it correlates with neuronal firing; however, the mapping between neural activity and subsequent registration of this activity is not straightforward. For instance, it is unclear whether the measured activity represents excitatory or inhibitory neuronal assemblies. However, recent studies strongly suggest that the activity of single neurons is indeed closely linked with increased oxygen consumption (Thompson et al., 2003), which is the fundamental assumption supporting Blood Oxygen Level Dependent (BOLD) fMRI

research. Nevertheless, Logothetis et al. (2001) showed that the fMRI BOLD response (in monkey visual cortex) is associated with local field potentials (reflecting the input signal), rather than spiking activity (output signal) of either single neurons or neuronal populations. Therefore, although the underlying assumption of coupling between different measurements of neuronal activity holds true, we may need to rely on several techniques, such as fMRI and EEG, to accurately map brain activity.

Further, hypotheses regarding functional circuits in the brain of both healthy subjects and clinical populations may be even more critical, since the BOLD signal may reflect the summed input activity over an extended network and lack the computational sensitivity to highlight dysfunctional loci in clinical groups. Since the experimental chapters of this thesis examine brain activity using fMRI, the next sections will briefly review the history and principles of fMRI, after a summary of the advantages and disadvantages of this neuroimaging method. Subsequently, data analysis methods are outlined, describing the transformation of raw images into meaningful neural activity, allowing comparison of activation in different groups. Excellent textbooks in this subject e.g. Jezzard et al. (2001) provide a thorough introduction to this field.

2.3.1.1 Merits of fMRI

1. With temporal resolution of 3-5 sec, fMRI improves the temporal resolution of PET (45 sec) and SPECT (> 60 sec; not depicted in Figure 2.1) (Volkow et al., 1997).

2. The spatial resolution of fMRI (1-1.5 mm) is superior to PET (4 mm), SPECT (6-8 mm) and EEG (10-15 mm; not depicted in Figure 2.1).

3. Safe and non-invasive. No radioactive isotopes used.

4. fMRI is less costly and more accessible in a clinical setting than MEG.

2.3.1.2 Disadvantages of fMRI

1. The temporal resolution of fMRI falls short of direct recording of electrical activity in the brain (EEG and MEG are both in the order of 1 msec (Volkow et al., 1997)). This method's spatial resolution is inferior to MEG.

2. fMRI does not measure absolute blood flow. Therefore studies measuring relative changes in flow, and hence activity, do not account for baseline activity in different populations.

3. This method observes subtle blood flow changes in capillaries, which may be obscured by large pulsating blood vessels, near activated regions. Furthermore, the signal may be observed in veins that are draining the neuronally active area. This means the signal may be dislocated from its neuronal source.

4. Potential sources of noise include:

    a. Susceptibility artefacts from air cavities, such as sinuses. This caveat is particularly relevant in psychiatric populations, where the activity of orbitofrontal and mesotemporal (amygdala and hippocampus) regions, which are more sensitive to these signal distortions, is of interest.

    b. Periodic noise such as respiration and heart beat.

5. Sensitive to subject movement (shared by MEG); may be confounded by agitated or restless patients in clinical studies.

Nonetheless, many of these disadvantages can be resolved (e.g. correcting for movement) or accounted for (e.g. physiological noise) during statistical analysis of the data. Compared to other neuroimaging methods, fMRI remains the most accurate and safe technique of probing brain function in humans.

2.3.2 The fundamentals of fMRI

Before the invention of methods measuring electrical and neurochemical activity in the brain, localisation of function was possible only by associating the region of brain damage (lesions; Figure 2.1) with loss of function. Since we currently cannot see brain activity without opening the skull, we use an indirect approach, looking at blood flow (haemodynamic response) and metabolism in the active brain, assuming that demands will increase to active parts of the brain, associated with the performance of specific tasks. While traditional neuroimaging methods such as PET and SPECT involve injection of radioactive substances and visualising areas of increased concentration (associated with increased metabolic rate) fMRI relies on the subtle increase in magnetisation of oxygenated blood (binding to the iron molecule in haemoglobin), compared to deoxygenated blood.

The strength of the magnetic field (typically 1.5-3 Tesla in human experiments) inside an fMRI scanner causes hydrogen (^1H) protons in the tissue to spin and precess around their axes (Figure 2.2a) at the same frequency (gyro-magnetic ratio; measured in MHz) but in random phase, aligned with (or opposite to) the direction of the magnetic field (along the z plane). The precession frequency (ω_0), which describes the absorption of the radio-frequency (RF) pulse energy by the atom, is

specified by the Larmour equation (2.1) to be dependent upon the strength of the magnetic field (B_0) and the gyro magnetic ratio (γ) of the specific atom:

$$\omega_0 = \gamma * B_0 \tag{2.1}$$

The ^1H protons are flipped by the RF pulse (Figure 2.2b) to the *xy* plane and start precessing in phase (Figure 2.2c). Relaxation of protons back to baseline is characterised by two independent processes, the T1 (longitudinal) and T2 (transverse) time constants (Figure 2.2d), measuring relaxation to baseline. T1 represents the rate at which hydrogen molecules return to alignment with B_0 (gaining longitudinal coherence). Conversely, the decay of T2 represents the loss of phase coherence among the hydrogen protons. The T2* effect measures the actual decay of the T2 signal, taking into account inhomogeneities of the surrounding magnetic field (Logothetis, 2002). Recovery of the T1 and T2* signal from different tissues such as grey and white matter, or oxygenated and deoxygenated blood, allows the detected signal to be reconstructed into different images. Anatomical images are based on the T1 signal, while the BOLD fMRI contrast, described in the next section, is based on the T2* signal.

Basic imaging parameters include the repetition time (TR), which describes the time between RF pulses and subsequent acquisitions of the same slice. An imaging sequence often excites the protons twice, first to 90^0 and subsequently to 180^0. The elapsed period between the two excitations is called the Echo Time (TE). The angle of the flipped ^1H protons following the RF pulse is simply called the flip angle (Figure 2.2b shows a flip angle of 90^0).

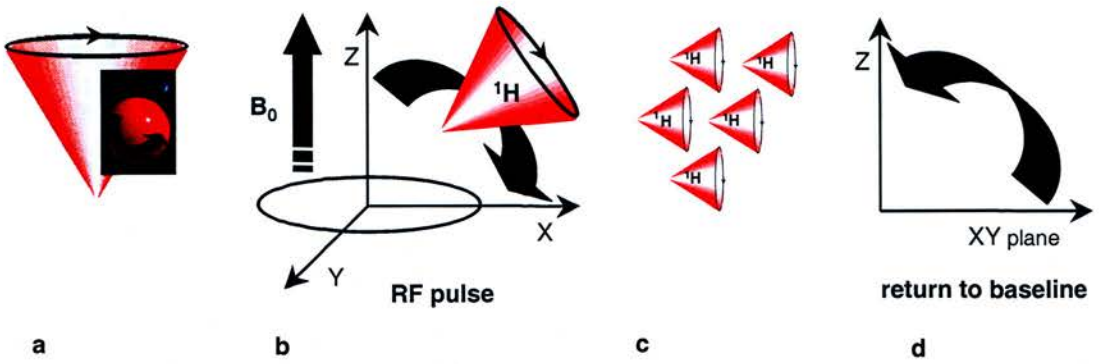

Figure 2.2: The properties of magnetisation inside the fMRI scanner. (a) Magnetic field; spinning and precessing of one hydrogen proton; (b) Flipping of the protons after RF excitation; (c) Protons aligned along the xy axis, preccesing in phase; (d) Return to equilibrium, loss of xy (transverse) phase coherence (T2*) and gain of coherence along the z (longitudinal) axis.

The BOLD contrast in fMRI, first observed in the rat by Ogawa et al. (1990), depicts changes in the magnetic field as oxygenated blood enters activated regions. In a T2* weighted image, increased MR (magnetic resonance) signal intensity is associated with oxygenation changes in blood flow around activated tissue, since the oxygenated blood does not dephase the hydrogen protons as much as the deoxygenated blood (Ogawa and Lee, 1990). These changes in blood flow (the 'haemodynamic response') occur approximately 4-8 seconds after the onset of a stimulus and are characterised by an initial increase in deoxygenated blood ('dip') followed by a longer period of increased (oxygenated) blood-flow to areas that were activated by the task. The temporal resolution of modern fMRI scanners is limited by the rate of the haemodynamic response and the scanning sequence used. However at 2-4 seconds per TR (the experimental paradigms described in this thesis) using 1.5 Tesla scanners, this method is a great improvement on both PET and SPECT.

During a typical fMRI experiment, active conditions are interspersed with periods of rest or with similar active conditions that can be differentiated in specific aspects. Comparing the images acquired during performance of these tasks by subtracting the activation of one task from the other (or from rest) reveals the relative changes in blood flow to specific regions that may be associated with the condition of interest.

In sum, fMRI is a very useful and widely used technique to measure blood flow associated with neuronal activity. The disadvantages of this method are mainly that its temporal resolution cannot directly detect neuronal events and the susceptibility artefacts which result from subject movement and from inhomogeneities of the magnetic field in the skull. Nonetheless, fMRI improves the temporal resolution of other, more traditional methods (such as PET and SPECT), and is relatively safe and accessible. In the next section, the transformation of the magnetic signal into meaningful activation images in different subject groups will be outlined.

2.3.3 Analysis of fMRI data

The raw data in fMRI is acquired in the frequency domain (k-space; Figure 2.3a). The analysis of this data involves image reconstruction using an inverse Fourier Transform (FT) and pre-processing, to increase the signal to noise ratio (SNR). Statistical analysis, comparing the observed signal to a model of expected activity using methods such as the General Linear Model (GLM), produces activation images (Figure 2.3d). These stages of data analysis, described below, pertain to Figures 2.3c and 2.3d.

2.3.3.1 Pre-processing

After the raw data matrix is transformed into image space, pre-processing procedures remove noise and movement artefacts in preparation for statistical analysis. This is crucial, since even the slightest movement of the subject's head inside the scanner may produce large signal changes around the edge of the brain that can be greater than the change in signal associated with neural response to the task. For this purpose, all the acquired scans are realigned to the first or average scan, accounting for translation and rotation parameters.

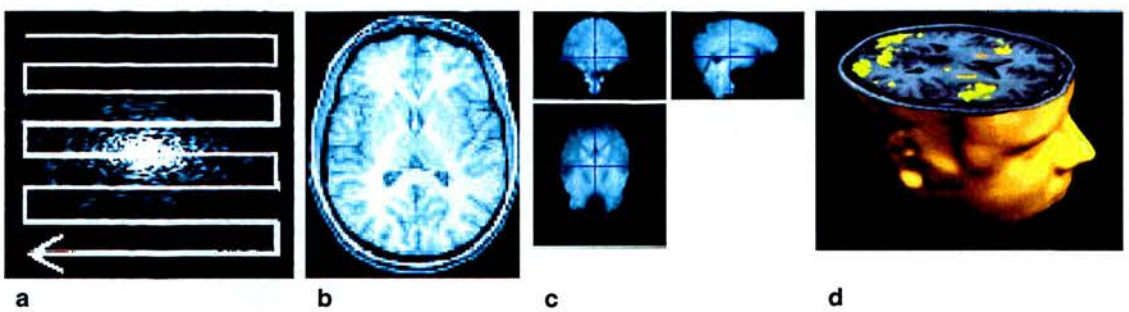

Figure 2.3: Image reconstruction in fMRI. (a) Activation is captured in k space using an EPI (Echo Planar Imaging) sequence. (b) High resolution anatomical scans and (c) low resolution functional scans are reconstructed using FT. (d) Subsequent statistical analysis measuring signal change associated with a specific activation paradigm, produces activation images. Here yellow denotes areas that were active during the task. Sources:
(a) http://www.hslmc.cam.ac.uk/index_hires.htm
(b-c) http://tezpur.keck.waisman.wisc.edu/images/fmri.jpg
(d) http://www.kun.nl/

To increase SNR, smoothing (filtering) can be performed both in time and in space. Smoothing in space is done by convolving the image with a Gaussian filter of a certain size (usually parameterised by the Full Width Half Maximum (FWHM)). Filtering can remove high frequency fluctuations (usually associated with physiological noise such as respiration or heart-beat) or low frequency drift

associated with scanner operation. The use of high and low pass filters is discretionary, as is the choice of the width of the Gaussian filter for spatial smoothing. Finally, normalisation to standard space such as the Talairach template (Talairach and Tournoux, 1988) enables comparison and averaging of activation images from individual subjects in standard space (as used in chapter 5).

2.3.3.2 Statistical analysis

An experimental paradigm is typically based on the hypothesis of change in activity across a network of areas in association with a specific stimulus or task, specified in a model (also known as a design matrix). In a block design for example, the task conditions (or phases) alternate with at least one form of a control condition consisting of either rest periods or different task conditions. The model of expected activity, expressing a linear relationship between predictor variables and neural response, is fitted to the time-course of every voxel.

$$Y = \beta * X + \varepsilon \qquad (2.2)$$

At its simplest form, model fitting involves parameter estimation for equation 2.2, where Y is a vector representing the neural response (the time-course of one voxel) across all scans; X represents a (design) matrix of predictor variables (that help account for the data, such as the difficulty of specific blocks, reaction time, or known confounders such as movement parameters for each block) for every time point; β represent the parameters of the regression line which we would like to estimate and ε represents the remaining error (or residuals) for each scan. Fitting the parameter β is typically performed using least squares minimisation.

Once the parameters have been estimated, various techniques can assess the statistical significance of the model at every voxel. For example, in the SPM (Statistical Parametric Mapping; Friston, 1997)) analysis package, a t-statistic for every voxel is computed and compared to the null hypothesis of no experimental effects (Worsley et al., 1996). This statistic is typically converted to a z-score in packages such as SPM to give a normalised value of neural activation. Alternatively, non-parametric statistics (as used in chapter 4) are preferred by several groups, since these do not assume that data are normally distributed (Brammer et al., 1997).

fMRI analysis typically involves many thousands of simultaneous comparisons. By the nature of statistical testing, some of these may give false positive results. For example if significance is assessed at the 95% confidence level, 5 out of every 100 results may be false positives. It is therefore necessary to correct for multiple comparisons (Nichols and Hayasaka, 2003). This can be done simply by Bonferroni corrections, multiplying the uncorrected p-values by the number of comparisons. However, this test is likely to be too conservative and create false negatives, since Bonferroni corrections treat each active voxel as if it was an independent measurement while fMRI data are temporally and spatially continuous. Thus, correction procedures such as Random Field Theory (in SPM) or False Discovery Rate (FDR) are adopted (Genovese et al., 2002), giving a corrected p-value for every activated voxel. These methods are less conservative than Bonferroni corrections, and deal with multiple comparisons in a robust manner.

The field of fMRI analysis is relatively young and therefore development of new imaging sequences and analysis techniques is ongoing. There are different commercial and freely available software packages for analysing these data. These include, among others: SPM (www.fil.ion.ucl.ac.uk): used for the first-level (localisation) analysis of the data in chapter 5; Afni (afni.nimh.nih.gov); Brain

Voyager (www.brainvoyager.de); and XBAMM (www-bmu.psychiatry.cam.ac.uk): a similar package was used for analysis of the neuroimaging data in chapter 4. Finally, only univariate analysis techniques (i.e. performing the analysis separately for each voxel) have been discussed here. Different multivariate techniques, such as Principle Component Analysis (PCA) and Independent Component Analysis (ICA) were considered to be beyond the scope of this thesis.

2.4 Structural changes

Associations between structural changes and behavioural deficits have been established in several ways. First, lesions in specific areas of the cortex have often been linked to specific disorders. Second, certain neurological illnesses, such as Huntington's disease (HD), affecting discrete brain areas, are often accompanied or even preceded by psychiatric symptoms. Third, morphological features, observed in both *post-mortem* studies and *in vivo* techniques such as voxel-based morphometry, may be used to compare the structure of normal brains to those of psychiatric populations. For example, increased incidence of white matter lesions, noted both in unipolar and bipolar patients (Videbech, 1997), suggest global connectivity impairments in these populations.

Arguably, changes in the activity pattern of a particular structure are not a reliable predictor for a particular affective disorder. Nonetheless, damage to certain structures or pathways yields a fairly consistent pattern of impairment, with a similar presentation to depression, mania and various language disorders (Starkstein, 1998).

2.4.1 Lesions

Before neuroimaging studies allowed us to observe activity in the healthy, living human brain, associations between neuroanatomy and behaviour were limited to the association of traumatic brain injuries (such as stroke, accidents or neurosurgery) with the devastation they caused (Cosgrove and Rauch, 2003; Seel et al., 2003). However, the cognitive deficits and altered emotional states produced by lesions (Rogers et al., 1998) are constrained by retrospective inferences and compensatory changes emerging as part of the recovery process (Seitz et al., 1999). Furthermore, the behavioural manifestations of stroke for instance (associated with older patients) may not be restricted to dysfunction in the area immediately surrounding the haemorrage, but is confounded by putative geriatric pathology.

2.4.2 Structural abnormalities in psychiatric populations

Structural changes in limbic associated areas have been identified by several groups. Volume reduction was found in temporal areas, linked with verbal memory deficits (Shah et al., 1998) and illness severity (Sheline et al., 1999). Glial cell loss was noted in the anterior cingulate of unipolar and bipolar patients with a family history of affective disorders (Drevets et al., 1997). Glial cell abnormalities were also reported in orbitofrontal cortex (OFC) and dorsolateral prefrontal cortex (DLPFC), where neuronal volume and density were correspondingly impaired (Rajkowska et al., 1999; Cotter et al., 2002). Conversely, increased cell numbers were noted in hypothalamus and dorsal raphe (Rajkowska, 2000). Dysfunction may be argued to focus around those areas in clinical subgroups with similar aetiology (e.g. a family history of mental illness). However, familial affective disorders may now be

evaluated using genetic tools, allowing earlier and perhaps better-informed targeting of pharmacological agents.

2.4.3 Genetic studies

Twin studies have traditionally been used to establish the heritability of specific psychiatric disorders (Zerbin-Rudin, 1987; Smoller and Finn, 2003). However, these studies can establish only an association between specific symptoms and diagnoses. Recent developments in the field of bioinformatics, using the micro-array (gene-chip) technologies, can highlight or identify specific dysfunctional loci. Unravelling the genetic phenotype associated with unipolar (Zubenko et al., 2002) and bipolar (Craddock and Jones, 1999) disorders may in turn inspire more accurate and focussed knockout studies in animal models.

2.5 Functional circuitry

Our grasp of functional circuitry in unipolar and bipolar depression may be obscured by several factors. First, our understanding of human connectivity is mostly based on anatomical studies in non-human mammals, where regional specificity and thus connectivity patterns are likely to differ from the human brain. Second, in human subjects, current imaging techniques (e.g. fMRI and PET) do not operate on a sufficiently sensitive time scale to detect neuronal events. Third, brain activity recorded during performance of specific tasks is likely to detect redundant information. Namely, functional imaging may reveal an extended network, which includes areas that do not participate in the functional circuit. An incomplete understanding of functional circuitry is more complex in conditions such as

unipolar or bipolar illness, where unclear aetiology, clinical heterogeneity and inconsistent experimental methodology are possible confounders. Furthermore, in patients suffering from affective disorders, it is often difficult to decouple trait (illness) and state (current mood state) related deficits (Harmer et al., 2002). Varying degrees of neuropsychological dysfunction are reported (Rossi et al., 2000), which may persist beyond remission (Paradiso et al., 1997).

The afflicted network of areas giving rise to these dysfunctions may extend beyond areas previously described as the "limbic lobe" (first delineated by Broca in 1878), to include prefrontal cortex and cerebellum, along with basal ganglia, amygdala, hippocampus and parietal cortex (Phillips et al., 2003). Some of these structures are highlighted in Figure 2.4. Structural and functional deficits, along with metabolic changes associated with different medications, have been found in these areas. Although a reparative role may account for functional (possibly compensatory) interactions between different regions, the precise nature of these interactions has so far been mainly descriptive. I will now outline findings implicating several key areas in further detail, trying to capture the putative coupling between neurobiological and behavioural phenomena. Some of these are seldom associated with affective disorders. However, they are likely candidates for the dysfunctional networks associated with depressive symptoms in unipolar and bipolar disorders. I highlight areas that may participate in neuronal-networks related to mood and cognition, to preface the modelling ideas presented in the next chapter.

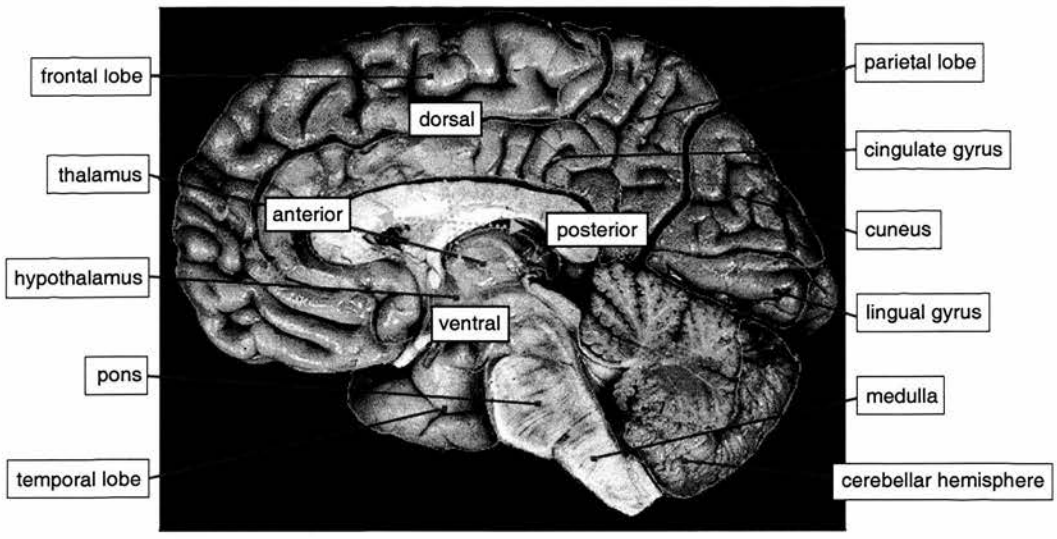

Figure 2.4: Medial view of the human brain (right hemisphere), highlighting the major cortical and subcortical structure, some of which may be impaired in affective disorders. Depressed patients show functional (cognitive) deficits in prefrontal and parietal lobes. The cingulate gyrus (especially subgenual and anterior cingulate, wrapping around the corpus callosum, which connects both hemispheres), is particularly vulnerable in both unipolar and bipolar disorders (Drevets et al., 1997). Figure adapted from digital anatomist. http://www9.biostr.washington.edu.

2.5.1 Basal ganglia

The basal ganglia (Figure 2.5) are often neglected in the study of affective disorders, where the focus is predominantly on prefrontal and limbic structures. However, these structures can be linked with unipolar and bipolar illness for two reasons. First, motor symptoms associated with depression may be comparable to motor dysfunction in basal ganglia related illnesses such as Parkinson's disease (Caligiuri and Ellwanger, 2000). Second, neuropathological processes in the basal ganglia, such as Huntington's disease (HD), have often been associated with mood impairment that preceded the characteristic motor symptoms (Rosenblatt and Leroi, 2000). The neurodegenerative process in HD is caused by a progressive pattern of cell death originating in the dorsal striatum, progressing ventrally until the whole structure

degenerates (Hedreen and Folstein, 1995). The exact nature of the relationship between the psychiatric manifestation of the neurodegenerative process in this illness is, however, unclear.

Neurochemical changes in the basal ganglia, such as changes in levels of dopamine, have also been linked with clinical changes in depressive illness. Increased striatal dopamine release has been linked with amelioration of depressive symptoms, following a night of sleep deprivation (Ebert et al., 1994) and after applying repetitive transcranial magnetic stimulation (rTMS) to the DLPFC (Strafella et al., 2001). However, enduring striatal hypometabolism was shared by both responders and non-responders to (the former) treatment (Wu et al., 1999). Thus, subcortical involvement can be associated with worsening of symptoms (psychomotor slowing), recurrence of illness episodes and impaired cognition (Hickie et al., 1999) in depressive illness.

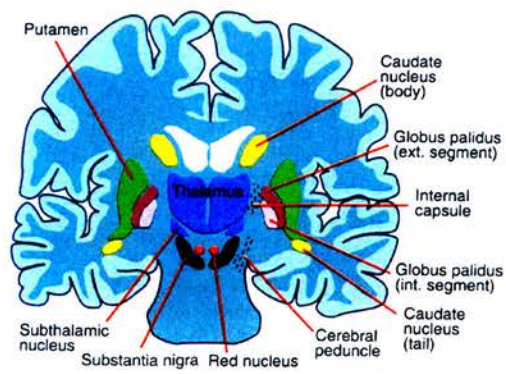

Figure 2.5: Axial slice of subcortical structures, including basal ganglia structures and thalamus. Image source: http://pharyngula.org/~pzmyers/neuro/chap9/basalganglia.jpg

2.5.2 Hippocampus and amygdala

The importance of the amygdala to recognise the emotive content of stimuli (Le Doux, 1992) and association of the hippocampus (GH) with memory and cognition (Rosenzweig and Barnes, 2003) suggests a functional decoupling between the two structures (depicted in Figure 2.6). However, no definitive causal relationship has been established between these discrete structural changes and aetiology of affective disorders.

GH is continually modified by means of long-term potentiation a process of synaptic activity dependent strengthening called LTP, a process that may be impaired by aging (Rosenzweig and Barnes, 2003); see Appendix A (Ebmeier and Kronhaus, 2001) for a review of the neuropathology and neurobiology associated with the aging process. The GH is vulnerable to chronic release of glucocorticoids (stress hormones), which may account for the cognitive and memory impairment experienced by depressed patients (Brown et al., 1999) and for the hippocampal atrophy associated with this illness (Shah et al., 1998; Bremner et al., 2000). These structural changes are independent of whole brain volume reduction or specific changes in amygdala, caudate, frontal or temporal lobe. Neurogenesis in the adult dentate gyrus is suppressed by glucocorticoid release in depressive illness (Jacobs, 2002) and enhanced by antidepressants, which also increase serotonin neurotransmission (D'Sa and Duman, 2002).

Amygdala enlargement has been associated with heightened emotional state in bipolar patients (Phillips et al., 2003), illness duration, and with medication history (Strakowski et al., 1999). Activation of the amygdala has been associated with fearful facial expressions or general vigilance to negative expressions (Yang et al., 2002). This effect was observed even when processing was not conscious, such as the backward masking paradigm (Whalen et al., 1998). In bipolar disorder, distinct

structural changes affect regions associated with processing of emotion. These changes include enlarged volume of amygdala (Altshuler et al., 1998; Strakowski et al., 1999; Brambilla et al., 2002) and also caudate nucleus (Aylward et al., 1994), along with suggested reduction in thalamic volume in adolescent patients (Dasari et al., 1999).

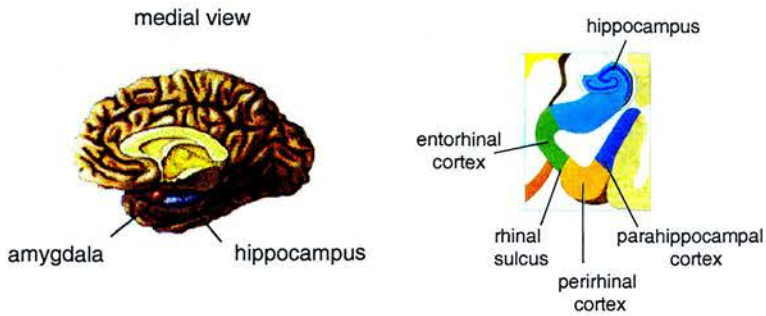

Figure 2.6: Sagittal slice showing location of amygdala and hippocampus (left) and a detailed view of the hippocampal formation (right).

Image source: http://dubinserver.colorado.edu/prj/sha2/amygdala.gif (medial view) http://departments.oxy.edu/cogsci/courses/2000/cs101/lecture-notes/linden/ (detailed view)

Structural abnormalities may precede depression or bipolar illness. Alternatively, these volume changes can be induced by the illness itself (Van Elst et al., 2001) or by prolonged use of psychotrophic medications.

2.5.3 Parietal cortex

Evidence for parietal cortex involvement in depression is increasing. This area could be reciprocally activated to complement or even compensate for prefrontal or temporal deficits. Remitted MDD patients (Mayberg et al., 1999), showed increased activity in DLPFC and inferior parietal regions, which were decoupled from the

activity of the subgenual anterior cingulate. Furthermore, increased prefrontal and parietal activity after a night of sleep deprivation compensated for decreased temporal lobe perfusion (Drummond et al., 2000). Finally, mutual activation of prefrontal and parietal cortices is often reported in working-memory tasks (see chapter 5). However, I know of no reports of structural deficits in parietal cortex of either unipolar or bipolar subjects.

2.5.4 Frontal cortex

Widespread hypoactivity is often reported in the prefrontal cortex (PFC) of psychiatric populations (al-Mousawi et al., 1996), termed hypofrontality. However, decreased activation of PFC may be due to neural dysfunction elsewhere. For example, an overactive region (such as the cingulate) may directly suppress PFC or alternatively, PFC may not receive sufficient excitation. Further, depressed patients may be unable to alter the activity of their PFC, adapting to increased task difficulty (Elliott et al., 1997), thus showing deficient plasticity rather than hypoactivity.

Increased dorsal PFC (associated with cognitive function) activity and decreased ventral PFC activity (associated with mood), upon recovery (Mayberg et al., 1999), suggests a decoupling of dorsolateral prefrontal cortex (DLPFC) from limbic regions such as the anterior cingulate. These systems may directly compete with each other through lateral inhibition, or perhaps participate in more extended loops, where competition can occur subcortically (e.g. between different structures in the basal ganglia). Therefore, the next section will examine the connectivity patterns between prefrontal areas that are associated with mood and with cognition.

2.5.5 Connectivity of affected areas

Both theoretical and analytical (effective connectivity; see chapter 3) models of functional networks are based on known anatomical connections in non-human primates. Connectivity patterns may suggest whether co-active areas are directly or indirectly related. However, the inconsistent nomenclature and different architectonic boundaries (Price, 1999; Ghashghaei and Barbas, 2001), make the task of defining anatomical networks rather difficult. A searchable database (www.cocomac.org) helps bridge some of the disparity in the field, or at least makes it explicit. Already informative in highlighting various details included in connectivity studies, this database may in future be enriched by allowing direct access to the parameters used by different groups, and encouraging direct comparisons of their findings.

The prefrontal cortex has been divided along functional outlines related to mood and cognition (Mayberg et al., 1999; Phillips et al., 2003). This demarcation suggests that these networks are also anatomically distinct, giving rise to their functionally disparate vulnerability to depressive illness. The following sub-sections focus therefore on delineation of the orbito-medial prefrontal cortex (OMPFC) and related structures, which have been linked with affective disorders.

2.5.5.1 Orbital and medial networks

Connections and architecture of the OMPFC have been described in the monkey by several groups (Price, 1999; Ghashghaei and Barbas, 2001). These areas have been divided into two distinct networks (Figure 2.7), medial and orbital (Carmichael and Price, 1995). The orbital network forms the input region, integrating information from visceral, somatosensory and visual areas, as well as amygdala and GH. By

contrast, the medial network is the output region, receiving both limbic and orbital inputs and sending afferent connections to the hypothalamus and the brain-stem (Price, 1999). The projections of different frontal areas are specific and topographical (Yeterian and Pandya, 1991; Morris et al., 1999), which may suggest specialized roles for areas displaying similar properties, such as connectivity patterns.

2.5.5.2 Amygdala and anterior cingulate connections

The amygdala receives most of its input from temporal cortex, but also the superior temporal gyrus, as well as small projections from the entorhinal cortex and the parahippocampal gyrus (Stefanacci and Amaral, 2000). Subgenual anterior cingulate (BA25) projects to amygdala and medio-dorsal thalamus (Freedman et al., 2000). Parietal afferent input is mainly restricted to dorsal cingulate (BA24) (Vogt and Pandya, 1987), but not in rostral BA24, which receives input from amygdala. Parietal connections to the posterior cingulate are more prominent than to anterior cingulate, where projections are sparse (An et al., 1998). See appendix A (Ebmeier and Kronhaus, 2001) for further details regarding cingulate function in depressive illness.

2.5.5.3 Hippocampal connections

As far as I am aware, studies of hippocampal neuroanatomy and connectivity have mostly been restricted to the rat. Therefore, due to the evolution of the prefrontal cortex in humans, any analogies drawn from these studies may not be relevant. However, the following findings in primates have been reported. Several medial orbital areas (Carmichael and Price, 1995) and OFC (Van Hoesen et al., 1993) receive

connections from GH. Reciprocal connections of the medial areas with GH are sparse (Carmichael and Price, 1995) or non-existent (Cavada et al., 2000) (but see also (Barbas et al., 1999)). Finally, an indirect projection from cingulate back to GH goes through ventromedial temporal areas (Van Hoesen et al., 1993).

2.5.5.4 Subcortical afferents

The medial and orbital networks (Figure 2.7) in the OMPFC connect to distinct areas of the striatum, which in turn connect to different portions of the mediodorsal nucleus of the thalamus. Orbital prefrontal areas connect to central rostral striatum (in a dorsal orientation to the connection site of the medial network). Medial prefrontal areas however, connect to ventromedial rostral striatum. Further, while in the orbital network striatal areas project to ventrolateral thalamus, the parallel connections in the medial network are to dorsomedial thalamus. Finally, thalamic nuclei project back to their respective prefrontal cortical afferents in either network.

2.5.5.5 Alternative delineations of PFC

By contrast, Mayberg et al. (1999) associates changes in activity of the dorsal (cognitive) and ventral (mood) prefrontal networks with depression and sadness. They argue that dorsal PFC is suppressed during depression while the ventral PFC including subgenual anterior cingulate, is over-active. After remission, this pattern is reversed. This argument is supported by anatomical evidence, showing that the subcortical projections of these respective frontal cortical areas is unique (Yeterian and Pandya, 1991). Whereas the dorsolateral and medial prefrontal areas connect to the dorsal and central section of the caudate, OFC connects to ventral and central

sections. Respective medial-orbital and dorsal-ventral topographical projections from PFC to similar orientations in the striatum have also been noted.

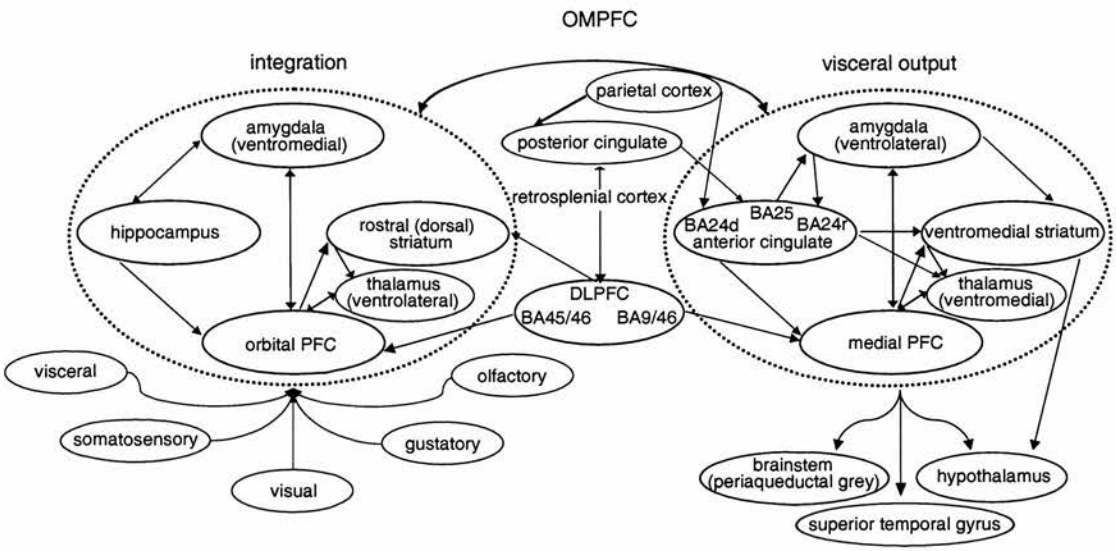

Figure 2.7: Connectivity diagram based on the medial and orbital delineation of prefrontal networks (Price, 1999). Input and output regions are specified outside the dotted lines, while subcortical efferents and afferents are included within the dotted lines. These networks appear to have a similar connectivity profile with cortical and subcortical afferents (albeit different portions of these structures, e.g. amygdala, striatum, thalamus and DLPFC). The orbital network is posited as the convergence zone for somatosensory and gustatory cortical inputs, while the medial network appears to send mostly afferent (output) connections. Both sections of the OMPFC are interconnected.

2.5.5.6 Functional implications of anatomical specificity

Distinctive functional assignment in the medial and orbital networks has been observed in the context of reward related behaviour. While the medial network has been associated with gambling tasks, the lateral orbital network is active when it is necessary to inhibit response to previously rewarded stimuli (Elliott et al., 2000). Simpson and colleagues (Simpson et al., 2001b; Simpson et al., 2001a) associated

activation of medial prefrontal network with anxious states and deactivation with increased cognitive (attentional) demands. Similarly specific delineation has been reported in other areas of the cortex, such as temporal and parietal lobes (Simpson et al., 2001a).

2.5.6 Evaluation and summary

The anatomical delineation of the neuronal networks associated with affective disorders can be useful in the process of identifying functional vulnerability, better targeting of therapy and finally in constructing and testing a model of culprit systems. However, the terminology used throughout experimental literature is often inconsistent, with different delineation along medial-lateral (Cavada et al., 2000) and medial-orbital (Carmichael and Price, 1995) or dorsal-ventral (Mayberg et al., 1999; Phillips et al., 2003) networks. Further, the nature of innervation in these areas is not always clear from experimental papers. Unless directly indicated, the density of connections is not known and it is also unclear whether connections converge on the same target neurons (Ferry et al., 2000). Furthermore, the computational implications of either can only be speculated.

Nonetheless, there appears to be some consensus regarding separation of the prefrontal cortex into two networks, defined by anatomy and function. The first network is more closely related to cognitive function (integration of information) and is therefore closely coupled with brain regions that are related to memory (e.g. GH) and sensory inputs. By contrast, the second network is more closely coupled with limbic brain regions and subcortical areas (e.g. the ventral striatum) that are related to the processing of emotion. The networks described by Price (1999) are limited to the OMPFC, which is separated both anatomically and functionally

(Figure 2.7) into a network that is responsible for integration of somatosensory input and a network for visceral output.

It is unclear to me whether the parallel networks in the OMPFC can account for the data (i.e. abnormal cognition and mood in affective disorders). Clearly, these two networks (Figure 2.7) are closely coupled and furthermore, delineation of the prefrontal cortex along different boundaries (e.g. dorsal and ventral, relating to cognition and emotion respectively) may be more appropriate. The dorsal and ventral prefrontal networks also appear to be differentially connected to sections of the striatum (Yeterian and Pandya, 1991). The connectivity patterns reported by these authors show that medial and dorsal PFC are connected to the dorsal striatum, while inferior and orbital PFC project to the ventral striatum.

However, in view of the connectivity patterns described above, the time course of the illness in patients with HD remains a mystery. As described in section 2.5.1, the neurobiological deficit in HD originates in the dorsal striatum, however the neurospsychiatric manifestation usually precedes motor or cognitive symptoms. This pattern suggests that the interaction between the prefrontal-subcortical networks related to emotion and cognition cannot be easily teased apart (Mayberg et al., 1999). Nonetheless, I tried to highlight the inter-dependency between the OMPFC, dorsal and ventral networks, and the associated brain areas. Identifying distinct prefrontal cortical networks associated with both cognitive and emotional processing deficits is crucial, both for theoretical and analytical models.

2.5.7 Cognitive impairment

Particular neuropsychological deficits such as perseverative behaviour or thought patterns, are shared by several mood disorders. Interaction with the environment is altered by way of increased sensitivity (amplification) or lack of response to stimuli, conveying fluctuating levels of attention to external and internal events. These common behaviours contribute to the 'continuum' hypothesis (Moller, 2003), suggesting that the boundaries between MDD and bipolar disorder may be blurred and some aspects of these illnesses may have a common neurobiological substrate. Alternatively, the sequential pattern of cognitive decline, expressed by a positive correlation between illness duration and the number of clinical episodes, may be shared by several psychiatric disorders.

Decreased prefrontal cortex (and cerebellar) blood flow and glucose metabolism, were observed both in unipolar and bipolar depression (see Soares and Mann (1997), for review). Discrete impairment in the prefrontal cortex was also discerned by Videbech (1997), where a review of the MRI literature revealed that lesions (which appear as signal hyperintensities), especially in the frontal cortex and the basal ganglia, positively correlated with cognitive impairment. Veiel (1997) reported a comparable pattern of globally diffuse impairment with an emphasis on frontal deficits. Reports of neuropathology in particular parts of the brain endeavour to further classify the different patient groups, by complementing reports of the associated clinical presentation.

The concepts of helplessness and hopelessness were developed by Seligman and Beck (see below) and have been used over the years to study both human and animal behaviour (such as the learned helplessness model, see chapter 3) with respect to prognosis and altered neurotransmitter pathways. Seligman's theory of helplessness posits an absence of contingency between behaviour and outcome

leading to emotional distress, anxiety and fear and consequently progressing to helplessness and depression (Seligman, 1978). These indications point to a close coupling between cognitive deficits and disease severity. The absence of hope has also been associated with a higher risk of suicide (Beck et al., 1985). Thus, cognitive decline may suggest a higher probability of relapse.

Cognitive deficits in depression can be divided into two categories. The first examines task performance of different patient groups under discrete conditions, evaluating the correlation between perceived dysfunction and neuropathology. For example, depressed subjects are particularly vulnerable to memory deficits (Veiel, 1997; Atre-Vaidya et al., 1998; Austin et al., 1999). The second assumes an intrinsic negative perceptual tendency (cognitive bias). This tendency predisposes an individual to a higher risk of depression (possibly related to personality type). It is expressed by prevailing negative thought patterns and could play an important role both in disease aetiology and in treatment response.

To conclude, although neuropsychological impairment and abnormal cortical activation during task performance were noted, the associated neuropathology is still unclear. The increased emotionality or lability at baseline may be distinct from the neuropsychological impairment or the associated failure to activate specific regions observed in these patients. Alternatively, characteristic patterns of brain activity may predispose patients to specific damage and persist throughout remission (Phillips et al., 2003).

2.5.8 Therapeutic strategies

The efficacy of treatments that are directed at a particular mechanism or structure can corroborate its participation in aetiology and in recovery. For example, if a depressed patient shows weak activation of the PFC in the clinical phase of the illness and direct excitation of this area is followed by clinical remission, we can deduce that hypoactivity in this region is associated with the clinical phase of the illness and with treatment response. This will inspire computational investigations of the interactions of PFC with other regions and the effects of PFC hypoactivity on the behaviour of the whole network. This section will explore some of these mechanisms in MDD and bipolar disorder.

Currently the choice of treatment is guided by symptoms, yet there is no deterministic way to predict improvement or relapse and the search for the appropriate medication is predominantly a process of trial and error. Characterising mental illness by neurobiological markers (Helmuth, 2003) and behavioural expressions could provide better understanding of the impaired dynamics which may render certain individuals more vulnerable to affective illness. The next section introduces an investigative tool which may enable direct study of excitatory and inhibitory stimuli on the activity of neuronal networks.

2.5.8.1 Brain stimulation techniques

Whole brain stimulation appears to be very effective in alleviating treatment-resistant depression. Transcranial magnetic stimulation (TMS) is performed by delivering a magnetic stimulus through an external coil over the target brain area, stimulating cortical neurons to fire (George et al., 1998). Stimulation over left DLPFC was found to produce an antidepressant effect

(Pascual-Leone et al., 1996; George et al., 1997). High frequency stimulation (10-20 Hz) was found to have the most persistent antidepressant properties. This frequency is believed to facilitate neuronal firing and therefore considered to be excitatory, whereas low frequency (1-5 Hz) is thought to be inhibitory (Speer et al., 2000; Cincotta et al., 2003). TMS was also used to study connectivity patterns (see section 3.2.2) and is particularly interesting in the context of computational modelling, since hypotheses generated by models regarding the activation or deactivation of specific brain regions can be tested using this technique.

2.6 Functional segregation and functional integration

Understanding brain function has been subject to the dichotomy of functional segregation (localisation) or functional integration (Horwitz et al., 2000; Friston and Price, 2001b). It can be argued that neuroimaging methods are mostly focussed on localisation of function (or the identification of dysfunctional loci, in the case of impairment associated with brain lesions), supporting an association between specific brain regions and a particular task. However, brain areas can support (integrate) a number of different behavioural or cognitive constructs. Therefore, the idea of functional specialisation clearly cannot convey the complexity of the human brain. The notion of functional integration therefore, purporting a network or systems approach to brain function, is an essential conjunct to the localisation approach. The two approaches have a complementary role in elucidating global brain function (Horwitz et al., 2000; Friston and Price, 2001b).

2.7 Summary

This chapter introduced a number of topics related to the study and the nature of neurobiological deficits in unipolar and bipolar illness. The different strands in this chapter included a review of the neuroimaging techniques which now allow us to study brain function both in healthy subjects and in clinical populations. The latter half of the chapter highlighted putative loci of dysfunction, where structural impairments were identified in patients. Connectivity patterns of these areas, suggest that localised dysfunction may translate into functional deficits in regions that are anatomically connected to them.

Examining the dysfunctional loci from both local and global perspectives, introduced the neuroimaging-based studies (chapters 4 and 5) in the thesis. In the next chapter I describe different approaches to modelling affective disorders, which will provide the rationale and computational background to my modelling efforts (chapters 6 and 7).

Chapter 3

Modelling psychiatric disorders

Disorders of mood are unique to the human condition. Feelings of hopelessness and despair, suicidal thoughts and, above all, cognitive changes that accompany depressive or manic episodes cannot easily be modelled, since the nature of the experience is so human and subjective. However certain aspects of these disorders, such as behaviours or the neurobiology associated with these behaviours, can be represented and manipulated through animal and computer modelling paradigms. These models are useful tools to study putative links between discrete variables such as the effect of localised brain damage, social interactions or environmental factors on behaviour. This chapter will present different modelling approaches to psychiatric disorders. The term modelling will be used to discuss representation and

independent manipulation of certain aspects of the data. These are extended to the class of computational generative models, which are not limited to faithfully reproducing the main elements in the data, but also predict certain behaviours on the basis of the known factors.

First, merits and limitations of the animal modelling paradigms will be discussed (section 3.1). The following two sections focus on modelling brain activity in human subjects. I will first outline approaches that aim to represent brain activity, or the principal influences which underpin this activity, by describing various approaches that chart connectivity in neuroimaging data (section 3.2). This will be followed by a general description of the modelling paradigms that have been applied to the study of human emotion and cognition (section 3.3). Although the general aim of the thesis is to investigate both unipolar and bipolar disorders, the main focus of the experimental work in thesis is depression and its effect on brain activity in both. Therefore, the modelling (both animal and computational) approaches reviewed here will mostly be limited to the study of depression.

3.1 Animal models

Causal relationships between neuroanatomy and behaviour are difficult to ascertain in humans. The animal models allow us to investigate these links, alongside the effect of psychotrophic medication on both brain and behaviour. This paradigm is an accepted and well-established technique (more so than theoretical methods) to study brain and behavioural abnormalities in affective disorders. Activity changes associated with mood disorders, such as exploratory behaviour or memory deficits, have been observed and associated with specific neural deficits in the animal model (Richardson, 1991; O'Neil and Moore, 2003).

3.1.1 Behavioural manipulation

A number of paradigms have studied the influence of stressful life-events on subsequent behaviour that resembles depression with corresponding neurobiological and physiological changes. The following paradigms illustrate this class of models:

1. Exposure to stress (chronic or acute) at a vulnerable stage in development elicits release of high levels of cortisol. This stress-response either at a critical stage or over a prolonged period of time may cause long-term damage to the septo-hippocampal pathway (Finkelstein et al., 1985; Korte, 2001).

2. The learned helplessness model emulates certain behaviours associated with depression, such as despair and hopelessness. Deficient levels of both norepinephrine and serotonin were found both in the learned helplessness animal model (Rojas-Corrales et al., 2002) while in humans, decreased neurotransmitter levels were associated with depression, fear and anxiety (Charney, 2003). In the animal model, these deficits seemed to respond to antidepressant treatment (Giral et al., 1988).

3. Prolonged separation of a young animal from its mother may be detrimental to normal development and cause autonomic responses such as sleep disturbances and decreased body temperature. These seem to persist beyond the experimental phase (McKinney, 1984). Since these autonomic responses resemble some of the autonomic changes associated with depression, manifestation of depression in later-life has been putatively linked to developmental stress (Riso et al., 2002).

3.1.2 Hippocampal function and pharmacology

The hippocampus and its susceptibility to stress have often been associated with depressive illness in humans, both in relation to specific working-memory difficulties (MacQueen et al., 2003) and structural deficits (Shah et al., 1998) in depressed patients. Recent reports showed hippocampal neurogenesis following the administration of antidepressant medication (D'Sa and Duman, 2002; Malberg and Duman, 2003). In rats, lesions effected early in development to ventral hippocampus were more likely to cause a persistent working-memory impairment (Lipska et al., 2002).

Several pharmacological studies in the rat have affected the function of the hippocampus. Desipramine and Mianserine (antidepressant medications), as well as Transcranial Magnetic Stimulation (TMS) reduced inhibition in dentate gyrus, enhanced LTP and reduced the modulating effects of serotonin (Levkovitz et al., 2001). Markedly these changes were found in young and adult rats, but were not observed in ageing animals (Levkovitz and Segal, 2001). Further, seizure level electroconvulsive stimulation, unlike antidepressant medication, induced axonal sprouting in granule cells of the rat dentate gyrus (Lamont et al., 2001). By contrast, in an animal model of psychosis, prefrontal networks were rewired when neurogenesis in hippocampal (GABAergic granule cells) was blocked by a single dose of metamphetamine (Dawirs and Teuchert-Noodt, 2001).

Finally, the triangulation between hippocampus, behavioural reaction to stress and memory were studied in the Wistar-Kyoto rat. The cholinergic impairment in the hippocampus of this animal strain appears to make it particularly vulnerable both to stress and impair its performance on a working-memory task (the Morris water maze), compared to wild-type (Grauer and Kapon, 1993).

3.1.3 Advantages and disadvantages of the animal model approach

Extrapolating from distinctive changes in animal behaviour to the complex nature of human disorders of mood is somewhat problematic. Further, an obvious disadvantage of these models may be the difficulty in transferring information across species at different stages of phylogenetic development and different definitions of structural boundaries within cortex. First, the experience of suffering associated with depressive illness, or the cognition associated with it, may be qualitatively different in animals. I can think of no way to compare these subjective experiences. Second, the fundamental differences in cortical structure and function in rodents, primates and humans may render a dubious analogy. Third, the episodic nature of this disorder, interspersing acute illness episodes with periods of euthymia or remission, has not been modelled in animals, as far as I know.

Nonetheless, animal models allow a direct investigation of both neurobiology and behaviour, which enables the putative long-term effects of both pathology and plasticity to be studied over a shorter time-course. These models allow the study of behavioural phenomena *in vivo* and in the context of a social environment. These models, therefore, offer a number of practical advantages:

1. Variables can be controlled to a greater degree in animal models than in human clinical studies. The three most useful paradigms in animal models are lesion studies, behavioural models and pharmacological models, which in turn emphasise two contrasting approaches. Disruption to the activity of specific structures, functional networks and specific neurotransmitter pathways can be achieved by localised lesions, response to pharmacological agents, or both. For example, animal models have been used to explore the specificity of different antidepressants with reference to modification of behaviours or discrete pathways.

2. Using these paradigms, further emphasis can be placed on the behavioural implications of the neurobiology.

3. Characteristic changes in brain activity and behaviour can be measured and subsequently modified by appropriate medication.

Although an association between psychotrophic medications and symptoms may be different in humans, animal models provide invaluable clues to support the links between specific neuropathology, pharmacology and behaviour. Nevertheless moral, economical and practical issues involving experiments with animals limit this line of research.

Next, I will describe developments in the study of neuronal-networks in the human brain through neuroimaging and activation data. The common scientific question among the models that will be described here is the nature of connectivity among brain areas and the integration of different areas during and for the purpose of performing a cognitive task. Given the large volume of data, computational methods are needed to sift through the data to establish meaningful links. The modelling approach in this thesis is closely linked with connectivity studies in neuroimaging data, as well as with straightforward data analysis techniques (the segregation and integration approaches described in chapters 2 and 3). In addition to these approaches, recent endeavours in the field of computational neuroscience may build upon the connectivity and basic activation studies to explore the dynamical interactions of the areas.

3.2 Analytical models

The dominant methods to explore brain activity from a network perspective, rather than on the level of interaction between brain-regions and particular tasks, are the analysis of functional and effective connectivity (Horwitz et al., 2000). These techniques model the data in terms of representing the cardinal interactions, capturing both the relative involvement of specific nodes (brain areas) in a task, as well as interactions (connection strengths) between those nodes. The representation of features is based on numerical analysis of covariance in the data describing the pair-wise interactions in what are believed to be the constituents of the network (which may be specified *a-priori*, especially in studies of effective connectivity). This section introduces the methods used later in the experimental studies in this thesis. Hence, chapter 5 uses functional connectivity methods and chapters 6 and 7 use an effective connectivity network (McIntosh et al., 1996) as the grounding for a dynamical model.

3.2.1 Introduction

Rather than focusing on specific regions and their interaction with the task, the network modelling approach to brain imaging analysis wishes to examine the interaction *between* task-oriented regions. These models are mostly descriptive, trying to capture the relative contribution of different regions and, in the case of effective connectivity models, the influence of these regions on each other (Friston, 1994). Recent developments in this field have highlighted the need for generative models (Friston and Price, 2001a; Friston et al., 2003), to examine the effects of change either in the structure of the input or in modification of connections, on the observed response (output). This section will briefly describe different methods and

approaches to the study of connectivity, first examining the study of functional connectivity using Transcranial Magnetic Stimulation (TMS). Second, the study of regional correlations will be explored through functional and effective connectivity methods. The section will conclude by looking at a new generative-modelling framework: Dynamic Causal Modelling (DCM).

3.2.2 Transcranial Magnetic Stimulation (TMS)

Transcranial magnetic stimulation (first mentioned in section 2.5.8.1) turns magnetic pulses into electrical activity both directly under the site (brain area) where stimulation is applied, and in remote areas that are connected to it (George et al., 1998). The therapeutic properties of this method have been studied by several groups (Pascual-Leone et al., 1996; George et al., 1997; Martin et al., 2002). Recently, however, TMS has been linked with the study of connectivity, since stimulation of discrete areas of cortex appears to change the activity of distant regions that may be anatomically or functionally connected (Paus et al., 1997). Furthermore, this method rendered convincing results in the study of connectivity patterns in depressive illness (Shajahan et al., 2002). In this study, neural activity in bilateral cingulate loop and ipsilateral dorsal prefrontal loop, after one day of repetitive TMS treatment in depressed patients, was elicited by stimulation of the left DLPFC.

3.2.3 Functional connectivity

Functional connectivity methods map the temporal correlations between pairs of brain regions. However, covariance between brain regions may be coincidental since no causal links can thus be established. For example, two areas may appear to have

a functional relationship when in fact they may both receive input from a common source. Further, computing the covariance between specific Regions Of Interest (ROI) may highlight, for example, task-associated regions which may participate in activity of several independent networks. I feel that the most obvious advantages of this technique can be attributed to its exploratory nature and the absence of prior assumptions about the mechanism that produces these correlations. The absence of model specification in this analysis enables the comparison of covariance structure in different populations, which may be informative in highlighting connectivity deficits in certain groups.

The within-group covariance structure however, may be more difficult to interpret. Highly correlated areas will then be described as functionally co-active while no direct relationship has been established between them. Several limitations are associated with this approach. First, connectivity analyses make several critical assumptions, for example, the choice of the ROI (or 'seed-voxels'; the origin from which covariance is computed). Second, functional connectivity studies are descriptive in nature and do not include a specification of either an anatomical or a functional model. Third, no causal links can be established.

Further, if the delineation of ROI is based solely upon activation data, the choice of seed-voxels for analysis may be somewhat arbitrary. This may cause two further effects. First, the ROI specified in the model may not represent the activation data faithfully. Second, the data may contain latent influences that may not be represented, in the absence of a model. To circumvent the effect of task-related co-activation in neuroimaging data, Lowe et al. (1998) used signal fluctuations at rest as a measure of functional connectivity. They found strong connectivity, at rest, between left amygdala motor and visual cortices. However, the concept of rest is questionable in the conscious human brain and especially in depressed subjects,

where rumination (persistent negative thoughts) may form part of the clinical course. Therefore, describing the rest condition as the absence of task-related activity may be more appropriate.

3.2.4 Effective connectivity

Effective connectivity models have been described as "the influence that one neural system exerts over another" (Friston, 1994). Structural Equation Models (SEM; see Schumacker and Lomax (1996) for an introduction), have been widely used (McIntosh and Gonzalez-Lima, 1994; Buchel and Friston, 1997) in the study of connectivity in neuroimaging data. In this context, SEM account for the anatomical connections between areas, and use maximum likelihood methods (Wall and Li, 2003) to estimate connection strengths or path coefficients between pairs of regions. The model, signified by its strength and polarity of its paths or connections in the network, is specified describing different task-conditions. This model is either accepted or rejected depending on a measure of its goodness of fit, using regression-based methods. The nodes in the network can be modelled as a set of measured or latent variables, with residual errors associated with every latent variable that cannot be explained by the path coefficients in the model. The error terms associated with every path in the SEM are assumed to be independent of each other (www.ssicentral.com/lisrel.htm).

Effective connectivity models endeavour to capture and explain the activity of specific regions through direct (pair-wise) and indirect couplings between different regions, termed the 'neural context'. The contextual pattern of processing is essentially based on the configuration of anatomical connections between brain areas that are active during the task. The relative contribution of each area to

different task conditions is determined by the relative efficacy of connections between them (McIntosh and Gonzalez-Lima, 1994). The number of regions included in effective connectivity models is usually fairly small, and therefore the number of comparisons that needs to be corrected for, is fairly limited. An automated algorithm was suggested by Bullmore et al. (2000), using boot-strapping methods for calculating path coefficients.

Albeit useful in capturing and representing causal relationships among a number of task-related areas, effective connectivity methods (e.g. SEM) have several disadvantages. First, SEM focus on neural activity across different task-conditions, and the connectivity of the model is constrained by anatomy. Thus, the power of SEM may be limited to a small number of regions where anatomical connections ought to be well-defined (Goncalves et al., 2001). Second, SEM do not allow for the study of the direct and indirect effects of different inputs on network activity and are therefore limited in their scope as generative models (Friston et al., 2003). A modelling framework to address some of these problems has been proposed recently and will now be described.

3.2.5 Dynamic Causal Modelling

Friston et al. (2003) suggest a novel framework for studying network connectivity, by using Bayesian statistical techniques. The dynamic causal modelling (DCM) framework uses a non-linear, generative model to predict the effect of different inputs on both the activity of specific units and the connection strengths between them. This is a departure from previous models such as SEM, since experimental manipulations, or inputs, are made explicit. Furthermore, DCM allows the modelling of changes in signal over time, a concept that is not included in the SEM

framework which only models task-oriented states. Temporal or cognitive effects are modelled in the DCM framework as the stimulus-independent modification of connection strengths which indirectly changes the activity of network constituents. Conversely, the stimulus is directed at specific units (representing brain areas) in a manner that accounts for task-oriented neural activity.

Network activity in DCM (Figure 3.1) can also be elicited by external activation of specific units, such as V1. Activity then propagates throughout the network modulated by specific connectivity patterns. The connections between different units can also be modulated. This state (or activity) is determined by a set of non-linear differential equations whose parameters are constrained by priors. These equations describe the coupling between neuronal activity and haemodynamic response. The modulating effects (termed 'contextual') can therefore represent the change of efficacy in specific pathways as a function of time or cognitive factors, such as attention or learning.

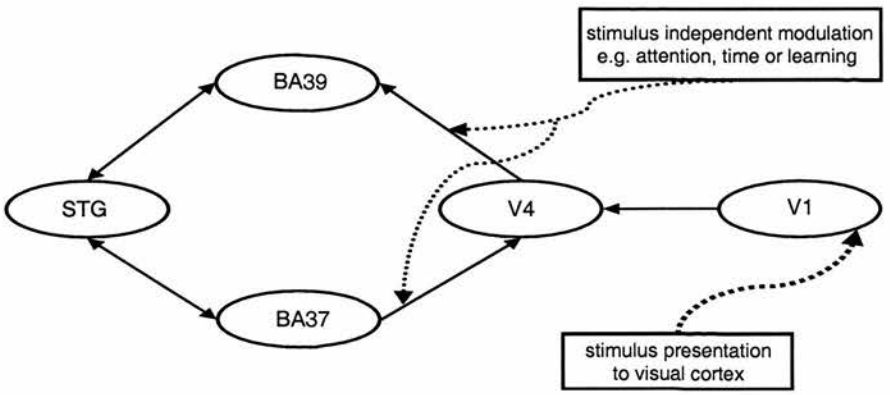

Figure 3.1: The DCM modelling framework. Visual input from an external source excites V1, which in turn activates a task-oriented loop of visual and temporal areas. Stimulus-independent input modifies the efficacy of specific connections. This type of indirect modulation provides the "neural-context" of activity in the network. The external direct and contextual (indirect) inputs are depicted as rectangles, while specific brain areas are encircled by ovals. Connections between regions are denoted by arrows. The specified modes for altering the efficacy of connections are for illustration purposes only. Modified from Friston et al. (2003).

In sum, the DCM modelling framework focuses both on the discrete effects of inputs on network activity and furthermore, it allows for external influences to modulate intrinsic activity patterns in the network. This framework has already been tested successfully on both simulated and real data. It seems to be a good successor to SEM by incorporating relevant dynamic aspects of neurophysiology.

3.2.6 Connectivity as a prelude to compensation

Chronic, repetitive and severe clinical episodes are often associated with residual cognitive impairment in euthymic unipolar and bipolar patients (Paradiso et al., 1997; Kessing, 1998; Quraishi and Frangou, 2002). However, conflicting evidence reporting no functional deficits in euthymic unipolar and bipolar patients with more pronounced deficits associated with aging (Fossati et al., 2002) may suggest either slighter neurobiological deficits in younger patients or compensatory strategies which recruit additional brain regions to prevail over age (Della-Maggiore et al., 2000) or illness associated decline.

3.2.7 Summary: studying regional-interdependence

The methods described in this section focus on studying the integration of task-associated regions into a network that accounts for experimental findings. The connectivity between regions or units in these networks can be specified *a priori*, based on anatomical data. Recent modelling efforts (Friston et al., 2003) decoupled the effect of inputs sources (directly) on the activity of specific units, from the indirect manipulation of activity through changing the value of connections (modulatory effects). The advantage of using functional connectivity methods in

that respect, may be their exploratory nature. However, the disadvantages associated with these methods are the possibility of co-activation being misinterpreted as connectivity, and the possibility that these methods may be excessively unconstrained. Conversely, the disadvantages associated with effective connectivity methods are therefore the chance of over-specification, or the inclusion of prior beliefs that may limit the model in an unrealistic manner.

The main advantages, however, of studying connectivity (both functional and effective) as a complement to using a region-specific approach, are as follows. First, the validation of task-specific neuronal networks through explaining (or even replicating) the mechanism by which task-associated neural activity can be achieved. Second, networks can be characterised in healthy subjects, allowing comparison with clinical populations. Thus, the neural basis of aberrant, task-related activity in clinical subjects may be revealed. Third, generative models can study the existing data or models using different perturbation parameters. Predictions made by the generative models, such as the modifying effects of specific inputs on areas or paths, can be subsequently tested by using methods such as TMS.

The next section will provide a brief introduction to the field of neural-network (also termed 'connectionist') modelling. Several studies have used these methods to investigate either brain function (based on neuroimaging results) or psychological phenomena in depressive illness. The studies presented in chapter 6 and 7 of the thesis are based on this modelling paradigm.

3.3 Introduction to theoretical models

Computational or theoretical models have been applied to both the study of cognitive and mental disorders. The interaction between either high or low-level factors (e.g. language deficits or molecular interactions) can be formally represented by arbitrary units. The activation of those units can thus be computed by equations describing the computation that takes place. Accordingly, this computation can be represented on a progressive scale of detail from the dynamics of ion channels to the abstract models describing brain function or social interaction (Rumelhart and McClelland, 1987). If human phenomena or data are represented faithfully in the models, they can hopefully enable the manipulation of parameters representing concepts that either cannot transcend the species barrier or alternatively, may be too complex for an *in vivo* study (e.g. cortical dynamics in the presence of an underlying pathology). Theoretical models allow us to quantify certain parameters that are suggested by previous hypotheses on a purely qualitative or descriptive basis. By reproducing a known behaviour or activity pattern, the manipulation of certain parameters and the predictions of the model could suggest further areas of research.

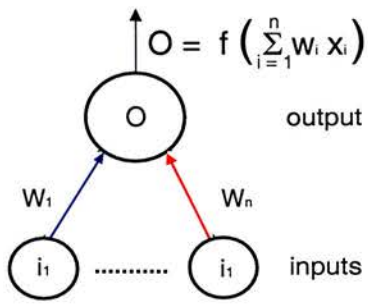

Figure 3.2: A simplified Artificial Neural Network. Activity in the input layer is modulated by connection weights and summed in the output neuron. an optional function f(X) can be used to modify the value of the output.

The activity of units in such models is computed as the summed, weighted output of the units that are connected to them (Figure 3.2). This output can be passed through a function, which assigns the internal activation of the unit to an output value. This paradigm has been used to represent neural architecture, relating the activity of a neuron (typically a firing rate) as the summed, weighted activation of other neurons. While this level of description may be an over-simplification of the neurobiological phenomena, inasmuch as neural activity can be represented as a varying input signal over time, these models have been useful in both recreating and predicting certain aspects of brain dynamics (Hertz, Krogh and Palmer, 1991).

Neural activity associated with either depression or mania cannot be easily addressed by theoretical models. These disorders appear to be both aetiologically and behaviourally heterogeneous. Furthermore, findings describing neural activity in unipolar and bipolar patients using different neuroimaging techniques such as PET and fMRI studies are divergent. Therefore, formulation of hypotheses to formally represent these abnormalities in theoretical models has been a challenging feat. Models of unipolar and bipolar depression described in the next section have mostly focused on the psychological and cognitive deficits in these disorders, often representing the activity of specific regions at a conceptual level (Siegle, 1999). I will briefly outline the theoretical framework of these models and conclude this section by discussing a biologically plausible framework which models brain activity based on PET and fMRI data. The reasoning for this ordering is based on my personal choices for theoretical modelling, since I am particularly interested in the neurobiological aspects of unipolar and bipolar illness and have therefore chosen to model activity from a neuropsychiatric perspective.

3.3.1 Prior work

There are relatively few neural-network (connectionist) models of unipolar and bipolar depression. The models are rather varied in terms of both scope and their approach to different aspects of the illness. My perspective on the behavioural and cognitive manifestations of these disorders has always been focussed on the putative links between these deficits and neurobiological abnormalities, which can be tested using different neuroimaging methods. It seems however, that most of the connectionist modelling of depression (over the last decade or so) has focused on the cognitive and emotional negative bias that has been associated with this illness. For comparison purposes and to illustrate modelling paradigms in other psychiatric disorders, I will briefly mention several neural-network models of schizophrenia and obsessive-compulsive disorder.

The architectures used to study psychiatric disorders include backpropagation (Ownby, 1998) and recurrent neural-networks (Stein and Ludik, 2000), used to model the well-defined neuropathology in obsessive-compulsive disorder (OCD) by severing specific connections or pathways that represented the effect of serotonergic and dopaminergic modulation of behaviour and of therapeutic strategies, for example. Further, perturbations describing neuropathological phenomena can be performed through severing ("overpruning") connections in a recurrent network, thus creating spurious activity patterns ("hallucinations") in models of schizophrenia (Hoffman and McGlashan, 2001). However although these models are based on neurobiological phenomena (i.e. decreased cortical connectivity in schizophrenia), the units in the models do not represent brain areas and the activity of the networks may be associated with network architecture rather than with the neurobiological phenomena they simulate. A methodological synopsis of this field has been addressed at the psychiatric community (Jeffery and Reid, 1997).

Nonetheless, few of these models appear to be closely linked to real neuroimaging studies or psychopathology in depression and bipolar disorder. This may be associated with either poorly defined (or perceived) neurobiological schema. In existing models, the behaviour of the network following different perturbations can often be associated with the architecture of the network rather than (for example) the specific brain region it is argued to represent.

Another application of neural networks in the study of psychopathology was to identify structure in large volumes of data. For example, classification of patients grouped by clinical parameters predicted their response to a specific psychotrophic medication (Franchini et al., 2001). The next section will therefore review several of the modelling paradigms that have been applied to the investigation of psychiatric disorders. I will also describe a model of neural-activity (Tagamets and Horwitz, 1998) which looked at the putative contribution of inhibition to the rCBF signal observed with PET. Although this model is unrelated to the study of clinical populations, I believe that modelling brain function in this context could provide additional tools for studying the neurobiological mechanisms underlying affective disorders.

3.3.2 Modelling cognition and emotion in Major Depressive Disorder

Human experience cannot be readily captured in the activity of artificial units in a neural-network model. Perhaps this is the reason most network models focused on the coupling between (biased) cognition and emotion in depression. However, many of the signs associated with depressed or sad mood can also have cognitive (which may be expressed through language) or motor manifestations. These include, among others, psychomotor slowing, perseveration (difficulties with performance of

cognitive tasks that require set-shifting), working-memory deficits and excessive fatigue. Further, a negative bias is classically associated with depressive cognition (Sackeim and Wegner, 1986) and associated with a higher probability of future relapse (Bouhuys et al., 1999). Hence, depressed patients are more likely to use negative words and attend to negative stimuli. They are also more likely to identify neutral faces as negative (Bouhuys et al., 1999).

Models of depression study this illness from the perspective of biased cognition; see (Siegle, 1998) for review. Nonetheless, a qualitative modelling framework such as the dorsal-ventral hypothesis (Mayberg, 1997; Mayberg et al., 1999) may render themselves to a computational investigation in due course.

3.3.2.1 The Siegle model of attentional bias in depression

A promising framework for studying interaction between cognitive and emotional biases in depression was suggested by Siegle (1999). Although these models are not based directly on brain activity as such, they are grounded in both psychological (Ingram et al., 1987) and neurobiological models (Le Doux, 1992), describing the interaction between hippocampus (cognitive stream) and amygdala (emotional stream) function in depressive illness. To implement learning, this modelling framework first used a supervised, back-propagation architecture, where the error is related back to the system; it subsequently used a Hebbian learning rule (Siegle, 1999).

Using a feed-forward mechanism, the network was required to perform a lexical decision task, with an output (signifying activity of PFC) through either semantic (cognitive; $n = 9$) or valence (emotive; $n = 3$) nodes representing the meaning of specific words that were used as input. Feedback connections between these two

processing modes (cognitive and emotive) can change the features associated with specific units. Context nodes representing attentional constructs can also provide direct excitation to either lexical or emotive nodes. The feedback mechanism between cognition and emotion until a lexical decision is made represents the temporal process of attention. Weights in the network decayed at a given rate to represent the psychological concept of forgetting and to keep the weights bound. To emulate depressive behaviour, the network was 'overtrained', i.e. the learning algorithm was implemented for longer on emotive rather than on cognitive stimuli. The results of this training regime clearly showed a bias towards negative words on which the network was overtrained and a stronger competition between recognition of those words and negative words that were not included in the overtraining regime. Therefore, this simulation predicted that depressed patients will have an attentional bias towards their internal (personally-relevant) negative representation of the emotive context of words.

Depressed patients also show an attentional bias towards mood-congruent visual images (Eizenman et al., 2003). Therefore the neural-network simulations were accompanied by physiological response data (pupil-dilation in depressed patients) suggesting that depressed patients do not attend to external stimuli and are more likely to attend to negative stimuli for longer (Siegle, 1999).

Relating these results to neuropsychological bias in depressed patients, Siegle (1999) suggests that unlike healthy individuals, depressed patients do not attend to external stimuli by processing and subsequently putting them out of their mind. Impaired attention in depressed subjects, coupled with a negative internal schema (rumination) causes patients to perpetuate the processing associated with their *internal* negative information, rather than with external stimuli.

3.3.3 Modelling cognition and emotion in bipolar illness

Neuropsychological phenomena associated with manic symptoms have been simulated by adding noise to an attractor neural-network (Hoffman et al., 2001). In this modelling framework, manic symptoms (termed "heat") perturb the activity of a recurrent neural-network. In this simulation stored 'memories' or patterns represented different orientations of the Necker cube. Each orientation (pattern) could be recalled by activation of one input unit. However, when noise was increased in the system the network rapidly switched between one recalled pattern (attractor) and another, emulating manic behaviour. These results were subsequently confirmed by a neuropsychological study with manic patients, who showed a similar reversal rate (choosing different representations of the Necker cube successively). However, it is unclear whether this behaviour can indeed be argued to represent manic symptoms, since introduction of noise to an attractor network may simply reveal behaviour that is associated with the architecture of the attractor-network. Specifically, it is unclear how the noise translated into neural activity in the brain of manic patients (although the authors suggest that elevated levels of norepinephrine during mania may be a compensatory mechanism for increased "neural noise". Alternatively, these authors suggested that a globally distributed projection from "rogue neurons" may act as noise generators in manic-spectrum disorders).

Siegle (1998) suggests that the dearth of models investigating psychological phenomena associated with bipolar illness may be associated with the scientific focus of investigation, stressing the biological basis of this illness. Therefore, he believes that modelling efforts of this illness should be grounded in and motivated by biology.

3.3.4 Modelling brain function in depression

There are few theoretical frameworks, such as DCM (section 3.2.5) investigating results from fMRI or PET studies using generative models and even fewer using a neural-network approach or studying data from neuroimaging experiments in depression or in mania. Although many conceptual models (Hoffman and McGlashan, 2001; Hoffman et al., 2001) may be related to brain activity associated with affective disorders, these studies do not model activity in brain areas as such, nor the interaction between different areas. However, a recent fMRI study (Siegle et al., 2002) confirmed predictions from previous modelling studies (summarised in Siegle, 1999) which addressed the role of the amygdala in the negative bias of information processing associated with MDD. The recent neuroimaging study thus identifed sustained amygdala activity in depressed patients (compared to healthy controls), predicted by the models (section 3.3.2.1).

3.3.5 Neural network classifiers

Neural networks can discover regularities in large datasets and thus learn to classify or associate between different items, based on the features of those items (Hertz, Krogh and Palmer, 1991). The application of these techniques to depressive studies has been mostly with reference to classification of signs and symptoms experienced by clinical populations with prediction of outcome (e.g. the therapeutic efficacy of specific pharmacological agents) (Jefferson et al., 1998; Winterer et al., 1998; Franchini et al., 2001). The architectures that have been used for classification in psychiatric literature include both supervised algorithms such as back-propagation (Franchini et al., 2001) and unsupervised algorithms, such as self-organising neural-networks (Gaetz et al., 2004).

3.3.6 Computational models based on functional imaging

Large scale, biologically realistic models of brain activity (Tagamets and Horwitz, 1998; Arbib et al., 2000) have contributed to the synthesis of neuroimaging findings with a computational neuroscience approach. These models study the global properties and activity among networks of neurons by representing brain activity at different dimensions or levels of description. The next section will describe a model which includes detail of excitation and inhibition at the neuronal level, incorporating neuronal populations to represent brain regions. Hence, the performance of the model was assessed by comparing the activity it produces both in terms of task performance and in terms of neural activity recorded by PET. Delineation of the neuronal activity that gives rise to the activation patterns in healthy subjects and subsequent perturbations of this activity may suggest either focal or progressive deficits that may be associated with neuropsychiatric abnormalities.

3.3.6.1 The Tagamets and Horwitz model of neural activity

PET and fMRI are two imaging techniques measuring brain activity at different spatio-temporal resolutions, but not at the level of single neurons or cortical columns. Quantitative data regarding transient events could be lost or misinterpreted, since the activity in these neuroimaging studies is usually averaged over time. Further, imaged data sums up synaptic events rather than neuronal firing and therefore can signify both excitatory and inhibitory synaptic activity (Horwitz et al., 2000). The role of inhibition in detected signal through different neuroimaging modalities is the subject of investigation in a model that examined both performance and neuronal dynamics in a working-memory network (Tagamets and Horwitz,

1998). In this model, both local and global excitatory and inhibitory dynamics were probed to see the effect of changing parameter values on retrieval-capacity and on the activity of the network (output). A Wilson-Cowan unit (including excitatory and inhibitory interactions within an element) represented a single cortical column (Figure 3.3) comprised of excitatory and inhibitory pairs. The connectivity patterns within the unit included feed-forward and feedback connections, with the "neural context" provided by input from outside areas. Weights (connection strengths) between the excitatory and inhibitory units, as well as excitatory feedback connections and afferent feed-forward input, were derived from anatomical data and primate studies. Regions were modelled by combining 81 basic units into 9 x 9 matrices, representing ~1 mm^2 of cortex.

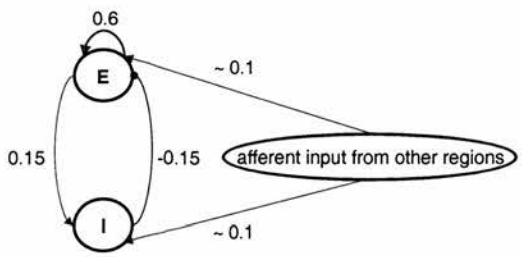

Figure 3.3: A basic unit representing a cortical column in Tagamets & Horwitz (1998) model. Excitatory (E) and inhibitory (I) populations modify each other's activity. Both can be driven by receiving afferent input from other areas varying between 0.1-0.2 in strength (Tagamets and Horwitz, 2001). The most dominant connections in this model are the recurrent excitatory connections, with an efficacy of 0.6. All connections sum up to 1 (roughly), denoting the proportional strength of every set of connections in a single unit, representing a cortical column. These proportional divisions (e.g. 60% of connections represent recurrent excitation) reflect results from anatomical studies in primates.

Using a sigmoidal activation function to limit the activity of the networks within bounds, they investigated the behaviour of the network under different parameter values and tested the effect of several modifications such as feedback vs. afferent input, excitation and inhibition on network behaviour. Finally, connectivity patterns

between different areas were explored by altering the density, spatial pattern and efficacy of connections. Task-related conditions were modelled by increasing the efficacy of feed-forward input, whereas maintenance in working-memory was expressed through increased feedback efficacy. The parameters of the model were based on PET data reporting changes in regional cerebral blood flow (rCBF) in the delayed match to sample task (Haxby et al., 1995).

The model was able to solve the delayed match to sample task by successfully retrieving simple encoded patterns after a certain delay. It emulated activation of the ventral visual path (Ungerleider and Mishkin, 1982), including visual, infero-temporal and prefrontal areas and was consistent with PET findings. In addition to the setup of regional matrices, a working-memory system (PFC) was incorporated into the model, with a weak input to one of the units representing an attended process. The model investigated several 'neural contexts', where inhibition played different roles either to dampen or enhance the signal (representing blood flow) observable by neuroimaging modalities. In this model, increased signal was expressed by summing up the *absolute* activity of the excitatory and inhibitory elements. Despite most local connections (60%) being excitatory, increased inhibition did not always decrease the overall signal. Counter-intuitively, if either local recurrent or feed-forward excitation was low (described as neural context), increased inhibition effectively enhanced the overall signal. The effect of inhibition on the network was also dependent upon the nature of inhibition. These findings highlight the potential discrepancy in the analysis of task related rCBF, where activity and excitation are not necessarily synonymous.

This modelling paradigm is to some extent conceptually challenging, because it coalesces two representational strata (both qualitative and empirical), into one architecture. In this respect, attention could be contended to engage additional

sub-cortical or limbic structures (such as the cingulate) in tandem with the prefrontal cortex and therefore the model may contain several hidden variables that remain unaccounted for. Further, it is unclear whether diffuse afferents from PFC are realistic; indeed a subsequent model (Tagamets and Horwitz, 2003) changed this prefrontal connection into discrete input. Nonetheless, I feel that basing modelling studies on neuroimaging data is a more direct approach to studying brain activity. Therefore, in chapters 6 and 7, I used a systems level model to consider the effects of impaired cortical dynamics on regional integration. Thus, local and global interactions could be studied in the context of the neurobiology of affective disorders.

3.3.7 Relative merits of theoretical vs. animal models of depression

To conclude, I suggest that computational models of depressive illness offer the following advantages and disadvantages:

3.3.7.1 Advantages

1. Theoretical models can be based on human neuroimaging data and therefore on the activity of the human brain.

2. Theoretical models can test existing descriptive models by putting them into a rigorous framework.

3. Using an empirical approach, theoretical models can guide further experimental studies. A model can suggest, for example, several competing mechanisms that can account for a specific activity pattern.

4. Computational modelling is relatively inexpensive compared to the cost of animal studies or neuroimaging experiments with human subjects. Theoretical models are in that sense similar to functional and effective connectivity models, since neither involve an additional experimental cost but rather draw on the experimental (neuroimaging) data that has already been acquired.

3.3.7.2 Disadvantages

1. The units represented in theoretical models are arbitrary, since by virtue of modelling the data, they will fail to include all the influences that are believed to be represented in the experimental data.

2. The model is often limited by the findings of the preliminary analysis, where some of the underlying activity may not have been observed or accounted for. In fMRI data analysis for example, task-independent fluctuations may have been removed as noise and are believed to be independent of the data and of each other. However, the residuals may contain valuable information that is ignored because they are not accounted for by the model.

3.3.8 Connectivity approaches and theoretical frameworks

Computational approaches bolster the qualitative descriptions based on neuroimaging experiments with a sound quantitative grounding. Both connectivity techniques and theoretical models can adopt a generative methodology to study unknown or poorly-understood factors in the wealth of findings that stem from neuroimaging experiments. By quantifying the different known factors in the data

and adopting an empirical framework, the neural activity of healthy subjects and clinical populations can be investigated. Both approaches can offer a valuable contribution, since both can accommodate and represent the data, albeit using different tools. Both approaches have the potential of addressing brain activity from a network perspective, yet also enable the investigation of the role of specific constituents within this network. One day, it may even be possible to relate the activity of this network to human behaviour and emotions.

Chapter 4

Selective attention in bipolar disorder: functional localisation of neural activity

4.1 Introduction

Cognitive impairment in patients suffering from bipolar disorder (American Psychiatric Press Association, 1994) appears to persist throughout remission, and is characterised by attention deficits and impaired performance of tasks involving executive function and working-memory. Bipolar patients are particularly vulnerable to attentional deficits (Harmer et al., 2002) which can be tested using the

Stroop task. The Stroop Colour Naming Task (Stroop, 1935) has classically been used to measure selective attention; reviewed by MacLeod (1991). A typical interpretation of this task suggests that when a conflict occurs between the meaning of words and the colour of the ink in which they are written (e.g. the word yellow, written in blue ink), subjects must inhibit automatic responses whilst attending to the stimulus. This has been described as the Stroop interference effect (Posner and Snyder, 1975), resulting in longer reaction-time for incongruous stimuli (i.e. when the colour of the ink and the meaning of the word differ) since absolute suppression of the meaning of the word cannot be achieved.

4.1.1 Impaired task performance in bipolar patients

Although there is some evidence for impaired Stroop task performance in symptomatic bipolar patients (Borkowska and Rybakowski, 2001; Clark et al., 2001), there are inconsistent findings regarding selective attentional impairments in remitted or euthymic bipolar patients. Findings from several studies indicate no impairment in euthymic bipolar patients (Paradiso et al., 1997; van Gorp et al., 1998; Cavanagh et al., 2002), while others report deficits in these patients (McGrath et al., 1997; Ferrier et al., 1999; Ali et al., 2000; Ferrier and Thompson, 2002). Bipolar patients appear to experience particular difficulties with sustained attention, even when euthymic (Clark et al., 2002). These difficulties seem unrelated to working-memory impairment (Harmer et al., 2002). Longer illness duration and increased severity of symptoms (Cavanagh et al., 2002; Cools et al., 2002) are associated with residual cognitive impairment in euthymic patients (Wilder-Willis et al., 2001).

4.1.2 Neurobiological abnormalities that may impinge on task performance

Neuropathological and structural neuroimaging studies of bipolar patients have indicated abnormalities in areas important for performance of tasks requiring selective attention. Extensive volume reductions (Lim et al., 1999), particularly in subgenual prefrontal cortex (PFC) (Drevets et al., 1998) and anterior cingulate gyrus (Hirayasu et al., 1999) have been demonstrated in bipolar patients, using both neuroimaging and histological techniques. These reductions may be attributed to decreased density of glial cells (Ongur et al., 1998), but also to a reduced number of non-pyramidal neurons in layer II of anterior cingulate gyrus (Benes et al., 2001) and reduced pyramidal cell density in layers III and V of dorsolateral prefrontal cortex (Rajkowska et al., 2001). Functional neuroimaging studies in these patients report decreased activity in similar regions, including middle, superior and inferior prefrontal cortices (Drevets et al., 1997; Sax et al., 1999; Lopez-Larson et al., 2002). Many of these dorsal and ventral prefrontal cortical regions have been associated with executive task performance (see Phillips et al. (2003) for review).

4.1.3 Delineating state-related and state-unrelated factors

Whilst a number of studies have demonstrated significantly greater functional and neuroanatomical abnormalities during executive task performance in symptomatic compared with euthymic bipolar patients (Baxter et al., 1989; Martinot et al., 1990; Blumberg et al., 2000; Ketter et al., 2001), other reports indicate additional mood-independent functional abnormalities in these patients (Blumberg et al., 2003). In the latter study, neural responses during Stroop task performance were examined in euthymic, manic and depressed bipolar patients. Decreased activity within left orbitofrontal cortex during task performance was demonstrated in all bipolar

patients compared with healthy volunteers, independent of current mood state. Further, a relative increase in activity within a different region in left ventral prefrontal cortex and a relative decrease in activity in right ventral prefrontal cortex were reported in depressed and manic bipolar patients, respectively. However, correlations of the magnitude of these abnormalities with symptom severity did not yield significant results (Blumberg et al., 2003).

Together, these findings suggest both state and trait functional neural abnormalities in bipolar patients during executive task performance. Furthermore, they suggest prevalent illness-related decreases in activity within left ventral prefrontal cortex, with specific depression-related increases in these patients. However, it remains unclear whether these functional neuroanatomic abnormalities, which may be partially related to the present mood, correlate positively with symptom severity.

4.1.4 Anxiety and performance of cognitive tasks

Several brain areas are particularly susceptible to the physiological effects of stress and anxiety. Among them are hippocampus (GH) and medial prefrontal cortex (MPFC). Damage to these regions may alter social function as well as cognitive processing. Hippocampal damage has classically been associated with prolonged or early exposure to the stress hormone cortisol causing susceptibility to depression (Brown et al., 1999; Sheline et al., 1999). However, hippocampal atrophy has also been associated with functional abnormalities in bipolar patients (Sax et al., 1999; Ali et al., 2000). Furthermore, in healthy subjects, anticipation of anxiety causes increased latency in visually evoked potentials over the temporal and pre frontal cortices, which was interpreted as increased inhibition (Gray et al., 2003). These authors also reported concomitant increased amplitude and decreased latency in the

occipital cortex, suggesting increased excitation. Higher levels of anxiety in healthy subjects were also associated with rCBF reduction in MPFC (Simpson et al., 2001a).

The MPFC is anatomically linked to the anterior cingulate (see Figure 2.7), where an anxious trait (rather than state) was linked to performance deficits and higher sensitivity to errors (Paulus et al., 2004). It is also reciprocally connected with the amygdala, which has been implicated in human response to anxiety and fear (Ninan, 1999). In children, evoked potentials in the MPFC were linked with higher levels of anxiety (Lewis and Stieben, 2004) suggesting that activity in this area can be linked with regulation of negative emotions. However, effortful control of emotion and behaviour have also been linked with the 'dorsal' prefrontal network (Phillips et al., 2003), which includes GH and dorsal anterior cingulate.

Animal studies show that MPFC lesions affect social interaction and exploratory behaviour (Gonzalez et al., 2000), yet Lacroix et al. (2000) found that lesions in this region decreased anxiety while increasing freezing behaviour. Finally, 5 weeks after medial PFC lesions were performed, elevated global levels of corticosterone were accompanied by decreased release of this hormone in response to a stressful stimulus (Rangel et al., 2003). Taken together, these findings suggest that MPFC appears to be processing social cues associated with vigilance, anxiety and fear.

4.1.5 Hypotheses

Using fMRI, we measured neural correlates of Stroop task performance in a group of euthymic and depressed bipolar patients. Subsequently, neural response in all subjects was correlated with mood and performance. The framework for studying the extent of the association between functional abnormalities in task associated

neural systems and the severity of depressive symptom bipolar disorder, was based on the following hypotheses:

1. Bipolar patients would demonstrate impaired task performance, including both an increased numbers of errors and longer reaction times (RT). In patients, RT is expected to be longer overall and especially during the incongruous Stroop condition.

2. Decreased activation in dorsolateral and ventrolateral prefrontal cortices will be associated with task performance in bipolar patients.

3. Increased activity in the left ventral PFC would be correlated positively with depression severity in bipolar patients, as implied by a similar study (Blumberg et al., 2003).

4. Anxiety will be associated with increased neural activity in the hippocampus and medial PFC in both subject groups.

In the methods and particularly in the results sections, the data will first be presented for control subjects, followed by the data for bipolar patients. The discussion however, will be focussed on the implications of these results for the study of affective disorders, situating this work into the general framework of my thesis. Therefore, the discussion section will emphasise results from the patient group.

4.1.6 Collaboration

This study was conducted in collaboration with Professor Mary Phillips, Dr Natalia Lawrence and colleagues at the Institute of Psychiatry (IOP) in London, who recruited and tested the patients, as well as acquired the neuroimaging data (sections 4.2.1-4.2.3; pages 79-81). Behavioural data (accuracy and reaction-time) were also analysed by Dr Lawrence (section 4.3.1; page 88). Some of this work has been presented previously in abstract form (Kronhaus et al., 2003; Kronhaus et al., 2004).

4.2 Methods

4.2.1 Subjects

Ten bipolar patients (six male and four female); age (given as mean ± SD): 40.9 ± 12.7 years; education: 15.7 ± 0.8 years, diagnosed with Bipolar I illness (duration: 16.8 ± 4.5 years; DSM-IV criteria, American Psychiatric Association, 1994), were recruited from the South London and Maudsley NHS Trust. Eleven healthy controls (six male and five female), matched for age (36.4 ± 10.4 years) and education (17.2 ± 2.8 years), were recruited from the local community. Bipolar patients had no major manic or depressive episodes 6 months prior to testing. All subjects completed the Beck Depression Inventory (BDI) (Beck et al., 1961), the Spielberger state anxiety scale (Spielberger et al., 1970), and the Mania Rating Scale (Young et al., 1978). The range of mania ratings scores (Young, 1978) was 2-7 in patients, indicating that no patient was in a manic phase of illness during the study. Mean BDI score was significantly higher in patients than controls (respectively, 14 ± 5.9 and 2.3 ± 2.3, $F_{(1,19)} = 37.6$, $p < 0.01$). Two bipolar patients were euthymic (BDI < 9) at the time of testing, seven patients presented with mild symptoms of depression (BDI 10-19) and one, moderate depression (BDI > 20). Our bipolar patients can therefore be described as remitted, with some suggestion of residual depression. The mean Spielberger anxiety score was also greater in patients than controls (respectively, 39 ± 11.9; 28.9 ± 7.3; $F_{(1, 16)} = 4.4$, $p = 0.05$).

All patients were medicated, receiving one or more of the following medications: Selective Serotonin Reuptake Inhibitors (SSRIs) (n = 6), atypical antipsychotics (n = 5); mood-stabilisers: lithium (n = 2), sodium valproate (n = 4), carbamazepine (n = 2) and lamotrigine (n = 1). All participants were right handed (Edinburgh Handedness Inventory; Oldfield, 1971). Exclusion criteria were as follows: a history

of head injury; illicit substance abuse, and, for healthy volunteers, a history of psychiatric illness. Ethical approval was obtained from the Ethical Committee of the South London and Maudsley Trust and the Institute of Psychiatry. All subjects gave written, informed consent.

4.2.2 Experimental paradigm

Subjects participated in a block-design Stroop paradigm (Stroop, 1935; Posner and Snyder, 1975), with five alternating blocks of incongruent Stroop and control conditions. Each Stroop block consisted of eight stimuli, with a white fixation-cross (1500 msec) against a black background preceding presentation of each Stroop stimulus (100 msec). Stroop stimuli comprised a colour word (yellow, green, red or blue) displayed in an incongruent colour (e.g. the word 'yellow' displayed in red ink). Each control block comprised eight 100 msec presentations of a row of X's of the same length as the colour words, with each stimulus preceded by a 1500 msec presentation of the white fixation-cross (1500 msec) against a black background. A blank screen (2900 msec) followed presentation of all stimuli, during which subjects' verbal responses were recorded using voice-activated software. Subjects were asked to name the colour of the ink, as quickly and accurately as possible. The experimental run lasted 6:18 minutes in total (36 s per block), discarding the first 4 volumes (18 s) due to susceptibility artefacts of the magnetic field. A compressed acquisition sequence was used (Amaro et al., 2002) to avoid acquisition of images during periods when subjects were responding. Accuracy scores were collected for all subjects, however due to technical difficulties reaction-time data from eight subjects was incomplete. Response accuracy rather than reaction-time (RT) was therefore used as the main dependent variable during task performance analysis and a subset of participants' RT data were analysed for between-group differences.

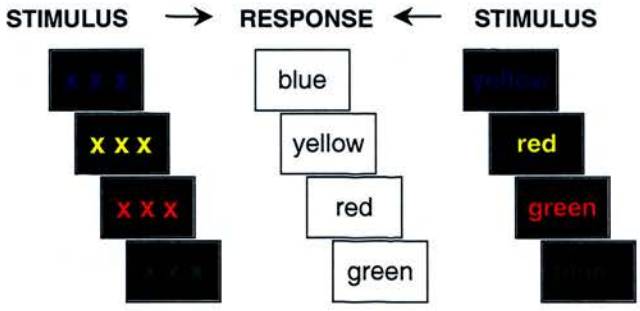

Figure 4.1: Design of the Stroop task. Either a string of X's or a word denoting colour, yet depicted in a different ink-colour, are shown in the control and Stroop conditions (task-phases) respectively. The subjects are asked to respond by naming the colour of the stimulus (which differs from the meaning of the colour word, in the incongruous Stroop condition).

4.2.3 Scanning protocol

Imaging data were acquired at the Maudsley Hospital, London, UK using a 1.5T, GE scanner (Milwaukee, WI), fitted with echo planar imaging (EPI) hardware and a quadrature birdcage headcoil for transmission and reception of the radio-frequency (RF) pulse. Both structural and functional scans were acquired during the same session.

High-resolution structural images (43 slices), providing whole brain coverage (thickness: 3 mm, inter-slice gap: 0.3 mm; planes parallel to the inter-commissural (AC-PC) line) were acquired using an inversion-recovery EPI: TE = 73 msec; TI = 180 msec; TR = 16 s; in-plane resolution = 1.72 mm; matrix size = 128 × 128 mm^2. Pixel size = 1.72 × 1.72 mm^2.

Functional images, acquired with gradient EPI pulse sequence (T2* weighted), measured BOLD response. These consisted of 80 volumes (after removing the first four scans) with 16 near-axial slices each (thickness: 7 mm; inter-slice gap: 0.7 mm:

TE = 40 msec; TR = 1.6 s; pixel size = 3.75 x 3.75 mm^2; matrix size = 64 x 64 mm^2; flip angle = 90°).

4.2.4 Single-subject and group activation maps

4.2.4.1 Basic analysis: task related neural response

Data were analysed with software developed at the Institute of Psychiatry, London, UK (Brammer et al., 1997; Bullmore et al., 1999b; Bullmore et al., 2001). Data were corrected for motion by realignment to the average scan (Bullmore et al., 1999b) Realignment to the average scan overcomes two potential pitfalls. First, it avoids the potentially disproportionate influence of an unrepresentative first scan, which may contain excessive movement or residual signal saturation. Second, the average scan integrates movement over the entire dataset. Therefore, correction parameters are likely to incorporate and correct for all movement artefacts. Linear low-frequency trends were removed using a high-pass filter, correcting for scanner drift. Finally, after spatial smoothing with a 7.2 mm Full Width Half Maximum (FWHM) Gaussian filter functional data were registered to each subject's own anatomical scan. Activation maps expressing the neural correlates of brain activation during Stroop vs. control task epochs were computed independently for each individual subject, in several steps. First, an activation model was fitted at each voxel by convolving the experimental design (on-off blocks) with two Poisson functions (with a mean of 4 and 8 seconds), representing the haemodynamic response. These functions provide a scaling factor for every model component. The least-squares fit of the weighted sum of these two convolutions at every voxel produced a goodness-of-fit statistic termed SSQ (sum of squares quotient), which expresses the ratio of the model to the sum of squares of its residuals.

$$SSQ = \frac{\sum_i (model_i)^2}{\sum_i (residuals_i)^2}$$

Model i represents the fitted time-course at the i^{th} voxel, while residual error represents subtraction of the fitted time-course (model) from the observed signal at voxel i. This operation calculates the average BOLD response over every active condition. These values are either positive or negative, a convention denoting either Stroop (on) or control (off) conditions, respectively. Following the above equation, the magnitude of the (absolute) SSQ value determines the size of the neural response relative to the residuals.

Permutation and randomisation methods are useful in controlling for nominal type I error, correcting for temporal auto-correlation (Bullmore et al., 2001; Nichols and Hayasaka, 2003). These methods preserve all non-random structure in residuals while removing the expected relationship between stimulus and response. The distribution of the SSQ statistic under the null hypothesis of no experimental effects (making no assumptions about the shape of the distribution) was computed by transformation of the time-series into the wavelet domain. The data were subsequently randomised ten times, which effectively eliminated statistical power from the experimentally related components of the residuals. We set a determinative threshold for the significance of each SSQ value further to obtaining the probability distribution for all randomised sets of SSQ ratios (Bullmore et al., 2001; Breakspear et al., 2003). Because SSQs are tested for significance using non-parametric statistics, they do not need to assume that data are normally distributed. In other respects however, they are analogous to F-statistics.

4.2.4.2 Group activation maps

The data were spatially transformed, first by rigid body registration to a high resolution structural scan for each individual subject, followed by transformation to the Talairach and Tournoux (1988) template (Brammer et al., 1997). Generic Brain Activation Maps (GBAMs) were then computed for each group, by combining median values for each randomised SSQ of every subject, at each voxel. Median values were used for computing group maps, since they are robust to the effects of individual subjects (outliers) on group maps (Brammer et al., 1997). Our group maps allowed fifty false positive voxels (number of voxels activated by chance) over the entire brain volume (21,409 voxels), representing an expected type I error rate of $p \leq 0.002$ (uncorrected).

4.2.4.3 3D cluster analysis

We extended our analysis to 3D clustering to bolster our voxel-wise GBAM findings. Cluster level inference is expected to limit the impact of the multiple-comparison problem and type I errors encountered in fMRI. Connecting contiguous voxels and extending our inference into the third dimension allowed us to include very small areas of strong activation that would not be considered significant in 2D analysis. The clustering algorithm integrates the sum of statistical mass over contiguous voxels, using the median SSQ ratios for each voxel. We estimated the probability of the occurrence of clusters by wavelet permutation of the time-series, allowing 1 false positive voxel per brain volume, which is equivalent to a cluster-wise error rate of $p = 0.001$ (Bullmore et al., 1999a). In this chapter, cluster analysis is only used for illustration purposes (Figure 4.2 and 4.3) and for between-group analysis using IOP software (see section 4.2.5.2).

4.2.5 Between group analysis

4.2.5.1 SSQ and between-group analyses

SSQ values of all the areas where significant activation was observed during group GBAM voxel analysis were noted in bipolar patients and healthy controls. To test whether these SSQ values differed between the two groups, we first calculated the mean SSQ over all voxels in the cluster, and then compared the mean SSQ between patients and controls with two-tailed t-tests. The p-values were then corrected for multiple comparisons, using the False Discovery Rate (FDR) correction procedure. These statistical tests were performed using R (www.r-project.org).

4.2.5.2 Between group ANOVA and 3D clustering

To confirm the above ROI analysis we performed an analysis of variance (ANOVA) by computing the mean SSQ values of each group at every voxel, looking for between-group differences across the whole brain volume. The null distribution of these differences was obtained by repeatedly randomising subjects' group membership and re-calculating the mean difference in SSQ values. This distribution was used to calculate the probability that these differences did not occur by chance (significance level of $p = 0.05$) and thus reject the null hypothesis of no experimental effects. Voxels that were found to be significant were clustered using procedures described above. We set the voxel-wise error rate p-value at 0.05 and the cluster-wise p-value to 0.01.

4.2.6 **Correlations with present state**

4.2.6.1 Correlations with mood and performance

Finally, we tested whether significant correlations existed between SSQ values, representing fMRI BOLD (neural) response, with several measures of mood-state and task performance. We computed correlations for task-related neural responses using Spearman's rank correlations and produced scatter plots for three sets of correlations:

1. Correlating SSQ values of all subjects at every (activated) cluster with their BDI scores (measuring depression); see section 4.2.1.

2. Correlating SSQ values with subjects' Spielberger state anxiety scores; see section 4.2.1.

3. Correlating subjects' SSQ values with measures of RT. These were calculated separately for the Stroop and control conditions. Correlations were also computed between the Stroop interference (which subtracts RT for the control condition from RT for Stroop) and neural response (SSQ value) for every cluster.

Three control subjects did not complete anxiety questionnaires and were therefore excluded from these analyses.

4.2.6.2 Interaction between medication and neural response

In bipolar patients, we also wished to examine the extent to which specific medications (i.e. lithium carbonate, antidepressants and antipsychotics) determined patterns of neural response during task performance. We therefore compared (using the Wilcoxon test) SSQ values in all clusters activated by bipolar medicated vs. unmedicated patients, with each type of medication, to test for differences.

4.3 Results

4.3.1 Task performance in patients and controls

Stroop task performance accuracy did not differ significantly between groups: Both groups performed at near-ceiling levels of accuracy (mean ± SD % accuracy for controls = 98.2 ± 2.5; for bipolar group = 98.6 ± 2.5). We retrieved RT data for six control subjects and from seven bipolar patients. In the Stroop phase, patients (RT: 865 ± 149 msec) responded slightly slower than controls (793 ± 128 msec). In the control phase, patients were also slightly slower (708 ± 140 msec) than controls (611 ± 77 msec). Repeated-measures ANOVA, with Stroop condition (control and stroop) as the repeated-measure and group (bipolar or control) as the between-groups factor, showed no overall significant difference in either group's RT ($F_{(1,11)} = 1.51$, $p = 0.245$), nor was there a group × stroop condition effect ($F_{(1,11)} = 0.48$, $p = 0.5$). There was a highly significant main effect of stroop condition on RT, however ($F_{(1,11)} = 86.18$, $p < 0.001$), revealing that RT was significantly slower in the Stroop phase relative to the control phase, confirming the traditional Stroop interference effect.

4.3.2 Group analysis: task associated neural response

4.3.2.1 Control subjects

During the Stroop condition with respect to the control condition, controls activated bilateral neural regions involved with visual processing, attention and verbal memory. The largest cluster was found in the left fusiform gyrus (BA37), with smaller clusters in left dorsolateral (BA46) and ventrolateral (BA47) prefrontal

cortices. Left precuneus (BA7), right hippocampus (Figure 4.2a) and left orbitofrontal cortex (BA 11) were also associated with the Stroop phase of the task. During the control condition relative to the Stroop condition, controls activated the right cuneus (BA19; Figure 4.2b), the right lingual gyrus (BA19) and left middle temporal gyrus (BA7; not shown) only. See Table 4.1 for coordinates and cluster size.

Cerebral Region	BA	Side	Size	Phase	Tal			Cluster
					x	y	z	number
Fusiform gyrus	37	L	10	Stroop	-30	-53	-2	44
Ventrolateral prefrontal cortex	47	L	8	Stroop	-28	40	-2	49
Hippocampus	-	R	6	Stroop	34	-35	-7	34
Dorsolateral prefrontal cortex	46	L	5	Stroop	-23	31	4	61
Orbitofrontal cortex	11	L	4	Stroop	-33	40	-18	16
Post cingulate gyrus	31	L	3	Stroop	-16	-19	42	102
Precuneus	7	L	3	Stroop	-12	-49	42	100
Lingual gyrus	19	L	3	Stroop	-18	-58	-2	45
Corpus striatum (WM)	-	L	3	Stroop	-23	31	9	69
Ventrolateral prefrontal cortex	47	L	3	Stroop	-31	42	-13	28
Posterior cingulate gyrus	31	L	3	Stroop	-13	-40	37	92
Cerebellum	-	R	3	Stroop	28	-46	-18	12
Fusiform gyrus	37	L	3	Stroop	-29	-52	-7	32
Cuneus	19	R	7	control	5	-74	31	85
Lingual gyrus	19	R	5	control	6	-56	4	52
Middle temporal gyrus	7	L	4	control	-31	-61	26	80
Cuneus	17/18	R	4	control	4	-72	20	76
Premotor cortex & SMA	8	L	3	control	-35	21	48	108
Precentral gyrus (premotor cortex)	6	R	3	control	49	2	42	103

Table 4.1: Group average of neural response for control subjects; voxel-analysis. Nineteen areas were activated during the Stroop and control conditions. Size represents cluster size (number of contiguous voxels) and Talairach coordinates (Tal x, y, z). Finally, the cluster number, which is an arbitrary assignment given by the program, is noted for reference in subsequent figures. Abbreviations include white matter (WM) and supplementary motor area (SMA).

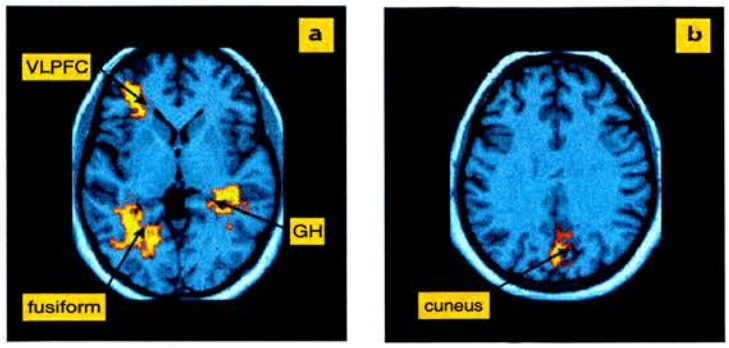

Figure 4.2: Cluster analysis of group-averaged neural activity in control subjects, to the (a) Stroop and (b) control conditions. (a) In the Stroop condition, neural response included an extensive network of areas in both hemispheres, including visual areas such as the fusiform gyrus, ventrolateral prefrontal cortex (labelled VLPFC), right hippocampus (GH) and parietal cortex (not shown). (b) The activation associated with the control condition was located mainly within right cuneus. Axial slices shown at (a) z = -2 and (b) z = 31.

4.3.2.2 Bipolar patients

During the Stroop condition, bipolar patients exhibited a unilateral pattern of activation, confined mainly to the right superior temporal gyrus (BA22) (Figure 4.3a) and right cerebellum (not shown). Deactivation associated with a control condition in bipolar patients was seen in several prefrontal regions: left medial (BA32) and left ventrolateral (BA47) prefrontal cortices, left orbitofrontal cortex (OFC; BA11), and left subgenual anterior cingulate gyrus (BA25) (Figure 4.3b), see Table 4.2 for more details. We therefore interpreted the pattern of recruitment in these left-sided prefrontal regions as a relative deactivation to the Stroop condition in bipolar patients compared with controls. See section 4.4.7 for further discussion.

Cerebral Region	BA	Side	Size	Phase	Tal			Cluster
					x	y	z	number
Cerebellum	-	R	4	Stroop	25	-35	-24	8
Superior temporal gyrus	22	R	3	Stroop	52	9	-2	35
Orbitofrontal cortex	11	L	10	control	-20	40	-13	26
Ventrolateral orefrontal cortex	47	L	8	control	-12	29	-24	10
Subgenual anterior cingulate gyrus	25	L	5	control	-3	24	-13	25
Medial frontal gyrus	32	L	5	control	-20	38	-7	30
Orbitofrontal cortex	11	L	5	control	-14	38	-29	5
Anterior cingulate gyrus	25	R	5	control	1	21	-18	19
Medial Frontal gyrus	32	L	3	control	-8	42	-7	31
Inf-post temporal lobe	37	L	3	control	-45	-62	9	43
Cerebellum	-	R	3	control	13	-47	-18	15
Meddle frontal gyrus	10	L	3	control	-24	53	9	46

Table 4.2: Group average of neural response for bipolar subjects; voxel-analysis. Twelve areas were activated in total, during the Stroop and control conditions. See Table 4.1 for conventions.

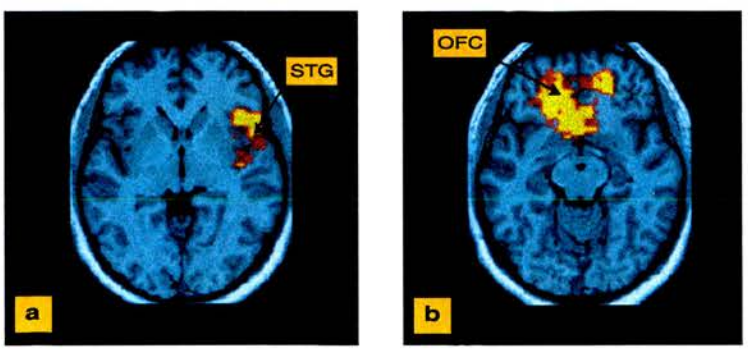

Figure 4.3: Cluster analysis of group-averaged neural activation in bipolar patients. (a) In the Stroop condition, neural responses were confined to the right superior temporal gyrus (STG). (b) During the control condition, which represents a relative decrease in neural response (deactivation) to the Stroop condition, bipolar patients show a relatively decreased neural activity in the left orbitofrontal cortex (OFC). Axial slices at (a) z = -2 and (b) z = -13.

4.3.3 Between group comparison

4.3.3.1 Comparing neural activity in both subject-groups using the two-tailed t-test

To perform between-group comparisons of task-associated neural response, SSQ values were extracted from all clusters in GBAMs (Tables 4.1 and 4.2), representing patient and control neural responses. Between-group comparisons using the two-tailed t-test were performed for each cluster, followed by corrections for multiple comparisons. Areas activated to a significantly greater extent by control subjects, compared with bipolar patients, included left-sided fusiform gyrus, dorsolateral and ventrolateral prefrontal cortices, posterior cingulate and left precuneus (Table 4.3), all increased during the Stroop condition. Conversely in bipolar patients, left-sided OFC and medial frontal gyrus (both activated during the control phase of the task) were activated to a significantly greater extent than in control subjects.

Brain area	Side	Size (voxels)	Phase	Tal x	Tal y	Tal z	BA	p-value	FDR	Cluster number
CONTROLS										
Lingual gyrus	L	3	Stroop	-18	-52	-2	19	0.0001	0.0038	45
Precuneus	L	3	Stroop	-12	-49	42	7	0.0006	0.0114	100
Ventrolateral PFC	L	8	Stroop	-28	40	-2	47	0.0019	0.0181	49
Fusiform gyrus	L	10	Stroop	-30	-53	-2	37	0.0048	0.0241	44
Posterior cingulate gyrus	L	3	Stroop	-13	-40	37	31	0.0057	0.0241	92
Dorsolateral PFC	L	5	Stroop	-23	31	4	46	0.0091	0.0280	61
Corpus striatum (WM)	L	3	Stroop	-23	31	9	-	0.0127	0.0322	69
BIPOLAR										
Orbitofrontal Cortex	L	10	control	-20	40	-13	11	0.0060	0.0454	26
Medial Frontal Gyrus	L	5	control	-20	38	-7	32	0.0068	0.0454	30

Table 4.3: Between group differences in neural response for both subject groups respectively, during the Stroop and control conditions. The p-value column depicts values of between group two-tailed t-tests (uncorrected) for each cluster; FDR depicts p-values (corrected for multiple comparisons, using FDR). Only clusters with $p < 0.05$ (corrected) are shown. Areas are ordered by significance after corrections.

4.3.3.2 Whole brain inference for between-group differences

To extend the region of interest analysis, which examined between-group differences in neural regions activated during task performance in both groups, we performed a between-group comparison, which examined between-group differences in neural response at each voxel in the whole brain. This analysis confirmed our previous findings (Table 4.1), highlighting significantly greater activation in left-sided visual areas, dorsolateral and ventrolateral PFC in controls compared with bipolar patients during the Stroop condition. By contrast, bipolar patients demonstrated significantly decreased activation during the Stroop condition compared with controls in left OFC, which was consistent with the pattern of increased activity within this region in bipolar patients during the control condition observed in the previous between-group comparison (Figure 4.4).

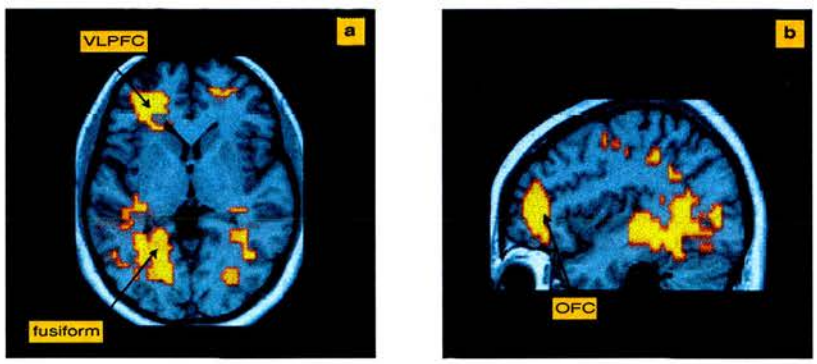

Figure 4.4: Between group differences in neural response to the Stroop and control conditions. (a) and (b) show between-group response. (b) Compared with controls, bipolar patients demonstrated significant decreases in neural response to the Stroop condition in left orbitofrontal cortex (labelled OFC). (a) By contrast, controls demonstrated significant increases in neural response to the Stroop condition in visual areas (fusiform), left dorsolateral (not shown) and ventrolateral prefrontal cortex (VLPFC). Axial and sagittal slices are shown at (a) z = -2 and (b) x = -37.

4.3.4 Task performance and clinical correlations

4.3.4.1 Associating neural activity with mood and anxiety

To further elucidate the relationship between brain activation and subjects' mood, we searched for correlations between SSQ values with clinical and behavioural measures.

Control subjects

In control subjects, there was no significant correlation between BDI scores and the magnitude of neural response within any of the regions activated by the task. There were positive correlations however, between state anxiety scores and the magnitude of neural response within the left precuneus, right hippocampus and left dorsolateral prefrontal cortex (Figure 4.5a-c), activated during the Stroop condition. There is an apparent negative correlation with the right cuneus (depicted in Figure 4.5d), which in control subjects was associated with the control phase of the task. However, assignment of a negative sign to SSQ values associated with the control condition is arbitrary (section 4.2.4.1) and therefore the relationship of correlations between neural activity and measures of mood state or performance should consider only the magnitude of neural response (*absolute* SSQ value at every cluster). This is particularly relevant to correlations with SSQ values in the bipolar group, where most of the neural activity was associated with the control condition. Hence, a negative correlation with neural response in the control condition is actually positive, whereas a negative correlation with the Stroop phase of the task is negative.

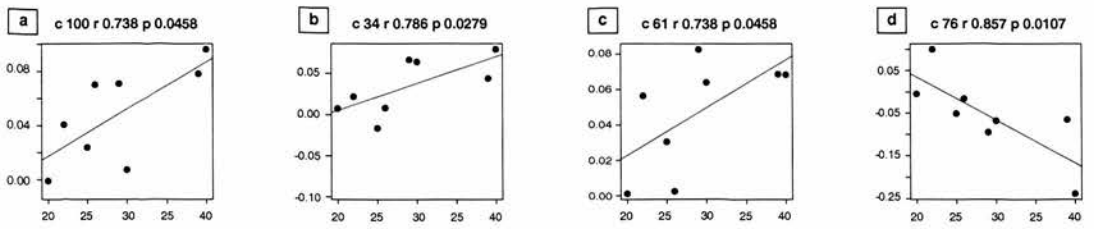

Figure 4.5: Correlations between SSQ values (shown on Y-axis) and anxiety scores (X-axis) in control subjects. (a) Clusters include left precuneus (Tal -12, -49, 42), (b) right hippocampus (Tal 34, -35, -7) and (c) left dorsolateral PFC (Tal -23, 31, 4) activated during the Stroop condition. Similarly, (d) the right cuneus, (Tal 4, -72, 20) activated during the control condition, was also *positively* correlated with anxiety. Thus, increased neural response to the control condition (denoted by negative values through convention), associated with larger anxiety scores. Cluster number (corresponding to the right-most column in Tables 4.1 and 4.2). Cluster number (c), as well as values for correlation coefficients (r) and significance (p-value; p) are noted above the plots.

Bipolar patients

In bipolar patients, two clusters were correlated with depressive mood, measured using BDI scores (Figure 4.6). First, activation of the cerebellum during the Stroop condition (Figure 4.6a) was positively correlated with BDI scores in bipolar patients. A further near-significant trend (Figure 4.6b) was found for a negative correlation (shown here as a trend for a positive correlation with negative SSQ values) between the magnitude of response within the left OFC during the control condition and BDI scores of bipolar subjects, i.e. decreased neural response with increased depression severity. When one patient outlier, whose BDI score (BDI = 1) was lower than that of the other patients (depicted in an open circle), was removed from the correlational analysis, a significant negative correlation was established between depression severity and magnitude of neural response within the OFC ($r = 0.757$; $p = 0.023$).

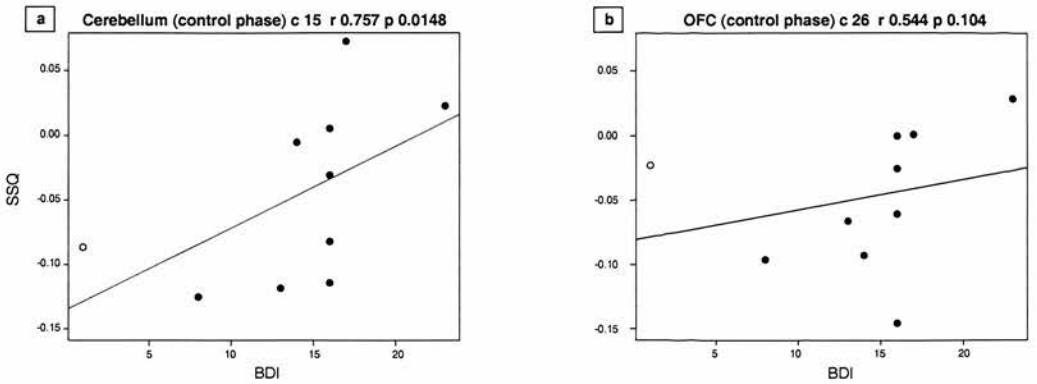

Figure 4.6: Correlation between SSQ values and depression severity (BDI scores) in bipolar patients. Between-group differences in neural response were demonstrated in (a) cerebellum (Tal 25, -35, –34) with a (b) non-significant trend in the orbitofrontal cortex. (b) This trend depicts a negative correlation between BDI and SSQ in the OFC, (Tal -20, 40, -13). The subject identified as a potential outlier is denoted by an open circle in (b). See Figure 4.5 for conventions.

The correspondence between anxiety and neural response in bipolar patients was associated with the same region in right cerebellum, which was also correlated with BDI scores. This suggests that activation of the cerebellum in bipolar patients could be associated with both anxiety and depression. By contrast however, neural response of the cerebellar cluster associated with the control condition was not correlated with anxiety.

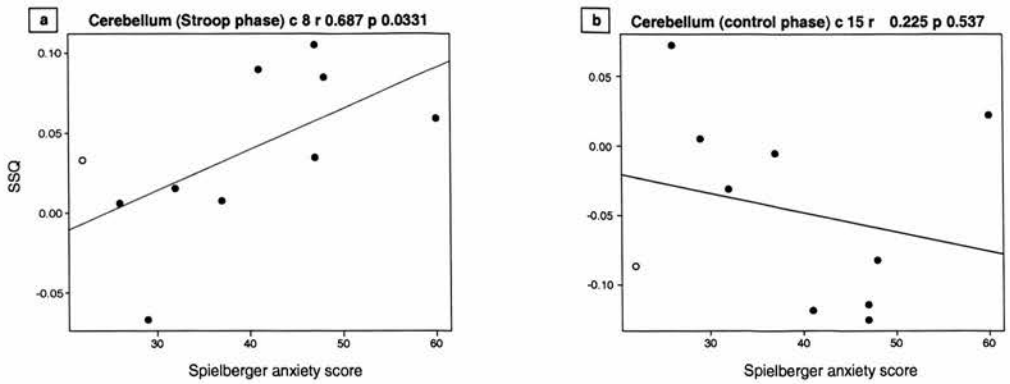

Figure 4.7: Correlations between SSQ and anxiety scores in bipolar patients. Activation of the right cerebellum (Tal 25, -35, -24) during the Stroop condition is positively correlated with anxiety, while the cerebellar cluster activated during the control condition (Tal 13, -47, -18) is not associated with anxiety. The subject identified in Figure 4.6 as an outlier (open circle), had a relatively low anxiety score (22). However, removing this subject from the correlation analysis, albeit changing the correlation values, did not make the correlation of anxiety scores with SSQ values (b) significant. See Figure 4.5 for conventions.

4.3.4.2 Associating neural activity with task performance

Given that no significant differences were noted between bipolar patients and control subjects either with respect to their response accuracy, or their RT, we did not expect to find correlations between these measures of performance and the SSQ values at each cluster, denoting neural response. Findings measuring the Stroop interference effect (the result of subtracting RT for the control condition, from RT for the Stroop condition), which was significant in both groups (see section 4.3.1), was also correlated with neural response at every cluster.

Control subjects

In control subjects, the magnitude of the Stroop interference effect was positively correlated with activation of the left lingual gyrus (Figure 4.8). Furthermore, a trend was noted between activation of right hippocampus (Tal 34, -35, -7) during the Stroop condition and anxiety scores in control subjects ($r = 0.829$; $p = 0.0583$); data not shown.

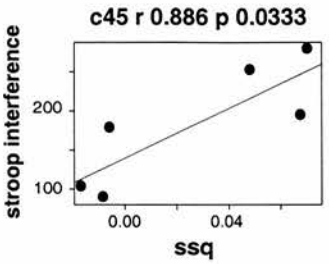

Figure 4.8: The Stroop interference effect is positively correlated with neural response in left lingual gyrus (Tal -18, -58, -2). Group: control subject; Stroop condition. The X-axis denotes SSQ values, while the Y-axis denote RT in msec.

Bipolar patients

The Stroop interference effect however, was negatively correlated with neural response in the cerebellum and in the middle frontal gyrus (Figure 4.9). Thus, a greater interference effect in both these areas was associated with diminished neural response. As described in section 4.3.4.1, a positive correlation with (negative) SSQ values for a cluster activated during the control phase of the task, is in fact negative.

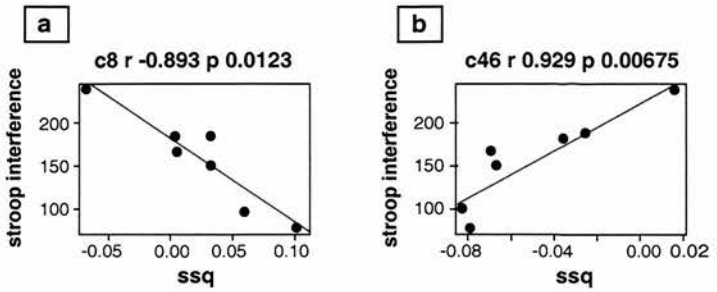

Figure 4.9: The Stroop interference effect (Y-axis, units denoted in msec) plotted against SSQ values (X-axis). This effect expresses the difference between RT during Stroop and control conditions. (a) The larger interference effect is negatively correlated with activation of the right cerebellum (Tal 25, -35, -34), which responded to the Stroop condition. (b) Correlations with left middle frontal gyrus (Tal -24, 53, 9), activated during the control condition, are also negative. Thus, diminished neural response in the middle frontal gyrus is associated with larger interference values.

4.3.4.3 Interaction between neural activity and medication status in bipolar patients

The magnitude of neural response (SSQ values) within regions showing between group significance (activated more strongly by the bipolar group, i.e. OFC and middle frontal gyrus; Table 4.3), was not affected by whether the patient was taking any type (antidepressants, antipsychotics, lithium) of medication. However, several clusters that were significantly activated by the bipolar group (Table 4.2), yet were not found to be significantly different in between group comparisons, appeared to be activated differently (significantly more or less) by medicated subjects (Table 4.4).

Region	Phase	Side	Tal			Medication type	p-value	M vs. U	Cluster
			x	y	z				
Orbitofrontal cortex	control	L	-14	38	-29	antidepressants	0.019	M < U	5
Medial frontal gyrus	control	L	-8	42	-7	antidepressants	0.0381	M < U	31
Crebellum	control	R	13	-47	-18	antidepressants	0.0667	M < U	15

Table 4.4: Significant differences in neural response between medicated (M) vs. unmedicated (U) patients. The neural response of patients receiving antidepressant medications was weaker than the neural response of unmedicated patients in left frontal cortex and right cerebellum. The table is ordered by p-value (Wilcoxon test), corrected for multiple comparisons.

4.4 Discussion

We aimed to study the relationship between current state of bipolar illness and both neural activity and performance of the Stroop task, by comparing performance of the task in remitted bipolar patients with healthy volunteers.

4.4.1 Major findings

We predicted that bipolar patients would demonstrate an abnormal pattern of neural response, predominantly within prefrontal cortex, as well as increased error rate and reaction-times in response to incongruent Stroop stimuli. Our findings indicate the following:

1. In bipolar patients a decreased response to the Stroop condition (deactivation) was noted in left ventrolateral PFC (confirming hypothesis 2 in section 4.1.5) and orbito-medial PFC (OMPFC).

2. Activation of the OMPFC showed a trend for negative correlation with depression severity (consistent with hypothesis 3).

3. Both depression and anxiety were linked with activation of the cerebellum in bipolar subjects.

4. Anxiety has been linked with increased neural response in the hippocampus (showing a near-significant trend), dorsolateral PFC, cuneus and precuneus in control subjects. This confirmed our hypothesis 4, showing a further link between anxiety and increased activation in areas involved with visual attention and in GH, which is vulnerable to stress.

5. Refuting our hypothesis 1 however, this abnormal pattern of neural response in bipolar patients emerged alongside an intact task performance, confirmed by similar response accuracy and reaction-times of subjects in both groups.

Medication may have contributed to these between-group differences in neural responses to Stroop stimuli. Our analysis revealed an association between antidepressant medication and neural response in the OMPFC and cerebellum. Nonetheless, the location of this OFC cluster (Tal -14, 38, -29) differed from the OFC cluster showing both a between-group effect (Table 4.3) and a trend for negative correlation with BDI scores (Figure 4.6b; Tal -20, 40, -13). It may be possible that these OFC activations (for example) may be related and therefore, the confounding effect of psychotrophic medications cannot be dismissed.

4.4.2 Task-associated neural response

Performance of the Stroop task is associated with a significant increase in attentional demand compared with the control task and has been demonstrated to recruit neural regions associated with attention, including dorsal regions of the anterior cingulate gyrus (Bush et al., 2000). In our study however, Stroop task-related neural response in control subjects included the fusiform gyrus, associated with visual object processing, and dorsolateral (BA46) and ventrolateral (BA47) PFC. The latter prefrontal cortical areas have been associated with cognitive task performance, including working-memory and error monitoring during reversal learning (Goldman-Rakic, 1999; Cools et al., 2002), processes which may be involved in Stroop task performance. Stroop task-related neural response in bipolar patients comprised few regions, namely right temporal gyrus and cerebellum, with relative

deactivation of left OMPFC, ventrolateral prefrontal cortex, subgenual anterior cingulate and medial frontal gyrus, since increased neural responses within these regions were demonstrated to the control compared with Stroop stimuli in the bipolar patients. Relative deactivation to Stroop stimuli was demonstrated by control subjects only within other visual processing regions, the cuneus, lingual gyrus and middle temporal gyrus.

4.4.3 The Stroop interference effect and neural activity

Significant differences between reaction times in the Stroop and control conditions confirmed the Stroop interference effect in both patients and controls. The pattern of neural response observed during the Stroop condition in controls was, however, within neural regions associated with cognitive task performance, visual attention and object processing. However activation was not observed in areas that are classically associated with the Stroop effect.

The block design nature of the Stroop task in the current study, which involved repeated performance of one task per block, may have rendered the task relatively easy for our subjects. Additionally, ample response-time was allotted for resolution of any potential conflict. Indeed, the absence of a dorsal anterior cingulate gyral response, together with the low error rate in either subject group, suggest that the task was too easy to induce activation in this area (Garavan et al., 2003). Nonetheless, previous work indicates that different versions of the Stroop task can bring about variation in neural response, depending on methodological issues (MacLeod and MacDonald, 2000; Salo et al., 2001). Therefore, the absence of cingulate activation may not be related to task performance *per se*.

4.4.4 State-related and state-unrelated neurobiological markers in bipolar disorder

Our findings indicate that bipolar patients have a relative deactivation in left OMPFC and ventrolateral PFC during the Stroop condition. Both findings are consistent with a recent report of decreased activity in left OMPFC-ventrolateral PFC in manic, depressed and euthymic bipolar patients, during Stroop task performance (Blumberg et al., 2003).

In addition to the role of the ventrolateral PFC in error monitoring during reversal learning, both orbitofrontal and ventrolateral prefrontal cortices have been linked to response inhibition based on emotional feedback (Hodgson et al., 2002) and fewer errors during the go-no-go task (Casey et al., 1997). Levesque et al. (2003) teased apart the respective roles of these areas in healthy subjects linking OFC (BA11) to increased inhibitory control and associating ventrolateral PFC (BA47) with the suppression of sadness.

4.4.5 Statistical significance and hypothesis testing

The results presented here (for example, in sections 4.3.4) were assessed at the 5% significance level, which is essentially a somewhat arbitrary assignment. With this stipulation in mind, the trend reported here (a negative correlation of OFC with BDI scores in bipolar patients and a positive correlation between hippocampal activation and Stroop RT in control subjects, reported in section 4.2.6) cannot be dismissed. These trends may in fact be more interesting than the *'significant'* correlation of anxiety with activation of the precuneus and cuneus in control subjects and (suggesting increased attention) and similarly, correlation of both BDI and anxiety with activation of the cerebellum in bipolar subjects (suggesting increased

irritability or lability). Hence, both the significant correlations and the suggested correlations (between OFC and depression in bipolar patients and between anxiety and neural response in the hippocampus of control subjects) are discussed next.

4.4.6 Correlations

Bipolar patients

Our data (section 4.3.4.1) show a negative correlation between depression severity and OFC activity during the control condition (i.e. relative deactivation during the Stroop condition), consistent with a previous report (Blumberg et al., 2003). These findings suggest that greater depression severity is associated with a "normalisation" of the functional neural abnormality in bipolar patients. It remains unclear, however, as to whether this activation is associated with improved performance on attentionally demanding tasks in depressed compared with euthymic patients. Interestingly, anxiety scores in control subjects were positively correlated with neural response in right dorsolateral PFC and left precuneus.

Control subjects

These data suggest that greater anxiety in control subjects was associated with increased recruitment of neural regions associated with attention and visual processing. These were associated with an increased evidence for the Stroop effect (section 4.3.4.2). Furthermore, activation of GH has also been putatively linked with the degree of anxiety in control subjects, suggesting that stronger activation of this area is positively correlated with longer RT in the stroop condition.

4.4.7 Two alternative hypotheses may account for the current findings

4.4.7.1 Hypothesis one: hypo-function

It may be possible, therefore, that the relative decreases in OMPFC and ventrolateral prefrontal cortical responses in bipolar patients during Stroop task performance in our study and in an earlier study (Blumberg et al., 2003) reflect a decrease in the recruitment of neural regions implicated in inhibitory control during task performance *per se*. This decrease may reflect suppression of this area during the Stroop condition, through direct inhibition from other areas. Although patients were not significantly impaired in task performance in the current study, this abnormal pattern of neural response may be associated with significant impairment in performance of tasks with greater attentional demands (see Figure 4.10).

4.4.7.2 Hypothesis two: hyper-function

An alternative interpretation of our findings in bipolar patients (Figure 4.10) is of a relative increase in OMPFC and ventrolateral prefrontal cortical activity during the control condition compared with the Stroop condition. In this case, recruitment of the OMPFC is continuous (i.e. it is excited both during Stroop and control phases of the task), however the excitation is suppressed during the Stroop condition and therefore can be detected only during the control condition. The OFC has been associated with emotion processing (Rolls, 1999) whilst increased activity in lateral OMPFC-ventrolateral PFC has been demonstrated previously to mood-congruent stimuli in depressed patients during an affective go-no-go task (Elliott et al., 2002). It is therefore possible that in the current study, relative increase in OMPFC and ventrolateral PFC activity in bipolar patients during the control condition may have reflected an illness-related, task-independent increased activity in neural regions

important for emotion, which decreased during Stroop task performance. The alternating, control-Stroop condition block design nature of the paradigm employed in the current study (Figure 4.10) renders it difficult to distinguish between these two interpretations of the data (although see chapter 8 for relevant discussion).

4.4.8 Associating depression with neural response

Our data show a negative correlation between depression severity and OFC activity during the control condition (i.e. relative deactivation during the Stroop task), consistent with a previous report (Blumberg et al., 2003). These findings suggest that greater depression severity is associated with a "normalisation" of the functional neural abnormality in bipolar patients. It remains unclear, however, as to whether this is associated with improved performance on attentionally demanding tasks in depressed compared with euthymic patients. Interestingly, anxiety scores in controls were positively correlated with neural response in right dorsolateral PFC and left precuneus. These data suggest that greater anxiety in control subjects was associated with increased recruitment of neural regions associated with attention and visual processing.

4.5 Conclusions

Patients show abnormal neural responses within regions associated with cognitive task performance during Stroop task performance, which may diminish during the depressed phase of bipolar illness. This may be interpreted as a simple measurement of hypofrontality in bipolar patients, as seen in other psychiatric populations (such as Major Depressive Disorder and Schizophrenia). However, we believe that the deactivation of the ventral prefrontal cortex in our study is more complex, since it appears to be "ameliorated" by depression and may reflect direct inhibition during the Stroop phase (see hypothesis two).

Hypothesis one implies suppression of the ventral prefrontal cortex during the Stroop phase. In depressed patients this suppression is weaker. However, even in the complete absence of suppression (e.g. for a very depressed patient) the OMPFC does not necessarily become active as might be expected from the activation we observed in control subjects. This is because we might observe different networks being recruited in the different subject groups. Under hypothesis two the OMPFC needs continuous excitation throughout the task, with additional suppression during the Stroop phase. This is in contrast to hypothesis one, where the OMPFC receives suppression only during Stroop phase. To account for data from depressed bipolar subjects, hypothesis two requires a change in the relative levels of excitation and suppression.

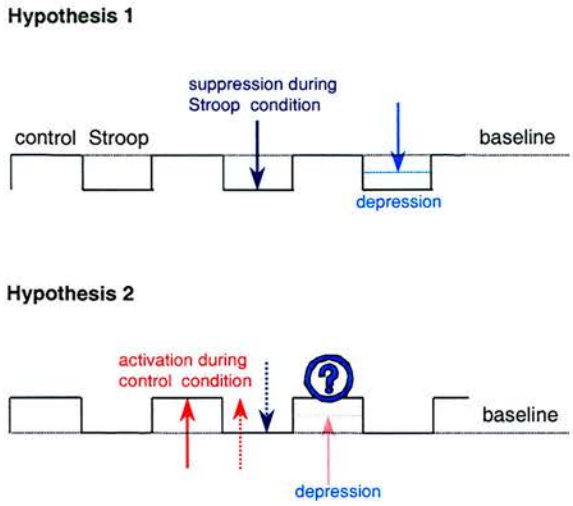

Figure 4.10: Two hypotheses accounting for neural response in the ventral PFC in bipolar patients. The diagram shows a simplified profile of neural response in three alternating control and Stroop blocks. In hypothesis 1, ventral PFC is deactivated during the Stroop condition, with depressed patients showing less deactivation (turquoise arrow). By contrast, in hypothesis 2 the ventral PFC is activated during the control condition. Here, activation during the Stroop condition may not be detectible due to concurrent suppression (dashed red and blue arrows). As above, this effect is 'dampened' (or perhaps actively suppressed by activity of other regions?), in patients who are currently depressed.

To investigate further the possible inter-regional deficits in affective disorders, chapter 5 will examine the functional connectivity in depressed patients and healthy control subjects, performing a working-memory task.

Chapter 5

Working-memory and unipolar depression

5.1 Introduction

Behavioural manifestations of neurobiological impairment can arise from either regionally specific deficits, or impaired integration of regions into a functional network (namely impaired connectivity), or both. The networks that might be of interest in the framework of this thesis are either task-related, for example a

working-memory task, or regions identified as vulnerable in the context of affective disorders. In chapter 4, we focussed on localisation function, where bipolar patients showed an altered pattern of neural recruitment. In this chapter, the aim was to investigate differences in correlations between task-associated areas and the rest of the brain in patients suffering from Major Depressive Disorder (MDD) and healthy control subjects (CTL).

Depression is often associated with a certain degree of cognitive impairment. Depressed patients, especially those suffering from melancholia (Austin et al., 1999; Rogers et al., 2004), exhibit performance deficits associated with short-term (working) memory. Both discrete impairments (such as under-activity of PFC or hippocampal atrophy) and functional interactions (slow or inappropriate recruitment of network constituents) may contribute to the observed behaviour. The N-back task has been classically used to study a parametric increase in the demands on working-memory resources. In this task, subjects are asked to recall a stimulus either directly after presentation (0-back), or a number of time steps after presentation of the target stimulus (time steps refer to presentation of subsequent stimuli). For example, a stimulus recalled 2 time steps after presentation of the target stimulus will represent a 2-back mode of recall (see section 5.2.2 for a full description of the paradigm). Thus, in this paradigm encoding and recall are done in parallel and the memory load increases parametrically as a function of delay. The fundamental issues include capacity limitations (possibly as a consequence of attentional or other deficits), either in the whole network or in specific elements. Alternatively, connections among network constituents (or even between them and other, anatomically connected but not task-related regions) could be at fault.

5.1.1 Performance and neural activity in healthy volunteers

Comparing 2- or 3-back and repetition (0-back) conditions activated prefrontal (BA46, BA9; BA6, BA8) and parietal (BA40, BA7) areas (Carlson et al., 1998), Jansma and colleagues (Jansma et al., 2000) found a large area of "load sensitive" activation in parietal cortex, whereas left primary sensorimotor cortex showed the greatest load-associated increase. Increased load sensitive activity in anterior cingulate was positively correlated with better performance. The authors suggest that recruitment of the cingulate was linked with efficient performance strategy, while a higher number of errors was negatively correlated with the size of activation of the right parietal cortex, independent of load specific effects (Jansma et al., 2000).

Nonetheless, increased working-memory load is not necessarily constrained by capacity. Impaired performance, which may relate to redistribution of resources, may be attributed to increased demands on other mechanisms such as encoding, retrieval or active maintenance of objects in working-memory. Temporal delay associated with increased load may also be a significant confounder (Honey et al., 2000).

Different patterns of activation, expressed as capacity profiles, were reported across the distributed network recruited by the N-back task. Three characteristic patterns were observed. First, an inverted U shape of activation was observed, in dorsolateral prefrontal cortex (DLPFC), but also in premotor thalamus, basal ganglia and superior parietal cortex. In these areas increased load (presumably beyond the capacity threshold) was associated with decreased neural response. The other two responses were capacity independent, including either an "all or nothing" activation pattern, which was triggered by a small load and remained constant thereafter (observed in the right inferior parietal lobule and precuneus). Alternatively,

increased load resulted in a consistent linear increase in activation (medial pericingulate; BA32) (Callicott et al., 1999).

To tease apart the effects of capacity restrictions from those of temporal delay, Honey and colleagues looked at inter-subject (n = 20 healthy volunteers) performance variability of the 2-back task. They compared reaction time across the whole group, which indicated restrictions imposed by limited resources (capacity). Prolonged reaction time, as an expression of increased difficulty, correlated with increased activity in bilateral parietal (BA40) cortex and supplementary motor area (SMA) (BA6, BA48) but not in prefrontal regions (Honey et al., 2000).

5.1.2 Delineating task-associated areas for this study

A comparative study (Casey et al., 1998), using experimental findings from four different institutions, with different scanners and analysis methods, found similar regions of activation associated with performance of the N-back task. This suggests that task-associated neural activity in specific regions is reliable and allows us to expect that activity in these regions would be manifested in this study. Specifically, connectivity of the medial prefrontal cortex (MPFC) with the rest of the brain was expected to be impaired. Studies that show consistency or reproducible activation in specific brain regions are extremely useful as a benchmark for localisation of task-related activity. Particularly in the context of the dataset used for the connectivity analysis in this chapter, the ability to set seed voxels for functional connectivity analysis based on an independent study (Casey et al., 1998) allowed me to verify that the voxels I was using were consistent with task-related neural activity in both the current study and consistent with the literature.

5.1.3 Working-memory deficits associated with depression

Depressive illness is often associated with neuropsychological abnormalities, particularly in cognitive tasks involving memory and executive function (see Zakzanis et al. (1998) for meta-analysis). The MPFC is a pertinent brain region both in terms of the N-back task (e.g. Casey et al., 1998) and in association with depressive illness (Drevets, 2000a; Wu et al., 2001). It forms connections with temporo-hippocampal regions (Suzuki and Amaral, 1994; Groenewegen et al., 1997), where changes in levels of glucocorticoid (Gartside et al., 2003) and structural deficits were associated with severity and duration of depressive illness (MacQueen et al., 2003; Shah et al., 1998). Reduction from baseline in MPFC activity was linked to cognitive processing where increased perfusion through this area was associated anxiety (Simpson et al., 2001b). In an animal model of anxiety however (Rangel et al., 2003; Shah and Treit, 2003), MPFC lesions attenuated stress-response.

Increasing task difficulty was followed by a linear augmentation in the activity of this area, associated with recruitment of the appropriate functional circuit in control subjects. By contrast, depressed patients showed decreased activity in the rostral prefrontal cortex, caudate nucleus and the anterior cingulate without the expected compensation of increased activity in DLPFC (Elliott et al., 1997). Further, regional activity in depression may be a consequence of characteristic structural and functional abnormalities or possibly, of limited capacity which may be governed by both impaired architecture and function (e.g. motivation, compensation, response to sensory input and so forth). Subjects may have a different arrangement for the dynamic allocation of resources throughout the network or reach their capacity boundaries in the absence of adaptive strategies. All these will invariably contribute to altered connectivity in patients compared to healthy controls.

Finally, the literature suggests that depression may be associated with decreased physical ability and patients may experience increased fatigue (Gold and Chrousos, 1999; Stahl, 2002). Therefore, patients were expected to express fatigue through impaired recruitment both on the global scale of neural activity as well as in decreased co-activation (impaired connectivity) of motor cortices.

5.1.4 Hypotheses and the approach taken in this study

The following hypotheses were constructed on the basis of prior literature:

1. Depressed patients will exhibit decreased connectivity as a measure of decreased activity of their prefrontal cortex (hypofrontality).

2. Depressed patients will exhibit further deficits in the covariance of structurally-vulnerable areas, such as GH (Shah et al., 1998), with the rest of the brain. Connectivity of GH with the MPFC is expected to be particularly sensitive to these structural deficits.

3. Depressed patients may experience a global dampening of neural activity across the entire cortex.

4. Depressed patients would activate task-independent regions (i.e. not prefrontal or parietal cortices) more than control subjects, in an effort to compensate for hypofrontality, for instance.

5. Depressed patients will be more affected by fatigue and would therefore show a global decline in activity, which will be associated with time.

Functional connectivity methods study the extent of correlations or covariance between specific brain areas. Correlations are normally calculated using pair-wise

comparisons between specific areas of interest (Friston, 1994); see chapter 3 for a general introduction to functional and effective connectivity analysis. This study examines the task-independent correlations between (what is assumed to be resting state fluctuations in) specific voxels of interest and the rest of the brain, comparing these correlations in healthy control subjects and in MDD patients.

5.1.5 Contributions to this project

The functional connectivity analysis in this study uses preliminary data and interim results from a larger study conducted by Dr E. J. Rose (Rose, 2004) and colleagues at Edinburgh University. Any results relating to the neuropsychological assessment and the functional localisation of neural activity therefore, are attributed to the original authors. My contribution to this project is the examination of functional connectivity or the correlation between specific areas of interest and the rest of the brain in SPM99, using the pre-processed data from a subset of subjects studied in the aforementioned study. The analysis software for the functional connectivity, consisting of batch scripts in Matlab analysis were written by Dr E. Simonotto. These scripts are documented elsewhere (Deary et al., in press). The analysis itself, including subsequent statistical inference and any remaining inaccuracies, are therefore my own. Specifically, sections 5.2.1-5.2.4 and 5.3.1 (pages 117-119 and 125), namely data acquisition and primary analysis were performed by Dr Rose et al., while all the analysis software, using methods described in sections 5.2.4 and 5.2.5 (pages 119-123) are acknowledged to Dr Simonotto. Some of this work was presented previously in abstract form (Kronhaus et al., 2002).

5.2 Methods

5.2.1 Subjects

Five patients suffering from Major Depressive Disorder (4 of them female); age (given as mean ± SE): 30.0 ± 2.82; IQ: 108.50 ± 2.56 and seven matched healthy control subjects (5 female); age: 30.3 ± 3.41; IQ: 112.86 ± 3.41, with no history of psychiatric illness took part in this study. Exclusion criteria were as follows: previous head injury; a history of drug or alcohol abuse; any serious physical illness. Additionally, patients' illness history did not include psychotic symptoms, recent changes in medication or recent electroconvulsive therapy (ECT) treatment. Prior to taking part in this experiment, all subjects completed a number of psychological tests to establish their mood and intellectual capacity (Rose et al., 2002).

5.2.2 Paradigm

Inside the fMRI scanner, subjects performed an N-Back task (Figure 5.1), testing their working-memory. In a two session parametric design, subjects were asked to recall the position of the stimulus either directly after its presentation (0 back), or after 1, 2 or 3 subsequent presentations of new stimuli. Each of the two sessions consisted of four experimental conditions (from 0- to 3-back). Instructions were read out before the start of every block. With parametric increase of difficulty, the first session progressed from 1 to 3-back, interspersed with 0-back (shadow) tasks, increasing task difficulty at every stage. Presentation order (and thus task difficulty) was reversed in the second session. Each session lasted 18:45 min.

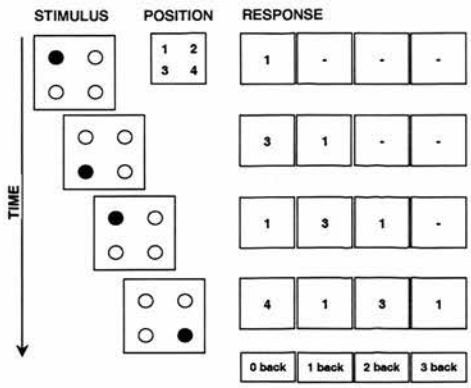

Figure 5.1: the N-back task. The squares on the left represent different stimuli (along the Y axis: progress in time). On the right, the correct response is represented, with different columns for every block. For example, the second row shows the correct response of 3 for the 0-back condition; 1 for the 1-back condition and subsequently no response for the 2 and 3-back conditions.

5.2.3 Scanning protocol

Subjects were scanned at the Western General Hospital in Edinburgh, Scotland, using a 1.5 Tesla GE Magnetic Resonance Imaging (MRI) scanner. Both T1 (anatomical) and T2* (functional) weighted images were acquired, using an EPI (Echo Planar Imaging) BOLD (Blood Oxygenation Level Dependent) sequence (see chapter two for details). For functional images, acquisition parameters included: TR (repetition time) = 2.5 sec; TE (echo time) = 40 msec; Flip angle = 90^0; FOV (Field of View) = 24×24 cm^2; with in-plane resolution (number of pixels for each scan) = 64×64 and near-axial plane orientation. Thirty contiguous slices (covering the whole brain volume) of 5 mm each were acquired using an interleaved acquisition sequence, during each TR. During each scanning session, a total of 450 scans were acquired for every subject. The first ten seconds of data from each session were discarded at the time of acquisition, due to transient inhomogeneities in transverse magnetisation.

5.2.4 Pre-processing and data analysis

Results were analysed with the Statistical Parametric Mapping (SPM99) software package, by Rose and colleagues (Rose, 2004). Functional images were reconstructed from k-space into Analyze format (http://www.mayo.edu/bir). In the pre-processing phase, data were realigned, corrected for movement, smoothed with a 6 mm FWHM Gaussian kernel and normalised to a Talairach template (Talairach and Tournoux, 1988). Temporal filtering was performed with a high pass filter cut-off period of 149 seconds and a low pass filter of 4 seconds. This removed global signal drift (that is related to the scanner rather than neural activity). These are the parameters used for the analysis of the full data set.

The General Linear Model (GLM) was used to estimate parameters and assess residual error. The design matrix consisted of fifteen regressors, one for every experimental condition (eight in total, including four instruction panels and four experimental conditions ranging from zero to three back), six regressors to account for movement (three dimensions each for translation and rotation), plus one regressor representing a constant. A simple box-car model was used, which was convolved with the haemodynamic response function (HRF, described in chapter 2) representing the temporal delay and shape of haemodynamic response following the onset of the stimulus. After the model was specified, multiple regression produced goodness of fit statistics which were assessed using multiple t-tests. Uncorrected values were corrected for multiple comparisons using Random Field Theory in SPM. Thus, functional localisation of brain activity identified significant areas of activation in the patient and the control groups separately, looking at the average effect among the specified group of subjects.

5.2.5 Functional connectivity

We wished to capture the networks that underpin different patterns of brain activity in depressed patients and control subjects during performance of the N-Back task. Further, we expected that impaired connectivity between regions that are known to be structurally-vulnerable in depressed patients contribute to the impaired activity pattern. Specifically, since MPFC and GH seem structurally impaired in unipolar patients (Shah et al., 1998; MacQueen et al., 2003) I expected that the co-activation of these regions with reference to the rest of the brain may be impaired.

In order to compute correlations between task related areas, I needed to choose a number of seed voxels, which served as anchor points for connectivity analysis. I investigated differences in connectivity between these points and the rest of the brain in depressed patients and healthy control subjects, computing both within group and between group significance tests (t-tests). For this analysis, I chose to focus on areas that were assessed by previous studies (Casey et al., 1998) to be crucially active during this task. Voxels (specified in Talairach coordinates) from this study were based on activation data from similar paradigms across four institutions. While the Talairach atlas (Talairach and Tournoux, 1988) is an accepted standard for normalisation of images, it is often criticised because it is based on a *post-mortem* analysis of one person and therefore it cannot be representative of the entire population. Therefore, many groups prefer to normalise individual scans to standard space, which is based on averaged coordinates (measuring the distance between specific points in the brain such as the anterior and posterior commissures). In SPM, the coordinates specifying the location of either neural activation or a particular between-group effect for example, are based on averaging of MRI scans from hundreds of normal, healthy subjects. The Montreal Neurological Institute (MNI) template is used to register activity of individual subjects, allowing

comparison of their neural activity in standard space. Table 5.1 displays the seed voxels (Casey et al., 1998) used for comparison of areas that were memory specific (memory vs. motor condition), in Talairach coordinates and MNI space. The transformation between Talairach and MNI coordinates was done using Matthew Brett's (www.mrc-cbu.cam.ac.uk/Imaging/Common/mnispace.shtml) non-linear transformation script in Matlab. In an exploratory analysis (where regions of interest are not specified *a priori*), I computed the covariance matrix between these eleven regions of interest and the remaining voxels in brain (throughout the task), for each subject in both groups. Using task related coordinates in structurally vulnerable areas while modelling out task effects, may allow us to discern the task-independent covariance of these areas with the rest of the brain.

The covariance matrix for voxel seeds and the rest of the brain is computed for the first session data only. Factoring out task related effects (using the design matrix described in section 5.2.4) in the pre-processed data, the cross correlation coefficients between the task-independent fluctuations (the signal that is not related to the block design of the task) were computed between seed voxels and every other voxel in the brain. Finally, the normalised data were smoothed with a 6 mm FWHM filter. Although I had access to data from both sessions, my results (see section 5.2.3) suggest that depressed patients (but not healthy controls) were showing between session differences and therefore only the first session data (rather than the mean of both sessions) was used in this analysis.

Seed	Area	Side	Talairach			MNI		
			X	Y	Z	X	Y	Z
1	Medial frontal gyrus BA 10	R	12	57	2	12	59	5
2	Superior frontal gyrus	L	-2	58	4	-2	60	7
3	Medial frontal gyrus BA 10	R	4	57	17	4	58	22
4	Precentral gyrus BA 9	R	38	25	35	38	24	39
5	Middle frontal gyrus	L	-44	16	41	-44	14	45
6	Insula	R	35	15	7	35	15	8
7	Parietal lobe, precentral gyrus BA2	R	53	-27	36	53	-30	38
8	Limbic lobe cingulate		0	-43	28	0	-46	28
9	Parietal lobe, postcentral gyrus	R	36	-46	62	36	-51	65
10	Parietal lobe	L	-24	-62	38	-24	-66	38
11	Parietal lobe	L	-15	-66	41	-15	-70	41

Table 5.1: Seed voxels used for functional connectivity analysis. Coordinates were taken from the Casey et al. (1998) comparative study. Side describes Left (L) or Right (R) hemispheres; Talairach coordinates from the paper were then translated to MNI coordinates to conform with SPM standards. Seed 8 (the cingulate) is not reported to be in the left nor right hemisphere, since the X coordinate is 0, indicating a midline voxel.

After correlation coefficients were computed separately for each subject for the eleven seed voxels (Table 5.1), cross correlation coefficients (from the covariance matrix of every subject) were normalised, since the activation data and likewise the residuals of all subjects were not expected to be normally distributed. Thus, applying the method proposed by Lowe et al. (1998), we corrected for inter-subject variability in the distribution of the cross correlations in functional connectivity maps, using Fisher's r to z (equation 5.1) transform followed by steps to normalise (mean = 0; SD = 1) the cumulative distribution of the cross-correlation coefficients. This operation allows us to make inferences about the sampling distribution from which correlation coefficients (ρ) are drawn (treating every subject as an independent sample). We can then make inferences about the relative distribution of individuals' score by transforming ρ values into Z space.

$$Z(\rho) = 0.5 \ln [(1 + \rho) / (1 - \rho)] \quad (5.1)$$

Subsequently, I assessed within and between group differences. First, a t-test evaluated within-group significant activity with stringent voxel-wise significance levels ($p_v \leq 0.001$; uncorrected) in SPM (see section 5.2.7). These were done separately for the first session data and for data derived from the difference between the first and the second session. Second, an Analysis of Variance procedure (ANOVA) tested for significance of between-group mean values in the first session transformed correlations.

5.2.6 Localisation of correlated areas

Using a Matlab script to translate the MNI coordinates into Talairach space, I subsequently used an online database server, the Talairach daemon (http://ric.uthscsa.edu/projects/talairachdaemon.html), to retrieve information about the location of the specific coordinates. I chose to include in tables 5.2-5.6 areas that may have been identified as borderline white matter (WM) for two reasons. First, the data has been extensively smoothed during analysis and therefore if the cluster is within a few mm of a structure, the signal may have originated from grey rather than white matter. Second, the coordinates shown in these Tables represent the voxel with the highest intensity within a cluster that may be composed of many contiguous voxels. Especially if clusters are large, at least some of their constituent voxels may indeed be located within the brain areas indicated in the tables.

5.2.7 Clustering and threshold levels in SPM

In accordance with the methods suggested in SPM, I did not correct for multiple comparisons at the voxel level, but instead used a stringent p-value threshold (p_v) of 0.001 (Z score of 3.09). Connected voxels were then grouped into clusters, using the default clustering from SPM. Clusters were tested for significance at the (p_c) 0.05 level after p-values were corrected for the entire volume (SPM). The results presented here, including Tables 5.2-5.6 and Figures 5.3, 5.4, 5.6b and 5.7a-b depict only significant activations ($p_c \leq 0.05$; i.e. the probability of finding a cluster this size, corrected for multiple comparisons in the entire search volume).

5.2.8 Computing caveat

Due to technical problems with SPM, only 4 out of the 5 available cross-correlation maps for the patient group could be used at any one time to compute within-group comparisons. I therefore tested all possible configurations of 4 subjects, to ensure that the results were replicable in at least 3 subgroups of 4. This was not a problem either for the control group (where all 7 maps could be used) or for the between-group computation, where 5 depressed patients' and 7 controls' cross-correlation maps were used. Evidently, these are small numbers of subjects and inferences should be made with great caution. However, taking stringent significance criteria, correcting for multiple comparisons and above all, formulating prior hypotheses about the structure of the data, may render these results more convincing.

5.3 Results

In order to substantiate the use of results from Casey et al. (1998) to specify the seed voxels (the origin) for computing the covariance matrix in the functional connectivity analysis, I needed to establish that task-related activation was concordant with this study. The seeds in table 5.1 were all present in the task-related activity maps (Figure 5.2). Hence these seeds were assumed to be valid for this study. Once I established that these areas were indeed active in both groups, I could proceed to factor out the task-associated signal and compute the correlation coefficients using only residual activity in the seed voxels, covaried with the whole brain. Figure 5.2 (Kronhaus et al., 2002) is based on previous analysis (Rose et al., 2002) and illustrates brain activity in the dataset used for functional connectivity analysis in this study.

5.3.1 Functional localisation

Patients and controls appear to activate a similar network of areas. However, there are several distinct differences between the two groups. Co-localisation of brain activity during task performance in both groups is suggested by the overlap of functional activation maps in Figure 5.2. Nonetheless, whereas parametric increase in task difficulty in both groups produces almost identical maps (with slight differences in the extent and p-value of activated clusters; Figure 5.2a), patients' deactivation of task related regions, as a function of time and increased difficulty, is significantly diminished (Figure 5.2b). This pattern suggests an overused system, where recruitment of the appropriate circuit of brain regions endures beyond what appears to be necessary for task performance.

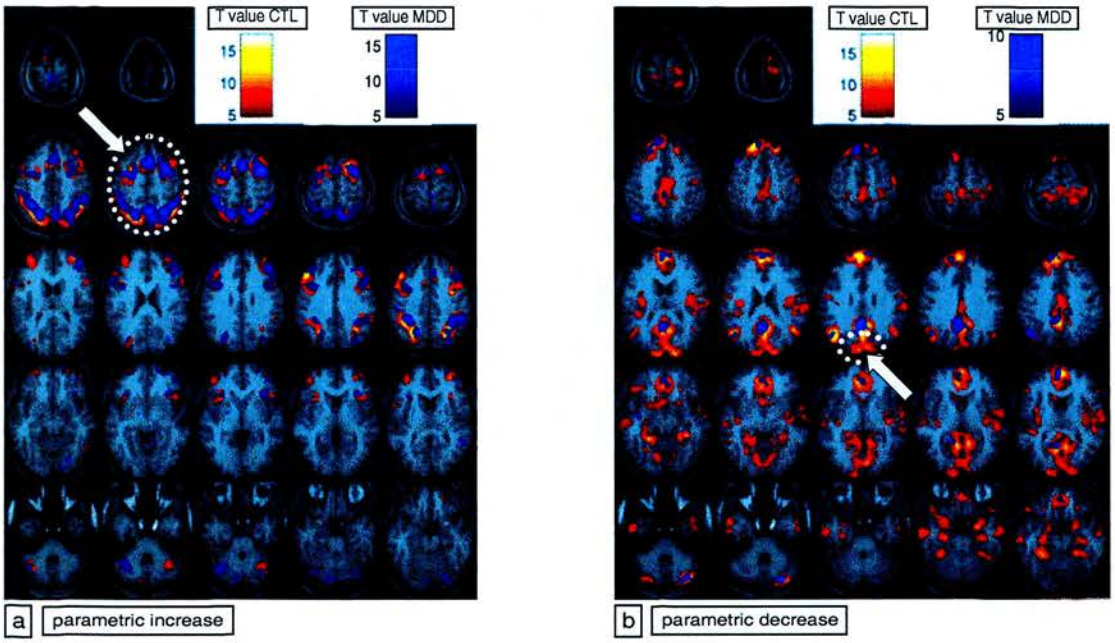

Figure 5.2: Parametric increase (a) and decrease (b) of brain activity as a function of task difficulty. Both plots show MDD (N = 5) activation (blue) superimposed on CTL (N = 7) activation (yellow-red). The areas showing task related activation include prefrontal, parietal and temporal areas, as well as occipital lobe and cerebellum. In MDD, the cluster size of the activated regions appears to be smaller than analogous measurements in control subjects. Coloured bars at the top of the plots depict the subject groups' respective T values. The white arrow in (a) points to prefrontal and parietal activation in both CTL and MDD, suggesting that both groups activate brain areas that are consistent with the literature and thereby justify the use of activation from a different study (Casey et al., 1998) as seed voxels in the functional connectivity analysis. The arrow in (b) points to occipital areas that in patients, unlike controls, do not show the expected decrease in neural activity that is associated with increased task difficulty (see section 5.3.2.2 for further discussion).

The task-related brain activity in patients, although qualitatively similar to control subjects, appears to be limited both in extent and significance (p-value). These differences allow us to form stronger hypotheses regarding the expected differences in functional connectivity between patients and control groups.

5.3.2 Functional connectivity

The vast number of brain voxels result in a considerable multiple comparisons problem. In this functional connectivity study, I chose to use SPM default values (which use a fairly stringent threshold at $p_v \leq 0.001$), performing both within and between group, one or two sample t-tests. These tests compare normalised correlation values using either group mean values (correlation values taken at every voxel, for every subject within each group) or the mean of each group against the null-hypothesis of no effects (correlation = 0). Therefore, particularly in the case of within group comparisons, I do not wish to make any claims regarding the exact location of the areas where either positive or negative correlations were noted with specific seed voxels. Nonetheless, I noted clear differences in the within-group analysis between connectivity profiles in patient and control groups. Therefore, the next section will illustrate within group comparisons of connectivity maps for two typical seed voxels, seed 7 (parietal cortex) and seed 8 (cingulate), for both groups, highlighting qualitative differences in their respective group activation profiles.

5.3.2.1 Within group analysis

Seed voxels 7 and 8 were chosen to represent the typical profile of within-group t-tests because these were two voxels where the between-group comparison showed significant results at the 0.001 threshold (p_v) level (see below: between group differences) with stronger connectivity for patients in seed voxel 7 and for controls in seed voxel 8. Tables 5.2-5.5 illustrate the connectivity values (normalised correlation coefficients), obtained for clusters over the whole brain volume with the seed voxel, based on within group t-tests.

Patients are comparable to control subjects in the specific areas that appear to be either positively (depicted in black in the tables) or negatively (depicted in red) correlated with specific seed voxels. However, when either the mean cluster size or the total number of correlated voxels (with each seed) are compared between patients and controls, a distinct hypo-function is illustrated by patients (Figure 5.3). For example, in the patients' correlation map for seed 7, mean cluster size (± standard deviation) for areas that are positively correlated with the parietal cortex is 32.13 (± 24.49) and the total number of voxels in all clusters is 257. By contrast, the control subjects' correlation map for seed voxel 7 shows a mean cluster size of 459.18 (± 751.61) subsuming a total of 5051 voxels. Tables 5.2- 5.3 show data for seed 7 for patients and controls respectively; Tables 5.4 – 5.5 show patients' and controls' data for seed 8.

MDD: significant correlations with seed 7

Brain region	side	MNI			Talairach			T	size	Z (r)	
		x	y	z	x	y	z			mean	SD
Cingulate	L	-12	12	32	-12	13	29	100.74	17	1.14	0.02
Middle frontal gyrus BA9	R	32	22	40	32	23	36	67.15	90	4.14	0.12
Frontal lobe (WM)	L	-8	32	40	-8	33	35	39.35	40	1.69	0.09
Superior frontal gyrus BA9	R	18	52	36	18	52	31	28.86	25	1.04	0.07
Frontal lobe	R	44	50	-6	44	48	-7	24.65	24	1.34	0.11
Superior frontal gyrus BA10	R	24	60	18	24	59	14	22.73	24	1.17	0.10
WM	L	-32	8	-8	-32	7	-7	19.47	20	0.64	0.07
Insula (WM)	L	-38	22	32	-38	23	28	16.61	17	1.99	0.24
Occipital lobe, precuneus	L	-16	-64	16	-16	-61	18	312.24	12	-1.13	0.01
Superior temporal gyrus	L	-58	-4	2	-57	-4	2	56.49	35	-0.71	0.03
Cerebellum	-	0	-70	-44	0	-70	-34	55.75	21	-0.76	0.03
Temporal lobe (WM)	L	-26	-50	16	-26	-48	17	36.84	14	-0.62	0.03
Anterior cingulate BA25	L	-2	2	-10	-2	2	-8	36.53	27	-0.85	0.05
Temporal lobe (WM)	L	-36	0	-34	-36	-1	-29	29.71	16	-0.73	0.05
Parietal lobe, postcentral gyrus	R	64	-20	14	63	-19	14	25.19	26	-0.83	0.07
Inferior parietal lobe, BA 40	L	-64	-38	22	-63	-36	22	23.62	30	-0.86	0.07
Superior temporal gyrus BA 42	R	64	-34	20	63	-32	20	20.96	24	-0.96	0.09
Supramarginal gyrus BA 40	L	-58	-48	28	-57	-45	28	19.42	11	-0.74	0.08
Superior temporal gyrus (WM)	L	-66	-38	6	-65	-37	7	16.16	14	-0.77	0.10

Table 5.2: Within group significant correlations with seed 7 (parietal lobe) in MDD group. Areas are listed in order of decreasing T value (i.e. more significant clusters appear first). Positive correlations are depicted in black, negative correlations in red. SPM output shown in column MNI, illustrating x, y, z coordinates for clusters that are positively (or negatively) correlated with seed 7. These coordinates are transformed to the Talairach space using a non-linear transformation, depicted in the Talairach column and translated into discrete brain areas using the Talairach daemon (see methods). The T column denotes a t-statistic and finally, cluster size (in voxels) and the mean and standard deviation (SD) of normalised correlation values for each subject are depicted in the columns size and distribution, respectively. Mean cluster size: positive = 32.13 (40.75 right hemisphere (RH); 23.5 LH)/ negative = 20.91 (25 RH; 19.88 LH); Total voxels: positive = 257 (94 LH) / negative = 230 (159 LH). The midline clusters, which are neither in the right nor in the left hemispheres (e.g. cerebellum, among the negatively correlated clusters in red ink) were not included in calculations of mean cluster size for RH / LH.

CTL: significant correlations with seed 7

Brain region	side	MNI			Talairach			T	size	Z (r)	
		x	y	z	x	y	z			mean	SD
Frontal lobe (WM)	L	-34	22	26	-34	23	23	32.68	446	1.11	0.09
Frontal lobe (WM)	R	42	10	46	42	12	42	32.05	2654	2.07	0.17
Medial frontal gyrus BA8	L	-10	30	46	-10	31	41	17.13	125	1.04	0.16
Parietal lobe, postcentral gyrus BA1	R	60	-28	42	59	-25	40	14.54	515	0.68	0.12
Frontal lobe (WM)	L	-12	16	60	-12	18	54	13.99	124	1.04	0.20
Frontal lobe, precentral gyrus BA9	L	-36	10	38	-36	11	34	10.84	213	1.20	0.29
Inferior parietal lobule BA 40	R	46	-58	54	46	-54	52	9.85	582	1.22	0.33
Inferior frontal gyrus BA13	R	44	22	10	44	22	8	8.59	76	0.85	0.26
Superior parietal lobule BA7	L	-34	-56	52	-34	-52	50	7.91	171	1.50	0.50
Inferior parietal lobule (WM)	L	-50	-40	48	-49	-37	46	7.49	73	1.44	0.51
Superior frontal gyrus BA6	R	12	6	64	12	9	59	6.53	72	1.05	0.43
Hippocampus	L	-26	-40	-8	-26	-39	-5	30.66	1271	-0.78	0.07
Middle temporal gyrus (WM)	L	-50	-20	-6	-49	-20	-4	24.09	74	-0.67	0.07
Parahippocampal gyrus BA36	L	-26	-28	-20	-26	-28	-15	21.94	177	-1.14	0.14
Inferiior temporal gyrus (WM)	R	46	-6	-34	46	-7	-28	21.16	902	-0.87	0.11
Parietal lobe, postcentral gyrus BA3	L	-18	-42	72	-18	-37	68	19.1	79	-0.85	0.12
Middle occipital gyrus (WM)	L	-18	-100	12	-18	-96	16	19.08	594	-0.77	0.11
Inferior frontal gyrus BA47	L	-26	14	-24	-26	13	-21	14.93	126	-0.88	0.16
Occipital lobe	L	-16	-88	-14	-16	-86	-7	14.31	342	-1.06	0.20
Insula	R	42	-14	14	42	-13	14	13.65	440	-0.77	0.15
Temporal lobe	L	-40	0	-48	-40	-2	-40	13.09	229	-0.66	0.13

Table 5.3: Within group significant correlations with seed 7 (parietal lobe) in CTL group. Mean cluster size positive = 459.18 (779.8 RH; 192 LH) / negative = 423.4 (671 RH; 361.5 LH); Total voxels: positive = 5,051 (1,152 LH) / negative = 4,234 (2,892 LH). See table 5.2 for conventions.

MDD: significant correlations with seed 8

Brain region	side	MNI			Talairach			T	size	Z (r)	
		x	y	z	x	y	z			mean	SD
Frontal lobe	L	-10	42	-22	-10	40	-20	172.48	16	0.60	0.01
Frontal lobe	R	46	38	28	46	38	24	73.23	33	1.32	0.04
Frontal lobe	L	-44	12	36	-44	13	32	57.07	231	3.69	0.13
Medial frontal gyrus BA8	L	-10	30	46	-10	31	41	53.25	12	1.15	0.04
Putamen	L	-18	8	8	-18	8	7	48.55	13	0.72	0.03
Putamen	R	18	4	10	18	4	9	31.7	24	0.98	0.06
Temporal lobe	L	-44	-16	-10	-44	-16	-8	146.12	30	-1.06	0.01
Superior temporal gyrus (WM)	L	-50	-24	-4	-49	-23	-2	38.48	12	-0.66	0.03
Parietal lobe, postcentral gyrus BA2	R	36	-42	62	36	-38	59	28.52	25	-0.49	0.03
Parietal lobe (WM)	R	12	-48	62	12	-44	59	26.33	12	-0.64	0.05
Temporal lobe	L	-42	-52	10	-42	-50	12	26.11	19	-0.99	0.08
WM	R	40	-40	-6	40	-39	-3	20.74	13	-0.78	0.08

Table 5.4: Within group significant correlations with seed 8 (cingulate) in MDD group. Mean cluster size: positive = 54.83 (28.5 RH; 68 LH)/ negative = 18.5 (16.67 RH; 20.33 LH); Total voxels: positive = 329 (272 LH) / negative = 111 (61 LH). See table 5.2 for conventions.

CTL: significant correlations with seed 8

Brain region	side	MNI			Talairach			T	size	Z (r)	
		x	y	z	x	y	z			mean	SD
Parietal lobe, precuneus BA7	-	0	-64	48	0	-60	47	27.55	364	1.57	0.15
Frontal lobe	R	18	62	16	18	61	12	21.33	265	1.31	0.16
Caudate	L	-14	4	12	-14	4	11	21.18	348	1.42	0.18
Parietal lobe	R	46	-54	56	46	-50	54	17.47	706	1.23	0.19
Occipital lobe	L	-26	-86	38	-26	-82	39	17.15	904	0.87	0.13
Middle frontal gyrus BA9	R	56	16	34	55	17	30	15.75	1013	1.39	0.23
Inferior frontal gyrus (WM)	L	-48	38	12	-48	37	9	15.02	427	1.03	0.18
WM (~striatum)	R	14	4	8	14	4	7	14.54	277	1.02	0.19
Middle frontal gyrus	R	46	48	-12	46	46	-12	11.23	251	1.03	0.24
Inferior temporal gyrus BA37	R	60	-54	-12	59	-53	-7	10.1	194	1.25	0.33
Frontal lobe	L	-38	26	32	-38	27	28	9.36	853	2.08	0.59
Medial frontal gyrus BA8	R	2	24	50	2	26	45	7.53	413	3.48	1.13
Superior frontal gyrus BA6	L	-24	12	66	-24	15	60	7.53	77	1.41	0.50
Insula	R	34	2	18	34	3	16	16.75	91	-0.84	0.13
Insula	R	44	-16	0	44	-16	1	11.67	187	-0.82	0.19
Superior temporal gyrus BA22	R	16	-28	62	16	-24	58	8.7	92	-0.41	0.12
Temporal lobe (WM)	R	42	-14	-22	42	-14	-18	7.88	74	-0.77	0.26

Table 5.5: Within group significant correlations with seed 8 (cingulate) in CTL group. Number of clusters: positive = 13 (5 LH) / negative = 4 (0 LH); Mean cluster size: positive = 468.62 (445.57 R; 521.8 LH)/ negative = 111 (all RH); Total voxels: positive = 6,092 (2,609 LH) / negative = 444 (0 LH). See table 5.2 for conventions.

Summary of within group analysis

Within group significant correlation suggests significant differences in the extent of correlations across the whole brain between patients and control subjects. Tables 5.2-5.5 show within group positive and negative correlations with respect to the parietal lobe (seed voxel seven) and the cingulate (seed voxel 8), in the two subject groups. Clearly, comparing the number of clusters in these tables in control subjects and in patients is not sufficient to indicate significant differences between patients and controls. However, the number of activated voxels suggests that the degree of correlation across the brain is larger by several orders of magnitude in control subjects (Figure 5.3). Furthermore, it appears that in control subjects similar areas in

frontal and parietal cortex are correlated both with parietal lobe (Figure 5.3a) and the cingulate (Figure 5.3b).

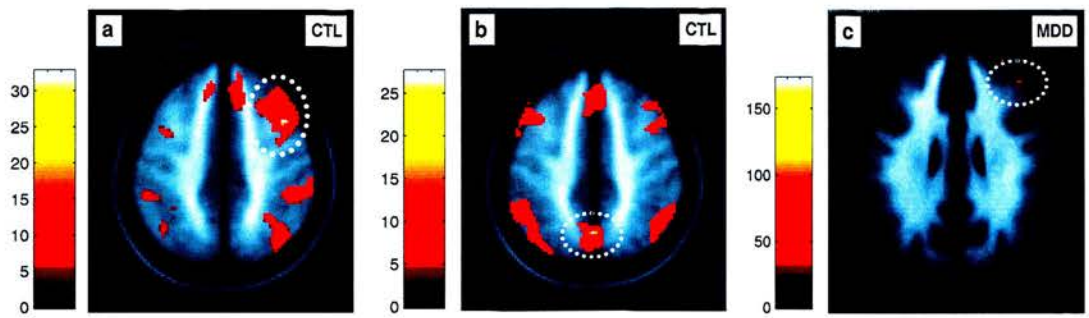

Figure 5.3: Within group task-independent positive correlations. (a) and (b) show significant areas that were correlated with seed 7 (parietal lobe) and seed 8 (cingulate), respectively. (c) Correlations within the MDD group with seed 8 were highly significant (coloured bar on the left of each figure indicates T value). However, cluster size was considerably smaller than in the control group. The figures show transverse slices at z level of (a) z = 46; white circle around the cluster coordinates [42, 10, 46]; (b) z = 48 ; white circle around the coordinates [0, -64, 48] and (c) z = 28 ; white circle around coordinates [46, 38, 28]. See tables 5.5, 5.3 and 5.4 regarding details such as cluster size and Z(r) value.

Between-group differences in correlations among different brain areas can provide important information regarding localised vulnerability in specific regions in the depressive group, if connectivity between affected regions is impaired compared to control subjects. Next, we will examine differences between subject groups, where one group shows a larger effect (stronger connectivity) between seed voxels and specific regions of the brain. If connectivity is in fact impaired in depressed patients, we can expect to find localised deficits that go beyond the *global* hypo-function suggested by the within-group analysis (Figure 5.3).

5.3.2.2 Between-group differences

This analysis highlighted three areas that were significant between subject groups.

Between group differences																
	Origin MNI			Seed	Region (origin)		Deficit MNI			Effect Talairach			Region (deficit)		Cluster size	P-value (corrected)
	x	y	z				x	y	z	x	y	z				
Patients > Controls	53	-30	38	7	R	parietal lobe	-14	-86	-14	-14	-85	-14	L	lingual gyrus BA18	143	0.025
Controls > Patients	0	-46	28	8		cingulate	-48	48	6	-40	43	3	L	frontal lobe (BA10)	132	0.035
	-15	-70	41	11	L	parietal lobe	-8	20	54	-10	22	53	L	frontal lobe (BA6)	149	0.041

Table 5.6: Between group differences. Patients show a stronger effect than controls in covariance between the right parietal lobe and the left lingual gyrus. Controls show stronger effect than patients in connectivity between the left frontal lobe and the cingulate and the left parietal cortex. Results are in descending order, noted by significance (lowest p-value, corrected at the cluster level). Cluster size displays the between-group comparison.

As expected, thresholding (p_v) the data at the 0.001 level yielded few significant clusters (Table 5.6). One cluster was more significant in the MDD group and two clusters were more significantly correlated in healthy controls. However, my results indicate that the clusters in Table 5.6 are indeed meaningful since these between group differences were echoed in association with different seeds (Figures 5.5; 5.9) using the 0.01 threshold level (p_v). The clusters reported in table 5.6 were corrected for multiple comparisons and only clusters with p_c-value < 0.05 are considered below (similar p_c thresholds were used with reference to the more lenient p_v threshold level).

The aim of the following section is twofold. First, I would like to present the results of between-group comparison, taken with stricter p_v threshold values. Second, I would like to present evidence supporting the methodology of taking these voxel-wise thresholding values, by showing that both the size of the between-group effect and the T values obtained for clusters from the more stringent analysis, are in fact more convincing with the stricter threshold.

Deficits in patients

The clusters situated in the frontal lobe (Table 5.6), showing a stronger effect in controls, with respect to connectivity with both the parietal cortex and cingulate may both be located in white matter. However due to extensive smoothing they are taken to be suggestive of stronger prefrontal connectivity in control subjects. Furthermore, this result is consistent with the prior hypotheses of hypofrontality in depressed subjects, which may give rise to the weaker covariance of left prefrontal areas with the rest of the brain. The first of these clusters, depicted in Figure 5.5, shows an area in the left prefrontal cortex (BA 10) where stronger connectivity was found with respect to the cingulate (seed 8) in control subjects.

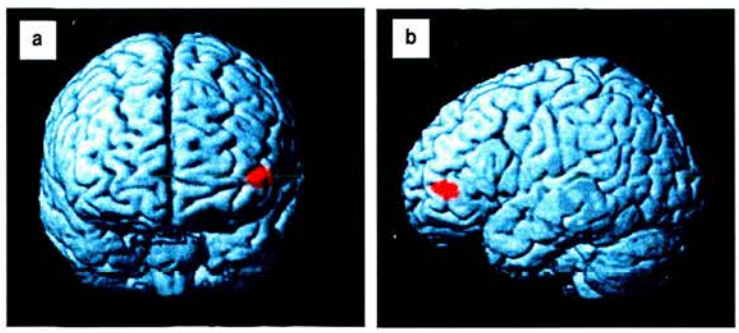

Figure 5.4: A left prefrontal cortical area (situated around BA10), which exhibited stronger connectivity with the cingulate in healthy control subjects, than MDD patients.

The between-group difference in the t-test (or one-way ANOVA), is calculated on the basis of the significance of differences between the respective mean values (normalised r scores), of the patients and the control subjects (Figure 5.5).

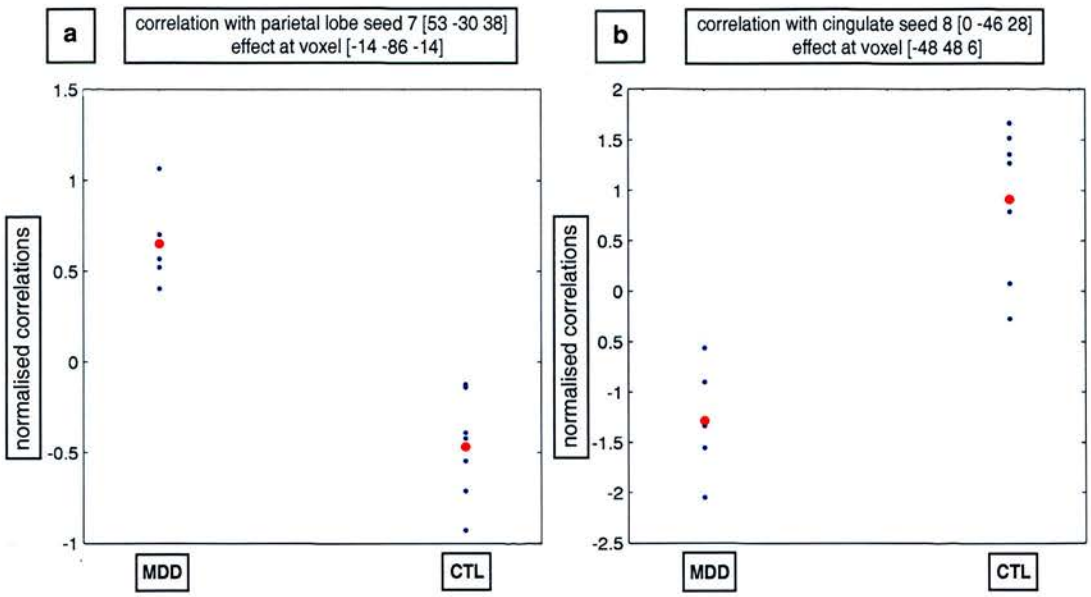

Figure 5.5: Between group differences, showing a stronger effect in MDD for connectivity with the seed located in the lingual gyrus (a); and for CTL (b), for connectivity of the cingulate with the frontal lobe. Blue dots indicate a normalised correlation value for every subject, red dots indicate group mean. The t-test or one-way ANOVA in this case, computes significance differences between respective group means. Location of the voxels in this and in subsequent plots and figures is given in MNI coordinates.

Further, control subjects show stronger connectivity between the left parietal lobe and left BA 6 (which I interpreted to be in close proximity to the pre-motor cortex; Figure 5.6b). These findings were echoed in seed 2 (superior frontal gyrus; Figure 5.6a) with a lower threshold level, where connectivity in control subjects was higher than in patients.

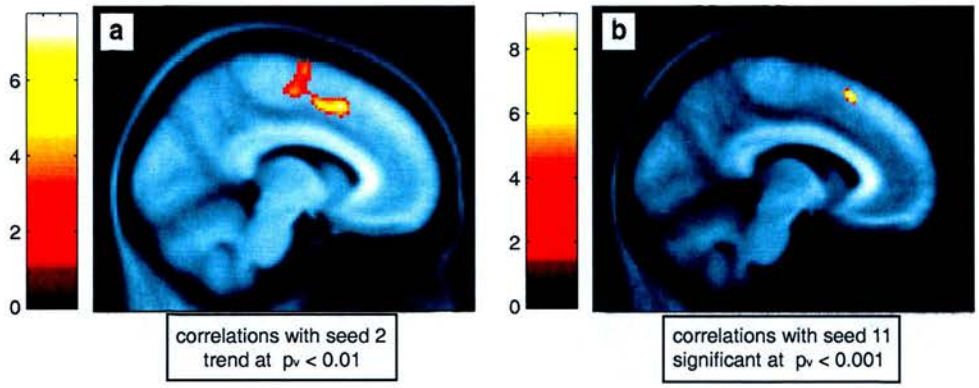

Figure 5.6: Between group differences, showing a stronger effect in CTL than in MDD. (a) and (b) depict stronger effect in similar regions (BA6), with respect to different seeds. Areas showing the effect, are strongly connected with the superior frontal gyrus, seed 2 (a); peak voxel at [-8, 14, 48]; p_c-value (corrected) 0.06);. Stronger connectivity in CTL with respect to the parietal cortex, seed 11 (b); showing coordinates peak voxel at [-8, 20, 54]), which is significant at the 0.001 level (p_v). The coloured bar on the left of each image indicates T values.

Stronger effect in patients

Patients show stronger connectivity of the occipital lobe (visual areas) with respect to task related areas such as the parietal lobe (Figure 5.7a-b), echoed by connectivity in another occipital area with respect to the medial frontal gyrus, BA 10 (seed 3; Figure 5.7-d). Interestingly, occipital areas were part of an extensive network (Figure 5.2b) that did not show the expected decrease in neural activity, which in control subjects was associated with increased task difficulty.

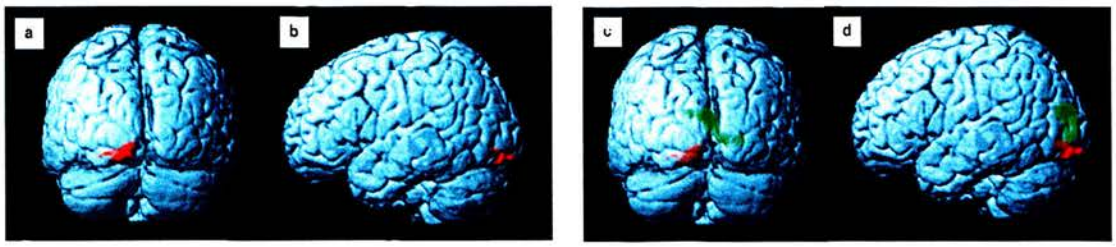

Figure 5.7: Between group differences, showing stronger connectivity between the occipital cortex MDD and both the parietal (a-d; red) and medial frontal gyrus (c-d; green). Locations of regions where differences were found. The occipital cortex of MDD patients is more strongly activated than in controls. (a-b) Connectivity with respect to the parietal cortex at a p_v threshold level of 0.001. (c-d) Clusters depicted in red are shown for comparison purposes (equivalent to a-b); clusters depicted in green are correlated with the prefrontal cortex, BA10, at a p_v threshold level of 0.01 (c-d).

5.3.2.3 Methodological issues

To conclude this section, I would like to motivate the rationale for use of higher p_v threshold of 0.001, despite highlighting relatively few within and between-group differences is demonstrated in figures 5.9 and 5.10, for healthy control subject and MDD patients respectively. Since a stronger effect was noted in control subjects at the lower p_v threshold level of 0.01 in both parietal (Figure 5.8a-b) and frontal (Figure 5.8c) cortices, I proceeded to investigate the difference between the effect in these areas, to ascertain why the parietal cluster did not appear significant (p_c (corrected) ≤ 0.05) at the stricter voxel-wise (p_v) threshold of 0.001.

Plotting the size of the effect in these respective clusters, it appears that a stronger effect at the frontal cortical cluster (Figure 5.9b) than in the parietal (Figure 5.9a) may have contributed to this. Figure 5.8 depicts parietal (a) and frontal (b) activation at the 0.01 p_v threshold level. Figure 5.9 shows a stronger mean effect in the frontal cluster (b), which underpins the significance of this cluster at the stricter threshold of 0.001.

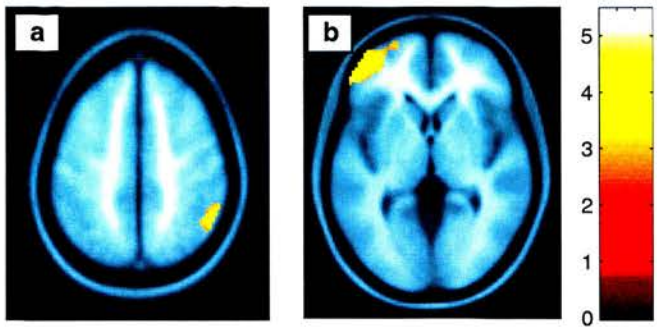

Figure 5.8: Stronger effect in CTL than MDD. Both plots show clusters at the 0.01 p_v threshold level. (a) Right inferior parietal lobule, BA 40, shows a trend ($p_c = 0.089$). (b) The prefrontal cluster, is positively correlated in CTL compared to MDD ($p_c = 0.018$) with respect to voxel 8 (cingulate). This area was also significant ($p_c = 0.035$) at the more stringent p_v threshold level of 0.001. Axial (a) and transverse (b) slices presented at y = -54 and z = 50 respectively for the parietal lobe cluster. The coloured bar on the right indicates T value. All p_c values indicated above are corrected for multiple comparisons.

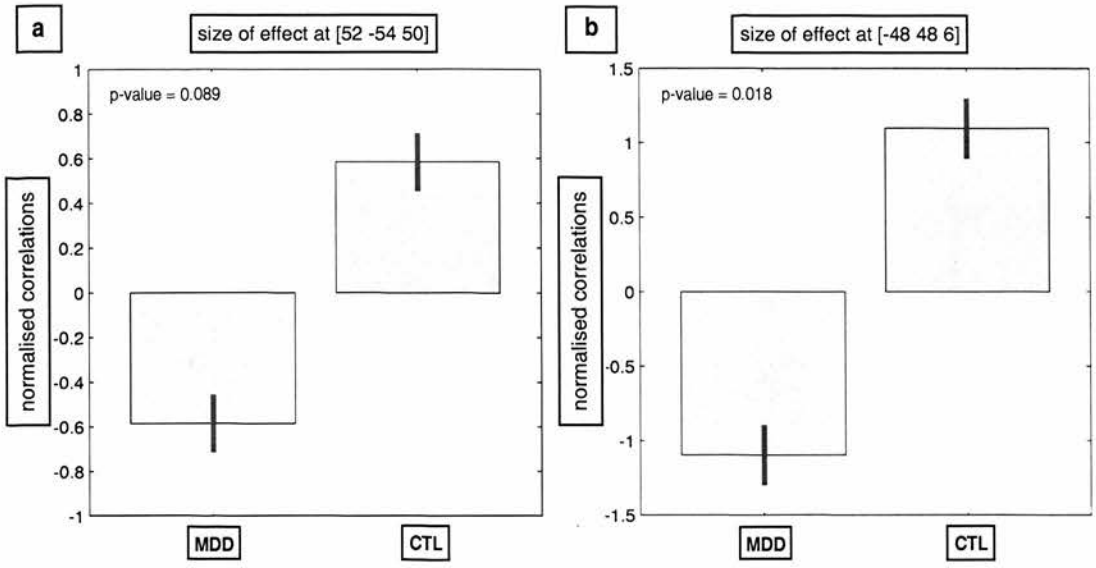

Figure 5.9: The size of effect at voxels [52, -54, 50] (area depicted in Figure 5.8 a) and [-48, 48, 6] (Fig 5.8 b) with respect to seed 8. While the prefrontal cluster (b) was significant both at the 0.01 and 0.001 p_v threshold level, the parietal cluster (a) only exhibits a trend at the 0.01 level and correspondingly, shows a smaller effect size than the prefrontal cluster. These plots depict the mean of the absolute of the two groups' Z scores (grey blocks) and ± 1 Standard Error of the Mean (SEM; red bar). Individual group's mean value (±SEM) are as follows: (a) CTL = 0.49 (± 0.14) / MDD = -0.68 (± 0.09), therefore plot (a) depicts the mean 0.58 (±0.13); likewise, (b) CTL = 0.91 (±0.22) / MDD = -1.28 (±0.13), therefore plot (b) depicts the mean 1.09 (±0.2).

Similarly, even though an effect was noted at the p_v 0.01 threshold level with respect to seed 2 (see Figure 5.7c-d; p_c (corrected) = 0.049), this effect was not significant at a p_v threshold of 0.001. Plotting the group responses (Figure 5.10c, patients plotted on the left), it seems that there is a lot of variance among the normalised correlation values among five patients and therefore, the between-group effect is not significant at the higher threshold.

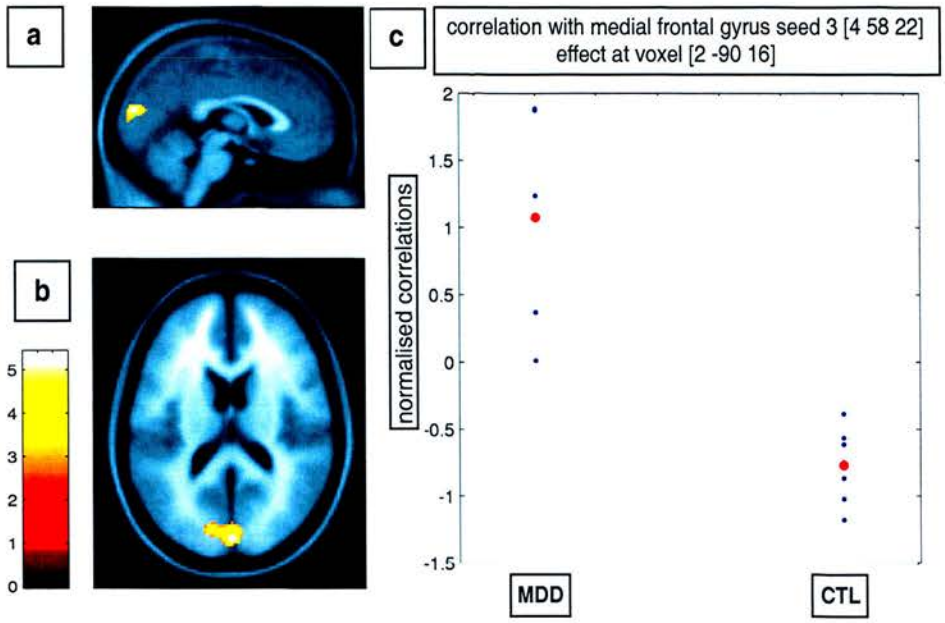

Figure 5.10: Between-group comparison of correlation between seed 3 and the occipital cortex, which is more strongly activated in patients than in controls. Images depict a sagittal slice (a) at x = 2 and a transverse slice (b) at z = 16. p_c-value (corrected) = 0.049; MDD = 1.08 (±0.19) / CTL = -0.77 (±0.11). See Figure 5.5 for conventions.

Summary of between group differences

My results suggest a global hypo-activity in depressed patients, combined with specific prefrontal impairment. Thus, within group effects show significantly smaller regions correlated with the voxel seeds in depressed patients, compared to control subjects. Between group differences highlighted stronger connectivity of the left lateral prefrontal cortex (Figure 5.4) in control subjects. Further, stronger connectivity of the lingual gyrus in depressed patients is consistent with localisation of function (Figure 5.2b), suggesting the absence of parametric deactivation of this area as a function of task difficulty. Careful examination of the size of effect (Figure 5.9) suggests that choosing stringent threshold values may produce more meaningful results, since the size of effect may be considerably smaller at this threshold level.

5.3.3 Between session differences

Finally, consistent with my prior hypothesis (see section 5.1.4), patients exhibited greater effects of fatigue, expressed through differences in brain activation, between the first and the second session. Table 5.7 shows five combinations of four patients each (since I was unable to include all five patients in the within group comparisons; see methods). In all groups, subtraction of the first from the second session shows areas that were significantly correlated with a specific voxel of interest (seed 11: parietal lobe in this example), as well as showing significant increase during the second session. These between-session differences were significant at the threshold 0.001 level and were typical of the within-group inference in the patient group, for all other seed voxels. The mean size for positively correlated clusters (± SD) was 52.72 voxels (± 6.07); while the negatively correlated clusters mean = 27.33 (± 9.92).

By contrast, no between-session differences were correlated with any of the seed voxels at the 0.001 p_v threshold level in control subjects (results not shown). Only one area showed between session differences in this group at the 0.01 level (p_v) with respect to seed 11, namely the pre-central gyrus, BA 6 (MNI coordinates [-12 -32 72]).

A few dominant areas exhibited between session differences in all sub-groups of depressed patients (Table 5.7), including prefrontal and parietal cortices, suggesting that these areas are the most sensitive in patients to the effects of fatigue. However, the calculation of between-session differences simply subtracts the normalised covariance map of the first session from the second. Values resulting from this subtraction can either be positive (stronger effect in the second session) or negative. Therefore, correlation coefficients with a positive sign could potentially express positive correlations with a positive value (session 1 > session 2) or negative correlations with a negative value (session 1 < session 2). Therefore, I refrain from further discussing the specific areas that show between session differences in the depressed group. Nonetheless, I feel that these results justify the use of only the first session data for the present functional connectivity analysis.

Group	Brain region	location P	side	MNI			Talairach			T value	size	
				x	y	z	x	y	z			
1	Frontal lobe	0.90	R	38	48	22	38	48	18	128.58	49	
	Parietal lobe	0.85	L	-36	-54	40	-36	-50	39	78.07	229	
	Frontal lobe	0.56	R	26	6	60	26	9	55	60.71	31	Mean: 62.67
	Parietal lobe	0.51	L	-56	-40	48	-55	-37	46	51.81	19	Sum: 376
	Frontal lobe	0.72	R	48	42	-12	48	40	-12	50.78	24	
	Frontal lobe	0.30	L	-42	34	34	-42	35	30	30.6	24	
	Frontal lobe	0.64	L	-10	46	52	-10	47	46	54.37	18	Mean: 28.5
	(anterior cingulate)		R	16	36	18	16	36	15	30.54	39	Sum: 57
2	Frontal lobe	0.70	L	-44	38	34	-44	38	29	78.22	40	
	Frontal lobe	0.79	R	28	48	34	28	48	29	76.92	29	
	Frontal lobe	0.91	R	20	18	-22	20	17	-19	66.01	18	Mean: 48.29
	Parietal lobe	0.47	L	-26	-62	50	-26	-58	49	43.79	78	Sum: 338
	Parietal lobe	0.66	L	-36	-56	62	-36	-51	60	41.04	76	
	Frontal lobe	0.60	R	24	10	60	24	12	55	37.17	43	
	Frontal lobe	0.90	R	38	48	22	38	48	18	28.63	54	
	Frontal lobe	0.64	L	-10	46	52	-10	47	46	47.99	16	Mean: 18.5
	Frontal lobe	0.68	R	14	-16	46	14	-13	43	47.44	21	Sum: 37
3	Frontal lobe	0.64	L	-42	42	34	-42	42	29	76.21	22	
	Parietal lobe	0.64	L	-42	-46	52	-42	-42	50	68.51	115	
	Parietal lobe	0.66	R	42	-52	44	42	-48	43	51.88	44	
	Frontal lobe	0.45	R	28	6	62	28	9	57	47.36	93	
	Parietal lobe	0.45	L	-28	-62	48	-28	-58	47	44.4	104	
	Cerebellum	0.93	L	-36	-44	-40	-36	-44	-31	39.71	28	Mean: 47.67
	Frontal lobe	0.89	R	42	46	16	42	45	12	36.95	42	Sum: 572
	Parietal lobe	0.28	R	18	-60	58	18	-55	56	34.74	36	
	Parietal lobe	0.55	R	42	-40	58	42	-36	55	33.9	21	
	Frontal lobe	0.53	L	-20	-2	64	-20	1	59	31.26	18	
	Frontal lobe	0.89	R	4	0	58	4	3	53	22.91	30	
	Parietal lobe	0.72	R	58	-34	48	57	-31	46	14.84	19	
	Parietal lobe	0.60	R	2	-54	32	2	-51	32	67.27	39	
	Parietal lobe	0.02	L	-34	-48	26	-34	-45	26	60.51	41	Mean: 43.6
	Frontal lobe	0.64	L	-10	46	52	-10	47	46	57.25	36	Sum: 218
	Frontal lobe	0.75	L	-6	58	12	-6	57	8	48.53	58	
	-		R	32	-20	26	32	-18	25	36.82	44	
4	Parietal lobe	0.72	L	-42	-44	58	-42	-40	55	111.31	140	
	Parietal lobe	0.38	R	38	-74	32	38	-70	33	75.92	16	
	Occipital lobe	0.68	L	-20	-70	-22	-20	-69	-15	59.5	15	
	Cerebellum	0.07										
	Cerebellum	0.87	L	-14	-74	-30	-14	-73	-22	50.71	37	
	Cerebellum	0.87	R	4	-74	-40	4	-73	-30	49.21	25	
	Parietal lobe	0.44	L	-28	-60	48	-28	-56	47	48.68	80	
	Cerebellum	0.23	R	2	-68	-18	2	-67	-12	41.12	43	Mean: 51.15
	Parietal lobe	0.60	R	22	-66	64	22	-61	62	38.37	89	Sum: 665
	Frontal lobe	0.45	R	28	6	62	28	9	57	35.43	54	
	Occipital lobe	0.06	L	-34	-58	-24	-34	-57	-17	34.29	75	
	Temporal lobe	0.75										
	Occipital lobe	0.36	R	22	-68	-22	22	-67	-15	34.12	30	
	Cerebellum	0.04										
	Frontal lobe	0.98	R	44	48	16	44	47	12	33.7	49	
	Cerebellum	0.91	L	-8	-78	-40	-8	-77	-30	17.02	12	
	Insula	0.66	L	-32	10	14	-32	10	12	114.08	18	
	Frontal lobe	0.64	L	-10	46	52	-10	47	46	44.8	17	
	Insula	0.06	L	-30	-18	18	-30	-17	17	37.34	20	
	-		L	-32	-40	-4	-32	-39	-1	36.3	20	Mean: 25.57
	Temporal lobe	0.79	R	58	2	-14	57	1	-12	35.58	18	Sum: 179
	Parietal lobe	0.53	R	44	-8	18	44	-7	17	33.37	69	
	Temporal lobe	0.11	L	-34	-44	-14	-34	-43	-10	27.79	17	
5	Parietal lobe	0.49	L	-24	-58	44	-24	-54	43	120.49	181	
	Frontal lobe	0.45	R	26	6	62	26	9	57	44.31	42	
	Frontal lobe	0.79	R	32	54	-14	32	52	-14	39.76	17	Mean: 53.83
	Parietal lobe	0.79	R	58	-52	42	57	-48	41	32.79	16	Sum: 323
	Frontal lobe	0.85	R	38	48	20	38	47	16	32.33	44	
	Frontal lobe	0.60	L	-38	-10	64	-38	-7	59	32.02	23	
	Frontal lobe	0.64	L	-10	46	52	-10	47	46	41.77	16	Mean: 20.5
	-		L	-34	-34	-12	-34	-33	-8	31.73	25	Sum: 41

Table 5.7: Between session differences in MDD group. Five combinations of four patients per-group. Differences between the second and the first session at seed 11 are correlated with the entire brain volume. Only clusters from the analysis using a p_v threshold at 0.001; p_c (corrected) < 0.05 are included. Group number is indicated on the left, positive clusters are depicted in black while negative clusters are depicted in red.

5.4 Discussion

This chapter provided an insight into neural systems associated with depression, using a functional connectivity approach. These results are both consistent with the literature and with prior hypotheses related to the particular design of this study. The advantage of using task-independent spatiotemporal correlations lies in the assumption that these correlations show real connectivity rather than simply provide circumstantial evidence for task related co-activation (Paus et al., 1997; Lowe et al., 1998; Hampson et al., 2002). In the present study, we do not use resting state data as such, but instead factor out task related neural activity by using the design matrix defined as part of the primary analysis. After summarising the main findings, this section will briefly discuss methodological questions and finally place this study in the context of the entire thesis.

5.4.1 Major findings

In sum, we note three key findings, in order of importance:

1. Depressed patients experience a global decrease in task-independent co-activation between areas that are known to be active during this task (and therefore are expected to have a large residual variance) and the rest of the brain. This confirmed the 3rd hypothesis (section 5.1.4).

2. Depressed patients show a localised deficit in connectivity of their left prefrontal cortex with both parietal cortex and cingulate (confirming the first hypothesis in section 5.1.4). The depressed group also exhibited stronger connectivity of visual areas, which may be related to a putatively compensatory mechanism (confirming hypothesis 4).

3. Depressed patients are more vulnerable to fatigue, which may in fact affect their cognitive performance (confirming the 5th hypothesis).

Thus, it appears that despite the modest number of subjects and the rigorous statistical testing, this study confirmed the expected deficits, both global (hypotheses 1 and 4 presented in section 5.1.4) and local (hypotheses 3 and 4), in depressed patients. Nonetheless, I did not confirm the 2nd hypothesis presented in the introduction, namely control subjects did not show stronger connectivity between medial prefrontal cortex and the hippocampal region, where structural deficits were observed in the MDD population.

5.4.2 Findings in context

The neural activation associated with this task is related to specific task components such as the central executive and memory (frontal and temporal regions), attention (parietal lobe) as well as motor and language regions (left temporal areas), dependent on the specific version of the task. Although task related neural activation of bilateral prefrontal cortical areas was noted in depressed patients who were less impaired than patients with schizophrenia (Barch et al., 2003), a number of groups report abnormalities of both neuropsychological function, along with specific deficits associated with working-memory and executive function, see Veiel, (1997) for meta-analysis, as well as impairments in neural response associated with cognitive task performance (Bench et al., 1992; Baker et al., 1997; Elliott et al., 1997; Okada et al., 2003).

In the context of the present study, Rose et al. (2002) found significant differences in task-accuracy, but not in reaction time, between the groups. Depressed patients appeared to have a higher error rate, which was positively correlated with task

difficulty. These differences were associated with decreased response of the left dorsolateral prefrontal cortex. My results are consistent with these findings, suggesting a specific prefrontal deficit in depressed patients. Furthermore, the absence of decreased activity in a large network of areas, including the visual (occipital) areas (Figure 5.2 b), suggests that the comparatively larger effect (increased correlation) between occipital areas and the parietal cortex (Figure 5.7a-b), and also prefrontal areas (Figure 5.7c-d), may serve as a compensatory mechanism for either global or localised deficits.

5.4.3 Functional connectivity and hypothesis testing

Studies examining connectivity between areas of interest often use pre-specified regions of interest for testing specific hypotheses about localised deficits in clinical populations; see Drevets (1999) and Phillips et al. (2003) for reviews. This seems sensible for two reasons. First, limiting the search space gives better control over the multiple comparisons problem presented with analysis of whole-brain volume, affording the use of more lenient correction procedures (www.fil.ion.ucl.ac.uk/spm/). Instead of performing many thousands of t-tests, the search can be limited to a small volume. Therefore corrections (even on the voxel-by-voxel level) are less intrusive. However, this approach limits the search space to areas where previous searches were conducted and thus potential new areas will not be discovered. Second, hypothesis-driven questions may give rise to more tractable searches, rather than creation of *a-posteriori* theories about brain function. The results presented in this chapter are consistent with the expected activation deficits in depressed subjects, although hypothesis testing in our case is limited since I would hesitate to over-interpret the within-group regional

correlations (the areas where significant positive or negative correlations with seed voxels were identified).

Depression is often expressed through physical symptoms of fatigue and lethargy (Gold and Chrousos, 1999; Stahl, 2002). Prior studies (Elliott et al., 1997; Veiel, 1997) suggested impaired task performance in depressed subjects, along with changes in the regional pattern of their brain activity, compared to healthy controls. This impairment could be a consequence of cognitive or attentional deficits, capacity limitations, or even psychomotor slowing *per se*. These factors may have been confounded by increased fatigue as a consequence of the duration (19 minutes) of the experimental sessions, which may affect patients' performance more noticeably than controls'. Consistent with this hypothesis, between-session differences were indeed observed in MDD patients (Table 5.7).

5.4.4 A critical review of methodology

The methods used in this study, although powerful, make the following assumptions. First, the study by Lowe et al. (1998) upon which we based our analysis tested connectivity in resting state fluctuations by looking in well-delineated areas, namely motor cortex, visual cortex and amygdala. Their acquisition (scanning) parameters allowed the examination of correlated fluctuations in great detail. For example, their slice thickness was 1 mm and repetition time (TR) was 134 msec (for single slice acquisition), while in the present study slice thickness was 5 mm and TR equalled 2.5 s. We have to assume therefore, that decreasing the resolution does not reduce the sensitivity of these methods in measuring task-independent fluctuations. Second, by factoring out task-related activity we assume that the residual error is completely task-independent, whereas

the residual error may be related to the task (for example, residuals may be correlated with task difficulty). Finally, we have to assume that the linear model, which is factored out in this task, fits neural response characteristics of both patients and controls, equally well.

Nonetheless, unlike simple localisation studies, functional connectivity methods enable a careful examination of correlated neural activity either in specified regions of interest or across the whole brain. Potentially, these methods are more sensitive to illness-associated changes in neural activity than the averaging of signal across blocks, which is part of the GLM analysis in block designs. Indeed, the sensitivity of this method clearly highlighted between group differences that were suggested by the functional localisation study (Rose et al., 2002). For example, decreased neural response in the left prefrontal cortex of depressed patients has been associated with a discrete difference in the covariance of this area with respect to the cingulate (Figure 5.4), in patients compared to control subjects. I believe that the analysis of task-related neural activity may have revealed suppression of the left prefrontal cortex in depressed patients; however I could not directly relate this suppression to the activity of the cingulate. Thus, functional connectivity between limbic (cingulate) and prefrontal (BA 10) areas may be particularly vulnerable in depression, as revealed by correlating task-independent fluctuations. Furthermore, the task-associated neural activity may have been sufficiently strong to activate either or both of these areas and could obscure the specific deficit highlighted here. Therefore, I believe that the results of my work can complement and enhance previous findings by looking at the task-independent signal.

5.4.5 Limitations and caveats

It is difficult to draw any meaningful conclusions about specific regional correlations in different populations on the basis of small sample sizes in clinical populations; see Appendix A (Ebmeier and Kronhaus, 2001). As with other neuroimaging studies, our findings may be influenced by a number of factors such as scanning methods; model specification (may differ for patients and controls: the neuronal-networks may be recruited differently in those subject groups, e.g. with a slight temporal delay in the case of the depressed patients). The main limitation nonetheless, is the size and the variability of the patient group – both subject groups are small and probably cannot be argued to form a homogeneous entity or represent the clinical population, either aetiologically or symptomatically and therefore in terms of their brain activity.

We should note however, that many important studies in the field often use data from a small number of well-classified subjects. For example, Casey et al. (1998) conducted their reproducibility study on the basis of data from five to eight subjects from every institution; Jansma et al. (2000) used data from twelve healthy subjects for their parametric study; while Lowe et al. (1998) used data from only three male subjects in their study. Indeed the data presented here for the depressed group appear homogeneous and their specific neural activity pattern with respect to the whole group analysis (as well as discrete deficits) are quite well defined. The technical difficulty I experienced with SPM has in fact proved to be fortuitous, since it forced me to compare 5 combinations of 4 patients each (Table 5.7) and convinced me that the effect I observed, especially with reference to my hypothesis 4 (section 5.3.3), is fairly robust.

5.4.6 Functional connectivity and parametric designs

Further to the general limitations of this mode of inference the methods described in this chapter may be enriched by dividing the time-series into task-related segments. Thus, correlation coefficients that are associated with particular memory loads (ranging from 0-back to 3-back) can be evaluated separately. This way, the distribution of the residuals may be examined against memory demands and what we assume to be resting state fluctuations can be compared at different stages of the task and under different conditions. However, this may be a useful exercise only if subject numbers are increased substantially, to achieve sufficient statistical power for these calculations. Furthermore, forming *a priori* hypotheses on the basis of functional localisation studies (associated with task related activity) may help address the problem associated with multiple comparisons.

5.4.7 Conclusions and suggestions for future work

In sum, this study appears to highlight both global and localised deficits in the depressed population. This project, based on Rose (2004) data, in tandem with the study presented in chapter 4 (comparing bipolar and control patients performing the Stroop task), offers an insight into discrete deficits in neural activity of clinical populations.

Future extensions to this study could include the following:

1. Choosing seed voxels that are derived directly from the functional localisation study of the same dataset: i.e. areas that were activated by both depressed patients and healthy controls.

2. Choosing seed voxels in areas that are affected by the illness, such as the ventral anterior cingulate (BA25), which was reported to be particularly vulnerable in depression (Mayberg, 1997).

3. Evaluating these results against the region-of-interest (ROI) approach used in connectivity analyses such as SEM.

4. Increasing the number of subjects.

Chapter 6

The delayed match to sample task: setting the scene for a systems level model

This chapter builds upon the results of the previous chapter by examining the effects of global and local changes in excitation and inhibition on a systems-level neural-network. This network models the results from an effective connectivity analysis (McIntosh et al., 1996) in healthy control subjects performing a memory task. Thus, the neuroimaging based projects in my thesis (chapters 4 and 5) are supplemented here by a computational investigation of the impact of structural and functional abnormalities in depression on a well-defined network of functionally associated areas.

6.1 Introduction

The examination of task-related neuroimaging data in healthy control subjects provides important clues to the specific associative pattern between brain areas. Here, the term association is used to denote the property of computation that is not necessarily dependent on the order of the elements that are used to produce the result. Specifically, we are interested in the interaction between different elements within the network, discerned by studying the internal dynamics that result from specific connectivity patterns, which are perceived to be more consequential than the initial input.

My aims in this work are twofold. First, I wished to study the dynamical properties of the proposed effective connectivity networks on which my models are based (McIntosh et al., 1996; McIntosh, 1999). These could be described as the default behaviours of these networks, since I remain faithful to the connectivity parameters suggested by the authors (see section 6.4.2). Second, I wanted to use the model to test the effects of simulating depression by varying certain parameters of the model. These include reduced efficacy of excitatory (glutamate) and inhibitory (GABA) neurotransmitters; see Sanacora et al. (2003) for review. These deficits may be ameliorated by activity changes in striatum and hippocampus (GH) associated with administration of antidepressant medications such as selective Serotonin reuptake inhibitors (SSRI) (Mayberg et al., 2002). Finally, structural abnormalities in areas such as the cingulate (Drevets et al., 1997), PFC (Rajkowska et al., 1999; Rajkowska et al., 2001) and GH (MacQueen et al., 2003) have been simulated using these models.

Using this paradigm, we can study the effects of global changes in excitation or inhibition on inter-regional connections or the dynamics of the entire network. Alternatively, modelling activity patterns in these networks may suggest a possible

explanation for the effects of changes (e.g. reduced size, denoting atrophy in specific regions) on the default dynamics of the network. The impact of these abnormalities on the intrinsic behaviours of a network that has been designed to cope with working-memory demands can be compared with their effect on a network that does not encode patterns. In this project, interactions between different brain-regions were modelled by means of a connectivity matrix, representing temporal correlations in neural activity between different areas during performance of a specific cognitive task.

This chapter will outline the decisions, assumptions and compromises that had been reached *en route* to constructing these dynamical models, followed by an outline of basic results. The next chapter (chapter 7) will describe experiments that explore the analogues of the physiology (activity) and the anatomy (structure) of these models. The former will be studied using different techniques to perturb the characteristic model activity (using the default parameters), while the latter will try to classify functional groupings or clusters in the network.

6.2 Structural Equation Modelling and dynamical networks

The networks, or effective connectivity models, pictured in Figure 6.1 (McIntosh, 1999) represent the results of Structural Equation Modelling (SEM) analysis of interactions (measured by PET) between 22 brain regions, in 10 healthy subjects performing the delayed match to sample task (Haxby et al., 1995). This is essentially a recognition task, where subjects are asked to identify a stimulus that was presented previously across different delay conditions, with or without presentation of distractor stimuli between the encoding and recall stages of the task. Unlike the N-back task, however, encoding and recall occur at different times and therefore this task can be simpler in certain respects. In the modelling work, I focussed on 2 of the 4 possible delay conditions: the perceptual matching and the long-delay conditions, to see the effect of variable delays on each network. In the matching condition, subjects were asked to match one of two faces to the one they were asked to previously encode (no intervening stimuli) and the long-delay network, representing a delay of 4 presentations of intervening (blank) stimuli (with an average of 21 s retention interval; McIntosh et al., 1996). Each stimulus presentation (both test and target) lasted 4 s, with 1 s inter-stimulus interval (Haxby et al., 1995).

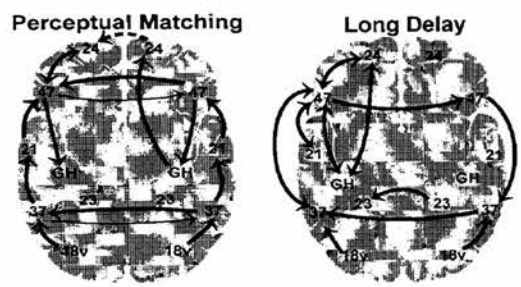

Figure 6.1: Network summarising path coefficients between specific aeas in the perceptual matching (left) and long-delay (right) networks (reproduced from McIntosh 1999).

Inter-regional covariance in activity between regions of interest (ROI) is assumed to indicate a functional relationship (connectivity) between those regions (see Lee et al., 2003 for an overview of current methods). The results (McIntosh et al., 1996) associated with the network describing the perceptual matching condition (the matching network), focused on activation of the bilateral inferior frontal regions (BA47) and hippocampi (GH), as well as on strong fronto-limbic connectivity, which summarises the activity of the ventral visual stream (Ungerleider and Mishkin, 1982). The bilateral inferior-frontal and occipito-temporal areas (BA37 and BA47) appear to be equally important in this network. By contrast, in the long-delay network activity is focussed on the left hemisphere, with feedback connections from (bilateral) frontal areas to BA37 and greater involvement of GH.

To analyse network activity quantitatively, McIntosh et al. (1996) applied SEM techniques. When applied to neuroimaging experiments, SEM combines anatomical information (usually derived from primate labelling studies) with activation data from neuroimaging studies in human subjects (McIntosh and Gonzalez-Lima, 1994). Searching for causal relationships between different variables, the direction, strength and polarity of direct and indirect connections between different nodes of the network of areas are computed (see chapter 3 for review). For the purpose of the neural-network models here and in chapter 7, path coefficients are interpreted as connection strengths between different nodes of the network.

This modelling framework allows me to examine the effects of neurobiological abnormalities found in patients with Major Depressive Disorder (MDD). The premise for disrupting the activity of the network to emulate disrupted brain function in depression is based on functional and structural changes reported in the literature. These include functional dysregulation between hyperactive limbic areas such as the anterior cingulate and hypoactive prefrontal cortical areas, reviewed by

Phillips et al. (2003). Illness-related structural abnormalities were reported in subgenual anterior cingulate (Drevets, 1999) and both neurons and glial cells in the prefrontal cortex (PFC) (Rajkowska et al., 1999; Rajkowska et al., 2001). It is expected, therefore, that these structural abnormalities would translate into functional deficits in remote areas, by increasing flow or metabolism either in these areas or in the associated network, for the purpose of compensation. A putative decrease in global metabolic rate was noted in MDD, while hyperactivity in limbic areas was also associated with depression or even sadness in healthy controls (Levesque et al., 2003; Stefurak et al., 2003). Finally, changes in global inhibition were also investigated, for two main reasons. First, I wished to relate this experiment to global changes in depression, such as decreased cortical excitability shown by post-exercise facilitation (Reid et al., 2002; Shajahan et al., 2002). Second, I planned to investigate the relative contribution of positive and negative correlations, expressed as path coefficients, to the dynamical activity patterns in the matching and long-delay networks, respectively.

6.2.1 Hypotheses

Several hypotheses guided the investigation of activity in these networks. These were based both on the basic characteristics of the effective connectivity network (McIntosh et al., 1996) and on the putative neurobiology underpinning the architecture of this network. Hypotheses are highlighted in bold.

1. McIntosh et al. (1996) describes the interactions between hemispheres and specific areas. **The specific differences between the matching and long-delay networks involve two significant differences:**

a. **The long-delay network will be characterised by a strong left-focussed activity while in the matching network, an inter-hemispheric pattern is expected, with a slight preference for focussed activity in the right hemisphere.**

b. **The long-delay network will have a slightly more recurrent nature than the matching network, where activity will propagate in a more feed-forward fashion.** This is expressed in the basic architecture of the network through bilateral feedback connections from BA47 to BA37 in the long-delay network that are absent from the matching network, as well as a bidirectional (left) connectivity between GH and BA24 (cingulate) that is only unidirectional (originating in GH) in the matching network. These interactions were described in McIntosh et al. (1996) and are based on the simplified version of the network, which is believed to represent the cardinal interactions (Figure 6.1) in the original networks, rather than the actual path coefficients (Figure 6.2).

2. Three frontal areas (BA46, BA10 and BA47) were concatenated into one frontal region, BA47, in Figure 6.1 (McIntosh, 1999). **Therefore, the activity in these regions is expected to be qualitatively similar. Furthermore BA47 is expected to be the dominant region among the three.**

3. **Further to the different global activity patterns associated with hypothesis 1, network activity in the long-delay condition is expected to be more vulnerable to deficits in the left hippocampus, anterior cingulate and BA47, since these three areas are reciprocally connected, forming a closed excitatory loop.** Moreover, clinical data suggests that

left GH is particularly vulnerable in treatment-resistant depressed subjects (Shah et al., 2002), which may be associated with developmental stress (Teicher et al., 2002). Likewise, left anterior cingulate deficits, such as decreased rCBF, may be associated with depression (Bench et al., 1992). I therefore expected these structural deficits to contribute to the hypofrontality reported in depressive illness assuming that GH, anterior cingulate and PFC were part of the same functional network.

4. **Increased activity in other areas, for example stronger activation of visual areas** (as was suggested by the functional connectivity study, chapter 5), **is expected to ameliorate the localised deficits described in hypothesis 3.** Thus, neural reorganisation was expected to effectively compensate for either age (Della-Maggiore et al., 2002) or mood-related (Gron et al., 2002) localised dysfunction.

5. **Changes in all excitatory and inhibitory weight values throughout the network (termed "global changes") are expected to affect network behaviour.** Although this may seem uncontroversial, it is impossible to envisage the exact nature of altering global levels of excitation or inhibition on specific behaviours, since I could not know in advance what shape this dynamic behaviour may take. However, I planned to examine the relative contribution of excitation and inhibition to characteristic behaviours in the matching or long-delay networks, respectively.

6.2.2 The modelling approach taken in this study

The networks (Figure 6.1) that have inspired the modelling work in this chapter are believed to be a snapshot of brain-activity during task performance. The path coefficients have been characterised by combining anatomical details about the presence or absence of connections between specific nodes with functional information. Using a computational model to characterise the activity of these networks has a threefold purpose. First, I wanted to examine which units were likely to be coactive and explore the parameter space that gives rise to this co-activation. Second, elements of this model of "normal function" were subsequently disrupted, to examine the effects of regional deficits in unipolar patients such as those described in the fMRI literature. Third, I wanted to examine the propagation of activity in the perceptual-matching network. This was described as co-activation of units, allowing me to effectively cluster areas functionally rather than topographically. Subsequently, in chapter 7, I assessed how changes in global parameters such as excitation and inhibition as well as changes in the output of specific units influence the behaviour of the network. The study of the long-delay network was guided by the findings of characteristic activity in matching network and enabled comparison between the respective behaviour of these networks, as well as the effect of perturbation upon this behaviour.

6.3 Methods

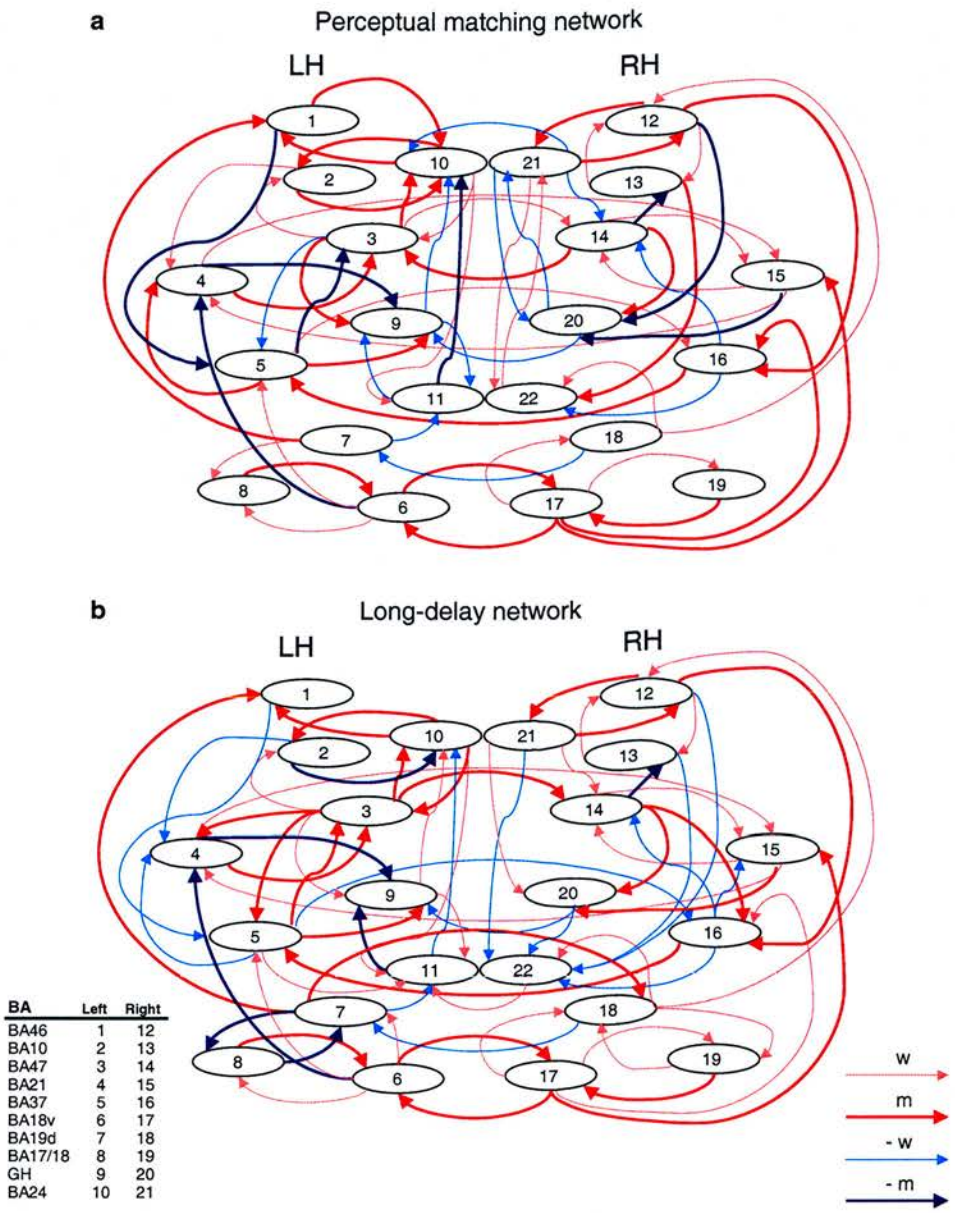

Figure 6.2: Connectivity diagrams depicting the cortico-cortical and cortico-limbic connections of left (LH) and right (RH) hemispheres in (a) the perceptual matching and (b) the long-delay conditions (McIntosh et al., 1996). LH units are labelled 1-11 and RH units 12-22, with Brodmann Area (BA) indicated in the key (bottom left). Cortical regions corresponding to Brodmann Areas (BA) depicted on the left are shown in Table 6.1. Discrete values were ascribed to weak and medium weights (positive and negative), to characterise network behaviour. Excitatory connections are depicted in shades of red and inhibitory connections are in blue; (a) is identical to the matrix representing the matching network in Figure 6.3.

6.3.1 Simulating the network

The matching and the long-delay networks depicted in Figure 6.2 were simulated and analysed by programs written in Matlab. The networks were constructed using the following components:

1. Activation vector, $\mathbf{a}_t$.

A row vector of 22 units representing 11 areas in the left and 11 areas in the right hemisphere (Table 6.1). The value of each element in vector $\mathbf{a}_t$ changes over time and reflects the changing activity in the corresponding brain region.

a

Region	BA	Left	Right
Middle frontal	46	1	12
Inferior frontal	10	2	13
Ventral inferior frontal	47	3	14
Middle temporal gyrus	21	4	15
Inferior temporal gyrus	37	5	16
Fusiform	18v	6	17
Cuneus	19d	7	18
Cuneus	17/18	8	19
Hippocampus	GH	9	20
Anterior cingulate	24	10	21
Posterior cingulate	23	11	22

b

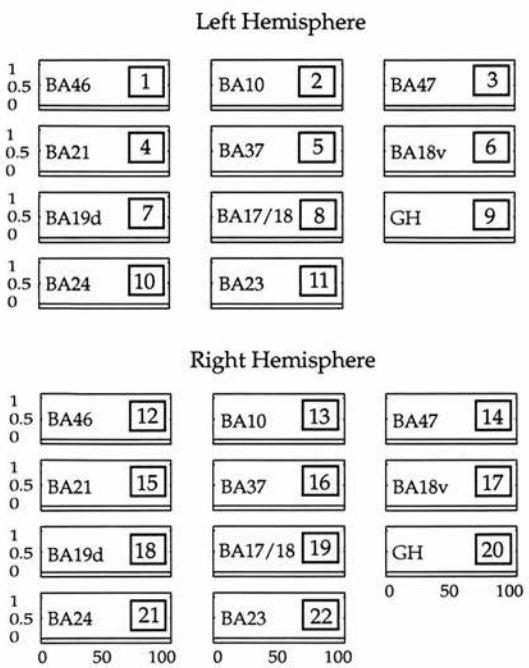

Table 6.1 (a): Areas from the McIntosh et al. (1996) study simulated in the model. (b) The figure shows activation in the 22 areas represented by the network; the top half of each plot shows activation of the 11 areas in the left hemisphere; right hemisphere activation is shown at the bottom. The name of the area appears above each plot. The plots are numbered from left to right and from top to bottom. The X-axis in these plots shows the first 100 (out of 1,000) time-steps and the Y-axis of each plot shows the activation of the area at that time (bounded between 0 and 1).

The vector $\mathbf{a}_0$, representing initial activity, is initialised with binary values, set by the user. Normally only 1 or 2 elements of $\mathbf{a}_0$ are set.

2. Connectivity matrix **W**.

W is a 22 × 22 matrix. Figure 6.3 shows the connectivity matrix for the 'matching' condition. The rows represent the source and columns represent the target of each connection. For example, element **W**(2,4) represents a weak positive connection from BA21 to BA10 in the left hemisphere, while the reciprocal connection **W**(4,2) is absent. Weak connections are given values of 0.1 or 0.35; likewise, medium-strength connections are either 0.36 or 0.65. Inhibitory connections are denoted by negative values.

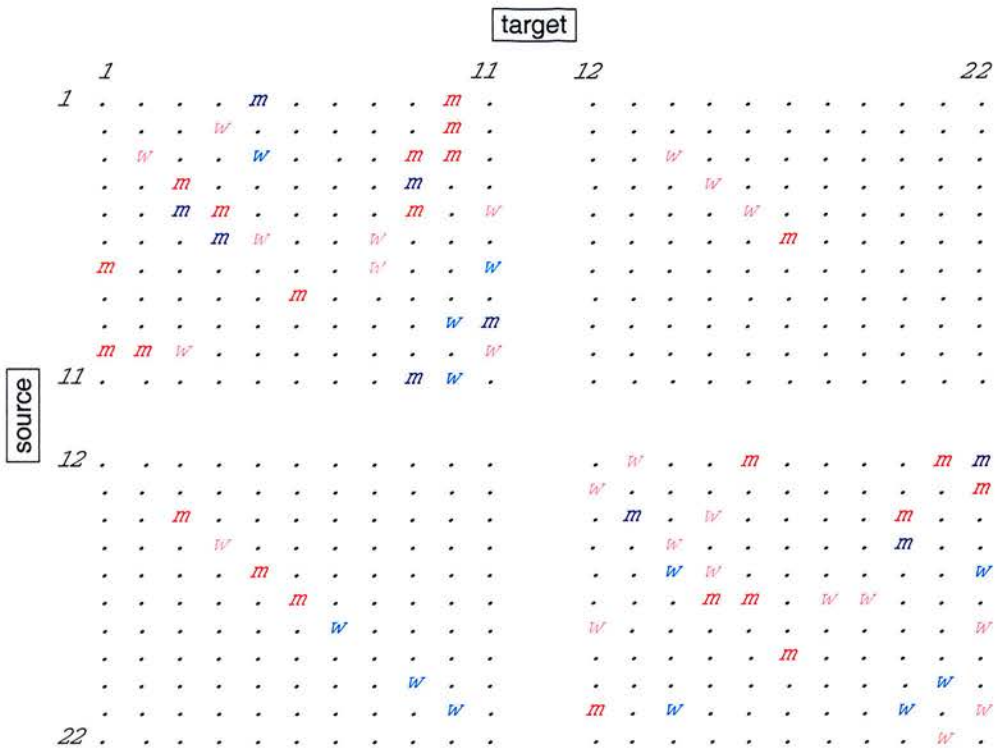

Figure 6.3: Path coefficients encoded into a weight matrix. Upper left quadrant: cortico-cortical and cortico-limbic connections in the left hemisphere. Lower right quadrant: connections within the right hemisphere. Upper right quadrant: left hemisphere connections to the right and the opposite direction in the lower left quadrant. Positive weights: m (values: 0.36/0.65; n=23); w (values: 0.1/0.35; n=23). Negative values: default set as for positive weights. -m (n=9); -w (n=12).

The connectivity matrix in Figure 6.3 was derived by studying the path-coefficients presented in Figures 2-6 of McIntosh et al. (1996). Personal communication with Professor A.R. McIntosh confirmed a number of inconsistencies in the connectivity diagrams (McIntosh et al., 1996), which were corrected in the computer programs used here. This matrix is identical to the matching network in Figure 6.2a. In McIntosh et al. (1996), 4 possible path coefficient ranges were encoded in the manuscript through the relative thickness of arrows connecting different brain regions. These included positive (solid line) and negative (dashed line) values for strong (0.66 to 1.0), medium (0.36 to 0.65) and weak (0.1 to 0.35) connections, as well as a thin dashed line representing a path coefficient of zero. Great care was taken to ensure that these were correctly encoded in the computer scripts. The arrows were mostly in the lower (medium, weak or zero) value-ranges; see section 6.4.2 for further details.

3. Update rule.

Given an initial activation vector $\mathbf{a}_0$, the dynamics of the network evolve over time using equations 6.1 and 6.2:

$$\mathbf{i}_t = \mathbf{a}_t * \mathbf{W} \tag{6.1}$$

Internal activation, $\mathbf{i}$, is a product of multiplying the current activity by the weight matrix. The internal activation is then passed through a sigmoidal squashing function, f, to get the activation at the next time step $\mathbf{a}_{t+1}$:

$$\mathbf{a}_{t+1} = f(\mathbf{i}_t) \tag{6.2}$$

4. Squashing function

The sigmoidal function is used as a squashing function because this function compresses a wide range of internal activation into a limited range of output and thus activity remains bounded. Furthermore, the specific form of the sigmoidal function used in this work, limited the output to exclusively positive values to prevent oscillations between positive and negative values.

$$f(\mathbf{a}_t) = 1/\ (1 + \exp(-10\ (\mathbf{a}_t - 1\ /\ 2))) \tag{6.3}$$

Therefore, each element of **a** will always be bounded in the range [0,1]. The constant 10 within f gives the sigmoidal a relatively sharp transition; lower values will give a broader sigmoidal. The constant 1/2 ensures that f (1/2) = half maximum.

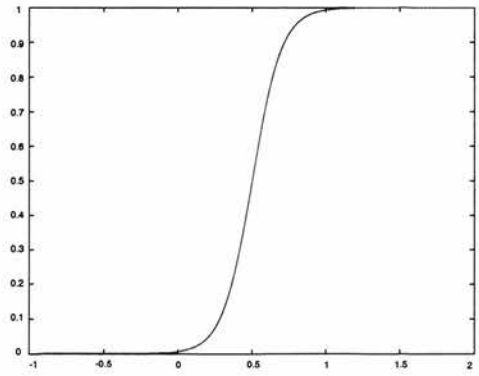

Figure 6.4: A typical sigmoidal function. The internal activation of a unit is passed through a squashing function and assigned a value in [0,1]. The X-axis denotes the internal activation of a unit i and the Y-axis shows the output, f(i) of the unit.

Starting from an initial activation vector, $\mathbf{a}_0$, the network activity is updated using the above equation for a pre-determined number (1,000) of iterations. We then examine the activation of each area over time.

Exploratory analysis of the network is carried out in two stages:

1. Characterising the activity of the network under specific parameters, pertaining to hypotheses 1 and 2.

2. Perturbing the network (chapter 7), pertaining to hypotheses 3 through 5:

    a. Global changes in excitation or inhibition.

    b. Local changes. The weight values from specific source units are changed, which effectively means that the participation or the impact of this source on network behaviour can be tested.

This describes the framework of the model. Further manipulations of the network to mimic particular biological phenomena will be described in the relevant sections.

6.3.2 General approach

Before testing the hypotheses outlined in the introduction (section 6.2.1), I made the following preliminary inquiries:

Calibrating the network: setting the framework for the dynamical models. This includes:

I. Highlighting the role for a limiting function on the output of the matching network (section 6.4.1).

II. Setting the range of weight values that are likely to produce activation (section 6.4.2).

The following two sets of experiments map onto the hypotheses described in section 6.2.1:

Experiment 1: Characterising the basic features of the matching (sections 6.5.1-6.5.3) and the long-delay (sections 6.6.1-6.6.2) networks. This set of experiments maps onto hypotheses 1 and 2.

Experiment 2: The final set of experiments will be described in chapter 7. These map onto hypotheses 3 through 5, exploring the role of global and localised changes in weight values, as well as the effects of compensation.

After presenting the general framework and setting up the parameters of these dynamical models (sections 6.4.1-6.4.2) the results are presented first for the matching network (section 6.5) and then for the long-delay (section 6.6) network.

6.3.3 Characterising network behaviour

Characterising network behaviours in the matching (and subsequently the long-delay) networks was performed by setting one unit (of the 22) at a time in $\mathbf{a}_0$. This highlighted a functional grouping of the matching network into functional sub-networks, or clusters, of co-activated units. This classification was done visually, by noting units that were oscillating together or displayed a similar behaviour (such as initial bursts or convergence at the upper limits of the sigmoidal function). The absence of activation (i.e. if the activation of any unit remained or decayed to 0), was not considered to suggest a pattern of co-activation. Once a sub-network was identified, I proceeded to determine which units were necessary for this pattern by individually clamping at 0 the activity of units that did not appear to participate in this pattern of behaviour. This was implemented for unit **i**

by enforcing $\mathbf{a}(i)_t = 0$. This stepwise elimination of units allowed me to determine which units were necessary for generating and maintaining certain patterns of activity and furthermore, to assess the consequence of removing certain units that may not be sufficient to disrupt the pattern on their own but are necessary for maintenance of this pattern. To gain insight into the nature of this activity, the activation values of the different units were noted and compared for different values, varying both inputs and weights.

6.3.4 Selection criteria for initial activity

The results presented in this chapter are from the analysis of both the matching and the long-delay networks. Naturally, given the different nature of the connectivity of these networks, it was sometimes difficult to find a common ground on which to pursue a comparative study of network behaviour. For example, activation through the visual areas appears to be the most sensible way of emulating the initial activation similar to the experimental procedure (Haxby et al., 1995; McIntosh et al., 1996). In the matching network, an initial input from left fusiform (BA18v; area 6) with the maximum weight values specified by McIntosh, (absolute values of $w = 0.35$ and $m = 0.65$), was sufficient to produce enduring activity in the network. By contrast, an initial input from the same unit (and the same weight values) in the long-delay network, produced only transient activity in several units (Figure 6.8a) without spreading to the dominant sub-network (Figure 6.8b). However, to compare the activity of these networks, I thought it would be helpful for the activation to be initiated by a visual unit and therefore, in the long-delay network initial input from BA18v (unit 6) is combined with input from a element of the dominant sub-network, e.g. inferior-temporal BA37 (unit 5; Figure 6.8c), which in turn triggers the characteristic coactivity pattern. The combination of these two inputs was compared

to co-activation of the other units taking part in this sub-network and was found to be typical of the activity pattern of any other (co-active) unit with unit 6. Hence, unit 5 was seen as a favourable and representative choice for a second area. Thus, my experiments with both activation and perturbation of the long-delay network are performed with initial activation from units 5 and 6.

6.3.5 Phase plots

The latter part of the analysis in this chapter (section 6.6.3), addresses the question of the specificity of neural activity in the long-delay network. Recurrent loops between prefrontal area BA47 and GH (Figure 6.1, from McIntosh et al., 1999) have been assigned the function of maintaining an encoded pattern in working-memory. As I was isolating the minimal constituents of the long-delay network, in a manner described in section 6.3.2, the relationship between the left prefrontal cortical areas and left GH became apparent (especially the correspondence between units 2 and 9). The maintenance of patterns in working-memory was expected (McIntosh et al., 1996) to be dependent upon this interaction and therefore, I wished to examine whether there is a relationship between these areas. Furthermore, as stated in hypothesis 2 (section 6.2.1), I wished to test whether this relationship holds for all 3 prefrontal areas in the network (i.e. BA46, BA10 and BA47). The activation of every unit of the matching and long-delay networks is normally plotted against time, here (Figures 6.6, 6.8) and in chapter 7 (Figures 7.1 and 7.3-7.7). This enables the visual evaluation of the concurrent activity in all units, which in the case of the matching network was straightforward since oscillations appear to have a period of two. However in the case of the long-delay network, especially when only the minimal constituents (Figure 6.9) were activated, this simple periodicity appears to have been disrupted. In section 6.6.3 therefore, phase plots are used to juxtapose the activity of

pairs of units and looked for periodicity in the signal by examining the activation values over time and by plotting the autocorrelation functions of different units in the statistical program R (www.r-project.org).

6.4 Preliminaries

Before using the network to investigate specific hypotheses, I performed several preliminary tests.

6.4.1 Limiting network activity (calibration I)

Network activity was constrained by the sigmoidal function (equation 6.3), which is a simple way of introducing both non-linearity and an activity-limiting constraint into the model. This is obviously an imposed limitation on network activity. However, confining the activity of the networks enables a more straightforward identification of clusters, i.e. groups of units that are likely to be co-active. In the absence of this function, activity rises or decays exponentially, oscillating between positive and negative values. In this network (which is largely excitatory) the absence of a squashing function allowed the activity to either rise or decay very quickly, depending on the discrete weight values in the matrix (Figure 6.3). If weight values are small and the activation does not exceed one the activity will die down (Figure 6.5a), whereas if activity exceeds one, oscillation will increase exponentially (Figure 6.5b).

This behaviour is expected from discrete dynamical systems theory (Scheinerman, 1995). However, it seems that this network can never achieve a stable state, where activity will neither grow nor decay over time.

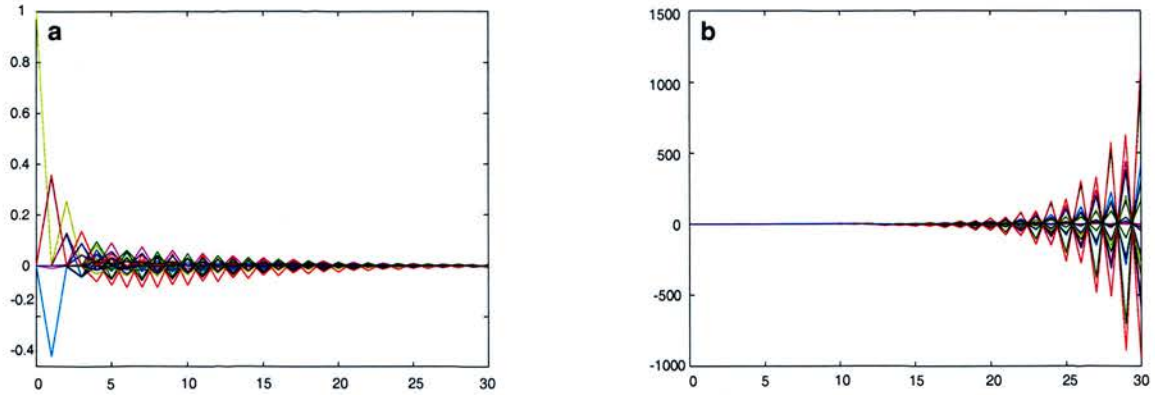

Figure 6.5: Typical activation of the matching network when no sigmoidal function is applied. Oscillations in an unconstrained network depend on the values of the weights. Here, the initial input is provided by unit 6. Absolute weight values (a) w = 0.35; m = 0.36; (b) w = 0.35; m = 0.65. Each plot shows the activation of a unit over time; X-axis denotes time and Y-axis denotes activation. The activation of every area is shown in a different colour. (a) If the weight values are too low to instigate a self-sustaining pattern, oscillations tend to decrease rapidly. (b) If weight values are high enough however, the oscillations will increase exponentially.

6.4.2 Setting weight values (calibration II)

Both matching and long-delay networks were characterised by a range of values (within the upper and lower limits) suggested by McIntosh et al. (1996), for weak and medium path coefficients. Therefore, weak values were specified as either 0.1 or 0.35, while medium weights were either 0.36 or 0.65, resulting in 4 combinations of weight values. Only the higher values (0.65 for the medium weights with either 0.1 or 0.35 for the weak values; more likely to be the latter) could produce sustainable activity in the network with some, but not all, inputs. Thus, the activity pattern in Figure 6.6a was only evident with values of w = 0.35; m = 0.65 while weaker values of w = 0.1; m = 0.65 failed to produce sustainable activity. Likewise, while units 1, 2 and 10 were recruited with weaker combinations than specified in the legend (namely: w = 0.1), units 3, 4 and 11, which echoed the activity in the dominant sub-network, were only recruited with stronger weight values of w = 0.35 and

m = 0.65. Therefore, I chose the absolute weight values of w = 0.35 and m = 0.65 as defaults for the remainder of this chapter (as well as for chapter 7), unless otherwise specified.

6.5 Activity patterns in the matching network (experiment 1)

6.5.1 Characterising activity in the matching network

To activate the matching network, initial input was provided by one element of the vector $\mathbf{a}_0$ (one unit) at a time. The activity of the network was then characterised by testing which elements or units are likely to be co-active. The nature of this coupling was captured in oscillations across several units. In the minimal case of co-activated units, the oscillations occur in left prefrontal areas BA46 and BA10 (units 1 and 2) and left anterior cingulate, BA24 (unit 10); see Figure 6.6b. This triangular loop could also be excited by input from visual areas by initially activating either unit 6 (Figure 6.6a) or contralateral unit 17 (not shown), which represent either left or right fusiform (BA18v) respectively. Despite this triangle forming an entirely excitatory loop, they exhibit an oscillatory activation pattern, which is a result of the initial activation (from one unit only) and the discrete (stepwise) update function. Thus, if for example only unit 10 is initially active, it will excite units 1 & 2 but not receive any input from them until the next update step and in the absence of concurrent input will be turned off. In the next step, units 2 and 1 will excite 10, yet their activation will return to zero in the absence of concurrent input from unit 10. If these areas are activated at the same time however, they will be co-active at the maximum value of one.

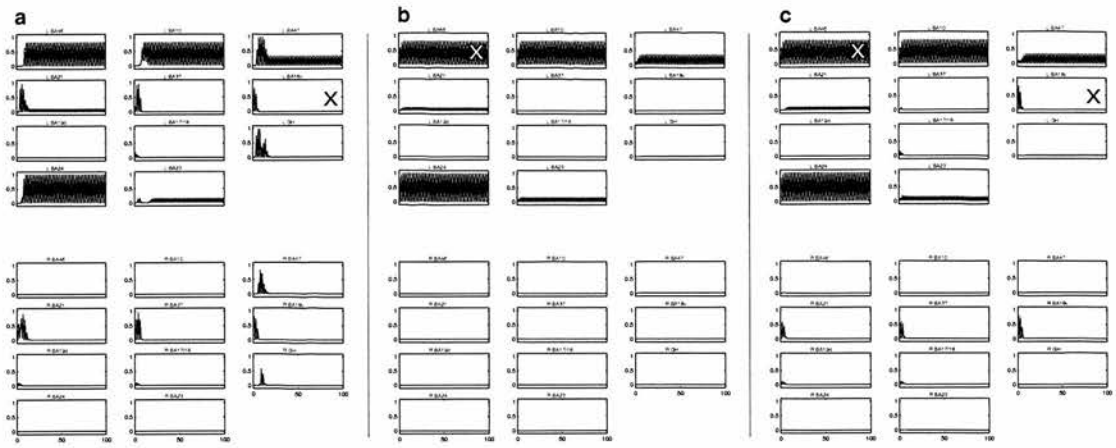

Figure 6.6: Characterising activity in the matching network. Three examples are shown, generated by different initial conditions. (a) The matching network can be activated by initial input is provided by unit 6 (fusiform), representing left BA18v (the input unit is marked by X here and in subsequent plots). This causes a short burst of activity in different units of the left (top right) and right (bottom right) hemispheres. (b) The initial input generates an activity pattern that recruits the 3 main units in the basic network, i.e. units 1, 2 and 10, which start oscillating. Subsequently, units 3, 4 and 11 echo this activity. (c) For comparison purposes (with the inputs to the long-delay network) both units 1 and 6 are initially active. This does not appear to change the activity pattern substantially, apart from reducing the transients in some units (e.g. units 3 and 9). Absolute weight values used in all plots: w = 0.35; m = 0.65 (default).

Since activity propagating from the left fusiform, BA18v (unit 6), will invariably pass through BA37 (unit 5) and BA24 (unit 10), we could expect these two areas to be the weakest links in the activation of this network. Namely, we may expect that change in their activity will have the most significant effect on the characteristic behaviour of the network (see section 7.3.3.1).

6.5.2 Identifying the minimal sub-network

To test which units were necessary (or sufficient) for production of these activation patterns, I isolated the units that participate in both patterns: the second pattern (Figure 6.6b) forms a closed excitatory loop and can develop and persist while all other units are set to zero. The first pattern, however (Figure 6.6a), is more widespread. When either unit 6 or 17 alone are initially active, the initial transient in an extended network is rapidly translated into activation in the primary cluster. I believe that the initial transient and persistent oscillations are independent patterns, with certain areas, especially unit 3, participating in both patterns.

The default weight values do not support the recruitment (activation) of the dominant sub-network with initial inputs from areas that are not part of, or related to, the dominant sub-network. However, due to the extended connectivity in both the matching and the long-delay networks, initial input from areas that may form separate clusters within the right hemisphere for example (such as units 22, 12 and 13 in the matching network) can engender activation of most units in the network if excitatory connections are strong enough (50% increase; data not shown). Invariably, the dominant sub-network is recruited because of higher weight values. Still, even when all units showed persistent oscillations, bilateral visual areas were silent due to the dearth of recurrent connections back to those units.

6.5.3 A summary of results and interim conclusions

This pattern of activity in the matching network led to several conclusions. First, observable and persistent activity in this network originated either in left fronto-limbic sub-network or in the extended network associated with either left or right fusiform (units 6 or 17). Second, the activity in the latter regions is closely

coupled by mutually excitatory connections. Through them, activity propagates to both left and right hemispheres. Interestingly, both in the matching and the long-delay network, these areas are reciprocally excitatory with medium strength connections. The other mutually excitatory couplings occur intra-hemispherically, for example, between units 1, 2 and 10 in the matching network. Further, inter-hemispherical excitation is more frequent in the matching (compared to the long-delay) network and therefore the dominance of the left-hemisphere in this network is somewhat unexpected.

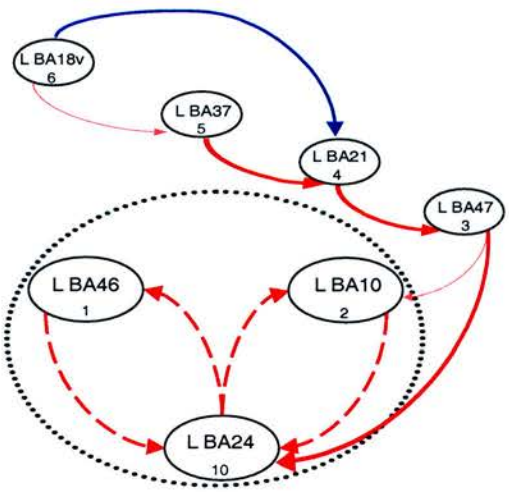

Figure 6.7: The minimal matching network: units necessary for creating the characteristic activation in the matching network. The dominant pattern of activity in this network consists of left frontal areas BA46 and BA10 (units 1, 2) which both send and receive excitatory input from the left anterior cingulate, BA24 (unit 10). This sub-network is excited by the ventral visual stream in the left hemisphere, originating in the fusiform BA18v, proceeding through BA37, BA21, BA47 and activating the dominant sub-network owing to a weak excitatory connection to BA10 and a medium excitatory connection to BA24. Area names appear above the unit number (see Table 6.1 and Figure 6.2 for conventions). Red lines represent excitation (a darker shade and thicker lines depict stronger weight values) and blue line represents inhibition. The dotted lines among the excitatory sub-network comprised of units 1, 2 and 10 (circled), indicating areas that oscillate together.

Dynamical activation of the matching network allowed me to evaluate a range of possible behaviours and achieve certain decisions regarding the activation parameters such as configurations of weight values, input patterns and the use of a squashing function. Furthermore, setting these parameters revealed a number of interesting behaviours, such as the possibility of creating self-sustaining activity in this network and the interactions or co-activation of specific clusters.

6.6 Activity patterns in the long-delay network (experiment 1)

Studying the long-delay network was more pertinent to the questions I wished to raise in this thesis, since working-memory deficits are classically associated with depression. The study of the matching network enabled comparison of both the common and unique properties of these networks. The study of the long-delay network is therefore based on the investigation of the matching network as well as expanding upon them, guided by the neurobiological and the neuropsychiatric questions. In the next chapter (section 7.6), a number of techniques in the study of the interaction of specific constituents of these networks will be presented.

6.6.1 Characterising the long-delay network

Unlike the perceptual-matching network, where the dominant sub-network was fairly isolated and the pattern of activity in this network was self-sustaining, the long-delay network appeared to be characterised by a more distributed activity pattern that included more areas and was thus less vulnerable to disruption. Here, an excitatory triangle of the dominant sub-network, analogous to the matching network, consists of units 3, 4 and 5 (Figure 6.9).

Likewise, oscillations occur as a product of the discrete activation and update function. However unlike the matching network, the activity here is closely coupled with the anterior cingulate (BA24; unit 10) and prefrontal areas (BA46 and BA10; units 1 and 2), as well as the hippocampus (GH; unit 9). To compare the activity in the matching and the long-delay networks and to express the essentially visual paradigm on which this model was based (Haxby et al., 1995), the fusiform (BA18v; unit 6) is initially activated and therefore included in the dominant sub-network.

The same characteristic activity as the control case (Figure 6.8b) pattern can be triggered by initial input from any of the 3 constituents of the dominant sub-network, namely left BA47, BA21 and BA37 (units 3, 4 and 5 respectively), the contra-lateral (right) area BA47 (unit 14) or left BA24 (unit 10). To compare visually-triggered activity in the matching and the long-delay networks, units 5 and 6 are set in $\mathbf{a}_0$ (Figure 6.8c), since BA18v (unit 6) alone is unable (Figure 6.6a) to trigger self-sustaining activity (see methods).

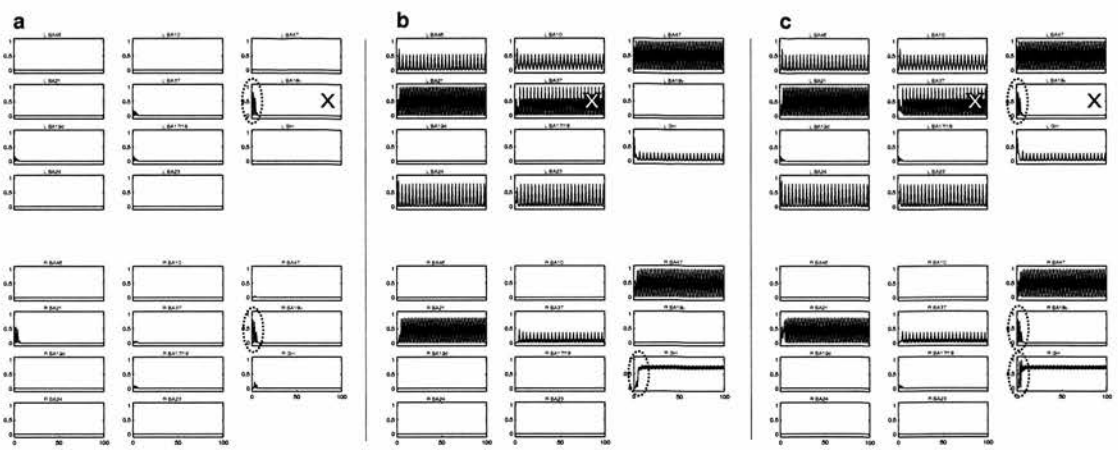

Figure 6.8: Typical activation patterns from the long-delay network. (a) Input from area BA18v, unit 6 and (b) BA37, unit 5. (c) Finally, a combination of both these inputs triggers a similar pattern to (b), with initial transients, such as those seen in units 6, 17 and 20 (dotted circles), associated with the visual input only (a).

6.6.2 Identifying the minimal sub-network

On the basis of observing activity in many trials, I have determined a minimal network that seems dominant. The minimal constituents of the long-delay network included a number of loops characterised by feedback connections. Here, as in the matching network, oscillations can be restricted to 3 mutually excitatory units, namely 3, 4 and 5. The sustainable activity in this dominant network can be triggered by one of these units and maintained while all the other units are silenced. However unlike the persistent pattern of activity in the matching network, the activity of the minimal long-delay network (Figure 6.9) cannot be triggered by the visual path (with initial input from unit 6). Furthermore, the relative contribution of each constituent of the minimal-network to the overall pattern cannot always be observed by visual inspection alone (see section 6.6.3).

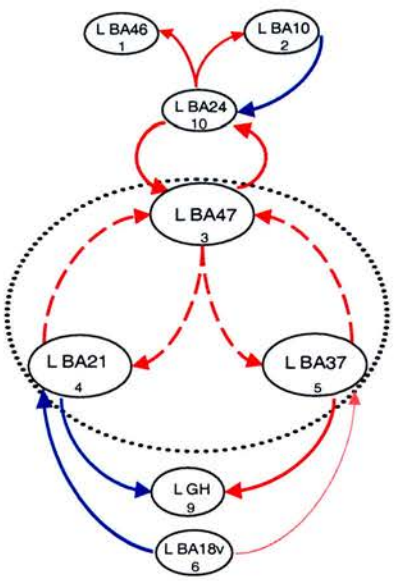

Figure 6.9: Minimal number of constituents participating in the activation of the long-delay network. Recurrent loops include the basic sub-network (units 3, 4 and 5), extending to fronto-limbic areas (units 10, 1 and 2) as well as hippocampus (unit 9). The activity in these recurrent loops cannot be triggered exclusively by the fusiform (unit 6), however this area is participating in the network by providing initial activation, together with one of the minor constituents of the dominant sub-network (unit 5; see Figure 6.8). See Figure 6.7 for conventions.

6.6.3 Outlining activity using phase plots

Figure 6.10 shows two plots that are seemingly identical (both include only units 1 through 10 of the network; units 11-22 are always silenced). However, while in (a) the visual units 6-8 are active, in (b) they are reset after every time-step. The activity in units 2 and 9 (BA 10 and left hippocampus respectively) appears to have a similar periodicity, yet the oscillations are somewhat irregular. Furthermore, the activity in BA47 appears to be unrelated to either of those. Visual inspection alone clearly could not distinguish between the two. Therefore, I used phase plots to chart the activity of these 3 areas against each other. This method allowed me to examine the activity of 2 pairs of units simultaneously, leading to the conclusion that the relationship between units 9 and 1 mirrored the relationship between 9 and 2 (Figure 6.11a). Detailed examination of the activation values in units 1, 2 and 9 revealed a dominant periodicity of 18 (twice the number of arms in Figure 6.11b).

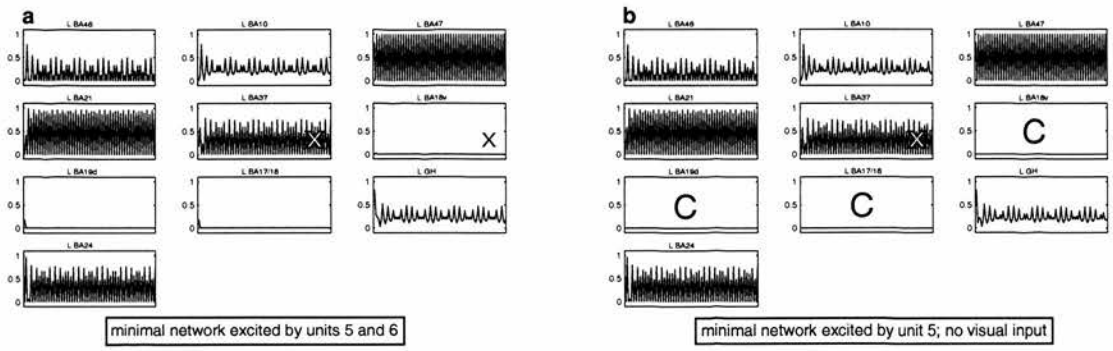

Figure 6.10: Minimal constituents of the long-delay network. Only units 1 through 10 are active, while the rest (11-22) are reset at every time-step. (a) Initial input from units 5 and 6, or (b) by unit 5, where activation of visual areas (C represents clamped units 6-8, where the activity is set to 0) is reset at every time-step. Default weight values are used in these experiments (see Figure 6.6 for conventions).

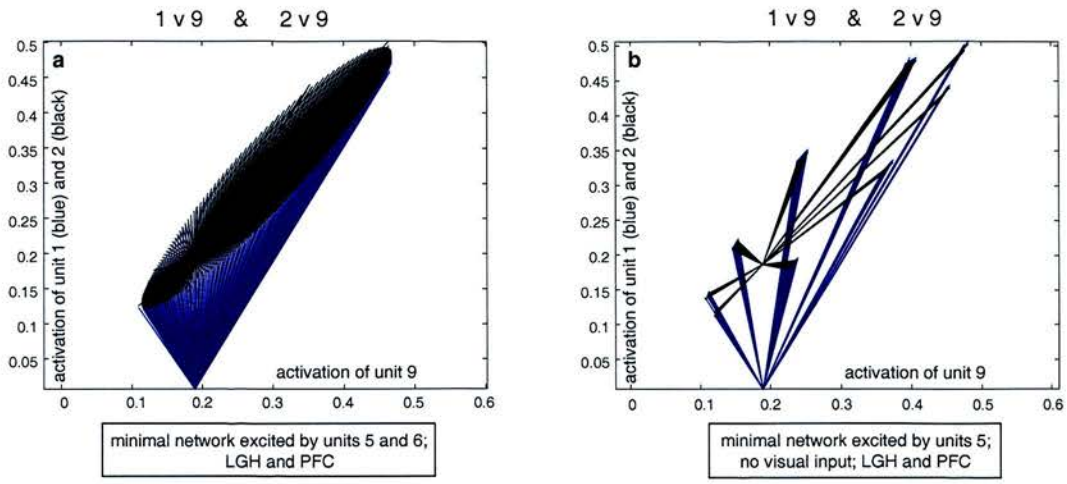

Figure 6.11: Phase plots of the activity in units 1, 2 and 9, which were plotted against time in Figure 6.10. The activity of the left GH (unit 9) is plotted along the X-axis, against BA46 (unit 1) and BA10 (unit 2). (a) Visual units can participate in this activity pattern or (b) are reset to zero at every time-step. The activity plotted here is for iterations 20-1000, ignoring initial transients.

Comparing the periodicity of unit 9 with units 1 and 2, to the periodicity of unit 9 plotted against every other unit (units 3, 4, 5 and 10; Figure 6.12) in the minimal network (excluding the visual units), we can see that this relationship is unique. Although both units 1 and 2 are excited by unit 10, the relationship between unit 10 and unit 9 (Figure 6.12d) does not resemble the interaction between the prefrontal areas (units 1 and 2) and the hippocampus (unit 9). Moreover, it appears that the activity in unit 3 (Figure 6.12a), which was chosen to represent all three frontal areas (Figure 6.1), does not resemble units 1 and 2.

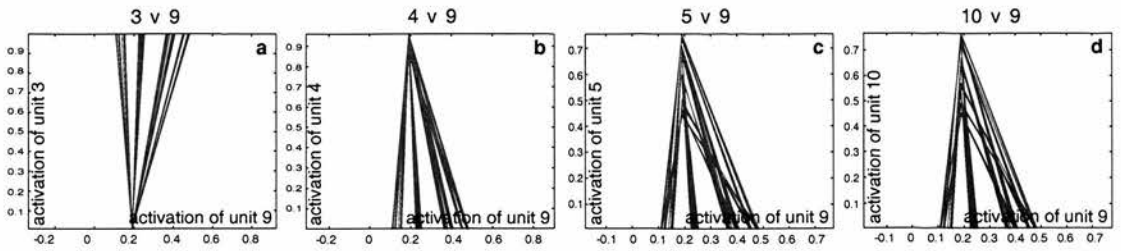

Figure 6.12: Corresponding activity in unit 9 and 4 other units in the minimal network. Phase plots of the activity of unit 9 against the activity in units (a) 3, (b) 4, (c) 5 and (d) 10. The activity of unit 9 is plotted along the X-axis. These plots correspond to the activity of individual units in Figure 6.10b.

The autocorrelation function measures the correspondence between two copies of the same signal shifted relative to each other. Peaks in the autocorrelation function at a given time-lag indicate periodicities at a certain interval. The periodicity of 18, revealed by the autocorrelation function (Figure 6.13), supports the periodicity observed in the examination of activation values of these units over time (directly reflecting the activation in Figure 6.10). This long periodicity reflects the complex nature of interaction in the long-delay network.

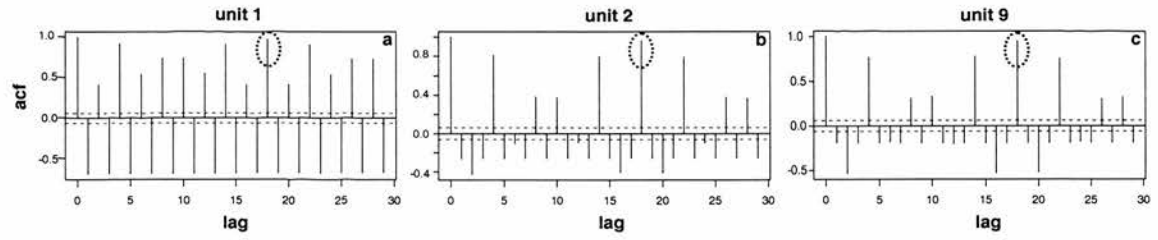

Figure 6.13: Autocorrelograms for the activity of three units (1, 2 and 9) in Figure 6.10b. This operation showed that in all three units the highest peak (periodicity) beyond the zero lag, is found at 18 (circled). The Y-axis represents the autocorrelation function (acf), showing both positive and negative correlations while the lag is plotted along the X-axis. The dotted blue line around 0 depicts the 95% confidence intervals, i.e. correlations within these bounds could have occurred by chance.

Discussion

Dynamical activation of the effective connectivity models suggested by McIntosh et al. (1996) highlighted fundamental differences between the networks characterising 2 experimental conditions in the delayed match to sample task. While constructing these models, certain assumptions or choices have often involved compromises, e.g. restricting the range of all possible values. For example, instead of using the range of values suggested by McIntosh et al. (1996) to encode path coefficients, I focused my efforts on the upper and lower limits of this range.

6.6.4 Summary of main findings

My network studies have shown the following

1. The matching network can be activated by direct input from either right or left fusiform (areas 6 or 17), while the long-delay network requires input from the prefrontal cortex, temporal regions or anterior cingulate. The activity of both networks however, appeared to be focused in the left hemisphere, thus refuting the expectations (hypothesis 1a) for a more balanced inter-hemispheric pattern in the matching network.

2. Further to the propagation of activity described in point 1, the dominant cluster in the long-delay network is more expanded than in the matching network. It includes more units, which are connected in a recurrent fashion through several feedback loops. Conversely, the matching network has a more feed-forward architecture, transcending the ventral visual stream and triggering activity in one dominant excitatory loop. This confirmed hypothesis 1b.

6.6.5 Caveats

Many of the parameters of this model had to be guessed (such as a limiting function) or approximated (such as the choice of weight values). Therefore, some of the behaviours of these networks are a product of imposed decisions. Nonetheless, the aim of revealing whether characteristic behaviour was fundamentally different in these two networks has been achieved.

The more general question is how long we would expect activity to persist in these networks with presentation of only one input. For example, the matching network is only supposed to perform a comparison with minimal involvement from PFC. However, PFC appears to be recruited almost instantly and the activity in this cluster persists beyond what I would expect visual activation to be associated with. By contrast, the long-delay network is expected to support maintenance and storage of patterns, perhaps by maintaining persistent activity and therefore, the sustained oscillations we observed in this network are not surprising.

Since I had limited expectations of the shape of activity, the assessment of activity in the network was defined as a measure of co-activation or functional clustering among units. Further experiments (chapter 7), testing the vulnerability of these networks to changing excitation or inhibition, can further highlight their unique architecture, through perturbation and compensation for both local and global deficits.

6.6.6 Neural context

McIntosh et al. (1996, 1999) suggested that finding specific regions related to task performance may be achieved through studying their interactions with other brain regions. This was termed the 'neural context' that supports observed behaviours.

This model supplements information available through simply observing the task-related neural activity highlighted by PET. In the framework of my thesis, this modelling project examines the mood-related neural context of activity in these networks. In this case, the neural context will be set by the clinical state of patients with major depressive disorder. Thus, ideas guiding the exploration of activity in illness-related brain regions (such as the anterior cingulate) and the investigation of their specific role of these regions in a task-associated neuronal networks (the matching and long-delay networks), were juxtaposed.

6.6.7 Solving the task

Although this model was not designed to study how the delayed match to sample task could be solved, this paradigm encoding the connections in the matching and long-delay networks (McIntosh et al., 1996) suggested several differences between them. These, in turn, may show how these networks are able to solve the delayed match to sample task. Naturally, the results presented here and in the next chapter can be evaluated only within the limits of the present modelling framework. Creating self-sustaining activity in the matching network for example, is superfluous to the recognition task this network is putatively specialised for. This paradigm allowed me to group and classify the minimal clusters. However, these networks (especially matching) do not need to maintain this activity over time. Further, it is unreasonable to assume that the activity is a product of only one input. This was an imposed parameter, to enable understating the minimal interaction in this complex structure.

Nevertheless, if we can accept that activity in the matching and long-delay networks is qualitatively different, I would suggest that the significance of the

prefrontal-cingulate loop (the dominant sub-network) may suggest the dissociation or transition between the straight-forward matching task (the initial burst in both hemispheres; Figure 6.6a) and the recruitment of frontal areas to account for the increased working-memory load, associated with different delays.

Further, I have suggested that persistent oscillations in the network are a product of the mode of input (a single unit set to 1 in $\mathbf{a}_0$) and the discrete update function. Nonetheless, one is tempted to relate the persistent activity among the closely coupled units 3, 4 and 5 in the long-delay network (Figure 6.10), to persistent activity recorded in the infero-temporal (represented here by unit 5) and prefrontal cortex of monkeys (Miyashita, 1988; Wilson et al., 1993). This persistent activity is thought to maintain familiar patterns in memory until a new stimulus is presented. This phenomenon was simulated previously with a recurrent neural-network architecture using biologically-plausible (integrate-and-fire) units that model neurons (Amit et al., 1994). The architecture used in the present study did not encode the activity of single neurons or even neuronal ensembles, and was based instead on an effective connectivity network describing this task in humans. However, dynamically modelling the coupling between areas the activity in the long-delay network seems to have captured the unique activation pattern associated with performance of the delayed match to sample task in non-human primates.

6.6.8 Comparing this approach with other modelling paradigms

Models of functional or effective connectivity are based on the analysis of both apparent and latent contributions to neural activity (Schumacker and Lomax, 1996), see chapter 3. This descriptive construct, however, has not been used to reproduce behaviour, unlike dynamical modelling paradigms such as Friston et al. (2003); see

chapter 3. Examining the connectivity patterns from a dynamical perspective can further the analysis of pair-wise interactions suggested by the network-analysis methods such as functional and effective connectivity.

The notion of modelling activity through dynamic representation of connectivity patterns, using the characteristic or representative features of task-related networks, has been addressed in this study. Unlike many artificial neural-network models of both psychiatric illnesses (e.g. Hoffman and McGlashan, 2001; Hoffman et al., 2001) and cognitive-tasks (Siegle, 1999) the units in this network represent task-associated neural activity or co-activation. Unlike biophysical models, which often endeavour to capture brain activity by including details at the molecular and cellular level (Amit and Mongillo, 2003), this model uses simple units that are controlled by an activation function and limited by a sigmoidal. It does not attempt to capture the activity of brain regions on a molecular level, since I believe that e.g. including ion channels in these units cannot help form a veridical representation of the summed activity in those areas. Arguably, some or even most of the findings in chapters 6 and 7 may be associated with the architecture and the parameter setting in these models. However, it seems that the behaviour of the networks is fairly robust within these bounds and furthermore, it is characteristically different in the matching and long-delay networks.

To conclude, the decisions that had to be made while setting up the framework for dynamic modelling of the effective connectivity networks (McIntosh et al., 1996) have highlighted a number of limitations of my paradigm. In turn, I believe that quantifying activation parameters and associating various values (e.g. weights) with specific behaviours made these networks more tangible and assured me that in the limited scope of my modelling paradigm, mindful of the reservations outlined in section 6.6.5, it is possible to characterise the behaviour of these network and predict

their response to changes in specific parameters on the basis of the typical behaviour described here.

Chapter 7 will therefore investigate the relative contribution of some of these parameters, such as the relative effect of excitation or changes thereof, on the typical behaviour of the network. These will map onto experiment 2 (which investigates hypotheses 3 through 5), outlined in section 6.2.1. In chapter 7, positive and negative path-coefficients will be discussed as if they represented excitation and inhibition in the network. It is not likely however that we can assume a direct correspondence between excitation and inhibition, with correlation or anticorrelations among units in the network (in the manner it is represented in the effective connectivity networks). I would like to stress therefore, that these are not taken as the direct influence of GABA or glutamate deficits in the depressed brain, but rather as coherent co-activation of network constituents.

Chapter 7

Physiology and anatomy of the matching and long-delay networks

7.1 Introduction

In the previous chapter, I described how the values of the experimental parameters in my modelling paradigm were set and characterised typical activity in the matching and long-delay networks. In this chapter I report different experiments, which were aimed at disrupting the characteristic activity in both networks and comparing the behaviour of these networks under different perturbations. In the following sections, I firstly summarise my results (see chapter 6), then describe the experimental framework and report my findings, separately for each network. This

part of the results (sections 7.3-7.5) will outline the "physiology" of the network, i.e. its behaviour under different parameter values. The latter part of this chapter (section 7.6) will describe the modelling analogue of examining the "anatomy" of the network. It will explore the possible delineations of different clusters based on the network's intrinsic properties (connectivity structure) rather than its dynamical activation.

7.1.1 Summarising interim results

Results so far (chapter 6) indicate the following general points:

Activity in the matching network (Figure 7.1a):

1. Activity in the dominant cluster (units 1, 2 and 10) is self-sustaining and does not require contribution from other units. This activity can be triggered by initial input from BA18v (visual unit 6).

2. The signal propagating from unit 6 activates the dominant sub-network, with only transient activity in the ventral visual stream (Ungerleider and Mishkin, 1982).

Long-delay network (Figure 7.1b):

1. The activity in the dominant cluster (units 3, 4 and 5) is self-sustaining and independent of other units. It can be triggered by a larger number of areas than the self-sustaining activity in the matching network (including units 10 and 14). It cannot however be triggered solely by an initial input from unit 6.

2. The long-delay network appears to include more feedback connections than the matching network and therefore can be expected to express a more robust, distributed pattern.

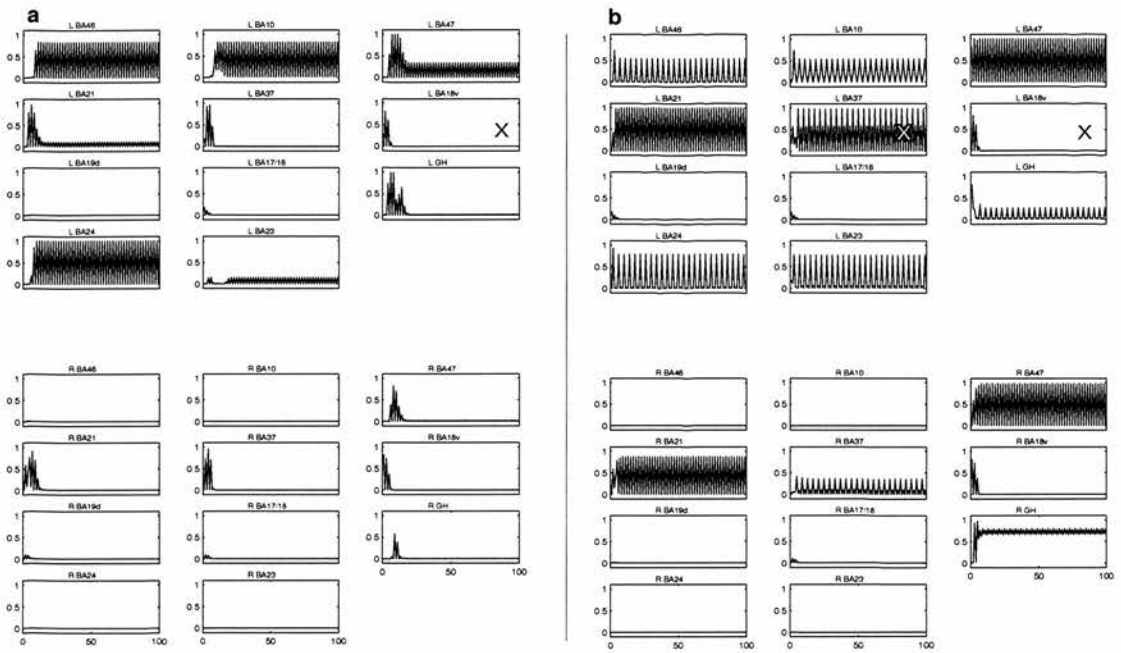

Figure 7.1: Characteristic activity patterns in the (a) matching and (b) long-delay networks. (a) The initial activation is provided by unit 6 in the matching network, where it is sufficient to trigger activity in the dominant sub-network. (b) Conversely, the same input from unit 6 alone in the long-delay network cannot trigger the activation of the dominant sub-network. Therefore here initial input is provided by both units 5 and 6. See Figure 6.6 for conventions. These characteristic patterns serve as the "control" or default patterns against which the experiments in this chapter will be compared.

7.1.2 Localised changes in the network

I wished to translate the deficits that were found in limbic areas of depressed patients, into a functional effect. For example, glial cell reduction in the pregenual anterior cingulate (Drevets et al., 1997) and metabolic reductions in dorsal anterior cingulate (Phillips et al., 2003) which appeared to normalise after successful

treatment (Kennedy et al., 2001), were represented through decreased output from unit 10, whereas hippocampal atrophy (Shah et al., 1998), was represented through decreased output from unit 9. Furthermore, since it is unclear whether structural abnormalities were indeed unique to these areas or whether localised atrophy may have been overlooked elsewhere, I investigated how a decrement in the efficacy of every unit (one at a time) affects network activity. To simulate the reduced effect of an area, I reduced the value of all its outgoing weights (both positive and negative) by some fraction. Default weight values were maintained throughout the rest of the network. The different perturbations to network activity have been performed on a unit by unit basis, both in the left and right hemispheres, however only changes to specific units in the left hemisphere appeared to have made a difference to network activity and therefore the apparent bias in my results can be attributed to the intrinsic properties of the network or its behaviour rather than to any prior decisions on my part.

7.1.3 Compensation

Depressed subjects often exhibit task performance or cognitive skills comparable to healthy control subjects (Grossman et al., 1994; Rogers et al., 2004) especially after remission (Phillips et al., 2003). However, neural activity deficits in key areas appear to persist beyond the clinical phase of the illness (Drevets, 2000b). Furthermore, as I found in the functional connectivity study (chapter 5), connectivity that may represent activity of specific areas is actually stronger in patients than in controls. This increased activity in depressed patients may represent an attempt to compensate for decreased activity elsewhere in the brain. Analogous results were reported by Della-Maggiore et al. (2000) where stronger cortico-limbic connectivity in older subjects suggested age-related deterioration in cognitive function. In the

present modelling study, after decreasing the weight output from BA37 (unit 5) and BA24 (unit 10), I examined the effect of increased activity in specific areas in compensating for these deficits. Compensation is defined therefore as restoration of sustainable activity in the network.

7.1.4 Visualisation of structural groupings

Several classification methods have been suggested to account for the functional organisation of brain regions into networks or functional clusters. Among them is the Multi Dimensional Scaling (MDS) technique. This method assesses the relative proximity or similarity between pairs of items in multi-dimensional space. Non-metric MDS has previously been applied to neuroanatomical data by Young (1992) and criticised by Simmen et al. (1994). The MDS method has also been applied to neuroimaging data by Friston et al. (1996), who related functional connectivity (correlations) to anatomical structure, using principal coordinates analysis (Gower, 1966). The Elastic Net algorithm (Durbin and Willshaw, 1987) takes an analogous approach to MDS, minimising the Euclidian distance between network constituents by re-ordering or clustering units that share similar properties (such as connectivity, or Euclidian distance), to other units.

In this thesis, I used a simple clustering technique to assess which functional clusters identified by the models presented here and in chapter 6, related to any groupings found by those clustering techniques. Thus, the clustering approach taken here complements the functional or activation studies in chapters 6 and 7.

Four separate results sections follow after an outline of methods. First, I will describe different perturbation procedures in the matching (section 7.3), long-delay (section 7.4) and both networks (section 7.5). These experiments investigate the

physiology of the network, since altering positive and negative weights in the network (termed excitation and inhibition), will engender changes in network activity or behaviour. The final results (section 7.6) examine the structure of both excitatory and inhibitory connections in the networks, relating this structural (anatomical) clustering to the functional groupings suggested by the functional experiments here and in the previous chapter.

7.2 Methods

7.2.1 Physiology of the networks

The second set of experiments (see section 6.3.2) explores the effects of global and local changes on the activity of the matching (section 7.3) and the long-delay (section 7.4) networks, using the following procedures:

1. Changing global values of either excitatory or inhibitory weights.

2. Isolating the relative contribution of specific units in the network to characteristic activity patterns, by decreasing the weights from specific areas to all other areas in the network, to simulate the effects of reducing the relative contribution of an area to the overall activity of the network (e.g. emulating significant structural or functional deficits in specific areas, that have been associated with depression). Thus, the reduction of the efficacy of specific areas is achieved, by changing elements of **W**.

3. Exploring the ability of specific units to compensate for a discrete reduction in the output of other areas may provide a quantitative underpinning for normal task in clinical populations in the presence of neural dysfunction.

7.2.2 Anatomy of the networks

The final phase of the analysis involved the examination of the intrinsic structure in the matching and long-delay networks. Areas in the 22 x 22 matching (Figure 6.3) and long-delay matrices were assigned a number in arbitrary order (albeit with some reference to topographical organisation) apart from separation of left and right

hemispheres. The same information (Figure 7.2) can be displayed in different ways. For example, permuting the order of the rows and columns (to allow grouping of areas that are closely connected) does not change the information in the matrix, however it may reveal additional information about possible functional relationships between adjacent units.

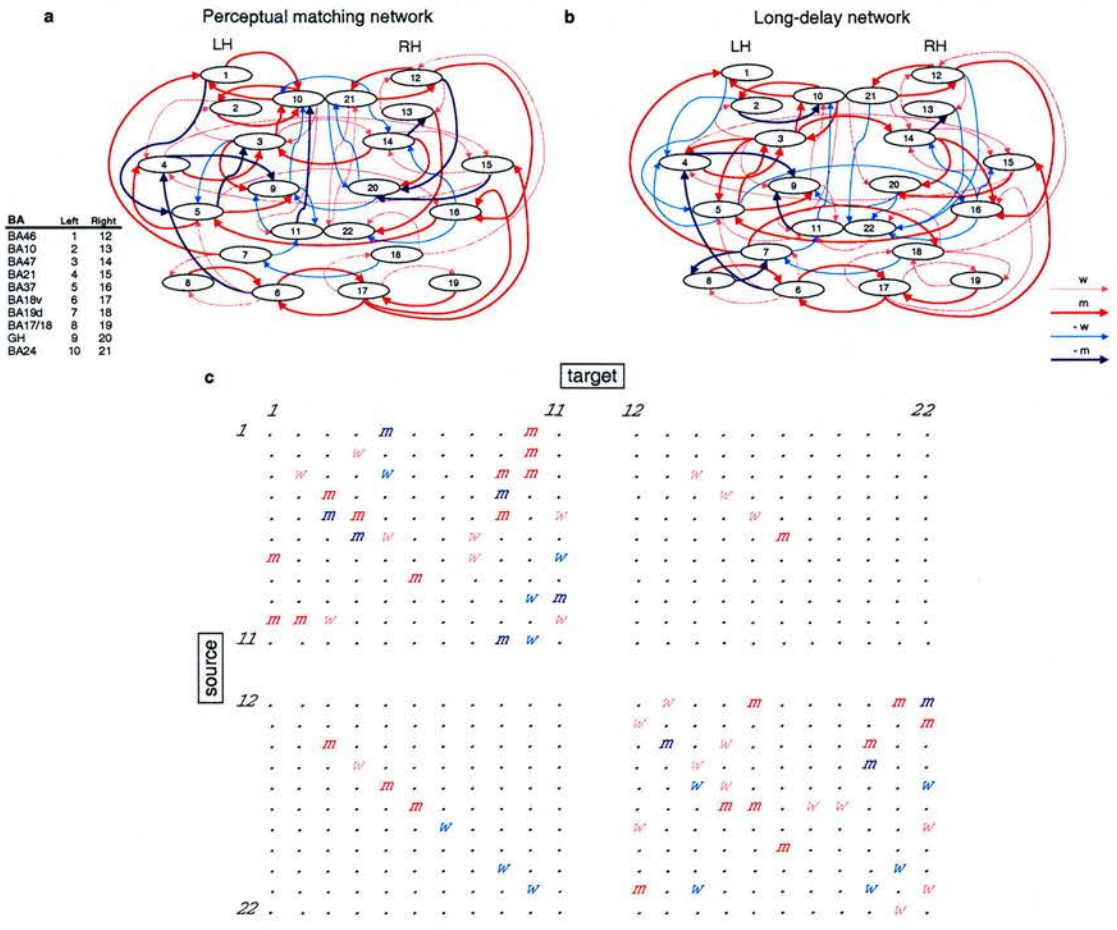

Figure 7.2: Connectivity diagrams of the (a) matching and (b) long-delay networks. The ordering of units, albeit arbitrary, is related to the topographical organisation (units are numbered in ascending order, from anterior to posterior direction). Excitatory connections are in red and inhibitory in blue. A darker shade denotes a stronger connection (higher weight value). (c) The matrix of connections equivalent to (a), using the same colour coding for positive and negative weights. Figure reproduces Figures 6.2 and 6.3.

To further our understanding of the functional groupings of units in these networks, two re-ordering algorithms were used. Both algorithms ignore the information regarding value of the weights and instead treat all non-zero connections as identical. First, the Reverse Cuthill-McKee (RCM) algorithm is an iterative process, which is intended to reduce the bandwidth of a matrix by pushing all the connections towards the diagonal axis. This effectively arranges reciprocal connections along the leading diagonal axis. Second, the Minimum Degree Ordering (MDO) algorithm accounts for extent connectivity (the number or degree of connections) of specific units and arranges the matrix in an ascending order of expansion (influence on other areas). Both algorithms are implemented in Matlab (www.mathworks.com). While the first algorithm can suggest functional organisation, I believe that the second highlights areas with the most extensive connectivity pattern and thus may suggest points of vulnerability, where localised deficits will cause the most disruption. Using these procedures to highlight functional clusters in both networks seems most effective when the excitatory and inhibitory connections are assessed separately.

Next, I will examine the effect of perturbation on the respective activity of the matching and long-delay networks. Modelling inhibitory and excitatory connections can in some sense emulate changes in excitatory and inhibitory dynamics in the brain. For example, decreased excitation can allude to decreased cortical excitability in depressed patients (Reid et al., 2002). Likewise changes in the efficacy of inhibition throughout the network can emulate increased cortical inhibition (Steele et al., 2000) or GABA deficits in depression (Leung and Xue, 2003; Kosel et al., 2004; Sanacora et al., 2004) and bipolar disorder (Krystal et al., 2002; Ketter and Wang, 2003).

7.3 Altering network connectivity: the matching network

The matching network appears to be more sensitive to changes in the efficacy of all excitatory connections (termed global excitation) rather than changes in the value of inhibitory weights across the network (global inhibition). Arguably, this may be attributed to the number of excitatory and inhibitory connections. Compared to 21 inhibitory connections (w = 12; m = 9), there are 46 excitatory connections (w = 23; m = 23). Therefore, we expected that any change in the global value of inhibition, will need to be stronger by (at least) a factor of two, compared to any change in global excitation to exert a similar effect on the whole network. Surprisingly however, contrary to hypothesis 5 (section 6.2.1), changes in levels of global inhibition had no effect whatsoever on the characteristic behaviour of the network (Figure 7.3).

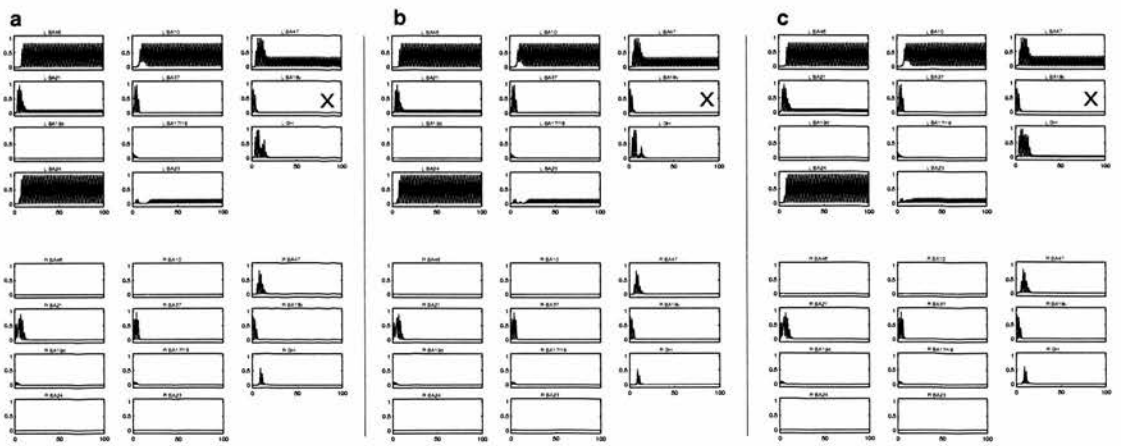

Figure 7.3: Changing the efficacy of inhibitory connections in the matching network does not affect the characteristic activity. (a) The control case, using the default weight values. (b) The value of all inhibitory (negative) connections is doubled, such that -w = -0.7 and -m = -1.3. (c) The value of inhibitory weights is reduced by 90%, such that -w = -0.035 and -m = -0.065. The excitatory connections are unchanged at the default values of w = 0.35 and m = 0.65.

7.3.1 Altered global excitation (experiment 2.1)

With stronger excitation, the dominant sub-network (Figure 7.4a) is more extended, recruiting left hippocampus (L GH; unit 9) and left posterior cingulate (L BA23; unit 11), which are mutually inhibitory. The activity depicted in Figure 7.4, shows how increasing excitation by 20% (Figure 7.4a-b) also increases the number of co-active units in the network, as well as the amplitude of the oscillations, until some units reach a steady state. Figure 7.4c shows how a small decrease (5%) in global excitation stops the characteristic activity pattern from developing. In the network associated with initial activation of the fusiform however (Figure 7.1a), a decrement of only 2% in excitation is sufficient to prevent the activity from propagating (data not shown).

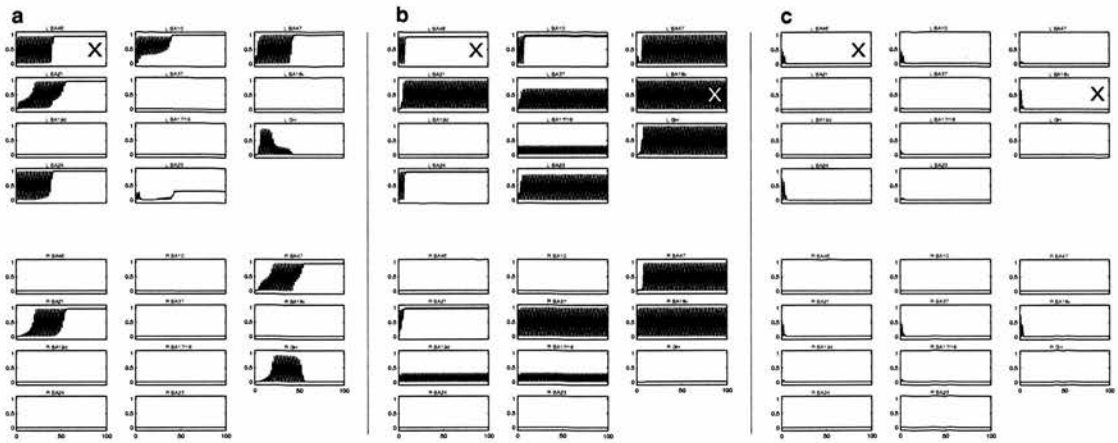

Figure 7.4: Changes in global excitation alter the characteristic pattern of activity in the matching network. (a) Increasing excitatory weights in the network by 20%, to w = 0.42; m = 0.78 causes transitory oscillations in the dominant sub-network. Thereafter, areas that were previously oscillating, as well as a few other contra-lateral areas, reach a steady state. (b) Combined initial inputs from units 1 and 6 change this pattern to some extent. For example, oscillations appear to persist in the hippocampus of both left and right hemispheres (units 9 and 20, where oscillations at very small amplitude are barely visible). (c) However, decreasing the excitatory weights in the network by 5% to positive values of w = 0.332; m = 0.617 suppressed activity in the dominant sub-network. Default inhibitory weight values remained unchanged.

7.3.2 Altered global inhibition (experiment 2.1)

Changing the value of only inhibitory weights in the matching network, e.g. doubling the negative weights to -w = -0.7 and -m = -1.3, did not appear to alter network behaviour. Likewise, decreasing inhibition in this network to one-tenth of its original values (90% decrease) did not affect network behaviour (Figure 7.3).

However, when excitation and inhibition were altered concurrently, varying inhibition subsequently changed the pattern of network behaviour. Furthermore, removing inhibition from the network entirely (negative weights set to 0) appeared to have an even greater effect compared to increasing the inhibitory weight values to -1. For example, with input from unit 1, if all excitatory weights were decreased by 4%, the characteristic oscillations in the sub-network of units 1, 2 and 10 disappeared. However, when inhibition was eliminated while excitation was still decreased (w = 0.336; m = 0.624), the usual pattern of oscillations was reinstated. Nonetheless, a different combination of positive weight values w = 0.12 and m = 0.78 (20% increase from respective baseline), which normally produced oscillations, was unaffected by large changes in values of inhibitory weights (either decrease to negative weight values of -1, or decrease to 0). Thus, this configuration appears to be even less sensitive to changes in inhibition (data not shown).

7.3.3 Localised changes in the matching network (experiment 2.2)

Modelling paradigms such as the one presented here allow us to quantify the effect of certain parameter values on the default behaviour of the network. In this instance, we have assumed that structural deficits imply a functional change in the behaviour of a unit, decreasing the output from the unit in question to the rest of the network. The ability to enumerate the discrete effects of these perturbations can suggest how

specific interactions may happen. For example, they may explain why the network is particularly sensitive to deficits in certain units and how these deficits can be corrected (through increased activity in other units).

7.3.3.1 Decreasing the efficacy of specific units (experiment 2.2)

The matching network is particularly sensitive to decreased weight value of 20% (output) from either BA37 or BA24 (units 5 and 10; Figure 7.5a and b respectively). These effects are in apposition to the absence of a notable effect while the weight value from every other source unit (one at a time) was either increased or decreased by 50%. The exception to this rule was area 4, where halving the weight output did not allow the activity to propagate to the dominant sub-network. Nonetheless, the sustainable activity in the network was more sensitive to decrement in the output from unit 10 than from any of the other units.

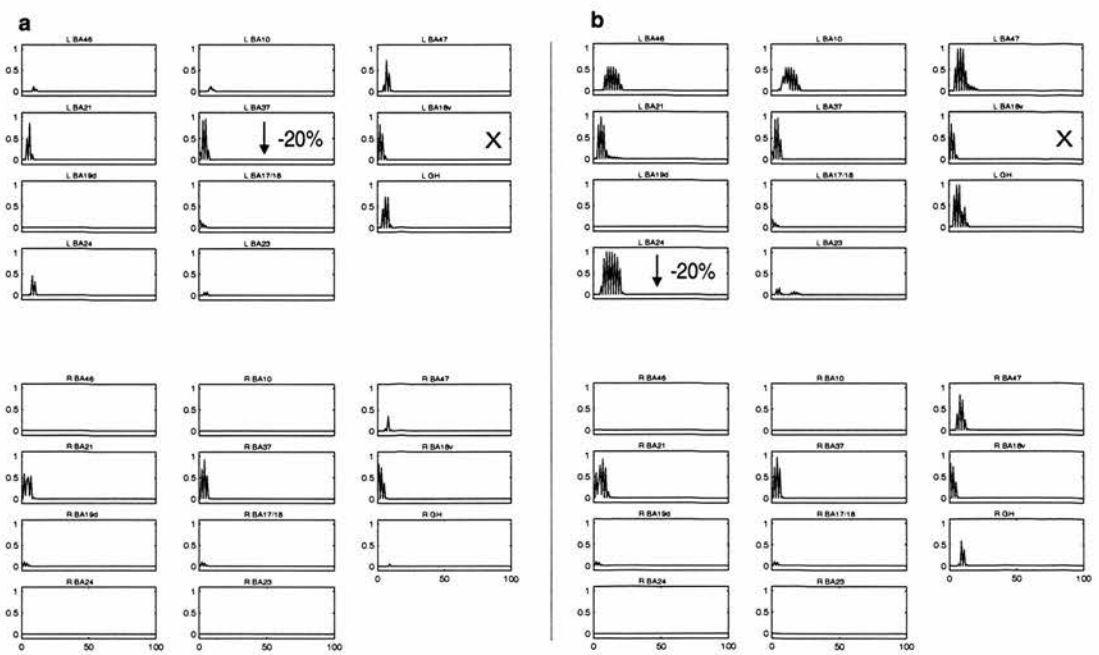

Figure 7.5: Activity fails to propagate through the matching network when the weights from (a) left BA37 (unit 5) or (b) left BA24 (unit 10), are decreased by 20%.

7.3.3.2 Compensation

Left inferior-temporal (unit 5) and anterior cingulate (unit 10) areas (BA37 and BA24 respectively) appeared to be the most vulnerable areas in the matching network (Figure 7.5). Namely, a relatively small decrement in the output from these areas prevented the characteristic, self-sustaining activity (Figure 7.1a), from developing. The critical role of both these units may be accounted for by their pivotal role in the propagation of activity. From an initial input provided by the fusiform (unit 6), activity propagates through a prominent input from inferior temporal BA37 (unit 5), allowing activity to propagate through temporal BA21 (unit 4) and frontal BA47 (unit 3), reaching the dominant sub-network, which includes frontal areas BA 46 (unit 1) and BA10 (unit 2), through anterior cingulate BA24 (unit 10).

Unlike BA24, where a decrement in its efficacy required a relatively large compensatory increment in output of other units in the network (such as an increase of 40% in the weight values from prefrontal units 1 or 2), reduction in activity of BA37 was relatively easy to correct for (probably because it is not included in the dominant sub-network or due to the distributed nature of this network). Namely, an increase of 10% in the output of one of several units (3, 4, 8, 15, 16 and 19) restored the characteristic pattern of oscillation. Likewise, an increase of 10% in the output of purely visual areas (units 6-8; Figure 7.6c) appears to restore the characteristic activity patterns and perhaps even over-compensate, whereby oscillations are now more widespread. Nonetheless, some areas fail to compensate for decreased output or weight values from these two units (5 and 10). For example, unit 1 cannot compensate for decreased weight values from area 5 (not shown) while unit 5 cannot compensate for the decrement in the weight output from unit 10 (Figure 7.6a).

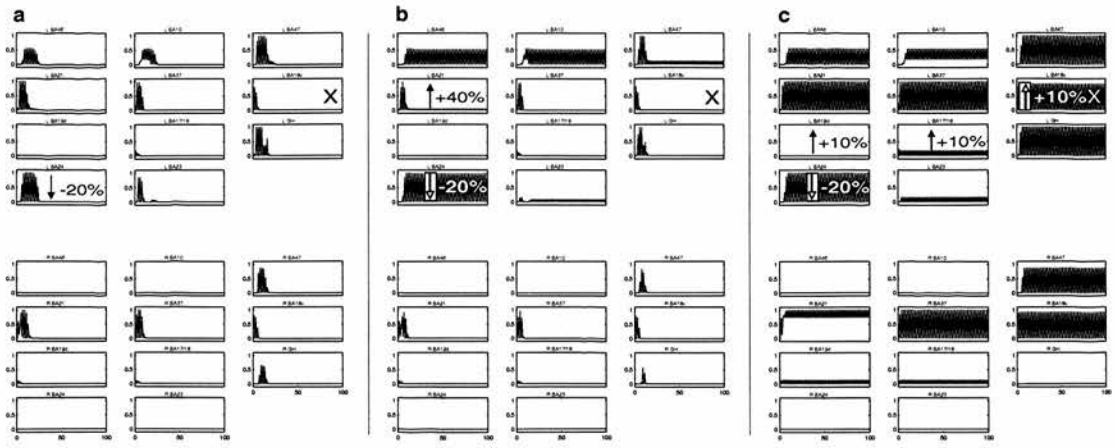

Figure 7.6: Compensating for decreased output from left BA24. The initial activation is provided by the fusiform (unit 6) while all output weights from unit 10 are decreased by 20%. (a) Doubling the output weights from area 5 fails to produce the expected pattern of oscillations. (b) Increased output by 40% from unit 4, restores the default pattern of activity. A similar effect occurred when compensating with either units 1 or 2 (not shown). (c) By contrast, a small (10%) increase in weight values from left visual areas (units 6-8), appears to overcompensate, producing oscillations in the dominant sub-network, but also in other units, unrelated to the original pattern.

7.3.4 Findings: the matching network

A number of interesting behaviours were revealed in the matching network:

1. Relatively small changes in global excitation affected the default behaviour of the network (Figure 7.4).

2. Inhibition does not play a key role in the activity of this network.

3. Left BA37 (inferior-temporal gyrus) and BA24 (the anterior cingulate) have an especially influential role in the activity pattern of the matching network (which is slightly more sensitive to decrement in the output weights from the anterior cingulate).

4. It is possible to compensate for decreased output from specific areas. Furthermore, BA37 is easier to compensate for than BA24.

5. An increase of 10% in output weight from visual areas (units 6-8, compensating for unit 10) is sufficient to restore (and perhaps over-compensate for) the default activation pattern. However, when compensation is provided by frontal areas (e.g. BA46 or BA10), an increase of 40% in the output weight values of these units is necessary to restore typical network activity.

7.4 Altering network connectivity: the long-delay network

Owing to the distributed pattern of activity in this network, changing global and local parameters did not create the extreme changes seen in the matching network.

7.4.1 Changing global excitation and inhibition (experiment 2.1)

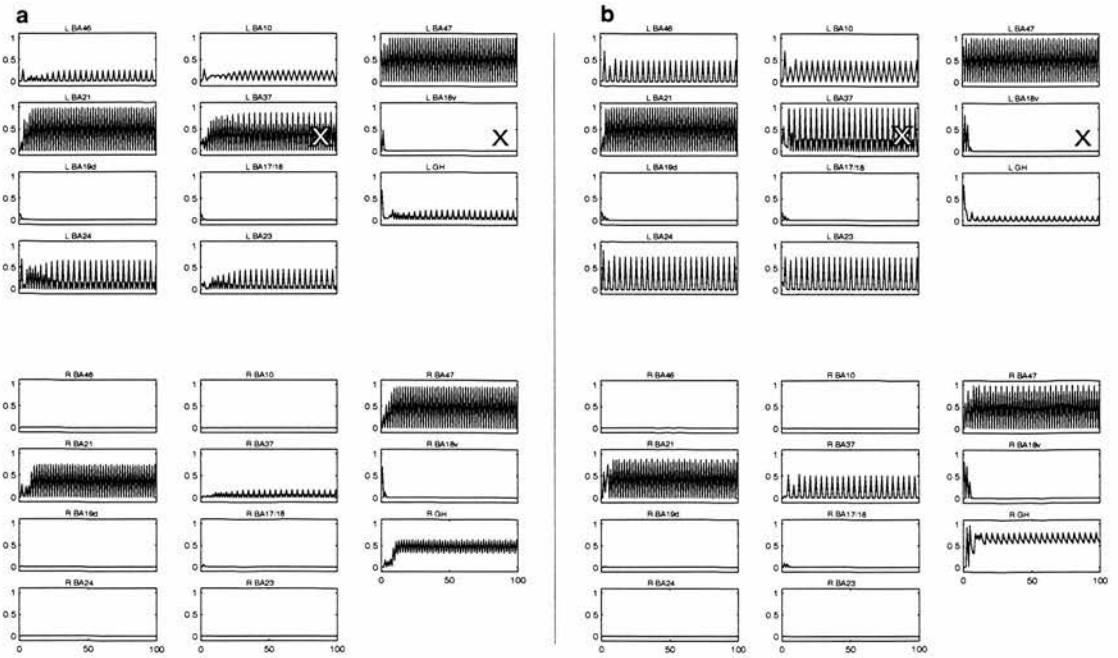

Figure 7.7: Decreased excitation (a) and increased inhibition (b) in the long-delay network produce little change to characteristic behaviour (Figure 7.1b). The typical pattern of oscillations (a) is slower to develop with decreased global excitation. Increasing global inhibition however, seems to affect the regularity of oscillations in bilateral hippocampi (units 9 and 20) most significantly. (a) Positive weight values were increased by 20% w = 0.315; m = 0.585. (b) Negative weight values were decreased by 50% to -w = -0.525; -m = -0.975. Negative weight values remain unchanged in (a), as do positive weight values in (b).

Increasing global excitation by 20% in the long-delay network increased the amplitude of oscillations or activated several areas at the maximum value of one. However, these oscillations did not extend to other units that did not participate in the characteristic pattern (Figure 7.1b). Moreover, unlike the matching network, decreasing global excitation did not have a similar catastrophic outcome (compare Figure 7.4c with Figure 7.7a).

Despite an initial disruption, after time-step 50 (about half-way along the X-axis), normal network activity has been reinstated. Increasing global inhibition by 50% seems to affect network behaviour by changing the frequency and/or amplitude of the characteristic oscillations (see for example unit 5, Figure 7.7b), where activity of both left and right hippocampi (units 9 and 20) may be particularly vulnerable. Decimating global inhibition (90% decrease) caused the amplitude of oscillations in all participant units to increase to the maximum (data not shown; see matching network, section 7.3.2, for comparison).

7.4.2 Localised deficits and the efficacy of compensation (experiment 2.2)

Using a similar testing procedure to the matching network (section 7.3.3.1), I tried to disrupt network activity by decreasing the weight values from one source unit at a time. However, unlike the matching network, even substantially reducing output from any unit by decreasing its output weight values did not prevent the characteristic pattern from developing. The effect of localised disruption (in the presence of global decrease in efficacy) in the matching and long-delay networks, may suggest that the compensatory strategy in the matching and long-delay tasks are different. This may be related to the compensatory strategies in depressive illness, where both the activity throughout the network is often suppressed

(Shajahan et al., 1999) and performance deficits associated with memory, when present, appear to be accompanied by an altered pattern of neural response (MacQueen et al., 2003).

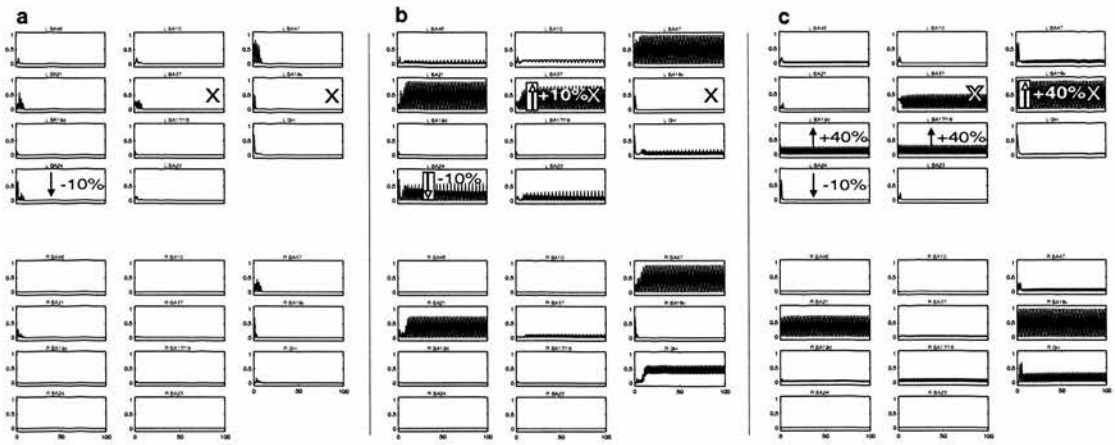

Figure 7.8: The long-delay network is vulnerable to (a) decreased output (weights) from anterior cingulate (left BA24; unit 10) by 10%. This only occurs when the excitation in the whole network is reduced by 10%, thus setting positive weight values at w = 0.315, m = 0.585. (b) Activity is resumed by increasing the weight values from one of the other areas in the dominant sub-network, such as BA37 (unit 5) by 10%. (c) However, compared to compensation for the disrupted activity in the matching network, weight values from the visual areas (units 6-8) need to be considerably higher (40%) than the analogous increase in (b), before the characteristic pattern is restored. Even then and similarly to the matching network, restoring self-sustaining oscillations by increased output from the visual areas appears to over-compensate.

Decreasing positive (with or without the negative) weight values throughout the network by 10% was followed by individually decreasing the weight values from every source unit, following the procedure described in the matching network (section 7.1.2). This highlighted the sensitivity of this network to decreased weights (representing reduced activation as a result of structural or functional abnormalities) from left BA24 (unit 10; Figure 7.8a) and surprisingly, the left GH (by 10% and 20% respectively).

The latter was unexpected because unlike the key participants in the dominant sub-network (units 3, 4, 5 and 10; all linked by excitatory reciprocal connections), the GH is excited by BA37 (unit 5) yet inhibited by BA21 (unit 4), two of the constituents of this excitatory network (see Figures 6.2 and 6.9). Furthermore, GH does not directly excite any of the constituents of this sub-network nor trigger the activity of this sub-network when it is set in $\mathbf{a}_0$. Nonetheless, an analogous decrement of 20% in weight values from any other source unit could not disrupt network activity.

7.4.3 Findings: the long-delay network

Further to the effect of global changes in excitation and inhibition on network behaviour, which are more constrained in the long-delay network due to its relatively distributed pattern, I would like to highlight the following phenomena:

1. Network activity is sensitive to disruption due to the effect of a single unit only in the presence of global decrease (-10%) in excitation. If default weight values are used (absolute values: w = 0.35; m = 0.65), even a large decrement in the output weight values does not affect the behaviour of the network.

2. Visual areas (units 6-8) can compensate more easily for decreased efficacy of the anterior cingulate (BA24) and inferior temporal gyrus (BA37) in the matching network (with a 10% increment), compared to their ability to compensate for the left anterior cingulate and GH in the long-delay network (requiring a 40% increment in their efficacy).

Sections 7.5.1-7.5.2 describe additional experiments performed on both networks, to prove that these behaviours can be generalised and are not unique to only a limited

range of weights and values of $\mathbf{a}_0$ (although values used here conform to McIntosh et al., 1996).

7.5 Specificity of parameter space determines activity patterns in both networks

7.5.1 The effects of initially activating several areas upon network activity

The cumulative effect of more than one input unit being set to 1 in $\mathbf{a}_0$ of the matching network, achieved the expected activation of either one or more sub-networks. Since the dominant force in this network is excitatory, no specific combination of initial activations could exert an inhibitory effect. In the long-delay network the activation of more than one unit changed the pattern of oscillations in the other units, however, this was typically expressed in the increase of either the amplitude or the frequency (or both) of oscillations. Interestingly however, if units 6 and 17 are co-activated in the matching network, the activity peaks and dies down very quickly (thus there is no chance for the activation of the dominant cluster to develop, since unit 4, which provides the link to units 1, 2 and 10 in the dominant sub-network (see Figure 6.7) is strongly inhibited by unit 6. Similarly, if an analogous co-activation of units 5 and 3 is set in $\mathbf{a}_0$ of the long-delay network, the frequency of oscillations in the dominant sub-network appears to be compromised to a certain extent (results not shown).

7.5.2 Testing the specificity of weight values in the matching and long-delay networks

Finally, to test the notion that activation in this network was uniquely linked to the specific weight values or range of values (upper and lower limits) set in the effective connectivity model, I tested the network with other combinations of weights, to see the effect that changing these values may have on network behaviour. Usually activity occurs with a combination of either w = 0.1 or 0.35 and m = 0.65. Decreasing these values by 0.05 stopped the characteristic activity patterns entirely. Therefore I would conclude that the dynamical activation of the network (subject to setting of the other activation parameters described in chapter 6) is dependent upon the upper limit of the specified range, while the lower limits cannot generate self-sustaining activity. Figure 7.9 shows the activation in the matching (a) and the long-delay (b) networks, with higher weight values. Increasing the weight values appears to recruit other units (that may belong to other clusters or sub-networks). However, when excitation in these networks is increased further, it is difficult to appreciate the more delicate interactions between different clusters since the activity is too widespread. Nonetheless, it should be noted that other aspects of network architecture (e.g. shape and limits of the sigmoidal) could be changed to restore characteristic activity after weights have been globally affected.

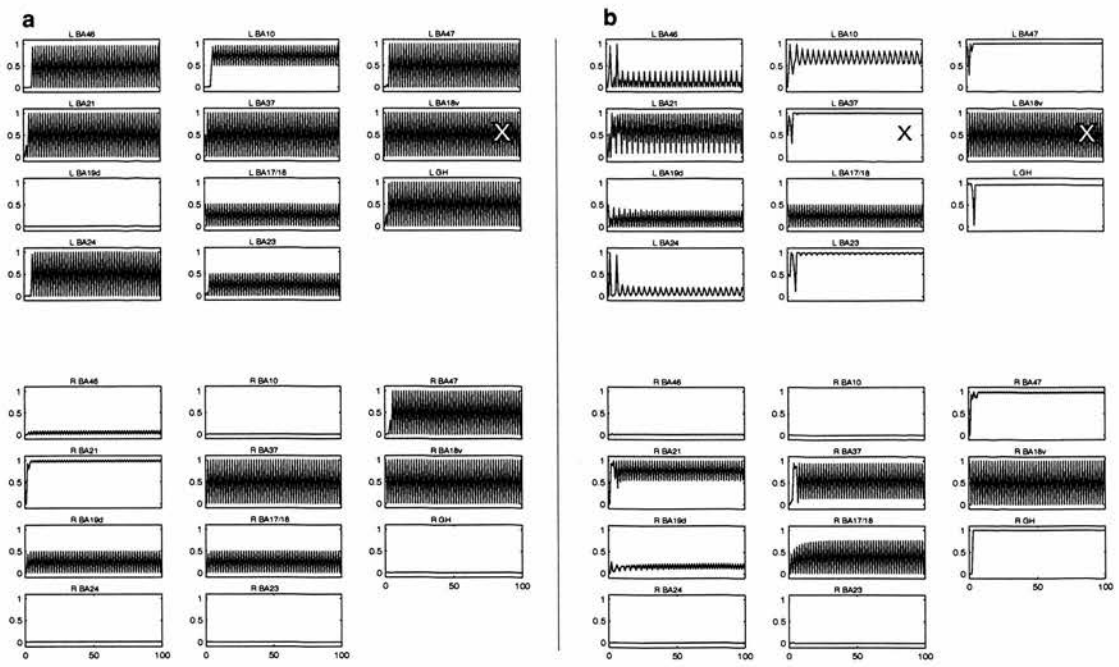

Figure 7.9: Testing the specificity of activation in the (a) matching and (b) the long-delay networks. Increasing the magnitude of all weight values in both networks extended the recruitment of units that were not normally activated by the default weight values. Absolute weight values for both plots: w = 0.5; m = 0.8.

Finally, section 7.6 suggests alternative techniques for evaluating activity in the matching and long-delay networks, based on the intrinsic (anatomical) connectivity patterns therein.

7.6 Clustering techniques: functional organisation?

The activity of the matching network was much less sensitive than the long-delay network to changes in the value of inhibitory weights despite the comparable number of excitatory and inhibitory connections in both networks. Several hypotheses could account for these differences:

First, I tried to establish if there was a difference between the overlap of excitatory and inhibitory connections in the matching and the long-delay networks. A significant difference could suggest that while the number of connections may be similar, the connectivity patterns may differ and therefore the loci of activity and overall network behaviour will invariably differ. Furthermore, if the degree of overlap were much higher between the excitatory than between the inhibitory connections, it may explain why excitation appears to affect both networks equally while inhibition does not.

Second, the distribution of either overlapping or disparate excitatory and inhibitory connections could suggest whether either polarity is clustered in specific regions of either network.

Third, the qualitative differences exhibited by these network may be related to the unique functional clustering in each. Specifically, the co-activation of clusters of units and the extent or nature (feed-forward or recurrent) of these functional clusters may explain their different behaviours. Table 7.1 provides a reference for the excitatory-inhibitory weight-ratio in the matching and long-delay networks.

Network	Excitatory connections (E)		Total (E)	Inhibitory connections (I)		Total (I)
	w	m		-w	-m	
matching	23	23	46	12	9	21
long-delay	25	24	49	14	5	19

Table 7.1: The number of excitatory and inhibitory connections in the matching and long-delay networks.

7.6.1 The overlap between excitation or inhibition in the connectivity matrices

Testing the first hypothesis presented in section 7.6, Figure 7.10 plots the location of excitatory connections (a) in the matching network, compared to (b) the long-delay network. Likewise, the inhibitory connections in the matching compared to the long-delay (c, d) networks are plotted. The number of non-zero (NZ) elements does not differ substantially between the respective excitatory and inhibitory connectivity matrices in either network, indicating that this is not an informative measure of functional clustering in these networks.

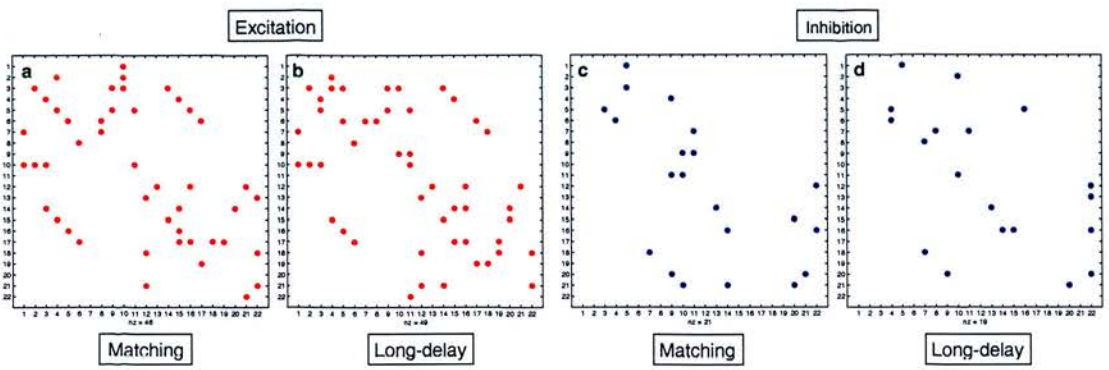

Figure 7.10: Excitatory and inhibitory connections in the matching and long-delay networks. The scatter plots show non-zero (nz) elements, for excitatory (a,b; depicted in red) and inhibitory (c,d; blue) weights in the matching and long-delay networks respectively. These plots do not differentiate between weak and medium connections. Area numbers are plotted along each axis with Y-axis representing the source area and X-axis representing the target area.

It seems therefore that the differences between these networks cannot be attributed to the ratio between excitatory and inhibitory weights, nor to the degree of overlap between weights of either polarity within these networks, since the ratio of

excitatory and inhibitory weights throughout the network is similar. The excitatory and inhibitory patterns do not overlap exactly, however differences between them seem minor. Furthermore, I do not believe that the distribution of weights (Figure 7.10) is informative.

7.6.2 Clustering in the matching network

The functional groupings observed in the networks may, to a certain extent, depend on the structural organisation of the network. In sparse matrices such as the matching and long-delay networks, it is often helpful to change the ordering of the rows and columns. This operation is aimed at grouping units that are closely connected, and reducing the band-width of the matrix by placing reciprocal connections near to the diagonal axis.

I expected clustering in the matching network to highlight mainly the excitatory cluster comprised of units 1, 2 and 10. Further, I expected this cluster to be related to the input from unit 6. These were indeed highlighted (Figure 7.11b). Examination of the matrix containing only positive values also highlighted a second cluster in the right hemisphere (Figure 7.11c). The highlighted clusters in the matrix of positive weights only (top left and bottom right), were functionally independent and were thus grouped by the clustering algorithm at either end of the matrix. However, re-organisation of the matrix with negative weights only did not highlight any functional clusters.

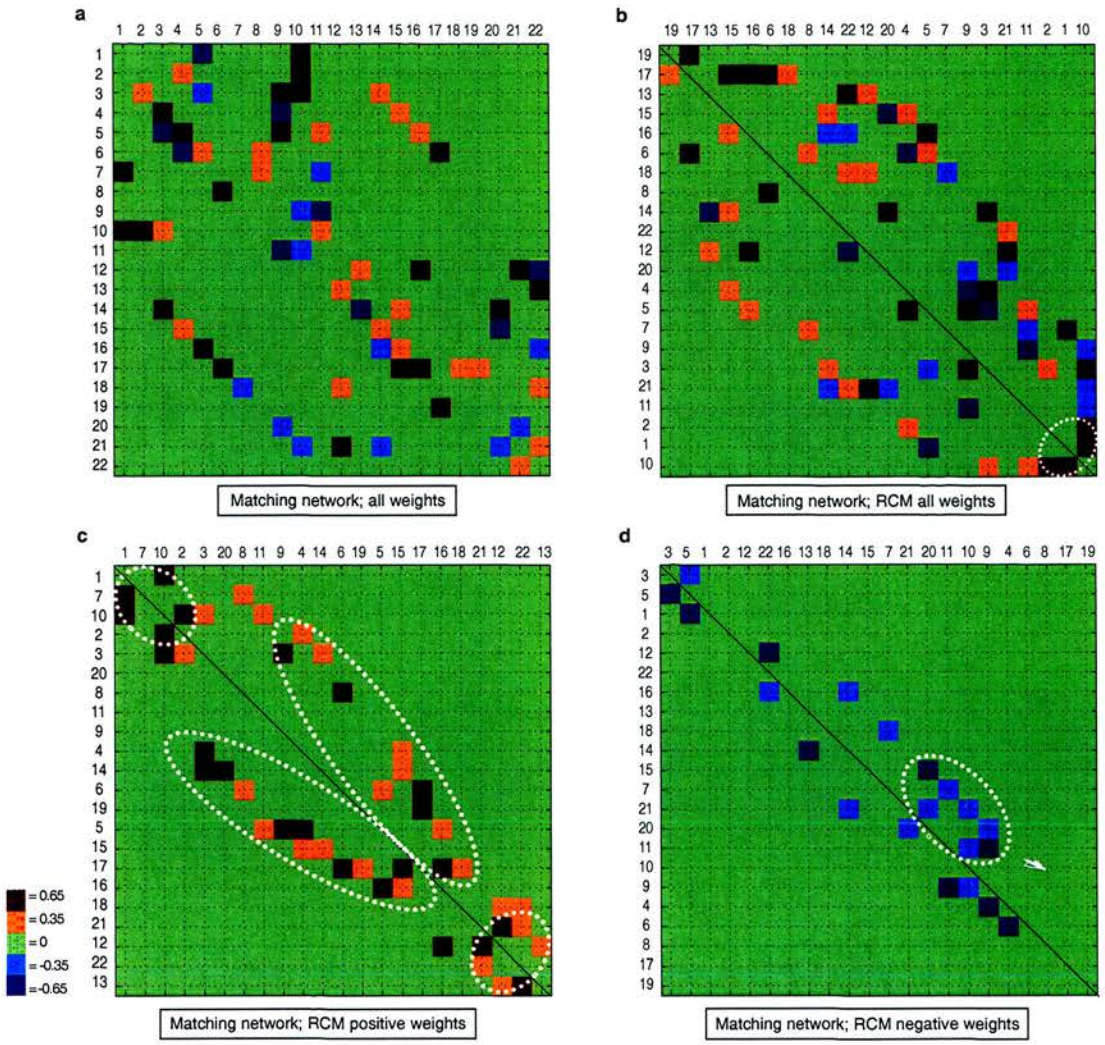

Figure 7.11: Re-plotting the matching network using the RCM algorithm. (a) All weights from the matching network; original arrangement of units. (b) When both positive and negative connections are arranged using RCM along the diagonal axis, the dominant sub-network is highlighted (white circle). (c) This classification hierarchy is preserved when only excitatory yet not (d) exclusively inhibitory weights are arranged along the diagonal axis, effectively reducing the bandwidth. Excitatory weights are depicted in shades of red, while inhibitory weights are in blue (indicated by a scale-bar). The relative arrangements of areas (numbered) appear above and on the left of each plot (see also Table 7.2). Other circled clusters are described in the text.

Grouping of the positive weights only also revealed two reciprocally connected clusters, either side of the diagonal line (Figure 7.11c). These units (circled in the centre of the matrix, outside the two main clusters) appear to mirror each other. To

the left (number of excitatory on the left central cluster NEL = 14; overall number on the left NEL = 24) and right (number excitatory right central cluster NER = 12; overall number on the right NER = 22) of the diagonal axis, expressing the clustering or similar connectivity patterns of neighbouring units. 6 reciprocal connections exist among units in the large clusters, whereas the small clusters on each side of them have 3 reciprocal connections each (12 in total).

Grouping of the negative connections (Figure 7.11d) highlighted a cluster (circled) to the right of the main diagonal, however distribution between left (number of inhibitory weights on the left NIL = 10) and right (number inhibitory right; NIR = 11) are fairly equal. When the RCM algorithm was applied to both excitatory and inhibitory units (Figure 7.11b) at once, most of the weight were on the right side of the leading diagonal (NER = 26; NIR = 14), compared to the left (NEL = 20; NIL = 7). It seems therefore, that the number of units on the right of the leading diagonal is considerably larger than the number of units on the left, even though the algorithm appears to have achieved its aim in reducing the bandwidth of the matrix. Nonetheless, there is no correspondence between the activity observed in the physiological experiments (chapter 6) and RCM clustering of both positive and negative weights (Figure 7.11b), while RCM using only positive weights (Figure 7.11c) was more successful.

Similar results were achieved with the MDO algorithm (Table 7.2). This algorithm grouped together areas units 5 and 10, whose efficacy was found to be most likely to disrupt network activity. However, other groupings observed from the physiological experiments have not been highlighted in this analysis.

7.6.3 Clustering in the long-delay network

When the RCM algorithm was applied to the long-delay network, groupings of units appear to be larger and both re-ordering algorithms (RCM and MDO) have highlighted them with greater success (Table 7.2). Although the 3 main units were not grouped together using the RCM analysis, the algorithm grouped together GH (unit 9) and several dominant areas (e.g. units 2, 4, 5 and 10). This area (GH) could not activate the network on its own, yet decreased weight output from it disrupted network activity if overall excitation was lowered. The MDO method also grouped together the most active units with GH (placing area 3 at the top of the ordered list, when the matrix containing only positive weights was ranked. The (secondary) visual input area (unit 6) was linked to the dominant activity cluster by the MDO examination of the matrix containing only negative weights.

Clustering only positive weights in the long-delay network (Figure 7.12c) reveals different characteristics to the matching network. First, a central cluster is highlighted, with 1 reciprocal connection. The large continuum of innervating areas are highlighted to the left of the diagonal (NEL = 17; overall number on the left NEL = 27). On the right, a cluster with a similar orientation has a much smaller number of connections (NER = 6; overall number on the right NER = 22). The clustering of negative weights in this network (Figure 7.12d) appears to have been most successful among all the examples above (both in the matching and long delay network) at reducing the bandwidth along the diagonal axis. There is little reciprocity among these connections however, and the left (NIL = 10) and right (NIR = 9) distribution is fairly equal.

The large elongated clusters either side of the diagonal have 3 reciprocal connections, with 3 more such connections remaining outside the highlighted areas. Finally, the clustering algorithm appears to have highlighted two large reciprocal

clusters (Figure 7.12b), which include units 10, 2, 9, 4 and 5. Surprisingly, unit 9 was included in this grouping, even though it appears to be outside the main excitatory loops. In the joint (excitatory and inhibitory) clustering map of the long-delay network, in contrast to the matching network, the weights were fairly evenly distributed either side of the leading diagonal (NEL = 23; NIL = 10; NER = 26; NIR = 9).

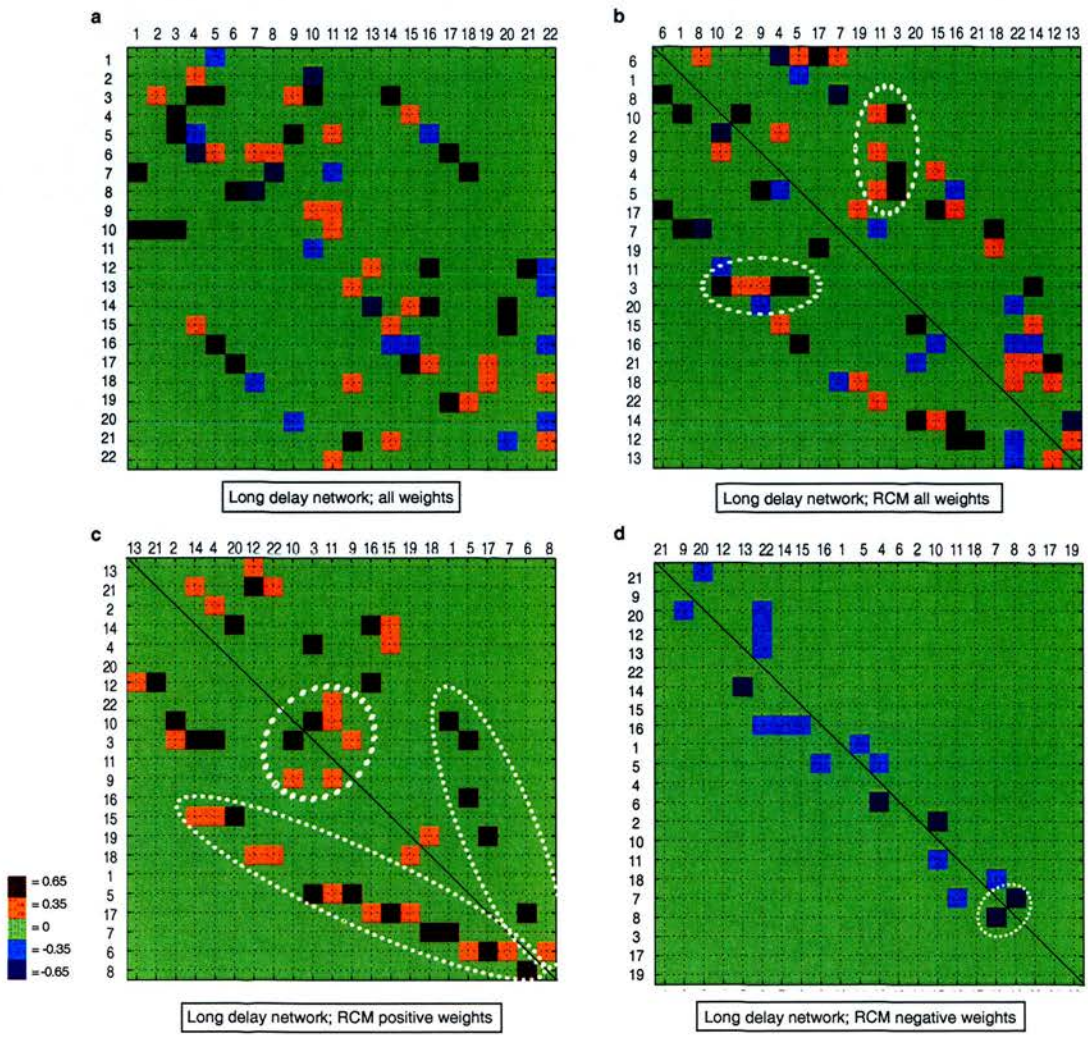

Figure 7.12: Application of the RCM algorithm to the long-delay network. Dominant clusters are highlighted (see Figure 7.11 for conventions).

7.6.4 Summary: comparison of relative clustering profiles in the matching and long-delay networks

The clustering analysis highlighted the following main points:

1. The matching network has twice the number of directly reciprocal excitatory connections compared to the long-delay network. The significant number of reciprocal connections in the matching network, characterise its activity on a two parallel (2D) strata, where activity in one cluster of units is immediately reflected in the activity of another.

2. Major constituents of the dominant networks have been highlighted by both RCM and MDO algorithms. However, I believe that the activity of the networks could not have been predicted *a-priori* by looking at the clustering configurations. Therefore, groupings in Table 7.2 are on the basis of prior knowledge (exploring structural and dynamic stability).

Table 7.2: Clusters in the matching and long-delay networks, highlighted by the RCM and MDO algorithms. Areas were grouped into frames based on functional organisation. The framed areas are suggested to be functionally-related, based on previous results (sections 6.5-6.6). If areas are closely coupled (for example, the dominant network in the matching network, highlighted in the RCM analysis of positive weights only), areas that are not functionally included in a cluster (e.g. area 7) were included in the frame. Unit numbers and corresponding area names are noted at the top of this table. The numbers chosen for different brain areas are arbitrary, however topographical organisation is generally preserved (see Figure 6.2).

REORDERING THE MATCHING AND LONG-DELAY NETWORKS, USING THE REVERSE CUTHILL-MCKEE AND THE MINIMUM DEGREE ORDERING ALGORITHMS

	1	2	3	4	5	6	7	8	9	10	11	12	13	14	15	16	17	18	19	20	21	22
	L BA46	L BA10	L BA47	L BA21	L BA37	L BA18v	L BA19d	L BA17/18	L GH	L BA24	L BA23	R BA46	R BA10	R BA47	R BA21	R BA37	R BA18v	R BA19d	R BA17/18	R GH	R BA24	R BA23
Matching																						
RCM																						
All weights	19	17	13	15	16	6	18	8	14	22	12	20	4	5	7	9	3	21	11	2	1	10
Positive	1	7	10	2	3	20	8	11	9	4	14	6	19	5	15	17	16	18	21	12	22	13
Negative	3	5	1	2	12	22	16	13	18	14	15	7	21	20	11	10	9	4	6	8	17	19
MDO																						
All weights	7	12	6	18	19	21	13	16	17	8	1	2	3	9	11	4	15	20	22	5	10	14
Positive	12	22	13	21	17	8	5	20	3	1	6	18	19	15	11	16	9	2	10	14	4	7
Negative	3	4	5	7	13	11	21	9	22	14	10	20	1	2	6	8	12	15	16	17	18	19
Long-delay																						
RCM																						
All weights	6	1	8	10	2	9	4	5	17	7	19	11	3	20	15	16	21	18	22	14	12	13
Positive	21	13	2	14	4	20	12	22	10	3	11	9	16	15	19	18	1	5	17	7	6	8
Negative	9	20	21	12	13	22	14	15	16	1	5	4	6	2	10	11	18	7	8	3	17	19
MDO																						
All weights	18	8	17	1	21	13	6	19	12	20	15	22	16	3	7	2	5	9	14	4	10	11
Positive	13	21	22	12	6	19	16	20	15	18	7	8	17	1	11	2	9	10	5	4	14	3
Negative	5	7	10	13	4	16	8	11	9	20	22	14	15	1	2	3	6	12	17	18	19	21

7.7 Discussion

Further to setting the basic framework for dynamical modelling of the effective connectivity networks described in McIntosh et al. (1996) and outlining the typical behaviours in the matching and long-delay networks in chapter 6, I proceeded to investigate the physiological (functional) and anatomical (structural) properties of the networks. Studying the effect of specific changes on the default connectivity pattern was taken to express the functional implications of discrete abnormalities associated with affective disorders. Some of the differences between the matching and long-delay networks, such as the different response of the networks to altered inhibition, could not be predicted without modelling the dynamics in these networks.

The functional and structural organisation of these networks can now be associated with specific values of different connections. The propagation of activity through these networks, has been manipulated using both local and global perturbation techniques. Evidently however, these observations (including putative differences between matching and long-delay networks) are limited by (and may be a product of) the parameters set in the basic framework.

7.7.1 A summary of the main findings

The analysis I used in this chapter, confirmed some of the hypotheses outlined in section 6.2.1. Findings are presented in order of importance:

1. Inhibition does not play a significant role in the matching network. The long-delay network however, is equally affected by changes in global excitation and inhibition, exhibiting resilience to small changes in either.

2. Activity in both networks is particularly sensitive to reduced output from left anterior cingulate (unit 10; BA24). Nonetheless, the long-delay network is only affected by localised deficits (including reduced output from BA24 and the left GH) when the global excitation is reduced. This finding is further to hypothesis 3, since the long-delay network was only vulnerable to disruption in those areas when global excitation was reduced.

This finding is particularly interesting, since the left anterior cingulate (BA24) is vulnerable in unipolar and bipolar patients with a family history of affective disorders (Drevets et al., 1997; Price, 1999).

3. Compensation, termed as restoration of the typical pattern of oscillations, is possible in these networks, however with different results. Visual areas can readily compensate for disrupted activity in the matching, but not in the long-delay network. Conversely, the prefrontal cortex is more effective at compensating for disrupted activity in the long-delay network.

4. Confirming hypothesis 1b in chapter 6, the minimal constituents in the matching and long-delay networks suggested different connectivity structures. Whereas the matching network appears to have relatively dominant feed-forward characteristics (leading to activation of the main loop), the long-delay network is more strongly recurrent. In this chapter, these different connectivity structures implied the comparatively robust response of the long-delay network to small global or localised changes.

These results did not confirm hypotheses 2 and 5, since the dynamical activation of both networks revealed that BA46 and BA10 may indeed be functionally related (section 6.6.3), consistent with the findings of Ranganath et al. (2003) who reported that anterior middle frontal gyrus (BA10/46) was activated during the recognition phases of both working and long-term memory tasks, while ventrolateral (BA47) and dorsolateral prefrontal (BA9/46) cortices were associated with encoding. In the current study, BA47 was functionally distinct and the activity of this area was more apparent in the long-delay network. Furthermore, BA46 and BA10 in both networks were activated predominantly through concurrent input from BA24 and therefore largely dependent on its unimpaired function.

7.7.2 Functional clustering

In the matching network, visual units 8, 6, 17 and 19 appear to be grouped. However, only units 6 and 17 are able to trigger activity in this network and clearly, this is not a dominant cluster in its own right. The main activity in this network is associated with prefrontal areas 1, 10, and 2 and to some extent 14, 5 and 4. An independent cluster is formed in the right hemisphere by units 12, 13 and 22. Activity in this cluster is triggered only when global excitation in the network is increased. The long-delay network is governed by the dominant activity of units 3, 4, 5 and 10 (thus shifting slightly the dominant activity in the matching network). Visual units 6, 7, 8 and 17, 18, 19 are still grouped together functionally; however in this network, despite their extended connectivity, they are less influential. Finally, in the right hemisphere, cluster 13, 12 and 21 is still apparent.

Functional delineation through simply examining the connectivity patterns or using classification algorithms such as RCM and MDO, can suggest a different way of

grouping units into clusters. The RCM algorithm has highlighted a large number of directly reciprocal connections among the excitatory weights in the matching network (twice the number in the long-delay network), which may explain the dominant role of excitation in this network. However, the algorithms used here only account for non-zero elements; they do not account for the actual value of weights, which seems to be crucial in these networks. Furthermore, ignoring the exact weight values in the networks will not enable the study of perturbing excitation or inhibition therein. Therefore, it may be desirable to discern interactions of sub-networks or a number of areas using activity, rather than connectivity alone.

7.7.3 Visualisation of activity

Graphical representation of architecture and activity in these networks has been instrumental in highlighting both the complexity (Figure 6.2) and the simplicity (e.g. Figure 6.7) of these dynamic interactions. Simultaneously plotting the activity of all areas encourages an awareness of change or novelty in the behaviour of network constituents over time. However simply viewing these plots cannot always reveal more complex interactions between specific constituents (Figure 6.10). Thus, plotting the activity of two prefrontal areas against the activity of GH (section 6.6.3), under two different conditions, (first including then excluding input from visual areas) highlighted discontinuity under the latter condition. One biological explanation for this could be putatively associated with the constant jitter associated with the activation of the visual system, where the continuous movement allows more efficient encoding of the visual scene. However, this is a speculative interpretation of the findings.

7.7.4 Caveats

Modelling inhibitory and excitatory connections in this network was suggested to be emulating inhibition (i.e. GABA efficacy) and excitation (e.g. glutamate) in the brain. This assumption may of course be incorrect, since anticorrelations (expressed as negative path coefficients) are not likely to represent direct inhibition and furthermore, the connections between cortical areas are reported as mostly glutamatergic (Somogyi et al., 1998). Moreover, the units in this effective connectivity network (McIntosh et al., 1996) are based on previous analysis of PET data (Haxby et al., 1995) and were sufficient to describe the data. However, certain latent interactions may be present yet not accounted for by the effective connectivity model. For example, sub-cortical structures such as striatum and thalamus are absent from this model, yet may be important for performance of this task (Rolls, 1994; Barrett et al., 2001). Furthermore, the striatum may also be functionally related to the dorsolateral PFC, since TMS over the latter area increased dopamine release in the caudate of healthy volunteers (Strafella et al., 2001). Though not necessary to describe the PET data, their presence in my models may have changed both the dynamical activity (perhaps modifying the excitatory loop between prefrontal cortex and anterior cingulate in the matching network) as well as the response of the network to changes in local or global efficacy.

7.7.5 Inferences

The exact nature of the interplay between excitation and inhibition in depressive illness is unclear. Though there are numerous findings reporting deficits in different neurotransmitters and neuromodulators, there is no clear delineation between these deficits and behavioural or cognitive dysfunction. I introduced global changes in

excitation and inhibition to examine whether the matching and long-delay networks have a similar response to these perturbations. Furthermore, I wished to associate these perturbations with deficits, such as decreased cortical excitability in depressed patients (Shajahan et al., 1999). In this sense, I would like to argue that decreased cortical excitability may have been expressed as decreased positive correlations among brain areas in the matching and long-delay networks. Nonetheless, although the various perturbations of the network in chapters 6 and 7 were discussed in the context of the neurobiological deficits, I would suggest that these positive and negative correlations (termed excitation and inhibition) may express coherence, or the absence of it, among different regions. Therefore, if we can accept that a natural activation or oscillatory pattern can be both task-independent and sustainable, this pattern was differentially affected in the matching and the long-delay network.

Hence, this study suggests a fundamental difference in the manner of neural recruitment in tasks that do (long-delay) or do not (matching) involve a memory component. During a relatively easy task, it is possible that presence of the positive correlations is instrumental for successful recruitment of task related areas, while any change in negative correlations is insignificant. By contrast, in the long-delay network both positive and negative correlations must be maintained, for successful completion of the task. Furthermore, the long-delay network is relatively robust to localised perturbation, however this resilience is expeditiously lost when excitation throughout the network is decreased. Thus, these results suggest a putative triangulation between the decreased excitability, specific working-memory deficits and cell loss (in the anterior cingulate), which are all associated with depression. Finally, we cannot directly relate deficits in glutamatergic excitation or GABAergic inhibition to perturbing the efficacy in the networks. However, the experimental decrease in global efficacy (either excitation or inhibition) in the modelling paradigm may be associated with white matter lesions even in mildly ill bipolar and

unipolar patients (Sassi et al., 2003), which may suggest an impaired intra-cortical connectivity (Kumar and Cook, 2002).

7.7.6 Future work and conclusions

Further to this project, I would like to pursue the following ideas:

1. Associate the network with performance of the delay match to sample task.

2. Implement learning in this network, to see whether the actual encoding of specific patterns in the matching network architecture may develop into a connectivity pattern resembling the long-delay network.

In sum, I believe that neither the characteristic activity patterns nor the different response of the matching and long-delay networks to perturbations could be observed by looking at the connectivity patterns alone. Furthermore, functional grouping may have been suggested by the close excitatory coupling among units. However, the coupling between GH and PFC in the long-delay network (Figure 6.11) is not apparent from the connectivity matrix, albeit suggested by the effective connectivity study (McIntosh, 1999). This project was informative and instructive on a number of levels, including the dynamical examination of a static effective connectivity model; the grouping of specific units into functional clusters using different reordering algorithms and finally, the outline of specific interaction or clusters within these networks.

Chapter 8

Conclusions

This thesis has been an exploration of the scientific questions in the context of various techniques that can be used for the study of different facets of neurobiological abnormalities associated with depression. This chapter brings together the contextual and conceptual aspects of my work. The neuroimaging related experimental projects (chapters 4 and 5) in the thesis have both inspired and instructed my modelling endeavours (chapters 6 and 7). Without studying the neural activity of bipolar and unipolar patients, I would not have been aware of the rationale upon which my models can be based or the implications of my findings.

After briefly summarising my major findings, I will describe my outlook on this subject, reflecting on the insight I have gained through the different studies.

Establishing the neurobiological basis of cognitive vulnerability in mood-disorders has been an important part of my thesis. I was involved at different stages of data analysis using datasets from two fMRI studies. In the first study, I examined neural-activity and its behavioural correlates in bipolar patients performing the Stroop task. In the second study, I computed task-independent correlations between seed-voxels and the whole brain, looking for significant between and within-group effects in unipolar patients performing the N-back task.

8.1 Neuroimaging data analysis

Neural activity in bipolar patients and healthy control subjects was examined during performance of the Stroop task. Bipolar patients are known to be particularly impaired in tasks involving attention (Harmer et al., 2002), a cognitive capacity which can be investigated by the Stroop task.

8.1.1 Depression in euthymic bipolar patients

The Stroop study (chapter 4) highlighted the following points:

1. The task-related network in bipolar patients differs both qualitatively (different areas) and quantitatively (smaller network) from healthy control subjects.

2. Despite using different networks, patients performed the task as well as control subjects.

3. The subjects' anxiety levels were associated with activation of the hippocampus in control subjects and cerebellum in patients.

4. Neural deficits in bipolar patients (i.e. deactivation of the orbitofrontal cortex) may be normalised by depression.

8.1.2 Implications

Confirming the findings of Blumberg (2003), we found that hypoactivity in orbito-medial prefrontal cortex (OMPFC) persists beyond remission in bipolar patients. This could delineate this area for purposes of diagnosis or as a possible candidate for directed therapy. For example, the effects of activating this area can be investigated in an analogous manner to activating dorsolateral prefrontal cortex (DLPFC) using transcranial magnetic stimulation (TMS) in depressed patients with unipolar disorder (Shajahan et al., 2002).

However, in the absence of an explicit baseline, in section 4.5 we suggested two alternative hypotheses to explain deactivation of OMPFC (see Figure 8.1). These are suppression of the OMPFC during the Stroop condition or, alternatively, activation of this area during the control condition. The former implies a prevalent pattern of hypofrontality in this group, which has also been observed in patients with schizophrenia and unipolar illness (al-Mousawi et al., 1996; Elliott et al., 1997). The latter suggests the opposite pattern of hyperfrontality, where OMPFC is active throughout the task yet suppressed during the Stroop condition. These hypotheses

may benefit from further examination in the context of both clinical and modelling studies.

I believe that the most intriguing finding in this study showed that depression appears to normalise OMPFC activation. This suggests that depression in bipolar disorder can be an adaptive strategy, which returns a hyperactive orbito-medial network (if the second hypothesis is indeed correct) to baseline. However, it is unclear whether symptoms of mania could be ameliorated by deactivation of this area and furthermore, the role of the OMPFC network or structures associated with it (such as the anterior cingulate, which is overactive in depressed patients (Mayberg et al., 1999)) has not been addressed.

8.2 A network approach to studying neural activity

Memory impairment is often associated with depressive illness (Zakzanis et al., 1998), which may be related to hippocampal deficits (MacQueen et al., 2003). Task-independent correlations across the brain may also be impaired in unipolar patients. These were examined in unipolar patients performing the N-back task, as a measure of functional connectivity that is unrelated to task performance as such. This investigation searched for characteristic differences in the patterns of connectivity between depressed patients and healthy controls, seeking out both global differences and areas where one group shows a stronger effect.

8.2.1 Functional deficits and compensatory strategies in unipolar patients

Examining the functional connectivity in unipolar patients and healthy controls, I found the following (chapter 5):

1. Patients show a significantly reduced pattern of correlations (in terms of number of voxels, as well as cluster size) across the brain, compared to control subjects.

2. Patients show a significant effect of fatigue across a lengthy experiment, compared to healthy controls.

3. Patients show a relatively reduced correlation between the cingulate (BA24) and prefrontal cortex (PFC; BA10), as well as between parietal lobe and BA6, compared to controls

4. Most importantly: patients show a stronger correlation than controls between the parietal lobe and visual areas (the lingual gyrus), possibly suggesting a compensatory strategy.

8.2.2 Compensation and cognitive deficits

This study examined task-independent correlations in neural activity, comparing depressed patients and healthy controls subjects. Following the rationale of Lowe et al. (1998), we argued that computing correlations between task-associated areas may erroneously highlight coincidental activation in remote regions that may respond to the task independently, rather than forming a functional network. Our findings therefore suggest that global suppression in depressive illness may hinder task performance by reducing the ability of regions to correlate rather than respond to

stimuli as such. Further, stronger correlations between visual areas and the task-oriented seed-voxels we used suggested a constant, task-independent coherence of the visual system with prefrontal areas. However, as well as suggesting compensation for cognitive deficits by stronger activation, this pattern may imply a global pattern of suppression. Therefore, it is possible that hypoactivity is pervasive throughout the cortex. Thus, contrary to the hypothesis I promoted in chapter 5, stronger correlations between the residuals in task-related areas and visual cortex may suggest the absence of de-coupling (between parietal and visual areas) rather than the presence of compensation.

8.3 Computational modelling

To complement my studies of neuroimaging data, I conducted various experiments using the neural-connectivity architecture proposed by McIntosh et al. (1996) for a working-memory task. The delayed match to sample task was used in this study, including data from a PET experiment (Haxby et al., 1995) where 4 experimental conditions were tested. In a visual task, subjects were asked to correctly identify a previously presented stimulus either immediately after its presentation (a perceptual matching condition) or following short, intermediate or long-delay periods. Dynamic modelling of the effective connectivity networks allowed me to investigate two of the architectures suggested by these authors, representing the matching and long-delay experimental conditions, from a global perspective (chapter 6). Further to this, I perturbed the default configuration of these networks and established putative links between structural abnormalities in depression and the different patterns of activity in either (chapter 7).

8.3.1 Modelling neuroimaging data

The first task I undertook was turning the effective connectivity networks in McIntosh et al. (1996) into dynamical models. These models highlighted the following differences between the matching and long-delay networks:

1. The matching network has stronger feed-forward characteristics compared to the recurrent nature of the long-delay network.

2. Dominant sub-networks are apparent both in the matching and long-delay networks. The activity of the main network constituents in the long-delay network has a longer and more complex periodicity than in the matching network.

3. In the long-delay network, there is a unique relationship between the left hippocampus (GH) with left BA46 (middle PFC) and left BA10 (inferior PFC) but not BA47 (ventral inferior PFC). All three areas (GH, BA46 and BA10) were not involved in the dominant loop and furthermore, this relationship was unique and not readily observable by looking at the activation of these areas over time.

8.3.2 Neural deficits and compensation

The subsequent experiments tested how perturbing global and local parameters affected the behaviour of the matching and long-delay networks, suggesting the following differences:

1. Unlike the long-delay network, the matching network is unperturbed by changing global inhibition levels.

2. The sustainable activity in both networks is sensitive to decreased output from left anterior cingulate (BA24; where structural deficits were observed in unipolar and bipolar patients with a family history of affective disorders (Drevets et al., 1997)).

3. The activity of the long-delay network was disrupted only when global activity in the network (expressed through weight values) was decreased.

4. Restoring the sustainable activity pattern (once it was disrupted) was more easily achieved with increased activity from visual areas in the matching network. By contrast, prefrontal and temporal areas were more likely to compensate for a similar disruption in the long-delay network.

8.3.3 Modelling psychiatric disorders

In the context of the thesis, the different perturbations to network activity highlighted the anterior cingulate as a potentially vulnerable area both in the matching and the long-delay networks.

8.3.3.1 The anterior cingulate and depression

Both in depression and in bipolar illness, it is unknown whether structural abnormalities in the cingulate (Drevets et al., 1997) are the cause or the effect of specific mood or cognitive deficits, nor is it clear which depressive symptoms may be associated with this particular deficit. The decreased output from the cingulate (BA24) in the matching and long-delay networks was the only instance where decreased output from one region disrupted the behaviour of both networks in an

analogous manner. This may be a consequence of the connectivity structure imposed on these networks, strategically placing BA24 in the intersection between the dominant sub-network and the units representing PFC. However, it may suggest that in the presence of this specific structural deficit in depression, compensatory strategies may differ in the perceptual-matching and long-delay (working-memory) tasks.

8.3.3.2 The hippocampus and depressive illness

Interactions between GH and PFC (McIntosh et al., 1996) were suggested to support maintenance of an encoded pattern in working-memory. Structural vulnerability in GH, as well as in the anterior cingulate, have often been associated with depression (Shah et al., 1998; MacQueen et al., 2003). The unique interplay between GH and both BA46 and BA10 suggests that deficits in hippocampal activity are most likely to affect these areas.

8.4 The power of numbers

The number of patients in neuroimaging studies is predominantly limited by financial constraints. Performing an fMRI experiment can cost thousands of pounds, even for small subject groups. It therefore seems important to investigate datasets beyond the first-level analysis of straightforward functional localisation. It also seems appropriate to make full use of the available data, combining different analytical and modelling techniques to study various aspects of the data (e.g. study aspects of activation or connectivity using generative models), testing specific hypotheses. Further, although it is certainly beneficial to increase sample sizes in

neuroimaging studies, it is also valuable to apply several complementary techniques to a given dataset to maximise the utility of the data. Thus, rigorous and multifaceted analysis with larger sample-sizes will render the most reliable results. The next section gives an example of this approach.

8.4.1 Case study: a computational model of neural activity in bipolar patients performing the Stroop task

The experimental study I analysed (chapter 4) showed that neural activity in bipolar patients differs from the activation in healthy control subjects, despite comparable task performance and reaction time. The study highlighted activation in the orbitofrontal and medial prefrontal cortices (OMPFC) as a potential correlate of mood in bipolar patients, showing that depression in these patients was associated with normalisation of activity in these regions. The deactivation of these areas may be related to the activity of the dorsolateral and ventrolateral prefrontal cortices (DLPFC and VLPFC respectively) in healthy controls during the Stroop task. However, it is unclear whether VLPFC and OMPFC, activated by control subjects and deactivated by bipolar patients during the Stroop task, may have been involved in a process of mutual inhibition with DLPFC in bipolar patients and therefore activation of neither was apparent.

We argued that activation of OMPFC may have been attributed either to active suppression from other regions during the Stroop condition or, alternatively, with deactivation during the control condition (see section 4.4.7 for a full account of our hypotheses, depicted in Figure 8.1). In the absence of a rest condition in the experimental paradigm, it was impossible to ascertain which of the two hypotheses may best account for brain activity in bipolar patients. Furthermore, it is unclear

how the modification associated with depressive illness may be related to the correlations we found between BDI scores (measuring depression, see section 4.2.1) and the activity of the OMPFC.

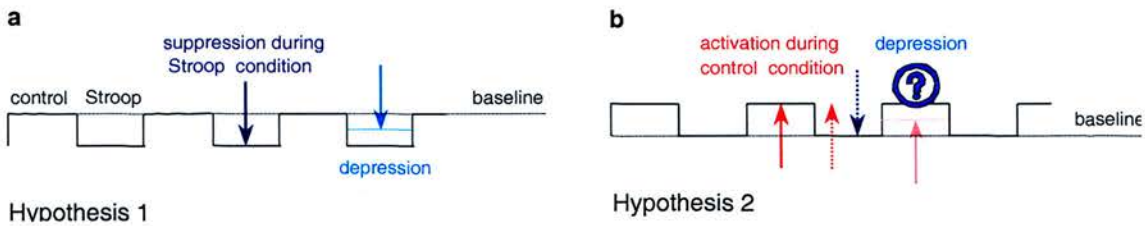

Figure 8.1: Alternative hypotheses for the activation of the OMPFC in depressed and euthymic bipolar patients, performing the Stroop task (repeating Figure 4.12).

The next section will therefore outline one (of several) possible modelling framework for investigating some of these questions, by proposing a simple architecture where mutual inhibition (suggested by hypothesis 2) can be addressed.

8.4.1.1 Proposed modelling framework

In its simplest form, the model (Figure 8.2) will contain two mutually inhibitory areas, receiving excitatory input from other cortical regions. These areas will represent interaction between OMPFC/VLPFC and DLPFC during the Stroop task in bipolar patients. I would like to test the following:

1. Explore the relationship between initial activity, continuous input and changing inhibition on network dynamics.

2. Investigate the effects of changing the values of afferent excitatory connections on mutually inhibitory units, varying both levels of excitation and inhibition.

3. Investigate the effects of synchronous and asynchronous input to the afferent units on network dynamics.

Further, I would like to test the discrete effects of VLPFC on network activity, by incorporating anatomical constraints into the model. Thus, superior temporal gyrus (which was activated by bipolar patients during the Stroop phase of the task) can be included in this framework either providing input to VLPFC, as suggested by Petrides and Pandya (2002), or acting as the output zone for the activity of the medial network in OMPFC, as suggested by Carmichael and Price (1995); see Figure 2.8. The effects of including this structure on network dynamics and especially on the activity of DLPFC can therefore be tested.

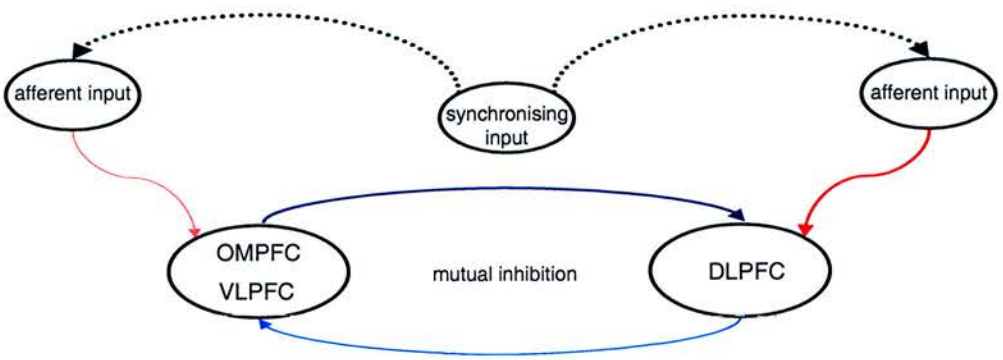

Figure 8.2: Synchronising input can provide a mediating signal to mutually inhibitory units in a circuit representing OMPFC activity in bipolar patients. Blue arrows represent a putative mutual inhibition between orbito-medial and ventrolateral PFC (OMPFC/VLPFC) and dorsolateral (DLPFC) in bipolar patients. Testing "winner-take-all" dynamics in this network, afferent excitation (red arrows) can cause one of these units to be more active and therefore suppress the activity of the other. The dotted black arrows represent a synchronising effect of the afferent input units. Different shades of red and blue represent the relative strength of these connections (testing the effect of strong and weak excitation respectively).

The modelling framework investigating the effects of synchronous input on laterally-inhibited neurons has been applied previously (Lumer, 2000), using integrate-and-fire neurons to simulate dynamics of a small patch of tissue. This author showed that synchronisation of neuronal firing prevents winner-take-all dynamics in the network. I would like to test lateral inhibition in a simplified network, to see how activity of external units (for example representing GH), affect these dynamics.

This modelling framework could only address the limited issues of lateral inhibition and the effect of synchronous input on winner-take-all dynamics. Such a hypothetical modelling study could help inform future experiments. Furthermore, with focussed experimental design, the question of variability, synchronous input signals and mutual inhibition between specific brain areas can be further explored through neuroimaging studies.

8.5 Conclusions

8.5.1 Background

Having developed a keen interest both in modelling and in neuropsychiatry, I was hoping to create a theoretical model that can capture and express the neural abnormalities associated with unipolar and bipolar illness. Since I wanted my findings to be based on real data, the analysis of neuroimaging data was invaluable. I believe that theoretical models can greatly benefit from being grounded in neuroimaging data and have therefore eschewed models that conceptualise the cognitive difficulties in affective disorders by looking at vague phenomena such as noise (Hoffman et al., 2001) or at negative emotional bias (Siegle, 1999). Although the experimental projects (chapters 4 and 5) have not directly contributed to my theoretical work, I feel that they have greatly contributed to my understanding of the field. Furthermore, these studies have provided a suitable grounding for my modelling ideas and will be invaluable both to the development of concrete models at a future date (section 8.4.1).

8.5.2 Connectivity and activity

The complexity of neuroimaging data is quite daunting. This is a relatively young field that is rapidly moving forward. Examples of recent developments in data analysis are the event-related design of studies (often replacing the popular block-design) and the transition to random-effects (replacing fixed-effects) analysis. These methods allow greater sensitivity and specificity in registration of neural activity and improve the computational reliability of the results.

However, the activity of specific regions cannot be detached from the activity of other brain areas. Therefore, the network or systems-level approach is now widely accepted (Horwitz et al., 2000). Network analysis looks at between-region correlations across the task, with or without specifying regions of interest. However, it seems that these methods are co-dependent, since usually functional connectivity is closely coupled with functional activity. After all, functional coupling is more likely to be found if function is present. Computational limitations dictate (McIntosh and Gonzalez-Lima, 1994) that study of effective connectivity (e.g. the construction of structural equation models) are to be limited to a small number of areas. With the advancement of technology through the development of more powerful scanners and faster (and more precise) scanning sequences, I believe that the activity of the human brain could be imaged with even greater accuracy. Combination of fine-grained methods such as EEG with fMRI is currently helping transcend the gap between recording activity at the neuronal and whole-brain level.

8.5.3 Limitations

In chapter 5 of the thesis I used data from a working-memory study (Rose, 2004) to explore task-independent fluctuations in depressed patients and healthy control subjects. In this study we did not use an ROI approach as such but rather performed an exploratory analysis, using a number of task-related yet study-independent seeds (see methods, chapter 5) and computing the correlations between those and every other voxel in the brain. By using exploratory analysis, we did not limit ourselves to task-related activity, nor did we enforce the expected areas where correlations could occur (of course, the origin of the correlations was set but not the target). The obvious disadvantage of this approach however, aside from the limitations imposed by selecting the origin seeds, is the huge multiple comparison problem. If 20,000

correlations are performed simultaneously, then simply by chance 1,000 of them may be significant at the 5% significance level. In this respect, limiting the number of correlations performed to ROIs appears to be a sensible idea.

At present, many of the assumptions about the structure of both the data and the noise (residuals) in healthy controls and clinical groups remain unstudied. Furthermore, the residuals are assumed to be completely independent (this is one of the assumptions supporting both the general linear model and structural equation models). Likewise, the residuals in patients may differ either during or between clinical episodes and in bipolar patients, the residuals (as well as the actual activity accounted for by the model) may have a different shape when patients are manic, depressed or euthymic. The assumption of independence may be incorrect and therefore, further work is needed to study the residuals in neuroimaging data and to compare these in controls subjects and in patients.

8.5.4 Why model if we can analyse connectivity?

I believe that the modelling approach can usefully complement data analysis for several reasons:

1. Examining neural activity or connectivity patterns from a dynamical perspective can highlight certain influences in the data that may not otherwise become apparent.

2. The modelling approach looks at the global activity rather than at pair-wise relationships.

3. Latent interactions can be modelled, to supplement the examination of visible structure of the data.

8.6 What is new and what can follow

The interdisciplinary nature of this project has made the amalgamation of these studies into a cohesive body of work both difficult and fascinating. Although depression is often described as the suffering of the human soul, I have been able to observe specific neurobiological deficits underpinning this experience. Further, in euthymic bipolar patients, depression was associated with normalisation of neural response. This might be evidence in support of the evolutionary hypothesis of depressive illness, suggesting that depression may aid self-preservation (Stevens and Price, 2000), with depressive hypo-function providing a temporary counterbalance to manic hyper-function in bipolar illness. However this interplay needs further clarification.

The most important finding in this thesis, I believe, is the compensatory capacity in the depressed brain. This has been shown through functional connectivity analysis in chapter 5, as well as suggested by my modelling studies in chapter 7. The modelling studies therefore, are not representing depression *per se*, but rather study patterns of activity under specific task-conditions. The different vulnerability loci in the matching and the long-delay networks may suggest how the structural deficits associated with depressive illness may be functionally expressed.

The experimental projects in the thesis did not address specific neural activity in manic patients, nor did they investigate the switch between mania and depression in bipolar illness. This switch can occur as a by-product in the course of anti-depressants (Parker and Parker, 2003; Tamada et al., 2004) or sleep-deprivation (Colombo et al., 1999). However, there have also been reports of mania induced by withdrawal of antidepressant treatment, both in unipolar and bipolar patients (Ali and Milev, 2003). Therefore it is possible that the under-specified 'switch'

mechanism in bipolar illness may be related to an analogous neural system in unipolar disorder, which may be disinhibited in mania. Moreover, fMRI studies with manic subjects may be complicated by subjects' behaviour inside the scanner, since this neuroimaging modality is susceptible to movement-associated noise (see section 2.3.1.2). I feel, therefore, that the modelling experience I have gained may help me address some of these questions in the future, using experimental findings from existing data, e.g. Blumberg et al. (2003) or Caligiuri et al. (2003), to inform computational investigations.

Perhaps better understanding of the neurobiological mechanisms associated with this disease may lead to the development of better cures. At the very least, the study of brain activity in the mentally-ill may dispel the stigma associated with "madness" or "malignant sadness" (Jamieson, 1996; Solomon, 2001) as affective disorders are sometimes colloquially labelled. Social acceptance and an awareness of the high prevalence of affective disorders in western society is rapidly increasing. The rising interest (and associated research) of these disorders among the neuroimaging and the computational modelling communities, and realisation that neurobiological abnormalities can to some extent be addressed and treated, may offer a ray of hope to those who are currently suffering.

Bibliography

al-Mousawi AH, Evans N, Ebmeier KP, Roeda D, Chaloner F, Ashcroft GW (1996) Limbic dysfunction in schizophrenia and mania. A study using 18F-labelled fluorodeoxyglucose and positron emission tomography. Br J Psychiatry 169:509-516.

Ali S, Milev R (2003) Switch to mania upon discontinuation of antidepressants in patients with mood disorders: a review of the literature. Can J Psychiatry 48:258-264.

Ali SO, Denicoff KD, Altshuler LL, Hauser P, Li X, Conrad AJ, Mirsky AF, Smith-Jackson EE, Post RM (2000) A preliminary study of the relation of neuropsychological performance to neuroanatomic structures in bipolar disorder. Neuropsychiatry Neuropsychol Behav Neurol 13:20-28.

Altshuler LL, Bartzokis G, Grieder T, Curran J, Mintz J (1998) Amygdala enlargement in bipolar disorder and hippocampal reduction in schizophrenia: an MRI study demonstrating neuroanatomic specificity. Arch Gen Psychiatry 55:663-664.

Amaro E, Jr., Williams SC, Shergill SS, Fu CH, MacSweeney M, Picchioni MM, Brammer MJ, McGuire PK (2002) Acoustic noise and functional magnetic resonance imaging: current strategies and future prospects. J Magn Reson Imaging 16:497-510.

American, Psychiatric, Press, Association (1994) Diagnostic and Statistical Manual of Mental Disorders., 4th Edition. Washington, DC: American Psychiatric Press.

Amit DJ, Mongillo G (2003) Spike-driven synaptic dynamics generating working memory states. Neural Comput 15:565-596.

Amit DJ, Brunel N, Tsodyks MV (1994) Correlations of cortical Hebbian reverberations: theory versus experiment. J Neurosci 14:6435-6445.

An X, Bandler R, Ongur D, Price JL (1998) Prefrontal cortical projections to longitudinal columns in the midbrain periaqueductal gray in macaque monkeys. J Comp Neurol 401:455-479.

Arbib MA, Billard A, Iacoboni M, Oztop E (2000) Synthetic brain imaging: grasping, mirror neurons and imitation. Neural Netw 13:975-997.

Atre-Vaidya N, Taylor MA, Seidenberg M, Reed R, Perrine A, Glick-Oberwise F (1998) Cognitive deficits, psychopathology, and psychosocial functioning in bipolar mood disorder. Neuropsychiatry Neuropsychol Behav Neurol 11:120-126.

Austin MP, Mitchell P, Wilhelm K, Parker G, Hickie I, Brodaty H, Chan J, Eyers K, Milic M, Hadzi-Pavlovic D (1999) Cognitive function in depression: a distinct pattern of frontal impairment in melancholia? Psychol Med 29:73-85.

Aylward EH, Roberts-Twillie JV, Barta PE, Kumar AJ, Harris GJ, Geer M, Peyser CE, Pearlson GD (1994) Basal ganglia volumes and white matter hyperintensities in patients with bipolar disorder. Am J Psychiatry 151:687-693.

Baker SC, Frith CD, Dolan RJ (1997) The interaction between mood and cognitive function studied with PET. Psychol Med 27:565-578.

Barbas H, Ghashghaei H, Dombrowski SM, Rempel-Clower NL (1999) Medial prefrontal cortices are unified by common connections with superior temporal cortices and distinguished by input from memory-related areas in the rhesus monkey. J Comp Neurol 410:343-367.

Barch DM, Sheline YI, Csernansky JG, Snyder AZ (2003) Working memory and prefrontal cortex dysfunction: specificity to schizophrenia compared with major depression. Biol Psychiatry 53:376-384.

Barrett NA, Large MM, Smith GL, Michie PT, Karayanidis F, Kavanagh DJ, Fawdry R, Henderson D, O'Sullivan BT (2001) Human cortical processing of colour and pattern. Hum Brain Mapp 13:213-225.

Baxter LR, Jr., Schwartz JM, Phelps ME, Mazziotta JC, Guze BH, Selin CE, Gerner RH, Sumida RM (1989) Reduction of prefrontal cortex glucose metabolism common to three types of depression. Arch Gen Psychiatry 46:243-250.

Beck AT, Steer RA, Kovacs M, Garrison B (1985) Hopelessness and eventual suicide: a 10-year prospective study of patients hospitalized with suicidal ideation. Am J Psychiatry 142:559-563.

Beck AT, Ward CH, Mendelson M, Mock J, Erbaugh J (1961) An inventory for measuring depression. Arch Gen Psychiatry 4:561-571.

Benazzi F (2004) Melancholic outpatient depression in Bipolar-II vs. unipolar. Prog Neuropsychopharmacol Biol Psychiatry 28:481-485.

Bench CJ, Friston KJ, Brown RG, Scott LC, Frackowiak RS, Dolan RJ (1992) The anatomy of melancholia--focal abnormalities of cerebral blood flow in major depression. Psychol Med 22:607-615.

Benes FM, Vincent SL, Todtenkopf M (2001) The density of pyramidal and nonpyramidal neurons in anterior cingulate cortex of schizophrenic and bipolar subjects. Biol Psychiatry 50:395-406.

Blumberg HP, Leung HC, Skudlarski P, Lacadie CM, Fredericks CA, Harris BC, Charney DS, Gore JC, Krystal JH, Peterson BS (2003) A functional magnetic resonance imaging study of bipolar disorder: state- and trait-related dysfunction in ventral prefrontal cortices. Arch Gen Psychiatry 60:601-609.

Blumberg HP, Stern E, Martinez D, Ricketts S, de Asis J, White T, Epstein J, McBride PA, Eidelberg D, Kocsis JH, Silbersweig DA (2000) Increased anterior cingulate and caudate activity in bipolar mania. Biol Psychiatry 48:1045-1052.

Borkowska A, Rybakowski JK (2001) Neuropsychological frontal lobe tests indicate that bipolar depressed patients are more impaired than unipolar. Bipolar Disord 3:88-94.

Bouhuys AL, Geerts E, Gordijn MC (1999) Depressed patients' perceptions of facial emotions in depressed and remitted states are associated with relapse: a longitudinal study. J Nerv Ment Dis 187:595-602.

Brambilla P, Barale F, Caverzasi E, Soares JC (2002) Anatomical MRI findings in mood and anxiety disorders. Epidemiol Psichiatr Soc 11:88-99.

Brammer MJ, Bullmore ET, Simmons A, Williams SC, Grasby PM, Howard RJ, Woodruff PW, Rabe-Hesketh S (1997) Generic brain activation mapping in functional magnetic resonance imaging: a nonparametric approach. Magn Reson Imaging 15:763-770.

Breakspear M, Brammer MJ, Robinson PA (2003) Construction of multivariate surrogates using the wavelet transform. Physica D - Nonlinear Phenomena 182:1-22.

Bremner JD, Narayan M, Anderson ER, Staib LH, Miller HL, Charney DS (2000) Hippocampal volume reduction in major depression. Am J Psychiatry 157:115-118.

Brown ES, Rush AJ, McEwen BS (1999) Hippocampal remodeling and damage by corticosteroids: implications for mood disorders. Neuropsychopharmacology 21:474-484.

Buchel C, Friston KJ (1997) Modulation of connectivity in visual pathways by attention: cortical interactions evaluated with structural equation modelling and fMRI. Cereb Cortex 7:768-778.

Bullmore E, Horwitz B, Honey G, Brammer M, Williams S, Sharma T (2000) How good is good enough in path analysis of fMRI data? Neuroimage 11:289-301.

Bullmore E, Long C, Suckling J, Fadili J, Calvert G, Zelaya F, Carpenter TA, Brammer M (2001) Colored noise and computational inference in neurophysiological (fMRI) time series analysis: resampling methods in time and wavelet domains. Hum Brain Mapp 12:61-78.

Bullmore ET, Suckling J, Overmeyer S, Rabe-Hesketh S, Taylor E, Brammer MJ (1999a) Global, voxel, and cluster tests, by theory and permutation, for a difference between two groups of structural MR images of the brain. IEEE Trans Med Imaging 18:32-42.

Bullmore ET, Brammer MJ, Rabe-Hesketh S, Curtis VA, Morris RG, Williams SC, Sharma T, McGuire PK (1999b) Methods for diagnosis and treatment of stimulus-correlated motion in generic brain activation studies using fMRI. Hum Brain Mapp 7:38-48.

Bush G, Luu P, Posner MI (2000) Cognitive and emotional influences in anterior cingulate cortex. Trends Cogn Sci 4:215-222.

Caligiuri MP, Ellwanger J (2000) Motor and cognitive aspects of motor retardation in depression. J Affect Disord 57:83-93.

Caligiuri MP, Brown GG, Meloy MJ, Eberson SC, Kindermann SS, Frank LR, Zorrilla LE, Lohr JB (2003) An fMRI study of affective state and medication on cortical and subcortical brain regions during motor performance in bipolar disorder. Psychiatry Res 123:171-182.

Callicott JH, Mattay VS, Bertolino A, Finn K, Coppola R, Frank JA, Goldberg TE, Weinberger DR (1999) Physiological characteristics of capacity constraints in working memory as revealed by functional MRI. Cereb Cortex 9:20-26.

Carlson S, Martinkauppi S, Rama P, Salli E, Korvenoja A, Aronen HJ (1998) Distribution of cortical activation during visuospatial n-back tasks as revealed by functional magnetic resonance imaging. Cereb Cortex 8:743-752.

Carmichael ST, Price JL (1995) Limbic connections of the orbital and medial prefrontal cortex in macaque monkeys. J Comp Neurol 363:615-641.

Casey BJ, Cohen JD, O'Craven K, Davidson RJ, Irwin W, Nelson CA, Noll DC, Hu X, Lowe MJ, Rosen BR, Truwitt CL, Turski PA (1998) Reproducibility of fMRI results across four institutions using a spatial working memory task. Neuroimage 8:249-261.

Casey BJ, Trainor RJ, Orendi JL, Schubert AB, Nystrom LE, Giedd JN, Castellanos X, Haxby J, Noll DC, Cohen JD, Forman S, Dahl RE, Rapoport JL (1997) A developmental fMRI study of prefrontal activation during performance of the go-no-go task. Journal of Cognitive Neuroscience 9:835-847.

Cavada C, Company T, Tejedor J, Cruz-Rizzolo RJ, Reinoso-Suarez F (2000) The anatomical connections of the macaque monkey orbitofrontal cortex. A review. Cereb Cortex 10:220-242.

Cavanagh JT, Van Beck M, Muir W, Blackwood DH (2002) Case-control study of neurocognitive function in euthymic patients with bipolar disorder: an association with mania. Br J Psychiatry 180:320-326.

Charney DS (2003) Neuroanatomical circuits modulating fear and anxiety behaviors. Acta Psychiatr Scand Suppl:38-50.

Cincotta M, Borgheresi A, Gambetti C, Balestrieri F, Rossi L, Zaccara G, Ulivelli M, Rossi S, Civardi C, Cantello R (2003) Suprathreshold 0.3 Hz repetitive TMS prolongs the cortical silent period: potential implications for therapeutic trials in epilepsy. Clin Neurophysiol 114:1827-1833.

Clark L, Iversen SD, Goodwin GM (2001) A neuropsychological investigation of prefrontal cortex involvement in acute mania. Am J Psychiatry 158:1605-1611.

Clark L, Iversen SD, Goodwin GM (2002) Sustained attention deficit in bipolar disorder. Br J Psychiatry 180:313-319.

Cohen MS, Bookheimer SY (1994) Localization of brain function using magnetic resonance imaging. Trends Neurosci 17:268-277.

Colombo C, Benedetti F, Barbini B, Campori E, Smeraldi E (1999) Rate of switch from depression into mania after therapeutic sleep deprivation in bipolar depression. Psychiatry Res 86:267-270.

Cools R, Clark L, Owen AM, Robbins TW (2002) Defining the neural mechanisms of probabilistic reversal learning using event-related functional magnetic resonance imaging. J Neurosci 22:4563-4567.

Cosgrove GR, Rauch SL (2003) Stereotactic cingulotomy. Neurosurg Clin N Am 14:225-235.

Cotter D, Mackay D, Chana G, Beasley C, Landau S, Everall IP (2002) Reduced neuronal size and glial cell density in area 9 of the dorsolateral prefrontal cortex in subjects with major depressive disorder. Cereb Cortex 12:386-394.

Craddock N, Jones I (1999) Genetics of bipolar disorder. J Med Genet 36:585-594.

D'Sa C, Duman RS (2002) Antidepressants and neuroplasticity. Bipolar Disord 4:183-194.

Dasari M, Friedman L, Jesberger J, Stuve TA, Findling RL, Swales TP, Schulz SC (1999) A magnetic resonance imaging study of thalamic area in adolescent patients with either schizophrenia or bipolar disorder as compared to healthy controls. Psychiatry Res 91:155-162.

Dawirs RR, Teuchert-Noodt G (2001) A novel pharmacological concept in an animal model of psychosis. Acta Psychiatr Scand Suppl:10-17.

Deary IJ, Simonotto E, M. M, Marshall I, Marshall A, Goddard NH, Wardlaw JM (in press) The functional anatomy of inspection time: an event-related fMRI study. NeuroImage.

Della-Maggiore V, Grady CL, McIntosh AR (2002) Dissecting the effect of aging on the neural substrates of memory: deterioration, preservation or functional reorganization? Rev Neurosci 13:167-181.

Della-Maggiore V, Sekuler AB, Grady CL, Bennett PJ, Sekuler R, McIntosh AR (2000) Corticolimbic interactions associated with performance on a short-term memory task are modified by age. J Neurosci 20:8410-8416.

Drevets WC (1999) Prefrontal cortical-amygdalar metabolism in major depression. Ann N Y Acad Sci 877:614-637.

Drevets WC (2000a) Functional anatomical abnormalities in limbic and prefrontal cortical structures in major depression. Prog Brain Res 126:413-431.

Drevets WC (2000b) Neuroimaging studies of mood disorders. Biol Psychiatry 48:813-829.

Drevets WC, Ongur D, Price JL (1998) Neuroimaging abnormalities in the subgenual prefrontal cortex: implications for the pathophysiology of familial mood disorders. Mol Psychiatry 3:220-226, 190-221.

Drevets WC, Price JL, Simpson JR, Jr., Todd RD, Reich T, Vannier M, Raichle ME (1997) Subgenual prefrontal cortex abnormalities in mood disorders. Nature 386:824-827.

Drummond SP, Brown GG, Gillin JC, Stricker JL, Wong EC, Buxton RB (2000) Altered brain response to verbal learning following sleep deprivation. Nature 403:655-657.

Durbin R, Willshaw D (1987) An analogue approach to the travelling salesman problem using an elastic net method. Nature 326:689-691.

Ebert D, Berger M (1998) Neurobiological similarities in antidepressant sleep deprivation and psychostimulant use: a psychostimulant theory of antidepressant sleep deprivation. Psychopharmacology (Berl) 140:1-10.

Ebert D, Feistel H, Kaschka W, Barocka A, Pirner A (1994) Single photon emission computerized tomography assessment of cerebral dopamine D2 receptor blockade in depression before and after sleep deprivation--preliminary results. Biol Psychiatry 35:880-885.

Ebmeier KP, Kronhaus DM (2001) Brain imaging in mood disorders. In: Textbook of Biological Psychiatry (D'Haenen H, der Boer JA, Westenberg H, Willner P, eds). New-York: John Wiley & Sons, Ltd.

Eizenman M, Yu LH, Grupp L, Eizenman E, Ellenbogen M, Gemar M, Levitan RD (2003) A naturalistic visual scanning approach to assess selective attention in major depressive disorder. Psychiatry Res 118:117-128.

Elliott R, Friston KJ, Dolan RJ (2000) Dissociable neural responses in human reward systems. J Neurosci 20:6159-6165.

Elliott R, Rubinsztein JS, Sahakian BJ, Dolan RJ (2002) The neural basis of mood-congruent processing biases in depression. Arch Gen Psychiatry 59:597-604.

Elliott R, Baker SC, Rogers RD, O'Leary DA, Paykel ES, Frith CD, Dolan RJ, Sahakian BJ (1997) Prefrontal dysfunction in depressed patients performing a

complex planning task: a study using positron emission tomography. Psychol Med 27:931-942.

Ferrier IN, Thompson JM (2002) Cognitive impairment in bipolar affective disorder: implications for the bipolar diathesis. Br J Psychiatry 180:293-295.

Ferrier IN, Stanton BR, Kelly TP, Scott J (1999) Neuropsychological function in euthymic patients with bipolar disorder. Br J Psychiatry 175:246-251.

Ferry AT, Ongur D, An X, Price JL (2000) Prefrontal cortical projections to the striatum in macaque monkeys: evidence for an organization related to prefrontal networks. J Comp Neurol 425:447-470.

Finkelstein Y, Koffler B, Rabey JM, Gilad GM (1985) Dynamics of cholinergic synaptic mechanisms in rat hippocampus after stress. Brain Res 343:314-319.

Fossati P, Coyette F, Ergis AM, Allilaire JF (2002) Influence of age and executive functioning on verbal memory of inpatients with depression. J Affect Disord 68:261-271.

Franchini L, Spagnolo C, Rossini D, Smeraldi E, Bellodi L, Politi E (2001) A neural network approach to the outcome definition on first treatment with sertraline in a psychiatric population. Artif Intell Med 23:239-248.

Frederick K, Goodwin MD, Jamieson KR (1990) Manic-Depressive Illness.: Oxfor University Press.

Freedman LJ, Insel TR, Smith Y (2000) Subcortical projections of area 25 (subgenual cortex) of the macaque monkey. J Comp Neurol 421:172-188.

Friston KJ (1994) Functional and effective connectivity in neuroimaging: a synthesis. Hum Brain Mapp 2:56-78.

Friston KJ (1997) Testing for anatomically specified regional effects. Hum Brain Mapp 5:133-136.

Friston KJ, Price CJ (2001a) Generative models, brain function and neuroimaging. Scand J Psychol 42:167-177.

Friston KJ, Price CJ (2001b) Dynamic representations and generative models of brain function. Brain Res Bull 54:275-285.

Friston KJ, Harrison L, Penny W (2003) Dynamic causal modelling. Neuroimage 19:1273-1302.

Friston KJ, Frith CD, Fletcher P, Liddle PF, Frackowiak RS (1996) Functional topography: multidimensional scaling and functional connectivity in the brain. Cereb Cortex 6:156-164.

Gaetz M, Iverson GL, Rzempoluck EJ, Remick R, McLean P, Linden W (2004) Self-organizing neural network analyses of cardiac data in depression. Neuropsychobiology 49:30-37.

Gartside SE, Leitch MM, McQuade R, Swarbrick DJ (2003) Flattening the glucocorticoid rhythm causes changes in hippocampal expression of messenger RNAs coding structural and functional proteins: implications for aging and depression. Neuropsychopharmacology 28:821-829.

Genovese CR, Lazar NA, Nichols T (2002) Thresholding of statistical maps in functional neuroimaging using the false discovery rate. Neuroimage 15:870-878.

George MS, Wassermann EM, Kimbrell TA, Little JT, Williams WE, Danielson AL, Greenberg BD, Hallett M, Post RM (1997) Mood improvement following daily left prefrontal repetitive transcranial magnetic stimulation in patients with depression: a placebo-controlled crossover trial. Am J Psychiatry 154:1752-1756.

George MS, HNahas Z, Speer AM, Kimbrell TA, Wassermann EM, Teneback CC, Molloy M, Bohning D, Risch SC, Post RM (1998) Transcranial Magnetic Stimulation: a new method for investigating the neuroanatomy of depression. In: New models for depression (Ebert D, Ebmeier KP, eds), pp 94-122. Basel: Karger.

Ghashghaei HT, Barbas H (2001) Neural interaction between the basal forebrain and functionally distinct prefrontal cortices in the rhesus monkey. Neuroscience 103:593-614.

Giral P, Martin P, Soubrie P, Simon P (1988) Reversal of helpless behavior in rats by putative 5-HT1A agonists. Biol Psychiatry 23:237-242.

Gold PW, Chrousos GP (1999) The endocrinology of melancholic and atypical depression: relation to neurocircuitry and somatic consequences. Proc Assoc Am Physicians 111:22-34.

Goldman-Rakic PS (1999) The physiological approach: functional architecture of working memory and disordered cognition in schizophrenia. Biol Psychiatry 46:650-661.

Goncalves MS, Hall DA, Johnsrude IS, Haggard MP (2001) Can meaningful effective connectivities be obtained between auditory cortical regions? Neuroimage 14:1353-1360.

Gonzalez LE, Rujano M, Tucci S, Paredes D, Silva E, Alba G, Hernandez L (2000) Medial prefrontal transection enhances social interaction. I: behavioral studies. Brain Res 887:7-15.

Gower JC (1966) Some distance properties of latent root and vector methods used in multivariate analysis. Biometrica 53:325-328.

Grauer E, Kapon Y (1993) Wistar-Kyoto rats in the Morris water maze: impaired working memory and hyper-reactivity to stress. Behav Brain Res 59:147-151.

Gray M, Kemp AH, Silberstein RB, Nathan PJ (2003) Cortical neurophysiology of anticipatory anxiety: an investigation utilizing steady state probe topography (SSPT). Neuroimage 20:975-986.

Groenewegen HJ, Wright CI, Uylings HB (1997) The anatomical relationships of the prefrontal cortex with limbic structures and the basal ganglia. J Psychopharmacol 11:99-106.

Gron G, Bittner D, Schmitz B, Wunderlich AP, Riepe MW (2002) Subjective memory complaints: objective neural markers in patients with Alzheimer's disease and major depressive disorder. Ann Neurol 51:491-498.

Grossman I, Kaufman AS, Mednitsky S, Scharff L, Dennis B (1994) Neurocognitive abilities for a clinically depressed sample versus a matched control group of normal individuals. Psychiatry Res 51:231-244.

Hampson M, Peterson BS, Skudlarski P, Gatenby JC, Gore JC (2002) Detection of functional connectivity using temporal correlations in MR images. Hum Brain Mapp 15:247-262.

Harmer CJ, Clark L, Grayson L, Goodwin GM (2002) Sustained attention deficit in bipolar disorder is not a working memory impairment in disguise. Neuropsychologia 40:1586-1590.

Haxby JV, Ungerleider LG, Horwitz B, Rapoport SI, Grady CL (1995) Hemispheric differences in neural systems for face working memory: a PET rCBF study. Human Brain Mapping 3:68-82.

Hedreen JC, Folstein SE (1995) Early loss of neostriatal striosome neurons in Huntington's disease. J Neuropathol Exp Neurol 54:105-120.

Helmuth L (2003) In sickness or in health? Science 302:808-810.

Hertz J, Krogh A, Palmer R (1991) Introduction to the theory of neural computation: Perseus Publishing.

Hickie I, Ward P, Scott E, Haindl W, Walker B, Dixon J, Turner K (1999) Neo-striatal rCBF correlates of psychomotor slowing in patients with major depression. Psychiatry Res 92:75-81.

Hirayasu Y, Shenton ME, Salisbury DF, Kwon JS, Wible CG, Fischer IA, Yurgelun-Todd D, Zarate C, Kikinis R, Jolesz FA, McCarley RW (1999) Subgenual cingulate cortex volume in first-episode psychosis. Am J Psychiatry 156:1091-1093.

Hodgson TL, Mort D, Chamberlain MM, Hutton SB, O'Neill KS, Kennard C (2002) Orbitofrontal cortex mediates inhibition of return. Neuropsychologia 40:1891-1901.

Hoffman RE, McGlashan TH (2001) Neural network models of schizophrenia. Neuroscientist 7:441-454.

Hoffman RE, Quinlan DM, Mazure CM, McGlashan TM (2001) Cortical instability and the mechanism of mania: a neural network simulation and perceptual test. Biol Psychiatry 49:500-509.

Honey GD, Bullmore ET, Sharma T (2000) Prolonged reaction time to a verbal working memory task predicts increased power of posterior parietal cortical activation. Neuroimage 12:495-503.

Horwitz B, Friston KJ, Taylor JG (2000) Neural modeling and functional brain imaging: an overview. Neural Netw 13:829-846.

Ingram RE, Kendall PC, Smith TW, Donnell C, Ronan K (1987) Cognitive specificity in emotional distress. J Pers Soc Psychol 53:734-742.

Jacobs BL (2002) Adult brain neurogenesis and depression. Brain Behav Immun 16:602-609.

Jamieson KR (1996) Touched with fire: manic depressive illness and the artistic temperament. New York: Free press.

Jansma JM, Ramsey NF, Coppola R, Kahn RS (2000) Specific versus nonspecific brain activity in a parametric N-back task. Neuroimage 12:688-697.

Jefferson MF, Pendleton N, Lucas CP, Lucas SB, Horan MA (1998) Evolution of artificial neural network architecture: prediction of depression after mania. Methods Inf Med 37:220-225.

Jeffery KJ, Reid IC (1997) Modifiable neuronal connections: an overview for psychiatrists. Am J Psychiatry 154:156-164.

Jezzard P, Matthews PM, Smith SM (2001) Functional MRI: an introduction to methods.: Oxford University Press.

Karkowski LM, Kendler KS (1997) An examination of the genetic relationship between bipolar and unipolar illness in an epidemiological sample. Psychiatr Genet 7:159-163.

Kennedy SH, Evans KR, Kruger S, Mayberg HS, Meyer JH, McCann S, Arifuzzman AI, Houle S, Vaccarino FJ (2001) Changes in regional brain glucose metabolism measured with positron emission tomography after paroxetine treatment of major depression. Am J Psychiatry 158:899-905.

Kessing LV (1998) Cognitive impairment in the euthymic phase of affective disorder. Psychol Med 28:1027-1038.

Ketter TA, Wang PW (2003) The emerging differential roles of GABAergic and antiglutamatergic agents in bipolar disorders. J Clin Psychiatry 64 Suppl 3:15-20.

Ketter TA, Kimbrell TA, George MS, Dunn RT, Speer AM, Benson BE, Willis MW, Danielson A, Frye MA, Herscovitch P, Post RM (2001) Effects of mood and subtype on cerebral glucose metabolism in treatment-resistant bipolar disorder. Biol Psychiatry 49:97-109.

Korte SM (2001) Corticosteroids in relation to fear, anxiety and psychopathology. Neurosci Biobehav Rev 25:117-142.

Kosel M, Rudolph U, Wielepp P, Luginbuhl M, Schmitt W, Fisch HU, Schlaepfer TE (2004) Diminished GABA(A) receptor-binding capacity and a DNA base substitution in a patient with treatment-resistant depression and anxiety. Neuropsychopharmacology 29:347-350.

Koukopoulos A (1999) Agitated depression as a mixed state and the problem of melancholia. Psychiatr Clin North Am 22:547-564.

Kronhaus DM, Rose EJ, Simonotto E, Goddard NH, Marshall I, Ebmeier KP, Willshaw DJ (2002) A rationale for using the N-back task for identifying brain areas affected in depressive illness. Poster presentation: Federation of Euopean Neuroscience Societies.

Kronhaus DM, Lawrence NS, Williams AM, Frangou S, Brammer MJ, Williams SCR, Andrew CM, Phillips ML (2004) Does depression reduce ventral prefrontal abnormalities associated with Bipolar disorder? Poster presentation: Association of European Psychiatrists Section of Neuroimaging.

Kronhaus DM, Lawrence NS, Williams AM, Frangou S, Brammer MJ, Williams SCR, Andrew CM, Willshaw DJ, Phillips ML (2003) Limbic activation in bipolar subjects during performance of the Stroop task. Poster presentation: Human Brain Mapping.

Krystal JH, Sanacora G, Blumberg H, Anand A, Charney DS, Marek G, Epperson CN, Goddard A, Mason GF (2002) Glutamate and GABA systems as targets for novel antidepressant and mood-stabilizing treatments. Mol Psychiatry 7 Suppl 1:S71-80.

Kumar A, Cook IA (2002) White matter injury, neural connectivity and the pathophysiology of psychiatric disorders. Dev Neurosci 24:255-261.

Lacroix L, Spinelli S, Heidbreder CA, Feldon J (2000) Differential role of the medial and lateral prefrontal cortices in fear and anxiety. Behav Neurosci 114:1119-1130.

Lamont SR, Paulls A, Stewart CA (2001) Repeated electroconvulsive stimulation, but not antidepressant drugs, induces mossy fibre sprouting in the rat hippocampus. Brain Res 893:53-58.

Le Doux J (1992) Emotion and the amygdala. In: The amygdala: neurobiological aspects of emotion, memory, and mental dysfunction. (Aggleton JP, ed), pp 339-351. New-York, NY: Wiley-Liss.

Leung JW, Xue H (2003) GABAergic functions and depression: from classical therapies to herbal medicine. Curr Drug Targets CNS Neurol Disord 2:363-374.

Levesque J, Eugene F, Joanette Y, Paquette V, Mensour B, Beaudoin G, Leroux JM, Bourgouin P, Beauregard M (2003) Neural circuitry underlying voluntary suppression of sadness. Biol Psychiatry 53:502-510.

Levkovitz Y, Segal M (2001) Aging affects transcranial magnetic modulation of hippocampal evoked potentials. Neurobiol Aging 22:255-263.

Levkovitz Y, Grisaru N, Segal M (2001) Transcranial magnetic stimulation and antidepressive drugs share similar cellular effects in rat hippocampus. Neuropsychopharmacology 24:608-616.

Lewinsohn PM, Allen NB, Seeley JR, Gotlib IH (1999) First onset versus recurrence of depression: differential processes of psychosocial risk. J Abnorm Psychol 108:483-489.

Lewis MD, Stieben J (2004) Emotion regulation in the brain: conceptual issues and directions for developmental research. Child Dev 75:371-376.

Lim KO, Rosenbloom MJ, Faustman WO, Sullivan EV, Pfefferbaum A (1999) Cortical gray matter deficit in patients with bipolar disorder. Schizophr Res 40:219-227.

Lipska BK, Aultman JM, Verma A, Weinberger DR, Moghaddam B (2002) Neonatal damage of the ventral hippocampus impairs working memory in the rat. Neuropsychopharmacology 27:47-54.

Logothetis NK (2002) The neural basis of the blood-oxygen-level-dependent functional magnetic resonance imaging signal. Philos Trans R Soc Lond B Biol Sci 357:1003-1037.

Logothetis NK, Pauls J, Augath M, Trinath T, Oeltermann A (2001) Neurophysiological investigation of the basis of the fMRI signal. Nature 412:150-157.

Lopez-Larson MP, DelBello MP, Zimmerman ME, Schwiers ML, Strakowski SM (2002) Regional prefrontal gray and white matter abnormalities in bipolar disorder. Biol Psychiatry 52:93-100.

Lowe MJ, Mock BJ, Sorenson JA (1998) Functional connectivity in single and multislice echoplanar imaging using resting-state fluctuations. Neuroimage 7:119-132.

Lumer ED (2000) Effects of spike timing on winner-take-all competition in model cortical circuits. Neural Comput 12:181-194.

MacLeod CM (1991) Half a century of research on the Stroop effect: an integrative review. Psychol Bull 109:163-203.

MacLeod CM, MacDonald PA (2000) Interdimensional interference in the Stroop effect: uncovering the cognitive and neural anatomy of attention. Trends Cogn Sci 4:383-391.

MacQueen GM, Campbell S, McEwen BS, Macdonald K, Amano S, Joffe RT, Nahmias C, Young LT (2003) Course of illness, hippocampal function, and hippocampal volume in major depression. Proc Natl Acad Sci U S A 100:1387-1392.

Malberg JE, Duman RS (2003) Cell proliferation in adult hippocampus is decreased by inescapable stress: reversal by fluoxetine treatment. Neuropsychopharmacology 28:1562-1571.

Martin JL, Barbanoj MJ, Schlaepfer TE, Clos S, Perez V, Kulisevsky J, Gironell A (2002) Transcranial magnetic stimulation for treating depression. Cochrane Database Syst Rev:CD003493.

Martinot JL, Hardy P, Feline A, Huret JD, Mazoyer B, Attar-Levy D, Pappata S, Syrota A (1990) Left prefrontal glucose hypometabolism in the depressed state: a confirmation. Am J Psychiatry 147:1313-1317.

Mayberg HS (1997) Limbic-cortical dysregulation: a proposed model of depression. J Neuropsychiatry Clin Neurosci 9:471-481.

Mayberg HS, Silva JA, Brannan SK, Tekell JL, Mahurin RK, McGinnis S, Jerabek PA (2002) The functional neuroanatomy of the placebo effect. Am J Psychiatry 159:728-737.

Mayberg HS, Liotti M, Brannan SK, McGinnis S, Mahurin RK, Jerabek PA, Silva JA, Tekell JL, Martin CC, Lancaster JL, Fox PT (1999) Reciprocal limbic-cortical function and negative mood: converging PET findings in depression and normal sadness. Am J Psychiatry 156:675-682.

McGrath J, Scheldt S, Welham J, Clair A (1997) Performance on tests sensitive to impaired executive ability in schizophrenia, mania and well controls: acute and subacute phases. Schizophr Res 26:127-137.

McIntosh AR (1999) Mapping cognition to the brain through neural interactions. Memory 7:523-548.

McIntosh AR, Gonzalez-Lima F (1994) Network interactions among limbic cortices, basal forebrain, and cerebellum differentiate a tone conditioned as a Pavlovian excitor or inhibitor: fluorodeoxyglucose mapping and covariance structural modeling. J Neurophysiol 72:1717-1733.

McIntosh AR, Grady CL, Haxby JV, Ungerleider LG, Horwitz B (1996) Changes in limbic and prefrontal functional interactions in a working memory task for faces. Cereb Cortex 6:571-584.

McKinney WT (1984) Animal models of depression: an overview. Psychiatr Dev 2:77-96.

Miyashita Y (1988) Neuronal correlate of visual associative long-term memory in the primate temporal cortex. Nature 335:817-820.

Moller HJ (2003) Bipolar disorder and schizophrenia: distinct illnesses or a continuum? J Clin Psychiatry 64 Suppl 6:23-27; discussion 28.

Morris R, Petrides M, Pandya DN (1999) Architecture and connections of retrosplenial area 30 in the rhesus monkey (Macaca mulatta). Eur J Neurosci 11:2506-2518.

Nichols T, Hayasaka S (2003) Controlling the familywise error rate in functional neuroimaging: a comparative review. Stat Methods Med Res 12:419-446.

Ninan PT (1999) The functional anatomy, neurochemistry, and pharmacology of anxiety. J Clin Psychiatry 60 Suppl 22:12-17.

O'Neil MF, Moore NA (2003) Animal models of depression: are there any? Hum Psychopharmacol 18:239-254.

Ogawa S, Lee TM (1990) Magnetic resonance imaging of blood vessels at high fields: in vivo and in vitro measurements and image simulation. Magn Reson Med 16:9-18.

Ogawa S, Lee TM, Nayak AS, Glynn P (1990) Oxygenation-sensitive contrast in magnetic resonance image of rodent brain at high magnetic fields. Magn Reson Med 14:68-78.

Okada G, Okamoto Y, Morinobu S, Yamawaki S, Yokota N (2003) Attenuated left prefrontal activation during a verbal fluency task in patients with depression. Neuropsychobiology 47:21-26.

Ongur D, Drevets WC, Price JL (1998) Glial reduction in the subgenual prefrontal cortex in mood disorders. Proc Natl Acad Sci U S A 95:13290-13295.

Ownby RL (1998) Computational model of obsessive-compulsive disorder: examination of etiologic hypothesis and treatment strategies. Depress Anxiety 8:91-103.

Paradiso S, Lamberty GJ, Garvey MJ, Robinson RG (1997) Cognitive impairment in the euthymic phase of chronic unipolar depression. J Nerv Ment Dis 185:748-754.

Parker G, Parker K (2003) Which antidepressants flick the switch? Aust N Z J Psychiatry 37:464-468.

Pascual-Leone A, Rubio B, Pallardo F, Catala MD (1996) Rapid-rate transcranial magnetic stimulation of left dorsolateral prefrontal cortex in drug-resistant depression. Lancet 348:233-237.

Paulus MP, Feinstein JS, Simmons A, Stein MB (2004) Anterior cingulate activation in high trait anxious subjects is related to altered error processing during decision making. Biol Psychiatry 55:1179-1187.

Paus T, Jech R, Thompson CJ, Comeau R, Peters T, Evans AC (1997) Transcranial magnetic stimulation during positron emission tomography: a new method for studying connectivity of the human cerebral cortex. J Neurosci 17:3178-3184.

Petrides M, Pandya DN (2002) Comparative cytoarchitectonic analysis of the human and the macaque ventrolateral prefrontal cortex and corticocortical connection patterns in the monkey. Eur J Neurosci 16:291-310.

Phillips ML, Drevets WC, Rauch SL, Lane R (2003) Neurobiology of emotion perception II: Implications for major psychiatric disorders. Biol Psychiatry 54:515-528.

Posner M, Snyder C (1975) Attention and cognitive control. In: Information Processing and Cognition: The Loyola Symposium. (Solso RI, ed). Hillsdale, NJ: Erlbaum.

Price JL (1999) Prefrontal cortical networks related to visceral function and mood. Ann N Y Acad Sci 877:383-396.

Quraishi S, Frangou S (2002) Neuropsychology of bipolar disorder: a review. J Affect Disord 72:209-226.

Rajkowska G (2000) Postmortem studies in mood disorders indicate altered numbers of neurons and glial cells. Biol Psychiatry 48:766-777.

Rajkowska G, Halaris A, Selemon LD (2001) Reductions in neuronal and glial density characterize the dorsolateral prefrontal cortex in bipolar disorder. Biol Psychiatry 49:741-752.

Rajkowska G, Miguel-Hidalgo JJ, Wei J, Dilley G, Pittman SD, Meltzer HY, Overholser JC, Roth BL, Stockmeier CA (1999) Morphometric evidence for neuronal and glial prefrontal cell pathology in major depression. Biol Psychiatry 45:1085-1098.

Ranganath C, Johnson MK, D'Esposito M (2003) Prefrontal activity associated with working memory and episodic long-term memory. Neuropsychologia 41:378-389.

Rangel A, Gonzalez LE, Villarroel V, Hernandez L (2003) Anxiolysis followed by anxiogenesis relates to coping and corticosterone after medial prefrontal cortical damage in rats. Brain Res 992:96-103.

Reid PD, Daniels B, Rybak M, Turnier-Shea Y, Pridmore S (2002) Cortical excitability of psychiatric disorders: reduced post-exercise facilitation in depression compared to schizophrenia and controls. Aust N Z J Psychiatry 36:669-673.

Richardson JS (1991) Animal models of depression reflect changing views on the essence and etiology of depressive disorders in humans. Prog Neuropsychopharmacol Biol Psychiatry 15:199-204.

Riso LP, Miyatake RK, Thase ME (2002) The search for determinants of chronic depression: a review of six factors. J Affect Disord 70:103-115.

Rogers MA, Bradshaw JL, Pantelis C, Phillips JG (1998) Frontostriatal deficits in unipolar major depression. Brain Res Bull 47:297-310.

Rogers MA, Bellgrove MA, Chiu E, Mileshkin C, Bradshaw JL (2004) Response selection deficits in melancholic but not nonmelancholic unipolar major depression. J Clin Exp Neuropsychol 26:169-179.

Rogers MA, Bradshaw JL, Phillips JG, Chiu E, Mileshkin C, Vaddadi K (2002) Mental rotation in unipolar major depression. J Clin Exp Neuropsychol 24:101-106.

Rojas-Corrales MO, Berrocoso E, Gibert-Rahola J, Mico JA (2002) Antidepressant-like effects of tramadol and other central analgesics with activity on monoamines reuptake, in helpless rats. Life Sci 72:143-152.

Rolls ET (1994) Neurophysiology and cognitive functions of the striatum. Rev Neurol (Paris) 150:648-660.

Rolls ET (1999) The brain and emotion.: Oxford university press.

Rose EJ (2004) PhD thesis. Cognitive changes in major depression: an fMRI study. In: Department of Psychiatry: University of Edinburgh.

Rose EJ, Goddard NH, Simonotto E, Marshall I, Ebmeier KP (2002) Working memory in depression - an fMRI study. In: Federation of European Neuroscience Societies. Paris.

Rosenblatt A, Leroi I (2000) Neuropsychiatry of Huntington's disease and other basal ganglia disorders. Psychosomatics 41:24-30.

Rosenzweig ES, Barnes CA (2003) Impact of aging on hippocampal function: plasticity, network dynamics, and cognition. Prog Neurobiol 69:143-179.

Rossi A, Arduini L, Daneluzzo E, Bustini M, Prosperini P, Stratta P (2000) Cognitive function in euthymic bipolar patients, stabilized schizophrenic patients, and healthy controls. J Psychiatr Res 34:333-339.

Rumelhart DE, McClelland JL (1987) Parallel Distributed Processing: Explorations in the Microstructure of Cognition: Psychological and Biological Models. Cambridge, MA: The MIT Press.

Sackeim HA, Wegner AZ (1986) Attributional patterns in depression and euthymia. Arch Gen Psychiatry 43:553-560.

Salo R, Henik A, Robertson LC (2001) Interpreting Stroop interference: an analysis of differences between task versions. Neuropsychology 15:462-471.

Sanacora G, Rothman DL, Mason G, Krystal JH (2003) Clinical studies implementing glutamate neurotransmission in mood disorders. Ann N Y Acad Sci 1003:292-308.

Sanacora G, Gueorguieva R, Epperson CN, Wu YT, Appel M, Rothman DL, Krystal JH, Mason GF (2004) Subtype-specific alterations of gamma-aminobutyric acid and glutamate in patients with major depression. Arch Gen Psychiatry 61:705-713.

Sassi RB, Brambilla P, Nicoletti M, Mallinger AG, Frank E, Kupfer DJ, Keshavan MS, Soares JC (2003) White matter hyperintensities in bipolar and unipolar patients with relatively mild-to-moderate illness severity. J Affect Disord 77:237-245.

Sax KW, Strakowski SM, Zimmerman ME, DelBello MP, Keck PE, Jr., Hawkins JM (1999) Frontosubcortical neuroanatomy and the continuous performance test in mania. Am J Psychiatry 156:139-141.

Scheinerman ER (1995) Invitation to Dynamical Systems: Prentice Hall.

Schumacker RE, Lomax RG (1996) A beginner's guide to Structural Equation Modeling. Mahwah, New Jersey: Lawrence Erlbaum Associates.

Seel RT, Kreutzer JS, Rosenthal M, Hammond FM, Corrigan JD, Black K (2003) Depression after traumatic brain injury: a National Institute on Disability

and Rehabilitation Research Model Systems multicenter investigation. Arch Phys Med Rehabil 84:177-184.

Seitz RJ, Knorr U, Azari NP, Herzog H, Freund HJ (1999) Visual network activation in recovery from sensorimotor stroke. Restor Neurol Neurosci 14:25-33.

Seligman ME (1978) Learned helplessness as a model of depression. Comment and integration. J Abnorm Psychol 87:165-179.

Shah AA, Treit D (2003) Excitotoxic lesions of the medial prefrontal cortex attenuate fear responses in the elevated-plus maze, social interaction and shock probe burying tests. Brain Res 969:183-194.

Shah PJ, Ebmeier KP, Glabus MF, Goodwin GM (1998) Cortical grey matter reductions associated with treatment-resistant chronic unipolar depression. Controlled magnetic resonance imaging study. Br J Psychiatry 172:527-532.

Shah PJ, Glabus MF, Goodwin GM, Ebmeier KP (2002) Chronic, treatment-resistant depression and right fronto-striatal atrophy. Br J Psychiatry 180:434-440.

Shajahan PM, Glabus MF, Gooding PA, Shah PJ, Ebmeier KP (1999) Reduced cortical excitability in depression. Impaired post-exercise motor facilitation with transcranial magnetic stimulation. Br J Psychiatry 174:449-454.

Shajahan PM, Glabus MF, Steele JD, Doris AB, Anderson K, Jenkins JA, Gooding PA, Ebmeier KP (2002) Left dorso-lateral repetitive transcranial magnetic stimulation affects cortical excitability and functional connectivity, but does not impair cognition in major depression. Prog Neuropsychopharmacol Biol Psychiatry 26:945-954.

Sheline YI, Sanghavi M, Mintun MA, Gado MH (1999) Depression duration but not age predicts hippocampal volume loss in medically healthy women with recurrent major depression. J Neurosci 19:5034-5043.

Siegle GJ (1998) Connectionist Models of Cognitive, Affective, Brain, and Behavioral Disorders. In.

Siegle GJ (1999) A neural network model of attention biases in depression. In: Prog Brain Res (Reggia JA, Ruppin E, Glanzman DL, eds), pp 407-432.

Siegle GJ, Steinhauer SR, Thase ME, Stenger VA, Carter CS (2002) Can't shake that feeling: event-related fMRI assessment of sustained amygdala activity in response to emotional information in depressed individuals. Biol Psychiatry 51:693-707.

Simmen MW, Goodhill GJ, Willshaw DJ (1994) Scaling and brain connectivity. Nature 369:448-450.

Simpson JR, Jr., Snyder AZ, Gusnard DA, Raichle ME (2001a) Emotion-induced changes in human medial prefrontal cortex: I. During cognitive task performance. Proc Natl Acad Sci U S A 98:683-687.

Simpson JR, Jr., Drevets WC, Snyder AZ, Gusnard DA, Raichle ME (2001b) Emotion-induced changes in human medial prefrontal cortex: II. During anticipatory anxiety. Proc Natl Acad Sci U S A 98:688-693.

Smoller JW, Finn CT (2003) Family, twin, and adoption studies of bipolar disorder. Am J Med Genet 123C:48-58.

Soares JC, Mann JJ (1997) The functional neuroanatomy of mood disorders. J Psychiatr Res 31:393-432.

Solomon A (2001) The noonday demon, UK Edition. London: Chatto & Windus.

Somogyi P, Tamas G, Lujan R, Buhl EH (1998) Salient features of synaptic organisation in the cerebral cortex. Brain Res Brain Res Rev 26:113-135.

Speer AM, Kimbrell TA, Wassermann EM, J DR, Willis MW, Herscovitch P, Post RM (2000) Opposite effects of high and low frequency rTMS on regional brain activity in depressed patients. Biol Psychiatry 48:1133-1141.

Spielberger CD, Gorsuch RL, Lushene RD (1970) Manual for State-Trait Anxiety Inventory. Plto Alto, CA: Consulting Psychologists Press.

Stahl SM (2002) The psychopharmacology of energy and fatigue. J Clin Psychiatry 63:7-8.

Starkstein E (1998) Neurological models of depression. In: New Models of Depression (Ebert D, Ebmeier KP, eds), pp 123-135. Basel: Karger.

Steele JD, Glabus MF, Shajahan PM, Ebmeier KP (2000) Increased cortical inhibition in depression: a prolonged silent period with transcranial magnetic stimulation (TMS). Psychol Med 30:565-570.

Stefanacci L, Amaral DG (2000) Topographic organization of cortical inputs to the lateral nucleus of the macaque monkey amygdala: a retrograde tracing study. J Comp Neurol 421:52-79.

Stefurak T, Mikulis D, Mayberg H, Lang AE, Hevenor S, Pahapill P, Saint-Cyr J, Lozano A (2003) Deep brain stimulation for Parkinson's disease dissociates mood and motor circuits: a functional MRI case study. Mov Disord 18:1508-1516.

Stein DJ, Ludik J (2000) A neural network of obsessive- compulsive disorder: modelling cognitive disinhibition and neurotransmitter dysfunction. Med Hypotheses 55:168-176.

Stevens A, Price J (2000) Evolutionary Psychiatry: a new beginning, 2nd Edition. London: Routledge.

Strafella AP, Paus T, Barrett J, Dagher A (2001) Repetitive transcranial magnetic stimulation of the human prefrontal cortex induces dopamine release in the caudate nucleus. J Neurosci 21:RC157.

Strakowski SM, DelBello MP, Sax KW, Zimmerman ME, Shear PK, Hawkins JM, Larson ER (1999) Brain magnetic resonance imaging of structural abnormalities in bipolar disorder. Arch Gen Psychiatry 56:254-260.

Stroop J (1935) Studies of interference in serial verbal reaction. Journal of Experimental Psychology 18:643-662.

Suzuki WA, Amaral DG (1994) Perirhinal and parahippocampal cortices of the macaque monkey: cortical afferents. J Comp Neurol 350:497-533.

Swann AC, Katz MM, Bowden CL, Berman NG, Stokes PE (1999) Psychomotor performance and monoamine function in bipolar and unipolar affective disorders. Biol Psychiatry 45:979-988.

Tagamets MA, Horwitz B (1998) Integrating electrophysiological and anatomical experimental data to create a large-scale model that simulates a delayed match-to-sample human brain imaging study. Cereb Cortex 8:310-320.

Tagamets MA, Horwitz B (2001) Interpreting PET and fMRI measures of functional neural activity: the effects of synaptic inhibition on cortical activation in human imaging studies. Brain Res Bull 54:267-273.

Tagamets MA, Horwitz B (2003) The use of large-scale modeling for interpreting human brain imaging data. In: Exploratory analysis and Data Modeling In Functional Neuroimaging (Sommer FT, Wichert A, eds). Cambridhe, MA: The MIT Press.

Talairach J, Tournoux P (1988) Co-Planar Stereotaxic Atlas of the Human Brain. Stuttgart, New York.: Thieme.

Tamada R, Issler C, Amaral J, Sachs G, Lafer B (2004) Treatment emergent affective switch: a controlled study. Bipolar Disord 6:333-337.

Teicher MH, Andersen SL, Polcari A, Anderson CM, Navalta CP (2002) Developmental neurobiology of childhood stress and trauma. Psychiatr Clin North Am 25:397-426, vii-viii.

Thompson JK, Peterson MR, Freeman RD (2003) Single-neuron activity and tissue oxygenation in the cerebral cortex. Science 299:1070-1072.

Ungerleider LG, Mishkin M (1982) Two cortical visual systems. In: Analysis of visual behaviour (Ingle DJ, Goodale MA, Mansfield RJW, eds), pp 549-586. Cambridge, MA: MIT Press.

Van Elst LT, Ebert D, Trimble MR (2001) Hippocampus and amygdala pathology in depression. Am J Psychiatry 158:652-653.

van Gorp WG, Altshuler L, Theberge DC, Wilkins J, Dixon W (1998) Cognitive impairment in euthymic bipolar patients with and without prior alcohol dependence. A preliminary study. Arch Gen Psychiatry 55:41-46.

Van Hoesen GW, Morecraft RJ, Vogt BA (1993) Connections to the monkey cingulate cortex. In: Neurobiology of the cingulate cortex and limbic thalamus: a

comprehensive handbook. (Vogt BA, Gabriel ME, eds), pp 249-284. Boston, MA: Birkhauser.

Veiel HO (1997) A preliminary profile of neuropsychological deficits associated with major depression. J Clin Exp Neuropsychol 19:587-603.

Videbech P (1997) MRI findings in patients with affective disorder: a meta-analysis. Acta Psychiatr Scand 96:157-168.

Vogt BA, Pandya DN (1987) Cingulate cortex of the rhesus monkey: II. Cortical afferents. J Comp Neurol 262:271-289.

Volkow ND, Rosen B, Farde L (1997) Imaging the living human brain: magnetic resonance imaging and positron emission tomography. Proc Natl Acad Sci U S A 94:2787-2788.

Wall MM, Li R (2003) Comparison of multiple regression to two latent variable techniques for estimation and prediction. Stat Med 22:3671-3685.

Whalen PJ, Rauch SL, Etcoff NL, McInerney SC, Lee MB, Jenike MA (1998) Masked presentations of emotional facial expressions modulate amygdala activity without explicit knowledge. J Neurosci 18:411-418.

Wilder-Willis KE, Sax KW, Rosenberg HL, Fleck DE, Shear PK, Strakowski SM (2001) Persistent attentional dysfunction in remitted bipolar disorder. Bipolar Disord 3:58-62.

Wilson FA, Scalaidhe SP, Goldman-Rakic PS (1993) Dissociation of object and spatial processing domains in primate prefrontal cortex. Science 260:1955-1958.

Winterer G, Ziller M, Linden M (1998) Classification of observational data with artificial neural networks versus discriminant analysis in pharmacoepidemiological studies--can outcome of fluoxetine treatment be predicted? Pharmacopsychiatry 31:225-231.

Worsley KJ, Marrett S, Neelin P, Vandal AC, Friston KJ, Evans AC (1996) A unified statistical approach for determining significant signals in images of cerebral activation. Hum Brain Mapp 4:58-73.

Wu J, Buchsbaum MS, Gillin JC, Tang C, Cadwell S, Wiegand M, Najafi A, Klein E, Hazen K, Bunney WE, Jr., Fallon JH, Keator D (1999) Prediction of antidepressant effects of sleep deprivation by metabolic rates in the ventral anterior cingulate and medial prefrontal cortex. Am J Psychiatry 156:1149-1158.

Wu JC, Buchsbaum M, Bunney WE, Jr. (2001) Clinical neurochemical implications of sleep deprivation's effects on the anterior cingulate of depressed responders. Neuropsychopharmacology 25:S74-78.

Yang TT, Menon V, Eliez S, Blasey C, White CD, Reid AJ, Gotlib IH, Reiss AL (2002) Amygdalar activation associated with positive and negative facial expressions. Neuroreport 13:1737-1741.

Yeterian EH, Pandya DN (1991) Prefrontostriatal connections in relation to cortical architectonic organization in rhesus monkeys. J Comp Neurol 312:43-67.

Young MP (1992) Objective analysis of the topological organization of the primate cortical visual system. Nature 358:152-155.

Young RC, Biggs JT, Ziegler VE, Meyer DA (1978) A rating scale for mania: reliability, validity and sensitivity. Br J Psychiatry 133:429-435.

Zakzanis KK, Leach L, Kaplan E (1998) On the nature and pattern of neurocognitive function in major depressive disorder. Neuropsychiatry Neuropsychol Behav Neurol 11:111-119.

Zerbin-Rudin E (1987) Psychiatric genetics and psychiatric nosology. J Psychiatr Res 21:377-383.

Zubenko GS, Hughes HB, 3rd, Maher BS, Stiffler JS, Zubenko WN, Marazita ML (2002) Genetic linkage of region containing the CREB1 gene to depressive disorders in women from families with recurrent, early-onset, major depression. Am J Med Genet 114:980-987.

Zubieta JK, Huguelet P, O'Neil RL, Giordani BJ (2001) Cognitive function in euthymic bipolar I disorder. Psychiatry Res 102:9-20.

Appendix A

Ebmeier KP, Kronhaus DM (2001)

Brain imaging in mood disorders

Textbook of Biological Psychiatry (D'Haenen H, der Boer JA, Westenberg H, Willner P, eds). New-York: John Wiley & Sons, Ltd.

XVIII-9

Brain Imaging in Mood Disorders

Klaus P. Ebmeier and Dina Kronhaus

INTRODUCTION

Depression, as the reversible psychiatric condition par excellence, is clearly an ideal object of functional neuroimaging studies. In theory, patients return to their initial (healthy) brain state so that any image changes observed during an affective episode should mark the brain structures and circuits involved in the expression of symptoms and signs. Authors have imaged patients when ill and after recovery and used a number of strategies to exploit short-term fluctuations of symptoms. Such fluctuations occur naturally, as in the typical diurnal variations of mood (Moffoot *et al.*, 1994b), or they can be provoked by interventions, such as mood induction (Baker *et al.*, 1997), sleep deprivation (Ebert *et al.*, 1994a) or tryptophan depletion (Smith *et al.*, 1999b). If, on the other hand, anatomical changes did exist in depression, they would be predicted in cases of treatment resistance (Shah *et al.*, 1998), in secondary or late-onset depression (Ebmeier *et al.*, 1998), or possibly a priori in certain patients with a genetic predisposition for the illness (Drevets *et al.*, 1998).

Anatomical systems involved are likely to be medial limbic, with the anterior cingulate cortex and orbitofrontal cortex playing a prominent role (Ebert and Ebmeier, 1996). There is also the well-rehearsed hypothesis of hypercortisolaemia, which occurs frequently in depression and, at least in animal models, leads to hippocampal damage. Hippocampal damage, in turn, would release the pituitary secretion of adrenocorticotropic hormone (ACTH) from hippocampal suppression and result in a positive feedback loop (Sapolsky *et al.*, 1986). This mechanism may not be specific to depression (Welberg *et al.*, 2001), as some authors have also used it to explain cognitive impairment or dementia (Hibberd *et al.*, 2000) and the sequelae of severe psychological trauma (Bremner *et al.*, 1995).

Neuropsychological tasks have been employed in imaging studies to activate brain systems thought to be implicated in depression, in particular using 'frontal' (e.g. word-generation) or 'temporal' (memory) tasks. In such experiments, limited task performance may be responsible for group differences. Attempts to control for such performance differences include pacing tasks at a speed that all patients can manage, and post-hoc correlation of brain activity with task performance, e.g. by using analysis of covariance. A further complication of functional imaging protocols is that it is now very difficult to recruit untreated patients in a psychiatric setting. Primary-care physicians have usually already treated their patients with a standard antidepressant (e.g. a selective serotonin reuptake inhibitor, SSRI) by the time of referral. The cost and effort required to recruit patients at the primary care level is usually seen as prohibitive. For this reason, many studies contain samples of medicated patients and have to be interpreted with caution. It also cannot be excluded that changes in brain activity or even brain anatomy may be caused by medication (DelBello *et al.*, 1999).

Medication is, of course, a particular problem for receptor ligand studies. Based on effective pharmacological treatment, there are a variety of hypotheses, particularly involving the serotonergic and noradrenergic transmitter systems, which are theoretically amenable to *in vivo* testing with neuroimaging (Delgado *et al.*, 1990). Not only the availability of untreated patients but also the availability of receptor ligands has limited such research. The latter may be partially responsible for the dearth of noradrenaline ligand studies. Not all ligands are suitable; their use may be limited by their specificity for the receptor concerned, their affinity (i.e. the likelihood to be displaced by endogenous ligand) and their nondisplaceable (nonspecific) binding fraction. In spite of these limitations, first results are now emerging that test some of the extant pharmacological hypotheses in depression.

Rather than giving a balanced review of all studies carried out in the field, we will focus on certain themes and future prospects that appear to be emerging. Our selection will no doubt be idiosyncratic, but we hope that we have captured the important paradigms and paths of current research. In order to limit the size of the chapter, we will focus on key publications of the last 5 years (at the time of writing), as earlier literature has been summarized well in a number of other reviews (Davidson *et al.*, 1999; Drevets, 1998; Kennedy *et al.*, 1997; Norris *et al.*, 1997; Stoll *et al.*, 2000; Videbech, 1997; Videbech, 2000). Rather than systematically dividing the imaging literature by image modality or diagnosis, we will attempt to present a logical narrative, proceeding from simple (e.g. neurochemical) hypotheses, such as the dopamine theory of psychomotor retardation in depression, to more complex models. Hypotheses that are, in a sense, post-hoc, i.e. exploit the natural history of depressive symptoms and their treatment, will be followed by experimental approaches, which imply complex neuronal systems and attempt to activate selectively such systems that are thought to be implicated in the expression of depressive symptoms. Mania is a rare condition that is very difficult to study with neuroimaging techniques, and reports are rare (Al-Moussawi *et al.*, 1996). This illness will, therefore, not be discussed, except when included in studies of bipolar depressed patients.

PHARMACOLOGY

Dopamine and Motor Function

Although dopamine is not thought to be involved primarily in the treatment and the experience of symptoms of depression, it may play an important role in the brain reward systems and in movement control. It has been implicated in retarded depression, both by the reduction of the dopamine metabolite homovanillic acid in cerebrospinal fluid (Jimerson, 1987) and by increased D2 receptor binding, particularly in psychomotor retarded patients (Ebmeier and

Biological Psychiatry: Edited by H. D'haenen, J. A. den Boer and P. Willner. ISBN 0 471 49198 5

Ebert, 1997). Increased postsynaptic receptor binding is interpreted mainly as evidence of reduced dopaminergic activity with resulting receptor supersensitivity or, alternatively, reduced displacement of the radioligand by endogenous dopamine (Shah *et al.*, 1997). Sleep deprivation, which may have an amphetamine-like effect, is associated with displacement of such ligands from their binding sites in the neostriatum (Ebert and Berger, 1998). Whether reduced availability of dopamine is ubiquitous in depression is, however, doubtful. At least one single photon emission computed tomography (SPECT) study (Klimke *et al.*, 1999) ($n = 15$) found a reduction in ligand binding to D2 receptors that normalized on clinical recovery and predicted response to SSRIs. Paillere-Martinot *et al.* (2001) reported a reduction in left caudate 18F-dihydroxyphenylalanine (DOPA) positron emission tomography (PET) only in blunted and retarded, but not in impulsive and anxious, depression. Examining presynaptic loci, 15 drug-naive patients with major depression showed significant increases in SPECT striatal dopamine transporter (DAT) binding capacity (Laasonen-Balk *et al.*, 1999). This may be interpreted similarly to the findings in D2 receptors, as a correlate of reduced availability of dopamine (see above). This effect, however, was not reported in 31 drug naive children. Serotonin transporter (SERT) binding (see below) but not DAT binding in the hypothalamus and midbrain was increased (Dahlstrom *et al.*, 2000). Interestingly, during acute cocaine abstinence ($n = 28$), associated with depressive symptoms and a 20% increase in striatal DAT binding capacity measured by SPECT, there was a negative correlation of tracer binding with Hamilton depression scores (Malison *et al.*, 1998a), suggesting an adaptive response. Basal ganglia involvement in depression is demonstrated by not only abnormal dopamine ligand studies but also imaging studies examining brain activation and blood flow. Hickie *et al.* (1999) reported a correlation between (delayed) reaction time and (reduced) left neostriatal activation from simple to choice reaction time tasks in psychomotor retarded patients. Finally, basal ganglia pathology may predispose to late-onset or secondary depression, as suggested by magnetic resonance imaging (MRI) lesion studies (Lauterbach *et al.*, 1997) and MRI studies of iron deposition (Steffens *et al.*, 1998).

Noradrenaline

Although noradrenaline has been implicated in depression for many years (Zis and Goodwin, 1982), there have been relatively few neuroimaging studies. After driving the noradrenergic system with clonidine, an alpha2 agonist, a study in six depressed and six healthy women found an increase in right prefrontal perfusion only in the depressed group, suggesting either presynaptic subsensitivity or a local supersensitivity of postsynaptic alpha2 receptors (Fu *et al.*, 2001). This may not be a specific finding, as Moffoot reported similar results for patients with Korsakoff psychosis (Moffoot *et al.*, 1994a).

Serotonin

Serotonergic Activation, Treatment Effects and Response

In accordance with the theoretical and practical importance of SSRIs in the treatment of depression, a number of studies have examined the effects of SSRIs on brain function, both explicitly and by comparing patients when they are ill and recovered. Mayberg *et al.* (1997) examined 18 hospitalized patients with unipolar depression and reported that rostral (anterior) cingulate (Brodman's area 24a,b) metabolism predicted response (hypermetabolism) and lack of response (hypometabolism) to fluoxetine. In a repeat measures study (Brody *et al.*, 1999), 16 depressed outpatients were imaged with 18F-fluorodeoxyglucose (FDG)–PET before and after treatment with paroxetine. SSRI responders showed a reduction in ventral prefrontal perfusion, but low (left) ventral anterior cingulate reduction before treatment predicted a better response. These findings could be in contradiction to the data of Mayberg *et al.* (1997). However, patients in that study were more clinically unwell, different SSRIs were used, and the target areas do not seem to be congruent.

In reversal of SSRI treatment, depletion of serotonin by a low-tryptophan amino acid drink can lead to a temporary lowering of mood in recovered depressed patients. Smith *et al.* (1999b) found that 'increasing levels of depression after tryptophan depletion were associated with diminished neural activity in ventral anterior cingulate, orbito-frontal cortex and caudate nucleus regions' during paced verbal fluency performance. In addition, depressive relapse attenuated cognitive task-related activation in the anterior cingulate. This study illustrates potential complications in design arising when behavioural conditions are mixed with pharmacological interventions in neuroimaging: although not obvious in this study, the pharmacological interventions may affect task performance as well as mood. The separation of drug and clinical effects, and the statistical definition of the interaction between the two, are, up to a point, arbitrary. The same group also confirmed the specific hypothesis that mood deterioration induced by low-tryptophan drink would increase activity in the projection from the habenula to the raphe, structures that are part of the feedback loop controlling the release of 5-hydroxytryptamine (5-HT) throughout the brain (Morris *et al.*, 1999). A reliable differential effect of the indirect serotonin agonist fenfluramine on brain perfusion in healthy volunteers and depressed patients has not been established. A study of 13 depressed and 18 healthy women showed identical effects in both diagnostic groups after intravenous infusion (Meyer *et al.*, 1998).

Serotonin Transporter

After an initial rush of interest in the association of certain SERT alleles with depression, a number of imaging studies have used SERT ligands with patients (Battersby *et al.*, 2001). Such studies are understandably difficult to conduct, as medicated patients cannot be used. Unipolar depressed patients exhibited a characteristic reduction of 18% in SERT in the brainstem, where the highest concentrations of receptors can be found, compared with healthy volunteers (Malison *et al.*, 1998b). Patients with seasonal affective disorder showed reduced SERT binding capacity in the thalamus and hypothalamus but not in the midbrain or pons (Willeit *et al.*, 2000). This effect, however, was reversed in the hypothalamus and midbrain, where increased SERT binding correlated with concurrent depression in a group of drug-naive children ($n = 41$). Increased binding could be attributed to a reduction of serotonin within the synaptic cleft (thus allowing increased tracer binding), with developmental differences accounting for contradictory results for adult and child transporter binding (Dahlstrom *et al.*, 2000).

5-HT2 Receptor

Post-mortem studies have suggested that a history of depression and, in particular, suicidal behaviour is associated with an increase in 5-HT2 receptors (Mann *et al.*, 1999). In contrast, a study of six drug-free, depressed patients examined with 18F-altanserin PET reported reduced binding in the right posterolateral orbitofrontal cortex and anterior insula with trends on the left side (Biver *et al.*, 1997). This apparent contradiction may be explained by receptor downregulation due to medication: eight of ten depressed patients who improved with desipramine showed a decrease in 18F-setoperone binding to the 5-HT2 receptor in many cortical areas (Yatham *et al.*, 1999). Further, an 18F-setoperone study before and

after 6 weeks of paroxetine medication in 19 depressed patients suggested a reduced binding capacity after treatment, which was found mainly in patients younger than 30 years of age. A study of 14, better controlled, drug- and self-harm-free (>6 months) depressed patients showed no abnormalities in prefrontal 18F-setoperone binding (Meyer *et al.*, 1999). Similarly, 11 elderly depressed patients did not show an *in vivo* reduction of 18F-altanserin binding capacity (Meltzer *et al.*, 1999).

5-HT1a Receptor

Rueter *et al.* (1998) have argued that antidepressant effects are due to a desensitization of 5-HT1a somatodendritic autoreceptors in the rat, which is responsible for the return to normal firing rate levels in the dorsal raphe nucleus. A single study has confirmed the hypothesized reduction in 5-HT1a binding capacity in depressed patients (Lesch *et al.*, 1990) using the PET ligand 11C-WAY-100635. Twelve primarily depressed patients with a family history of the illness showed reductions in binding capacity in the brainstem raphe, medial temporal cortex and possibly other cortical areas. This effect was greatest in bipolar patients and patients with a family history of bipolar illness (Drevets *et al.*, 1999).

'NATURAL EXPERIMENTS': CLINICAL PROFILES, TREATMENT RESPONSE AND TREATMENT RESISTANCE

What can neuroimaging studies tell us about depression that clinical description could not? Comparison of pretreatment and post-treatment neural activity is the most obvious way to associate *in vivo* neurobiological markers with depressive symptoms, cognitive ability or deficits. There is also mounting evidence for a correspondence between pretreatment metabolism in specific areas and treatment outcome. Characteristic changes in perfusion may help to classify patients with similar neuropathology. Changes in functional circuitry may emerge as predictors of treatment response and residual dysfunction whenever remission is not synonymous with recovery. Because a substantial placebo or spontaneous remission effect contributes to the drug treatment of depression, it is unclear whether changes in cortical dynamics upon recovery are associated with the nature or the extent of drug-induced changes (Andrews, 2001).

Neuroanatomical and functional deficits may already be identifiable as vulnerability factors in patients' families, or they may, at the other extreme, be the correlate of lingering abnormalities, such as perturbed cortical dynamics and impaired cognitive performance that are present beyond remission (Abas *et al.*, 1990). Persistent abnormalities can be a consequence of several factors. First, chronic administration of antidepressant, anticonvulsant or antipsychotic medication may contribute to the enduring brain changes (DelBello *et al.*, 1999). Second, impaired function during (or between) clinical episodes may compromise a system that is already fragile or affected in some way, and thus cause enduring damage (Sapolsky *et al.*, 1986). Finally, since affective disorders are often characterized by recurrent episodes over time, the normal process of ageing may be a confounder or may interact with the illness process (Kapur *et al.*, 1994). The interpretation of treatment progress in depression is also not straightforward. Change in behaviour, cognition or motor activity may not necessarily imply an associated modification in functional circuitry with return to normal activity (Goodwin *et al.*, 1993). Psychopharmacological agents target one or more neurotransmitter systems. Nonetheless, if the activity of one of the widely projecting neurotransmitter systems (dopamine, noradrenaline, 5-HT) increases, then global cortical dynamics will also be affected. Functional connectivity changes in mood disorders will be associated with abnormalities at rest (baseline) or, more likely, an abnormal pattern of recruitment during cognitive or motor activity. Where structural abnormalities have been reported in unipolar and bipolar depression, it is not unreasonable to assume that baseline and task-associated functional connectivity changes may occur. Brain imaging provides an assessment tool for the course of both illness-induced changes and active mechanism of recovery or compensation. In accordance with Alexander's (Alexander *et al.*, 1986) and Swerdlow and Koob's (1987) theories of functional cortico-subcortical loops, cortical areas (such as the frontal, temporal and parietal cortices), subcortical areas (such as the basal ganglia and thalamus), and most of all areas related to the limbic system (such as the anterior cingulate, hippocampus and amygdala) will be affected.

In order to better understand blood-flow abnormalities in affective disorders and consequent remission effected by different forms of treatment, findings can be separated into a number of distinct categories: pretreatment perfusion, post-treatment perfusion, activity in responders and nonresponders, and the comparison of either or both with control subjects. Some studies do not include healthy volunteers; therefore, it is impossible to tell whether remission is associated with normalization of perfusion. The use of diverse methodologies in clinical studies makes the comparison between their findings difficult. The neuroanatomical maps or delineation of specific brain regions (Brodman's areas) used to localize activation may not be identical throughout the literature. Despite anatomical proximity, these areas may have very different connectivity patterns. For example, the medial or orbital frontal networks receive input from very different areas of the cortex (Barbas *et al.*, 1999; Bhashghaei and Barbas, 2001). Methodological constraints on studies in a clinical setting include great variations in the size of samples, which are often small and occasionally nonuniform in terms of age, medication and clinical history. Medication can influence outcomes in both neuropsychological and imaging studies, although the duration of medication effects is not known (Elliott *et al.*, 1998). An agreed standard for response to medication lies around 6 weeks, but it may take longer to establish remission. Therefore, brain imaging carried out at a later stage (Pizzagalli *et al.*, 2001) may be recording the long-term behavioural gain of therapeutic intervention, rather than incidental drug effects.

An alternative to measuring regional metabolic changes is to examine functional connectivity. Mallet *et al.* (1998) found decreased interhemispheric connectivity along with reduced connectivity within the right hemisphere (in a cortical–subcortical as well as anterior–posterior orientation) in schizophrenia, obsessive–compulsive disorder and unipolar depression. In depressed subjects, these deficits were mostly resolved on remission. A distinct 'melancholic pattern' was noted, with decreased correlation between the orbitofrontal cortex and the dorsolateral prefrontal cortex compared with controls and non-melancholic depressed subjects (Mallet *et al.*, 1998).

TREATMENT METHODS

Sleep Deprivation

Up to 60% of patients can improve after a night of total sleep deprivation (TSD) (Ebert and Berger, 1998). In contrast to the delayed cumulative effects of antidepressant medication, TSD has an immediate effect that does not appear to extend beyond the next full night's sleep (Ebert and Berger, 1998). The experimental advantage of TSD is that patients do not have to be medicated to show a short-term clinical improvement. The effects of TSD have been explained with increased dopamine release in the basal ganglia, which results in increased displacement of the D2/D4 receptor radio ligand 123I-iodobenzamide (IBZM) by endogenous dopamine, i.e.

reduced ligand binding (Ebert *et al.*, 1994b). However, an allele of the D4 dopamine receptor, which has been suggested previously to increase susceptibility to this treatment, was not linked to treatment response in 124 bipolar patients (Serretti *et al.*, 1999). A growing body of evidence is documenting hyperperfusion in the medial prefrontal cortex as a state or trait related change (Ebert and Berger, 1998; Ebert *et al.*, 1996). Allied with limbic hyperperfusion, a number of studies describe dorsolateral prefrontal cortex hypoperfusion in depression and during mood induction in normal volunteers (Mayberg *et al.*, 1999). The early sleep deprivation literature reported increased perfusion in the orbitofrontal cortex that was found in the right anterior cingulate and bilateral orbitofrontal cortex and basal cingulate. Increased right hippocampal pretreatment flow was associated with greater treatment response (Ebert *et al.*, 1994a). Similar findings, indicating the association between successful drug treatment and pretreatment limbic hyperperfusion, have since been reported by a number of groups. Comparing glucose metabolism in hospitalized unipolar patients, Mayberg *et al.* (1997) reported hyperperfusion in the rostral anterior cingulate (Brodman's area 24a/b) to be indicative of a favourable treatment outcome. Although subsequent nonresponders were reported to be marginally more impaired than responders on neuropsychological performance, no other correlation between perfusion and clinical ratings was found. Hypoperfusion in responders was greater than in nonresponders in the dorsolateral prefrontal cortex (Brodman's area 45/46), anterior insula and inferior parietal cortex (Brodman's area 40). Pretreatment premotor cortex activation, on the other hand, was greater in responders.

The prognostic capacity of anterior cingulate activity with reference to the extent of treatment response can also be measured with electroencephalography (EEG) (Smith *et al.*, 1999a). Higher θ (6.5–8 Hz) activity in the rostral cingulate was associated with a greater response after 4–6 months of treatment with nortriptyline. A greater degree of response was associated with increased pretreatment θ activity in the medial frontal cortex (Brodman's area 24, 32), consistent with previous functional imaging reports (Mayberg *et al.*, 1997).

Pretreatment metabolism in the medial prefrontal cortex (Brodman's area 32), ventral anterior cingulate (Brodman's area 24) and posterior subcallosal gyrus (Brodman's area 25) was found to be higher in responders to TSD than in nonresponders and healthy volunteers (Wu *et al.*, 1999). Normalization upon recovery was noted with decreased flow in the medial prefrontal cortex (Brodman's area 32) and the frontal pole (Brodman's area 10). All depressed subjects had a lower striatal (putamen) metabolic rate than controls, which persisted after treatment and, by contrast, decreased in normal volunteers. Frontal and occipital cortex metabolism was also higher in both groups before treatment. The activity in the right lateral prefrontal cortex (Brodman's area 46) and higher superior temporal cortex and right insula increased in responders. Perfusion was decreased in the lateral prefrontal cortex of controls. Moreover, in comparison with control subjects, the neuropsychological performance of all depressed patients deteriorated markedly after a night of TSD. Normal subjects performing a verbal learning task following 35 hours of sleep deprivation exhibited a pattern of increased activation in the prefrontal and parietal cortices, whereas activity in their temporal lobe was decreased (Drummond *et al.*, 2000). Decline in subjects' performance of a free recall task was correlated positively with activation of their parietal lobe. Bilateral prefrontal cortex activation, which was related closely to personal perception of fatigue, was interpreted as a competitive mechanism associated with the homeostatic urge for sleep. Compensation for decreased temporal lobe activity appears to be achieved by increased perfusion in the bilateral parietal lobes in verbal tasks, which are not associated with this area in the control condition. Just as TSD created characteristic changes in blood flow during verbal learning challenge, elevated pretreatment regional cerebral blood flow (rCBF) in the right orbitofrontal cortex and basal cingulate of patients was normalized in responders to partial sleep deprivation (in the latter part of the night). Post-treatment left inferior temporal flow was correlated with treatment response (Volk *et al.*, 1997).

In summary, these studies appear to suggest that elevated metabolism and blood flow in the prefrontal or medial prefrontal cortex areas is an adaptive marker aiding response to different forms of therapeutic intervention, especially sleep deprivation. Depressed patients may share an abnormal functional network (decreased flow in subcortical structures) (Wu *et al.*, 1999) or persistent abnormalities throughout the temporal cortex (where structural changes have also been reported) (Shah *et al.*, 1998; Sheline *et al.*, 1998; Sheline *et al.*, 1999) that may accommodate behavioural changes by compensating for hypoperfusion elsewhere. In certain patients, this mechanism may later cease to be effective.

Sleep disturbance during rapid eye movement (REM) and nonrapid eye movement (NREM) sleep are well documented in patients suffering from affective disorders (Kupfer and Reynolds, 1992). Ho *et al.* (1996) studied the δ stage of slow-wave (high-amplitude) sleep of NREM sleep with FDG–PET in depression and found that metabolism was elevated in the occipital and parietal cortices to a greater degree than elsewhere. Limbic structures, such as the posterior cingulate, amygdala and hippocampus, were more active in depressed patients; however, metabolism in midline structures and the neostriatum (including the medial prefrontal cortex, medial thalamus, anterior cingulate, bilateral caudate, putamen and the head of the caudate) was reduced compared with controls. In conjunction with an EEG investigation, Nofzinger *et al.* (2000) studied the link between β EEG frequency (characterized by higher frequency and lower amplitude) and glucose metabolism in different areas of the cortex, defined on the basis of findings from control data. β-Wave frequency had been coupled previously with secretion of cortisol (Chapotot *et al.*, 1998) and, in this study, was present for longer in depressed subjects and was associated negatively with subjective sleep quality. No hypofrontality was found in this study; however, orbitofrontal cortex (including Brodman's areas 11, 25, 32) metabolism was higher in depressed patients than in controls, which may be indicative of dysfunctional arousal. Finally, the contrast between waking and REM sleep revealed that, unlike controls, depressed subjects failed to recruit anterior paralimbic areas (right parahippocampal gyrus, right insula and anterior cingulate). Instead, temporal-limbic areas (amygdala, subiculum, inferior temporal cortex, sensorimotor cortex) were activated (Nofzinger *et al.*, 1999).

Light Therapy

In patients suffering from seasonal affective disorder, light therapy produced dissimilar blood flow changes in responders and nonresponders. Responders expressed a globally increased activity, measured with hexamethyl-propyleneamine-oxim (HMPAO)–SPECT, relative to the cerebellum mainly in the frontal and cingulate cortices along with the thalamus (Vasile *et al.*, 1997).

Pharmacotherapy

Ogura *et al.* (1998) found in an HMPAO–SPECT study of patients with major depression that the severity of depression was correlated negatively with perfusion in the left superior frontal, right lateral temporal and right parietal cortex. After treatment with tricyclic antidepressants (clomipramine and amoxapine), remitted patients' perfusion did not differ significantly from that of controls.

Brody *et al.* (1999) reported that a better response to the serotonin reuptake inhibitor paroxetine was associated with lower pretreatment glucose uptake in the left ventral anterior cingulate. In

responders, values returned to normal in the ventrolateral prefrontal cortex and orbitofrontal cortex, but not in the dorsolateral prefrontal cortex or the inferior frontal gyrus. Hamilton depression score changes were correlated with changes in glucose metabolism in some areas (ventrolateral prefrontal cortex and inferior frontal gyrus). Remission was associated with increased baseline perfusion in the left premotor and supplementary motor area, along with decreased left ventral anterior cingulate metabolism (Brody *et al.*, 1999). These findings do not fit the Mayberg *et al.* (1997) study, but patients in Brody's study were more depressed and the researchers identified an area that lies ventral to Mayberg's 'rostral cingulate'.

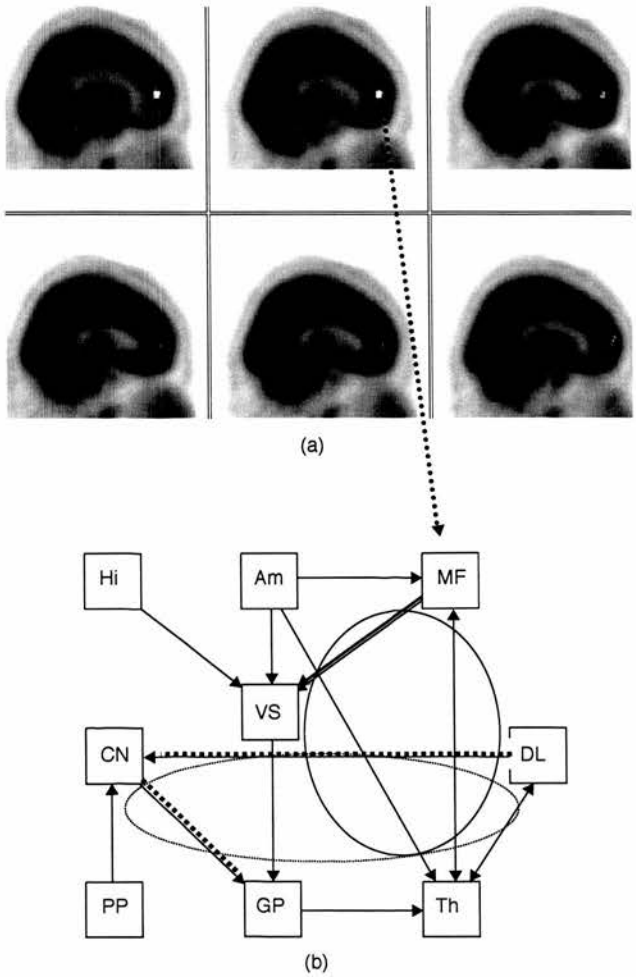

Figure XVIII-9.1 Effect of one session of TMS (5–20 Hz at motor threshold over the left dorsolateral prefrontal cortex) on rCBF during a word-generation task. (a) Statistical parametric map of areas with $P < 0.01$ for effect size (z) and contiguous area (k), using Statistical Parametric Mapping, version 1996. (b) Neuroanatomical projections. Am, amygdala; CN, caudate nucleus; DL, dorsolateral prefrontal cortex; GP, globus pallidus; Hi, hippocampus; MF, medial orbitofrontal cortex; PP, posterior parietal; Th, thalamus; VS, ventral striatum; Dotted ellipse, dorsolateral prefrontal loop; continuous ellipse, limbic loop; dotted arrow DL to CN, increase in regression coefficient c with significance levels in left dorsolateral loop ($c = 2.45$, $P < 0.05$); dotted arrow CN to GP, increase in regression coefficient c with significance levels in left dorsolateral loop ($c = 2.15$, $P = 0.05$); continuous arrow MF to VS, bilateral limbic loop (left: $c = 2.51$, $P < 0.05$; right: $c = 2.89$, $P < 0.05$) (see Plate XVIII-9.1)

Physical Therapies

Electroconvulsive treatment (ECT) has anticonvulsant effects, which suggests a reduction in cortical activity after a course of treatments (Ketter *et al.*, 1999; Post *et al.*, 2000). Using glucose uptake as a measure of cortical activity 5 days after a course of bilateral ECT in ten patients, Nobler *et al.* (2001) were able to support this hypothesis. Yatham *et al.* (2000) had previously failed to detect a significant change in five patients 1 week after a course of ECT, likely to be an effect of insufficient power.

Transcranial magnetic stimulation (TMS) has been used extensively to investigate cortical function in healthy volunteers and psychiatric patients (George *et al.*, 1998). A number of the simple hypotheses underlying the use of TMS in the treatment of psychiatric illness are based on the assumption that low-frequency TMS suppresses cortical activity (quenching) while high-frequency stimulation increases cortical excitability. Speer *et al.* (2000) were able to support this notion using 1- and 20-Hz stimulation over the left dorsolateral prefrontal cortex in a cross-over study of ten depressed patients. They found rCBF increases under the stimulation site and in associated paralimbic structures after 20-Hz stimulation and decreases in more restricted frontal, temporal and subcortical structures after 1-Hz stimulation. Similarly, Zheng (2000) found increases in cerebral perfusion in areas remote from the stimulation site after stimulation over the left dorsolateral prefrontal cortex.

In a parallel design study comparing 5, 10 and 20 Hz applied over the left dorsolateral prefrontal cortex in depressed patients, we found localized increases in the anterior cingulate after the first day's treatment, in combination with increased functional connectivity in the ipsilateral dorsolateral prefrontal loop and bilateral in the cingulate (limbic) loop (Figure XVIII-9.1).

In summary, recent studies have suggested an association between anatomical and functional changes in different prefrontal areas and their associated structures on one hand and disordered cognition and affect on the other. Such changes have been documented extensively in cingulate activity following successful treatment (e.g. Ebert *et al.*, 1996; Mayberg *et al.*, 1999; Volk *et al.*, 1997). Cingulate pretreatment perfusion differentiates between responders and nonresponders (Mayberg *et al.*, 1997; Wu *et al.*, 1999). Furthermore, abnormalities in glial density (Drevets, 1999) and even changes in neuronal size (Rajkowska *et al.*, 1999) were found in the prefrontal cortex of unipolar patients. Finally, the cingulate is activated differentially in cognitive tasks (e.g. Stroop) involving attention or motivation (Whalen *et al.*, 1998), possibly denoting subregions that can be involved in specific tasks, promising a more differentiated understanding of the cognitive and emotional aspects of depression.

EFFECTS OF AGE, CHRONICITY AND TREATMENT RESISTANCE: IRREVERSIBLE AND REVERSIBLE CHANGES

Depression has been perceived as a transitory state where, on remission, brain function and altered or compromised cognition return to normal. This is no longer considered to be accurate in every case. Neuropsychological studies have discovered persistent abnormalities in cognitive performance, pertaining to the duration and severity of the illness (Abas *et al.*, 1990; Shah *et al.*, 1998). A number of imaging studies have also found possibly enduring deficits (e.g. Abas *et al.*, 1990; Shah *et al.*, 1998; Sheline *et al.*, 1999). Shah *et al.* (1998), in addition to a mere group difference, described a correlation between abnormal verbal memory and left medial temporal lobe grey matter deficits in the impaired group. Just as for certain unipolar depressed patients, structural abnormalities in bipolar depression include white-matter lesions, decreased cerebellar size, and sulcal as well as ventricular enlargement (see Stoll *et al.*,

2000 for review). Structural MRI in 24 hospitalized bipolar patients (Strakowski *et al.*, 1999) has also revealed an increase in size of the amygdala with a similar trend in the globus pallidus, thalamus and striatum. These changes did not appear to correlate with other clinical measures, such as illness duration, medication, substance abuse, or the presence of previous episodes, although antipsychotic use would be a likely candidate.

Pathological studies have shown an excess of atheromatous disease in elderly depressed patients (Thomas *et al.*, 2001). In fact, some authors used the term 'MRI-defined vascular depression' (Krishnan *et al.*, 1997) to describe a group of elderly depressed patients with mainly later age of onset, nonpsychotic subtype, functional disability, anhedonia and a relative absence of family history (Krishnan *et al.*, 1997). Although these patients did not have a significantly worse prognosis than nonvascular depressives, a subgroup with late onset of the illness did (Krishnan *et al.*, 1998). In a large epidemiological study of cardiovascular health, small vascular lesions of the basal ganglia but not severity of white-matter lesions were associated with increased reporting of depressive symptoms as measured by the Centre for Epidemiological Studies Depression Scale (Steffens *et al.*, 1999). In a subsample, however, the MRI vascular changes in basal ganglia and nonbasal ganglia structures appeared to exert their effects on depressive symptoms via functional consequences of vascular disease, such as physical disability and cognitive impairment (Sato *et al.*, 1999). On the other hand, a case–control study of 96 elderly patients with late- and early-onset depression found the former to be associated with more white-matter hyperintensities, enlarged ventricles and hypertension (Lavretsky *et al.*, 1998).

MRI white-matter hyperintensities thus appear to be a hallmark of late-onset depression. Hyperintensities are also associated with treatment resistance (Lavretsky *et al.*, 1999; Simpson *et al.*, 1998). and future residual dysfunction, as well as cognitive decline (Hickie *et al.*, 1997; Jenkins *et al.*, 1998; Kramer-Ginsberg *et al.*, 1999) White-matter lesions seem to go with medical comorbidity, relatively independently of whole-brain and frontal atrophy, which are also more common in late-life depression (Kumar *et al.*, 2000). In particular, frontal lobe atrophy is correlated with severity of depression (Kumar *et al.*, 1998). A recent Newcastle study found that frontal white-matter changes were also more common in depressed patients with dementia. Finally, white-matter changes and frontal atrophy may be more common in depressed elderly patients with delusions (Kim *et al.*, 1999; O'Brien *et al.*, 1997a).

A combined MRI and SPECT study conducted in Edinburgh suggested greater temporal perfusion abnormalities in late- than early-onset depression and an association between cognitive deterioration and deep white matter changes (Ebmeier *et al.*, 1997b; Ebmeier *et al.*, 1998). Similar (left medial) temporal lobe changes were reported in late-onset depression (Greenwald *et al.*, 1997), suggesting a possible link between late-onset depression and Alzheimer's disease. A large study comparing 61 depressed patients with 77 demented patients suggests, however, that temporal lobe volumetry can distinguish clearly been these two groups (O'Brien *et al.*, 1997b). Similar results were obtained using hippocampal width alone (Ebmeier *et al.*, 1997b).

Research in younger but also elderly depressed patients suggests that there may be a subgroup with long-lasting or treatment-resistant illness who show (medial) temporal lobe structural and functional changes (Shah and Ebmeier, 1998; Sheline *et al.*, 1999; Vakili *et al.*, 2000). Although there is little corroborating clinical evidence, some authors have argued that hypercortisolaemia associated with clinical depression may be responsible for the hippocampal damage observed in elderly patients. Contrary to this assumption, there is some limited evidence that temporal lobe changes are more common in late-onset, i.e. shorter-lasting, depression (Ebmeier *et al.*, 1998; Lavretsky *et al.*, 1998).

Age Effects

As in younger patients, in elderly patients variation of depressive symptoms is associated with changes of brain activity in (medial) prefrontal structures. This can be shown in sleep deprivation studies (Smith *et al.*, 1999a), in follow-up studies of depressed patients (Halloran *et al.*, 1999), and in cross-sectional studies of clinical correlates in elderly depression (Awata *et al.*, 1998; Ebmeier *et al.*, 1997b). and even Alzheimer's disease (Hirono *et al.*, 1998).

Depression in children and adolescents has been attracting researchers' attention in recent years. Although the prevalence of affective disorders in childhood is now accepted to be on a par with the adult form of the illness, the contribution of the child's environment, along with cognitive and neuroanatomical developmental factors, is unclear. Data on functional brain activity in early onset depression are consistent with findings in adults reporting left anterolateral hypoperfusion. Nonetheless, it is not certain whether the association between haemodynamic response and neural activity are analogous across the lifespan (Davidson and Slagter, 2000). Decreased frontal volume and increased choline-to-creatinine ratios in the anterior medial frontal lobe have been reported in depressed children and adolescents (reviewed in Steingard, 2000). Bipolar, just as schizophrenic, adolescents ($n = 35$) were reported to have reduced intracranial volume with enlarged ventricles and increased frontal and temporal sulci (Friedman *et al.*, 1999).

Treatment Resistance

Shah *et al.* (1998) demonstrated in 20 young patients with treatment-resistant unipolar depression, all of whom had been ill for more than 2 years, that temporal lobe structures, including the hippocampus, were reduced in grey matter density. The reduction in left medial temporal lobe grey matter density was correlated with poor performance in an auditory verbal memory task. Mervaala *et al.* (2000) examined 34 drug-resistant patients with major depression and were able to replicate the reduction in volume of the left hippocampus. In addition, the mesial temporal lobe choline/creatinine ratio was raised, suggesting membrane breakdown. Sheline *et al.* (1999) imaged 24 women with recurrent major depression and found that hippocampi were reduced in volume bilaterally in proportion to illness duration and after controlling for age effects. Interestingly, patients also performed poorly in a verbal memory task, which may be a correlate of hippocampal reductions. Vakili *et al.* (2000) measured hippocampal volumes in 38 patients with primary depression. Although as a group patients had normal-sized hippocampi, treatment response to 20 mg fluoxetine for 8 weeks was associated with relatively larger right hippocampi in women. Somewhat at variance with these results, a study focusing on temporal lobe epilepsy patients reported amygdala enlargement to be associated with dysthymia and depressive symptoms (Tebartz van Elst *et al.*, 1999; Tebartz van Elst *et al.*, 2000). The discrepancy may be explained by different pathology underlying mood changes in epilepsy, by divergent changes in amygdala and hippocampus, or by a different timepoint in the natural history of depression. Ketter *et al.* (2001) examined 43 treatment-resistant bipolar patients and found a contrast between cortical and subcortical glucose metabolism (18FDG–PET). Normalized effects indicating increased metabolism were reported in subcortical areas (ventral striatum and right amygdala) as well as in the posterior cortex, thalamus and cerebellum. Depressed bipolar patients also showed an absolute prefrontal, temporal and anterior paralimbic hypometabolism. Elevated metabolism in posterior cortical areas (including posterior thalamus and cerebellum) persisted beyond remission (i.e. in euthymic patients),

indicating a trait marker unique to bipolar patients. Cognitive task activation (in this case, an auditory task) may be recruiting qualitatively different circuits in patients and controls, a concern shared by all studies employing neuropsychological activation paradigms (Ketter *et al.*, 2001).

Cellular Changes

Both neuronal and glial volume changes have been reported. The latter can be a consequence of a number of factors. As a result of the chronic use of antipsychotic medication, increased volume of glial cells was noted in the prefrontal cortex of rhesus monkeys (Selemon *et al.*, 1999). Reports of a laminar as well as a regionally specific pattern of glial but also neuronal reduction, where neurons decreased both in size (dorsolateral prefrontal cortex) and density (orbitofrontal cortex), was observed in the prefrontal cortex of unipolar patients (Rajkowska *et al.*, 1999). By contrast, post-mortem studies in both unipolar and bipolar patients with a family history of depression have not revealed any differences in the neuronal population, while glial density was decreased; glial volume of schizophrenic patients was unchanged (Drevets *et al.*, 1997; Ongur *et al.*, 1998). Finally, age-associated glial changes in primate grey matter reached statistical significance only in the cingulate (Sloane *et al.*, 2000). It is apparent that some association between changes in glial density and pathological or restorative processes has been established in patients suffering from affective disorders. Nonetheless, it is still unclear whether these changes are adaptive, compensatory or incidental. Further, the functional effect of such changes is still undetermined.

The association between neuronal activity and the metabolic processes measured by various functional brain-imaging modalities (haemodynamic response in functional magnetic resonance imaging (fMRI), glucose utilization in FDG–PET, and so forth), is not without question. Furthermore, it is apparent that astrocytes as well as neurons may contribute to the signal changes observed in FDG–PET (Magistretti and Pellerin, 1996; Magistretti and Pellerin, 1999). In the presence of glial reduction in anterolimbic structures reported by a number of groups (Drevets *et al.*, 1998; Rajkowska *et al.*, 1999), it is unknown whether, and to what extent, glucose utilization and its associated PET signal are altered as a result.

Lithium and valproate have been suggested to have neurotrophic and neuroprotective effects. An increase of 3% in the cortical grey matter volume of bipolar patients after 4 weeks of lithium administration is attributed to neurotrophic factors rather than to cell swelling (Moore *et al.*, 2000). Mood stabilizers could be involved in the regulation of gene expression by increasing levels of mRNA for PEBP2β (polyomavirus enhancer-binding protein 2 beta subunit), which controls coding for the neuroprotective protein BCL2 (B cell lymphoma protein 2) in the frontal cortex. Increased neuronal survival and increased regeneration are all effected by BCL2 upregulation, protecting against excitotoxic damage (Chen *et al.*, 1999; Chen and Chuang, 1999). It is unclear whether recent post-mortem findings of increased neuronal numbers throughout the hypothalamus and the dorsal raphe could be related to chronic use of medication (Rajkowska *et al.*, 1999).

Small structures such as the brainstem raphe nuclei are imaged with difficulty. It is, therefore, fortuitous that ultrasound sonography can be applied using a preauricular acoustic bone window to image the mesencephalic brainstem with structures such as the red nucleus and the rostral pontine brainstem. Becker *et al.* (1995) examined 40 unipolar, 40 bipolar depressive and 40 schizophrenic inpatients, as well as 40 healthy volunteers. Reduced midline echogenicity relative to the red nucleus, which can be interpreted as structural disruption of the raphe nuclei, was found only in the unipolar depressed patients.

EXPERIMENTAL APPROACHES TO DEPRESSION: COMPLEX MODELS

Introduction

Cognitive performance in depression and its relationship with the disturbance of emotion or mood have been examined in a number of contexts. Along with an investigation of cognitive impairment in subjects suffering from affective disorders, there is a large body of literature reporting different procedures of precipitating depressed or dysphoric mood in healthy subjects (mood induction). A number of conceptual questions are inherent in this literature. Above all, it is unclear to what extent sad mood is analogous with clinical depression. The transient time course of the neuropsychological impairment brought about by mood induction is usually far shorter than the experience of clinical depression. Similarly, induced mood may be of a different quality from morbid depression, although biological symptoms, such as depressive retardation, can be observed after experimental mood induction (Ebert *et al.*, 1996). The absence of biological markers often associated with depression (such as hypercortisolaemia), along with structural and functional differences, hinder direct comparison. In this sense, even if the neural systems recruited in healthy controls during mood induction are analogous to the neuroanatomical circuit activated in depressed patients at rest, the dynamics of the circuit may be different in the two conditions due to selective dysfunction in specific components or the connectivity between these. It is even possible that some of the differences between patients and controls can be explained by simple mechanisms, e.g. that depressed patients are slower to recruit the appropriate neuronal systems or their components.

Since neuropsychological studies are described in detail in Chapter XVIII-7 and XIX-8 of this book, we will focus on neuronal systems implicated by clinical and mood induction paradigms. We will try to integrate structural and functional findings reported earlier in the chapter in an attempt to assemble some of the complex interactions between specific structures and the systems they comprise in the manifestation of affective illness.

Neuropsychological studies suggest that cognitive deficits may be the consequence of competition between cognitive and affective functional resources. If this holds true, such that neural pathways identified in the induction paradigm are analogous to those affected in the specific mood disorder they are trying to emulate, then transient sadness or elation in normal volunteers can provide a useful insight into the neural correlate of cognitive performance in mood disorders. However, covariation between the degree of depression, impaired task performance and (in-)activity of relevant functional circuits does not necessarily imply a causal relationship between the three. Thus, apparently similar short-term deficits of neuronal activity observed both in clinical depression and after mood induction could be grounded in dissimilar processes. In the long term, these may be of no consequence for healthy volunteers, but they could result in the significant deficits noted in patients with recurrent and severe depression (Shah *et al.*, 1998).

The following section includes studies emphasizing perfusion changes associated with emotional states. Most studies report impaired cognitive performance as a consequence of transient mood change, although their methods may differ greatly. Anatomical structures that are grouped classically under the definition of 'limbic lobe' are involved in circuits responsible for both cognitive function and the generation of affect. These include the cingulate cortex, hippocampus, amygdala and thalamus, as well as other prefrontal and subcortical structures. Both mood-induction and clinical studies report altered dynamics in the limbic and prefrontal circuits, comprising activation or deactivation under specific conditions, compensatory effects, and the interplay between different regions (e.g. cortical and subcortical, limbic and dorsolateral prefrontal cortex,

etc). The role of the cingulate has been emphasized by authors such as MacLean (1985). He saw the phylogenetic emergence of the cingulate cortex as fundamental to the development of maternal care in mammals. There is therefore a convergence of paradigms (Stevens and Price, 2000) between psychodynamic speculation about attachment and loss (Bowlby, 1969) and the understanding of limbic brain function in depression (Ebert *et al.*, 1996).

Such theories are now amenable to empirical testing. Lorberbaum *et al.* (1999) employed fMRI in four recent mothers listening to recordings of infants' cries and white noise as a control condition. Increased brain activity could be demonstrated in the anterior cingulate and right medial prefrontal cortex. These regional activations are probably not very specific, as similar areas are activated during pain and are thought to be related to affective and attentional concomitants of pain sensation (Peyron *et al.*, 2000; Schnitzler and Ploner, 2000). However, with careful experimental procedures, hypotheses about the specific role of the medial prefrontal cortex in emotion are testable, in principle.

Supporting the imaging studies in humans, there is also an animal model of congenitally helpless rats with reductions in brain activity in the dorsal frontal, medial orbital and anterior cingulate cortex, and increases in the subgenual cingulate (Shumake *et al.*, 2000).

Mood Induction and Neuropsychological Paradigms

Neuropsychological studies use cognitive tasks in order to recruit associated functional circuits through their component structures. Specific functional vulnerability can be described by either impaired performance of a particular task or impaired activation of characteristic circuits or their constituents. Neuropsychological tasks have been designed to probe activity in brain regions associated with them. Frontal areas are activated by tasks such as the Wisconsin card sorting test (WCST) or the Tower of London (TOL) task, both of which involve the application and manipulation of rules, adaptive skills and flexibility necessary for set shifting. Tasks that involve memory are expected to be particularly sensitive to structural and/or functional discontinuity in (mesial) temporal structures, such as the hippocampus. Finally, the involvement of subcortical structures in the experience of clinical and experimental mood is expressed by both perseverative responses (the inability to change strategies) and psychomotor slowing, experienced predominantly by melancholic patients (Austin *et al.*, 1999; Austin *et al.*, 2001). It appears that similar limbic-subcortical circuits are involved in different experimental mood induction procedures; however, different substructures may be affected, possibly due to inconsistent methodology of experimental paradigms and the different affects involved.

Studies: Mood Induction

Baker *et al.* (1997) induced sad and elated mood in controls and examined brain activity following performance of a verbal fluency task. They reported anatomical dissociation between mood and cognitive function. Both mood states curtailed the activity normally associated with the verbal fluency task throughout the left prefrontal, premotor and cingulate cortex, as well as the thalamus. Reduced activation in the rostral medial orbitofrontal cortex and anterior cingulate was associated uniquely with sad mood.

Mayberg *et al.* (1999) proposed a simplified model of brain responses. They hypothesized a general increase in limbic-paralimbic perfusion coupled with a decrease in neocortical perfusion to accompany induction of sadness in healthy volunteers, while reciprocal changes were predicted during the resolution of dysphoric symptoms in depressed patients. These authors also observed an inverse correlation between right dorsolateral prefrontal and subgenual cingulate perfusion, supporting this notion. These finding can be interpreted as corollary evidence for the inverse relationship between depressed mood and attention.

Beauregard *et al.* (1998) studied patients' and controls' ($n = 7$) responses to mood induction. Transient sadness (triggered by film clips with emotional content) produced activation in the medial and inferior prefrontal, middle temporal cortex, cerebellum and caudate. Significantly greater activation in the left medial prefrontal cortex (Brodman's area 8) and right cingulate gyrus (Brodman's area 32) was observed in depressed patients, suggesting that these two structures may have a role in pathological sadness.

Elliott *et al.* (1997) postulated a catastrophic reaction to failure as a specific neuropsychological mechanism underlying poor performance in depression. They examined performance feedback responses in six patients and controls. Depressed patients did not show the expected activation in the medial caudate and ventromedial orbitofrontal cortex found in controls. Patients' brains were, therefore, insensitive to changes in both task and feedback conditions, consistent with the a priori hypothesis.

Schneider *et al.* (1996) found activation in a network related to performance feedback during the attempt at solving unsolvable anagrams; perfusion increased in healthy subjects ($n = 12$) in the mamillary bodies and the amygdala, and decreased in hippocampus. Solvable tasks were associated with increased perfusion in the latter. Increased frontal and temporal perfusion was associated with both conditions.

The Stroop interference task has been typically associated with activation of the cingulate gyrus (Pardo *et al.*, 1990). A different activation pattern was observed in depressed patients ($n = 11$), who failed to activate the left cingulate in comparison with control subjects. Reduced perfusion in patients' right cingulate was balanced by stronger activation of the left dorsolateral prefrontal cortex and the visual cortex (George *et al.*, 1997). A variant of the Stroop interference task (the emotional counting Stroop paradigm) showed a unique activation of the rostral anterior cingulate using fMRI in normal volunteers (Whalen *et al.*, 1998). Comparing perfusion between trials containing affective (such as murder) and neutral words associated negative content with increased perfusion in the anterior cingulate, without a change in reaction. Performance of this form of the Stroop task compared with fixation *per se* was associated with overall decreased perfusion. These findings may suggest an association between pathological anxiety and an inability to reduce cingulate activation during task compared with fixation.

Correlation between higher global perfusion and increased cognitive demands was associated with task switching. The superior parietal cortex was reported to have a specific role in task switching, although this effect may be task specific (Kimberg *et al.*, 2000). Illness severity in this subtype correlates with increased perfusion in frontolimbic structures parahippocampal gyrus and cingulate (Ebmeier *et al.*, 1997a).

Induction of depressed and elated mood can, at times, be associated with overlapping or diverging neural circuitry. Dissociable recruitment of subcortical and cortical structures in healthy subjects ($n = 16$) during experience of both positive and negative affect was associated with specific changes in subcortical structures (especially the amygdala) but not frontotemporal structures (Schneider *et al.*, 1995). Both happy and sad mood correlated with increased blood oxygen level-dependent (BOLD) fMRI response in the left amygdala of healthy subjects ($n = 12$) (Schneider *et al.*, 1997). De Raedt *et al.* (1997) used a modified Velten procedure to induce mood both 'within and out of the realm of attention'. The latter involved a combination of dichotic listening and subliminal stimulation. Right lateral reduction in thalamic perfusion was found during both conditions compared with responses to neutral stimuli. Increased hippocampal perfusion was limited to subliminal stimulation conditions.

Divergent circuits were found in the evaluation of negative versus positive affective content. While the former was associated

with increased perfusion in the right frontal gyrus and thalamus, the latter produced activation of the bilateral insula and the right inferior frontal gyrus. Neither showed associated changes in amygdala perfusion (Teasdale *et al.*, 1999). In a different study, subcortical limbic structures (amygdala, associative cortex, primary visual cortex, cerebellum) were activated through evaluation of unpleasant stimuli, while pleasant stimuli activated cortical structures (medial prefrontal cortex, dorsolateral prefrontal cortex, and the right orbitofrontal cortex (Paradiso *et al.*, 1999). Spatiotemporal differences in activation of the neuroanatomical correlate of positive and negative affect, expressed through characteristic activation of either the orbitofrontal cortex or the prefrontal cortex, were shown in healthy volunteers (n = 10). Recruitment of the medial prefrontal network in the context of negative affective content was established faster than the activation of the lateral prefrontal circuit, which was associated with positive affect (Northoff *et al.*, 2000). Finally, retrieval of episodic memory with affective content was associated with anterior temporal lobe activation and the left amygdala (Dolan *et al.*, 2000), a pattern mirrored by McGaugh and Cahill (1997) and Hamann and Adolphs (1999) in encoding of similar memories.

Hypofrontality along with specific prefrontal deficits has been reported extensively in the literature. Both depressed (n = 6) and control subjects performing the TOL task exhibited a pattern of deactivating the medial prefrontal cortex, superior temporal gyrus and posterior cingulate. For control subjects, increased difficulty was associated with a linear augmentation in the recruitment of the appropriate functional circuitry. By contrast, depressed patients presented with decreased activity in the rostral prefrontal cortex, caudate nucleus and the anterior cingulate without the expected compensation by the dorsolateral prefrontal cortex (Elliott *et al.*, 1997). Parietal cortex activation did not reach threshold in this experiment. Neural dissociation between cognitive and affective activation denoted specific activity-related changes in the medial frontal cortex. A reduction from baseline activity in the medial prefrontal cortex was linked to cognitive activation. Practice was associated with decreased perfusion in the medial prefrontal cortex, while performance anxiety was linked to increased perfusion in the same region. In a different experiment, elevated perfusion in the medial prefrontal cortex was reported during the anticipation of painful stimuli, and was correlated negatively with anxiety rating (i.e. increased anxiety produced a smaller reduction from baseline). Corresponding changes in flow were noted in the hypothalamus and midbrain. Thus, a decrease from baseline activity in the prefrontal cortex is thought to be a consequence of recruiting the network related to attention (Simpson *et al.*, 2001a; Simpson *et al.*, 2001b).

Systems

We conclude the chapter by discussing the neuronal circuits or systems putatively linked with affective illness. To the best of our current knowledge, there is no clear or direct correspondence between neurobiological factors and their effect on emotional experience or expression. Structural changes in areas such as the hippocampus, prefrontal cortex, cingulate or amygdala are perfect candidates for theories of dysfunctional loci. However, as we have indicated throughout this chapter, neurobiological abnormalities are not entirely predictive of functional deficits. Furthermore, dysfunction in affective disorders may involve long-term mechanisms of compensation and deterioration over time, which may not be explicit in present theories of unipolar and bipolar depression.

The limbic system is, of course, a natural candidate for many neuroimaging investigations. The evolutionary angle described earlier in this chapter (Bowlby, 1969; MacLean, 1985) places structures associated closely with environmental feedback, particularly in a social context, at the locus of a system associated with integrating internal and external states. For example, specific behaviours or neuropsychological tasks yield an associated activation in structures such as the cingulate gyrus (maternal separation cry, Stroop), amygdala (fear), hippocampus (autobiographical memories) and dorsolateral prefrontal cortex (TOL task), to name but a few. It is important to note that in brain regions not classically associated with the limbic system (and thus not salient in many investigations), such as the parietal cortex, reports of functional abnormalities are increasing (Davidson *et al.*, 1999; Drummond *et al.*, 2000; Ho *et al.*, 1996; Mayberg, 1997) Since regions of functional interest are often defined a priori in neuroimaging studies, a bias towards the well-documented structural and functional changes in limbic regions may be perpetuated.

Behavioural response to long-term stress in a social context seems to be adaptive, in the sense that initial alarm and resistance will lead ultimately to exhaustion and acceptance (Selye, 1936). Similarly, rank theories in mood disorders postulate acknowledgement of subordinate status and a 'yielding' motor response in the presence of higher rank (Stevens and Price, 2000). The limbic system is therefore assumed to unite behaviour and neuroanatomy, where conflict between external and internal input can be resolved, a role associated particularly with the cingulate. The impact on both psychomotor and prefrontal-cognitive associated capacity is inherent in these theories.

Expanding Papez's early theories of limbic circuit connectivity and function, current neuroimaging tools are instrumental in facilitating both understanding and advancement of functional circuitry in depression and mania. Careful attention to experimental design (such as activation under different experimental conditions), as well as the development of new chemical tracers and more powerful imaging technology, will contribute towards a better appreciation of the various phases associated with affective disorders. We are nearing a qualitative coupling between systems with either function or dysfunction. This is achieved by direct and indirect comparison between patients and healthy control subjects performing tasks under similar conditions. Nonetheless, quantitative knowledge regarding activity in distinct systems is, for now, sketchy.

Common to both prefrontal and limbic structures is the overlap between sensory and affective processes (LeDoux, 1996), where a visceral system provides feedback through endocrine and other neurobiological mechanisms. It is possible that inhibition by the prefrontal cortex may be involved in feedback control (not only the classically inhibitory orbitofrontal cortex but also the lateral prefrontal cortex, both denoting different strategies of associative learning) (Roberts and Wallis, 2000). Consequently, activity, or lack thereof, in frontal regions may lead to limbic hyperperfusion via nonlinear excitatory or inhibitory operational modes.

Hypofrontality has been reported extensively in different contexts. Thus, the interaction between cognitive and affective circuits with the frontal cortex has been described by neuroanatomical (Barbas *et al.*, 1999; Price *et al.*, 1996), neuropsychological and neuroimaging studies (Mayberg *et al.*, 1997; Rogers *et al.*, 1998). These circuits appear to have functional as well as structural regional specificity, whereby connectivity to other (remote) regions throughout the cortex and the subcortex are clearly defined.

The limbic system has been separated into affective and cognitive components, supported by neuroanatomical studies in humans and primates (e.g. Devinsky *et al.*, 1995; Mayberg *et al.*, 1999; Mega *et al.*, 1997; Price, 1999a). The integration of viscerosensory and affective information, yielding endocrine and motor changes (Price, 1999b) contributes to an extended network, which cannot be explicable by lesion studies alone (Frith and Dolan, 1998).

A number of compensatory mechanisms can be deduced from the extensive neuroimaging literature in the field. The amygdala

and orbitofrontal cortex appear to activate in synergy, where the orbitofrontal cortex is activated more strongly in response to amygdala dysfunction (Drevets, 1999). In healthy subjects, compensatory strategies require greater activity in the prefrontal and parietal cortices to balance for decreased temporal lobe perfusion and associated performance deficits after a night of TSD (Drummond *et al.*, 2000). By contrast, Elliott *et al.* (1997) showed that depressed patients lacked an adaptive capacity, which was expressed by their inability to recruit prefrontal as well as subcortical structures during performance of the TOL task. Further, correspondence between hyperperfusion in the cognitive and affective divisions of the cingulate reported by Mayberg *et al.* (1999) could arguably have a compensatory role in depression and recovery.

Therefore, a hyperactive limbic (or 'ventral'; see Mayberg *et al.*, 1999) system was noted by a number of groups, where increased perfusion can imply higher probability for response to treatment (Mayberg *et al.*, 1997; Wu *et al.*, 1999) or, alternatively, increased likelihood of more severe illness (Austin *et al.*, 1992). In the long term, connections to temporal (amygdala, hippocampus), parietal, prefrontal and subcortical structures will help us understand the extent to which an extended network can compensate for limbic hyperperfusion.

Blood flow and glucose metabolism in subcortical structures, the dorsolateral prefrontal cortex and the cingulate have been linked extensively with affective disorders through neurological and movement disorders, lesion studies, and functional activation and imaging at rest (Cummings, 1993; Mega and Cummings, 1994, Soares and Mann, 1997). Furthermore, basal ganglia and frontal lesions carry a higher probability for cognitive impairment (Rogers *et al.*, 1998; Videbech, 1997). It is apparent that subcortical involvement can be associated with increased pathophysiology (e.g. psychomotor retardation), recurrent episodes and cognitive decline (Hickie *et al.*, 1997; Hickie *et al.*, 1999; Simpson *et al.*, 1998). The anterior cingulate may play a cardinal role in this context, due to its widespread connections and functional association with the prefrontal cortex (Ebert *et al.*, 1996; Koski and Paus, 2000). This is, at present, not clearly specified, ranging from theories of a 'somatic marker' (Damasio, 1994), of motivation, attention and error detection (Carter *et al.*, 1999) to its specificity in the integration of cognition and affect. It is confounded by the structural changes in specific subgroups of unipolar and bipolar patients (Drevets *et al.*, 1997).

Finally, since hippocampal volume reduction is associated with the severity of depressive illness (Sheline *et al.*, 1999) and, by association (Drummond *et al.*, 2000), transient hypoactivity in the temporal cortex, its function maybe balanced by prefrontal and parietal regions. It would be interesting to probe such functional correspondences between two or more structures in a clinical context. To conclude, a unified theory of affective disorders is developing through the application of different imaging methods and consideration of both animal and human neuroanatomical data. Future studies will no doubt consider a larger, distributed functional network, coupled with better understanding of the long-term effects of clinical deterioration, medication and the ageing process. What emerges, is a functional interplay of brain modules that are associated with specific mood states, attention and nonspecific emotional factors, and specific aspects of the neuropsychological tasks used. We now have the tools to test relevant hypotheses in the living brain. The groundwork will have to be done with fMRI and possibly TMS in healthy volunteers, although in the last analysis, studies in sufficiently large, homogeneous and representative groups of patients will be necessary. The understanding that has come from studies so far is that dimensions of mood are indeed interlinked closely with cognitive categories, and that experimental studies may necessitate our rethinking of clinical and psychological constructs.

REFERENCES

Abas, M.A., Sahakian, B.J. and Levy, R., 1990. Neuropsychological deficits and CT scan changes in elderly depressives. *Psychological Medicine* 20, 507–520.

Alexander, G.E., DeLong, M.R. and Strick, P.L., 1986. Parallel organisation of functionally segregated circuits linking basal ganglia and cortex. *Annual Review of Neuroscience* 9, 357–381.

Al-Moussawi, A.H., Evans, N., Ebmeier, K.P., Roeda, D., Chaloner, F. and Ashcroft, G.W., 1996. Limbic system dysfunction in schizophrenia and mania—a study using 18F-fluorodeoxyglucose and positron emission tomography. *British Journal of Psychiatry* 169, 509–516.

Andrews, G., 2001. Placebo response in depression: bane of research, boon to therapy. *British Journal of Psychiatry* 178, 192–194.

Austin, M.-P., Dougall, N.J., Ross, M., Murray, C.L., O'Carroll, R.E., Moffoot, A., Ebmeier, K.P. and Goodwin, G.M., 1992. Single photon emission tomography with 99mTc-exametazime in major depression and the pattern of brain activity underlying the endogenous/neurotic continuum. *Journal of Affective Disorders* 26, 31–43.

Austin, M.-P., Mitchell, P., Wilhelm, K., Parker, G., Hickie, I., Brodaty, H., Chan, J., Eyers, K., Milic, M. and Hadzi-Pavlovic, D., 1999. Cognitive function in depression: a distinct pattern of frontal impairment in melancholia? *Psychological Medicine* 29, 73–85.

Austin, M.-P., Mitchell, P. and Goodwin, G.M., 2001. Cognitive deficits in depression. *British Journal of Psychiatry* 178, 200–206.

Awata, S., Ito, H., Konno, M., Ono, S., Kawashima, R., Fukuda, H. and Sato, M., 1998. Regional cerebral blood flow abnormalities in late-life depression: relation to refractoriness and chronification. *Psychiatry and Clinical Neurosciences* 52, 97–105.

Baker, S.C., Frith, C.D. and Dolan, R.J., 1997. The interaction between mood and cognitive function studied with PET. *Psychological Medicine* 27, 565–578.

Barbas, H., Ghashghaei, H., Dombrowski, S.M. and Rempel-Clower, N.L., 1999. Medial prefrontal cortices are unified by common connections with superior temporal cortices and distinguished by input from memory-related areas in the rhesus monkey. *Journal of Comparative Neurology* 410, 343–367.

Battersby, S., Ogilvie, A.D., Blackwood, D.H.R., Shen, S., Muqit, M.M., Muir, W.J., Teague, P., Goodwin, G.M. and Harmar, A.J., 2001. Presence of multiple functional polyadenylation signals and a single nucleotide polymorphism in the 3′ untranslated region of the human serotonin transporter gene. *Journal of Neurochemistry* 72, 1384–1388.

Beauregard, M., Leroux, J.M., Bergman, S., Arzoumanian, Y., Beaudoin, G., Bourgouin, P. and Stip, E., 1998. The functional neuroanatomy of major depression: an fMRI study using an emotional activation paradigm. *Neuroreport* 9, 3253–3258.

Becker, G., Becker, T., Struck, M., Lindner, A., Burzer, K., Retz, W., Bogdahn, U. and Beckmann, H., 1995. Reduced echogenicity if brainstem raphe specific to unipolar depression: a transcranial color-coded real-time sonography study. *Biological Psychiatry* 38, 180–184.

Bhashghaei, H.T. and Barbas, H., 2001. Neural interaction between the basal forebrain and functionally distinct prefrontal cortices in the rhesus monkey. *Neuroscience* 103, 593–614.

Biver, F., Wikler, D., Lotstra, F., Damhaut, P., Goldman, S. and Mendlewicz, J., 1997. Serotonin 5-HT2 receptor imaging in major depression: focal changes in orbito-insular cortex. *British Journal of Psychiatry* 171, 444–448.

Bowlby, J., 1969. *Attachment and Loss*. Tavistock Institute of Human Relations, London.

Bremner, J.D., Randall, P., Scott, T.M., Bronen, R.A., Seibyl, J.P., Southwick, S.M., Delaney, R.C., McCarthy, G., Charney, D.S. and Innis, R.B., 1995. MRI-based measurement of hippocampal volume in patients with combat related post-traumatic stress disorder. *American Journal of Psychiatry* 152, 973–981.

Brody, A.L., Saxena, S., Silverman, D.H., Alborzian, S., Fairbanks, L.A., Phelps, M.E., Huang, S.C., Wu, H.M., Maidment, K. and Baxter, L.R.J., 1999. Brain metabolic changes in major depressive disorder from pre- to post-treatment with paroxetine. *Psychiatry Research* 91, 127–139.

Carter, C.S., Botvinick, M.M. and Cohen, J.D., 1999. The contribution of the anterior cingulate cortex to executive processes in cognition. *Reviews in the Neurosciences* 10, 49–57.

Chapotot, F., Gronfier, C., Jouny, C., Muzet, A. and Brandenberger, G., 1998. Cortisol secretion is related to electroencephalographic alertness in human subjects during daytime wakefulness. *Journal of Clinical Endocrinology and Metabolism* 83, 4263–4268.

Chen, G., Zeng, W.Z., Yuan, P.X., Huang, L.D., Jiang, Y.M., Zhao, Z.H. and Manji, H.K., 1999. The mood-stabilizing agents lithium and valproate robustly increase the levels of the neuroprotective protein bcl-2 in the CNS. *Journal of Neurochemistry* 72, 879–882.

Chen, R.W. and Chuang, D.M., 1999. Long term lithium treatment suppresses p53 and Bax expression but increases Bcl-2 expression — a prominent role in neuroprotection against excitotoxicity. *Journal of Biological Chemistry* 274, 6039–6042.

Cummings, J.L., 1993. Frontal-subcortical circuits and human-behavior. *Archives of Neurology* 50, 873–880.

Dahlstrom, M., Ahonen, A., Ebeling, H., Torniainen, P., Heikkila, J. and Moilanen, I., 2000. Elevated hypothalamic/midbrain serotonin (monoamine) transporter availability in depressive drug-naive children and adolescents. *Molecular Psychiatry* 5, 514–522.

Damasio, A.R., 1994. *Descartes Error: emotion reason and the human brain*. GP Putbans Sons, New York.

Davidson, R.J. and Slagter, H.A., 2000. Probing emotion in the developing brain: functional neuroimaging in the assessment of the neural substrates of emotion in normal and disordered children and adolescents. *Mental Retardation and Developmental Disabilities Research Reviews* 6, 166–170.

Davidson, R.J., Abercrombie, H., Nitschke, J.B. and Putnam, K., 1999. Regional brain function, emotion and disorders of emotion. *Current Opinion in Neurobiology* 9, 228–234.

DelBello, M.P., Strakowski, S.M., Zimmerman, M.E., Hawkins, J.M. and Sax, K.W., 1999. MRI analysis of the cerebellum in bipolar disorder: a pilot study. *Neuropsychopharmacology* 21, 63–68.

Delgado, P.L., Charney, D.S., Price, L.H., Aghajanian, G.K., Landis, H. and Heninger, G.R., 1990. Serotonin function and the mechanism of antidepressant action. *Archives of General Psychiatry* 47, 411–417.

De Raedt, R., D'haenen, H., Everaert, H., Cluydts, R. and Bossuyt, A., 1997. Cerebral blood flow related to induction of a depressed mood within and out of the realm of attention in normal volunteers. *Psychiatry Research* 74, 159–171.

Devinsky, O., Morrell, M.J. and Vogt, B.A., 1995. Contributions of anterior cingulate cortex to behavior. *Brain* 118, 279–306.

Dolan, R.S., Lane, R., Chua, P. and Fletcher, P., 2000. Dissociable temporal lobe activations during emotional episodic memory retrieval. *Neuroimage* 11, 203–209.

Drevets, W.C., 1998. Functional neuroimaging studies of depression: the anatomy of melancholia. *Annual Review of Medicine* 49, 341–361.

Drevets, W.C., 1999. Prefrontal cortical-amygdalar metabolism in major depression. *Annals of the New York Academy of Sciences* 877, 614–637.

Drevets, W.C., Price, J.L., Simpson, J.R., Todd, R.D., Reich, T., Vannier, M. and Raichle, M.E., 1997. Subgenual prefrontal cortex abnormalities in mood disorders. *Nature* 386, 824–827.

Drevets, W.C., Ongur, D. and Price, J.L., 1998. Neuroimaging abnormalities in the subgenual prefrontal cortex: implications for the pathophysiology of familial mood disorders. *Molecular Psychiatry* 3, 220–226.

Drevets, W.C., Frank, E., Price, J.C., Kupfer, D.J., Holt, D., Greer, P.J., Huang, Y., Gautier, C. and Mathis, C., 1999. PET imaging of serotonin 1A receptor binding in depression. *Biological Psychiatry* 46, 1375–1387.

Drummond, S.P.A., Brown, G.G., Gillin, J.C., Stricker, J.L., Wong, E.C. and Buxton, R.B., 2000. Altered brain response to verbal learning following sleep deprivation. *Nature* 403, 655–657.

Ebert, D. and Berger, M., 1998. Neurobiological similarities in antidepressant sleep deprivation and psychostimulant use: a psychostimulant theory of antidepressant sleep deprivation. *Psychopharmacology* 140, 1–10.

Ebert, D. and Ebmeier, K.P., 1996. The role of the cingulate gyrus in depression: from functional anatomy to neurochemistry. *Biological Psychiatry* 39, 1044–1050.

Ebert, D., Feistel, H., Barocka, A. and Kaschka, W., 1994a. Increased limbic blood-flow and total sleep-deprivation in major depression with melancholia. *Psychiatry Research-Neuroimaging* 55, 101–109.

Ebert, D., Feistel, H., Kaschka, W., Barocka, A. and Pirner, A., 1994b. Single-photon emission computerized-tomography assessment of cerebral dopamine D2 receptor blockade in depression before and after sleep-deprivation–preliminary results. *Biological Psychiatry* 35, 880–885.

Ebert, D., Feistel, H., Loew, T. and Pirner, A., 1996. Dopamine and depression-D2 receptor SPECT before and after antidepressant therapy. *Psychopharmacology* 126, 91–94.

Ebmeier, K.P. and Ebert, D., 1997. Imaging functional change and dopaminergic activity in depression. In: Beninger, R.J., Palomo, T. and Archer, T. (eds), *Dopamine Disease States*, vol. 3, pp. 511–522. Cerebro y Mente Press, Madrid.

Ebmeier, K.P., Cavanagh, J.T.O., Moffoot, A.P.R., Glabus, M.F., O'Carroll, R.E. and Goodwin, G.M., 1997a. Cerebral perfusion correlates of depressed mood. *British Journal of Psychiatry* 170, 77–81.

Ebmeier, K.P., Prentice, N., Ryman, A., Halloran, E., Rimmington, J.E., Best, J.K. and Goodwin, G.M., 1997b. Temporal lobe abnormalities in dementia and depression: a study using high resolution single photon emission tomography and magnetic resonance imaging. *Journal of Neurology, Neurosurgery, and Psychiatry* 63, 597–604.

Ebmeier, K.P., Glabus, M.F., Prentice, N., Ryman, A. and Goodwin, G.M., 1998. A voxel-based analysis of cerebral perfusion in dementia and depression of old age. *Neuroimage* 7, 199–208.

Elliott, R., Baker, S.C., Rogers, R.D., O'Leary, D.A., Paykel, E.S., Frith, C.D., Dolan, R.J. and Sahakian, B.J., 1997. Prefrontal dysfunction in depressed patients performing a complex planning task: a study using positron emission tomography. *Psychological Medicine* 27, 931–942.

Elliott, R., Sahakian, B.J., Michael, A., Paykel, E.S. and Dolan, R.J., 1998. Abnormal neural response to feedback on planning and guessing tasks in patients with unipolar depression. *Psychological Medicine* 28, 559–571.

Friedman, L., Findling, R.L., Kenny, J.T., Swales, T.P., Stuve, T.A., Jesberger, J.A., Lewin, J.S. and Schulz, S.C., 1999. An MRI study of adolescent patients with either schizophrenia or bipolar disorder as compared to healthy control subjects. *Biological Psychiatry* 46, 78–88.

Frith, C. and Dolan, R.J., 1998. Images of psychopathology. *Current Opinion in Neurobiology* 8, 259–262.

Fu, C.H., Reed, L.J., Meyer, J.H., Kennedy, S., Houle, S., Eisfeld, B.S. and Brown, G.M., 2001. Noradrenergic dysfunction in the prefrontal cortex in depression. *Biological Psychiatry* 49, 317–325.

George, M.S., Ketter, T.A., Parekh, P.I., Rosinsky, N., Ring, H.A., Pazzaglia, P.J., Marangell, L.B., Callahan, A.M. and Post, R.M., 1997. Blunted left cingulate activation in mood disorder subjects during a response interference task (the stroop). *Journal of Neuropsychiatry and Clinical Neurosciences* 9, 55–63.

George, M.S., Nahas, Z., Speer, A.M., Kimbrell, T.A., Wassermann, E.M., Lawandales, C.C., Molloy, M., Bohning, D., Risch, S.C. and Post, R.M., 1998. Transcranial magnetic stimulation (TMS)–a new method for investigating the neuroanatomy of depression. In: Ebert, D. and Ebmeier, K.P. (eds), *Biological Psychiatry: new models for depression*, vol. 19. Karger, Basel.

Goodwin, G.M., Austin, M.-P., Dougall, N.J., Ross, M., Murray, C.L., O'Carroll, R.E., Moffoot, A. and Prentice, N., 1993. State changes in brain activity shown by the uptake of 99mTc-exametazime with single photon emission tomography in major depression before and after treatment. *Journal of Affective Disorders* 29, 243–253.

Greenwald, B.S., Kramer-Ginsberg, E., Bogerts, B., Ashtari, M., Aupperle, P., Wu, H., Allen, L., Zeman, D. and Patel, M., 1997. Qualitative magnetic resonance imaging findings in geriatric depression. Possible link between later-onset depression and Alzheimer's disease? *Psychological Medicine* 27, 421–431.

Halloran, E., Prentice, N., Murray, C.L., O'Carroll, R.E., Glabus, M.F., Goodwin, G.M. and Ebmeier, K.P., 1999. Follow-up study of depression in the elderly. Clinical and SPECT data. *British Journal of Psychiatry* 175, 252–258.

Hamann, S.B. and Adolphs, R., 1999. Normal recognition of emotional similarity between facial expressions following bilateral amygdala damage. *Neuropsychologia* 37, 1135–1141.

Hibberd, C., Yau, J.L. and Seckl, J.R., 2000. Glucocorticoids and the ageing hippocampus. *Journal of Anatomy* 197, 553–562.

Hickie, I., Scott, E., Wilhelm, K. and Brodaty, H., 1997. Subcortical hyperintensities on magnetic resonance imaging in patients with severe depression — a longitudinal evaluation. *Biological Psychiatry* 42, 367–374.

Hickie, I., Ward, P., Scott, E., Haindl, W., Walker, B., Dixon, J. and Turner, K., 1999. Neo-striatal rCBF correlates of psychomotor slowing in patients with major depression. *Psychiatry Research* 92, 75–81.

Hirono, N., Mori, E., Ishii, K., Ikejiri, Y., Imamura, T., Shimomura, T., Hashimoto, M., Yamashita, H. and Sasaki, M., 1998. Frontal lobe hypometabolism and depression in Alzheimer's disease. *Neurology* 50, 380–383.

Ho, A.P., Gillin, J.C., Buchsbaum, M.S., Wu, J.C., Abel, L. and Bunney, W.E., 1996. Brain glucose metabolism during non-rapid eye movement sleep in major depression — a positron emission tomography study. *Archives of General Psychiatry* 53, 645–652.

Jenkins, M., Malloy, P., Salloway, S., Cohen, R., Rogg, J., Tung, G., Kohn, R., Westlake, R., Johnson, E.G. and Richardson, E., 1998. Memory processes in depressed geriatric patients with and without subcortical hyperintensities on MRI. *Journal of Neuroimaging* 8, 20–26.

Jimerson, D.C., 1987. Role of dopamine mechanisms in the affective disorders. In: Meltzer, H.Y. (ed.), *Psychopharmacology: the third generation of progress*, pp. 505–511. Raven Press, New York.

Kapur, S., Meyer, J., Houle, S. and Brown, G., 1994. Functional anatomy of the dopaminergic system: PET study in humans. *Neuropsychopharmacology* 19(3S), Part 2, 17S.

Kennedy, S.H., Javanmard, M. and Vaccarino, F.J., 1997. A review of functional neuroimaging in mood disorders: positron emission tomography and depression. *Canadian Journal of Psychiatry* 42, 467–475.

Ketter, T.A., Kimbrell, T.A., George, M.S., Dunn, R.T., Speer, A.M., Benson, B.E., Willis, M.W., Danielson, A., Frye, M.A., Herscovitch, P. and Post, R.M., 2001. Effects of mood and subtype on cerebral glucose metabolism in treatment-resistant bipolar disorder. *Biological Psychiatry* 49, 97–109.

Ketter, T.A., Kimbrell, T.A., George, M.S., Willis, M.W., Benson, B.E., Danielson, A., Frye, M.A., Herscovitch, P. and Post, R.M., 1999. Baseline cerebral hypermetabolism associated with carbamazepine response, and hypometabolism with nimodipine response in mood disorders. *Biological Psychiatry* 46, 1364–1374.

Kim, D.K., Kim, B.L., Sohn, S.E., Lim, S.W., Na, D.G., Paik, C.H., Krishnan, K.R. and Carroll, B.J., 1999. Candidate neuroanatomic substrates of psychosis in old-aged depression. *Progress in Neuropsychopharmacology and Biological Psychiatry* 23, 793–807.

Kimberg, D.Y., Aguirre, G.K. and D'Esposito, M., 2000. Modulation task-related neural activity in task-switching: an fMRI study. *Cognitive Brain Research* 10, 189–196.

Klimke, A., Larisch, R., Janz, A., Vosberg, H., Muller-Gartner, H.W. and Gaebel, W., 1999. Dopamine D-2 receptor binding before and after treatment of major depression measured by [I-123]IBZM SPECT. *Psychiatry Research—Neuroimaging* 90, 91–101.

Koski, L. and Paus, T., 2000. Functional connectivity of the anterior cingulate cortex within the human frontal lobe: a brain-mapping meta-analysis. *Experimental Brain Research* 133, 55–65.

Kramer-Ginsberg, E., Greenwald, B.S., Krishnan, K.R., Christiansen, B., Hu, J., Ashtari, M., Patel, M. and Pollack, S., 1999. Neuropsychological functioning and MRI signal hyperintensities in geriatric depression. *American Journal of Psychiatry* 156, 438–444.

Krishnan, K.R., Hays, J.C. and Blazer, D.G., 1997. MRI-defined vascular depression. *American Journal of Psychiatry* 154, 497–501.

Krishnan, K.R., Hays, J.C., George, L.K. and Blazer, D.G., 1998. Six-month outcomes for MRI-related vascular depression. *Depression and Anxiety* 8, 142–146.

Kumar, A., Jin, Z., Bilker, W., Udupa, J. and Gottlieb, G., 1998. Late-onset minor and major depression: early evidence for common neuroanatomical substrates detected by using MRI. *Proceedings of the National Academy of Sciences of the United States of America* 95, 7654–7658.

Kumar, A., Bilker, W., Jin, Z. and Udupa, J., 2000. Atrophy and high intensity lesions: complementary neurobiological mechanisms in late-life major depression. *Neuropsychopharmacology* 22, 264–274.

Kupfer, D.J. and Reynolds, C.F., 1992. Sleep and affective disorders. In: Paykel, E.S. (ed.), *Handbook of Affective Disorders*, 2nd edn, pp. 311–323. Churchill Livingstone, Edinburgh.

Laasonen-Balk, T., Kuikka, J., Viinamaki, H., Husso-Saastamoinen, M., Lehtonen, J. and Tiihonen, J., 1999. Striatal dopamine transporter density in major depression. *Psychopharmacology* 144, 282–285.

Lauterbach, E.C., Jackson, J.G., Wilson, A.N., Dever, G.E. and Kirsh, A.D., 1997. Major depression after left posterior globus pallidus lesions. *Neuropsychiatry, Neuropsychology, and Behavioral Neurology* 10, 9–16.

Lavretsky, H., Lesser, I.M., Wohl, M. and Miller, B.L., 1998. Relationship of age, age at onset, and sex to depression in older adults. *American Journal of Geriatric Psychiatry* 6, 248–256.

Lavretsky, H., Lesser, I.M., Wohl, M., Miller, B.L. and Mehringer, C.M., 1999. Clinical and neuroradiologic features associated with chronicity in late-life depression. *American Journal of Geriatric Psychiatry* 7, 309–316.

LeDoux, J., 1996. *The Emotional Brain*. Simon & Schuster, New York.

Lesch, K.P., Mayer, S., Disselkamp-Tietze, J., Hoh, A., Schoelnhammer, G. and Schulte, H.M., 1990. Subsensitivity of the 5-hydroxytryptamine1A (5HT1A) receptor mediated hypothermic response to ipsapirone in unipolar depression. *Life Sciences* 46, 1271–1277.

Lorberbaum, J.P., Newman, J.D., Dubno, J.R., Horwitz, A.R., Nahas, Z., Teneback, C.C., Bloomer, C.W., Bohning, D.E., Vincent, D., Johnson, M.R., Emmanuel, N., Brawman-Mintzer, O., Book, S.W., Lydiard, R.B., Ballenger, J.C. and George, M.S., 1999. Feasibility of using fMRI to study mothers responding to infant cries. *Depression and Anxiety* 10, 99–104.

MacLean, P.D., 1985. Brain evolution relating to family, play, and the separation call. *Archives of General Psychiatry* 42, 405–417.

Magistretti, P.J. and Pellerin, L., 1996. The contribution of astrocytes to the 18F-2-deoxyglucose signal in PET activation studies. *Molecular Psychiatry* 1, 445–452.

Magistretti, P.J. and Pellerin, L., 1999. Cellular mechanisms of brain energy metabolism and their relevance to functional brain imaging. *Philosophical Transactions of the Royal Society of London. Series B: Biological Sciences* 354, 1155–1163.

Malison, R.T., Best, S.E., van Dyck, C.H., McCance, E.F., Wallace, E.A., Laruelle, M., Baldwin, R.M., Seibyl, J.P., Price, L.H., Kosten, T.R. and Innis, R.B., 1998a. Elevated striatal dopamine transporters during acute cocaine abstinence as measured by [123I] beta-CIT SPECT. *American Journal of Psychiatry* 155, 832–834.

Malison, R.T., Price, L.H., Berman, R., van Dyck, C.H., Pelton, G.H., Carpenter, L., Sanacora, G., Owens, M.J., Nemeroff, C.B., Rajeevan, N., Baldwin, R.M., Seibyl, J.P., Innis, R.B. and Charney, D.S., 1998b. Reduced brain serotonin transporter availability in major depression as measured by [123I]-2 beta-carbomethoxy-3 beta-(4-iodophenyl)tropane and single photon emission computed tomography. *Biological Psychiatry* 44, 1090–1098.

Mallet, L., Mazoyer, B. and Martinot, J.L., 1998. Functional connectivity in depressive, obsessive-compulsive, and schizophrenic disorders: an explorative correlational analysis of regional cerebral metabolism. *Psychiatry Research—Neuroimaging* 82, 83–93.

Mann, J.J., Oquendo, M., Underwood, M.D. and Arango, V., 1999. The neurobiology of suicide risk: a review for the clinician. *Journal of Clinical Psychiatry* 60(Suppl 2), 7–11.

Mayberg, H.S., 1997. Limbic-cortical dysregulation: a proposed model of depression. *Journal of Neuropsychiatry* 9, 471–481.

Mayberg, H.S., Brannan, S.K., Mahurin, R.K., Jerabek, P.A., Brickman, J.S., Tekell, J.L., Silva, J.A., McGinnis, S., Glass, T.G., Martin, C.C. and Fox, P.T., 1997. Cingulate function in depression: a potential predictor of treatment response. *Neuroreport* 8, 1057–1061.

Mayberg, H.S., Liotti, M., Brannan, S.K., McGinnis, S., Mahurin, R.K., Jerabek, P.A., Silva, J.A., Tekell, J.L., Martin, C.C., Lancaster, J.L. and Fox, P.T., 1999. Reciprocal limbic-cortical function and negative mood: converging PET findings in depression and normal sadness. *American Journal of Psychiatry* 156, 675–682.

McGaugh, J.L. and Cahill, L., 1997. Interaction of neuromodulatory systems in modulating memory storage. *Behavioral Brain Research* 83, 31–38.

Mega, M.S. and Cummings, J.L., 1994. Frontal-subcortical circuits and neuropsychiatric disorders. *Journal of Neuropsychiatry and Clinical Neurosciences* 6, 358–370.

Mega, M.S., Cummings, J.L., Salloway, S. and Malloy, P., 1997. The limbic system: an anatomic, phylogenetic, and clinical perspective. *Journal of Neuropsychiatry and Clinical Neurosciences* 9, 315–330.

Meltzer, C.C., Price, J.C., Mathis, C.A., Greer, P.J., Cantwell, M.N., Houck, P.R., Mulsant, B.H., Ben-Eliezer, D., Lopresti, B., DeKosky, S.T. and Reynolds, C.F., 1999. PET imaging of serotonin type 2A receptors in late-life neuropsychiatric disorders. *American Journal of Psychiatry* 156, 1871–1878.

Mervaala, E., Fohr, J., Kononen, M., Valkonen-Korhonen, M., Vainio, P., Partanen, K., Partanen, J., Tiihonen, J., Viinamaki, H., Karjalainen, A.K. and Lehtonen, J., 2000. Quantitative MRI of the hippocampus and amygdala in severe depression. *Psychological Medicine* 30, 117–125.

Meyer, J.H., Kennedy, S. and Brown, G.M., 1998. No effect of depression on [(15)O]H2O PET response to intravenous D-fenfluramine. *American Journal of Psychiatry* 155, 1241–1246.

Meyer, J.H., Kapur, S., Houle, S., DaSilva, J., Owczarek, B., Brown, G.M., Wilson, A.A. and Kennedy, S.H., 1999. Prefrontal cortex 5-HT2 receptors in depression: an [18F]setoperone PET imaging study. *American Journal of Psychiatry* 156, 1029–1034.

Moffoot, A., O'Carroll, R.E., Murray, C., Dougall, N., Ebmeier, K.P. and Goodwin, G.M., 1994a. Clonidine infusion increases uptake of 99mTc-exametazime in anterior cingulate cortex in Korsakoff's psychosis. *Psychological Medicine* 24, 53–61.

Moffoot, A.P.R., O'Carroll, R.E., Bennie, J., Carroll, S., Dick, H., Ebmeier, K.P. and Goodwin, G.M., 1994b. Diurnal variation of mood and cognitive function in major depression with melancholia. *Journal of Affective Disorders* 32, 257–269.

Moore, G.J., Bebchuk, J.M., Hasanat, K., Chen, G., Seraji-Bozorgzad, N., Wilds, I.B., Faulk, M.W., Koch, S., Glitz, D.A., Jolkovsky, L. and Manji, H.K., 2000. Lithium increases *N*-acetyl-aspartate in the human brain: *in vivo* evidence in support of bcl-2's neurotrophic effects? *Biological Psychiatry* 48, 1–8.

Morris, J.S., Smith, K.A., Cowen, P.J., Friston, K.J. and Dolan, R.J., 1999. Covariation of activity in habenula and dorsal raphe nuclei following tryptophan depletion. *Neuroimage* 10, 163–172.

Nobler, M.S., Oquendo, M.A., Kegeles, L.S., Malone, K.M., Campbell, C., Sackeim, H.A. and Mann, J.J., 2001. Decreased regional brain metabolism after ECT. *American Journal of Psychiatry* 158, 305–308.

Nofzinger, E.A., Nichols, T.E., Meltzer, C.C., Price, J., Steppe, D.A., Miewald, J.M., Kupfer, D.J. and Moore, R.Y., 1999. Changes in forebrain function from waking to REM sleep in depression: preliminary analyses of [18F]FDG PET studies. *Psychiatry Research* 91, 59–78.

Nofzinger, E.A., Price, J.C., Meltzer, C.C., Buysse, D.J., Villemagne, V.L., Miewald, J.M., Sembrat, R.C., Steppe, D.A. and Kupfer, D.J., 2000. Towards a neurobiology of dysfunctional arousal in depression: the relationship between beta EEG power and regional cerebral glucose metabolism during NREM sleep. *Psychiatry Research* 98, 71–91.

Norris, S.D., Krishnan, K.R.R. and Ahearn, E., 1997. Structural changes in the brain of patients with bipolar affective disorder by MRI: a review of the literature. *Progress in Neuropsychopharmacology and Biological Psychiatry* 21, 1323–1337.

Northoff, G., Richter, A., Gessner, M., Schlagenhauf, F., Fell, J., Baumgart, F., Kaulisch, T., Kotter, R., Stephan, K.E., Leschinger, A., Hagner, T., Bargel, B., Witzel, T., Hinrichs, H., Bogerts, B., Scheich, H. and Heinze, H.J., 2000. Functional dissociation between medial and lateral prefrontal cortical spatiotemporal activation in negative and positive emotions: a combined fMRI/MEG study. *Cerebral Cortex* 10, 93–107.

O'Brien, J.T., Ames, D., Schweitzer, I., Desmond, P., Coleman, P. and Tress, B., 1997a. Clinical, magnetic resonance imaging and endocrinological differences between delusional and non-delusional depression in the elderly. *International Journal of Geriatric Psychiatry* 12, 211–218.

O'Brien, J.T., Desmond, P., Ames, D., Schweitzer, I., Chiu, E. and Tress, B., 1997b. Temporal lobe magnetic resonance imaging can differentiate Alzheimer's disease from normal ageing, depression, vascular dementia and other causes of cognitive impairment. *Psychological Medicine* 27, 1267–1275.

Ogura, A., Morinobu, S., Kawakatsu, S., Totsuka, S. and Komatani, A., 1998. Changes in regional brain activity in major depression after successful treatment with antidepressant drugs. *Acta Psychiatrica Scandinavica* 98, 54–59.

Ongur, D., Drevets, W.C. and Price, J.L., 1998. Glial reduction in the subgenual prefrontal cortex in mood disorders. *Proceedings of the National Academy of Sciences of the United States of America* 95, 13290–13295.

Paillere-Martinot, M.-L., Bragulat, V., Artiges, E., Dolle, F., Hinnen, F., Jouvent, R. and Martinot, J.-L., 2001. Decreased presynaptic dopamine function in the left caudate of depressed patients with affective flattening and psychomotor retardation. *American Journal of Psychiatry* 158, 314–316.

Papez, J.W., 1937. A proposed mechanism of emotion. *Archives of Neurology and Psychiatry* 38, 725–743.

Paradiso, S., Johnson, D.L., Andreasen, N.C., O'Leary, D.S., Watkins, G.L., Ponto, L.L.B. and Hichwa, R.D., 1999. Cerebral blood flow changes associated with attribution of emotional valence to pleasant, unpleasant, and neutral visual stimuli in a PET study of normal subjects. *American Journal of Psychiatry* 156, 1618–1629.

Pardo, J.V., Pardo, P.J., Janer, K.W. and Raichle, M.E., 1990. The anterior cingulate cortex mediates processing selection in the Stroop attentional conflict paradigm. *Proceedings of the National Academy of Sciences of the United States of America* 87, 256–259.

Peyron, R., Laurent, B. and Garcia-Larrea, L., 2000. Functional imaging of brain responses to pain. A review and meta-analysis. *Neurophysiology Clinics* 30, 263–288.

Pizzagalli, D., Pascual-Marqui, R.D., Nitschke, J.B., Oakes, T.R., Larson, C.L., Abercrombie, H.C., Schaefer, S.M., Koger, J.V., Benca, R.M. and Davidson, R.J., 2001. Anterior cingulate activity as a predictor of degree of treatment response in major depression: evidence from brain electrical tomography analysis. *American Journal of Psychiatry* 158, 405–415.

Post, R.M., Speer, A.M., Weiss, S.R.B. and Li, H., 2000. Seizure models: anticonvulsant effects of ECT and rTMS. *Progress in Neuropsychopharmacology and Biological Psychiatry* 24, 1251–1273.

Price, J.L., 1999a. Networks within the orbital and medial prefrontal cortex. *Neurocase* 5, 231–241.

Price, J.L., 1999b. Prefrontal cortical networks related to visceral function and mood. *Annals of the New York Academy of Science* 877, 383–396.

Price, J.L., Carmichael, S.T. and Drevets, W.C., 1996. Networks related to the orbital and medial prefrontal cortex: a substrate for emotional behavior? *Progress in Brain Research* 107, 523–536.

Rajkowska, G., Miguel-Hidalgo, J.J., Wei, J.R., Dilley, G., Pittman, S.D., Meltzer, H.Y., Overholser, J.C., Roth, B.L. and Stockmeier, C.A., 1999. Morphometric evidence for neuronal and glial prefrontal cell pathology in major depression. *Biological Psychiatry* 45, 1085–1098.

Roberts, A.C. and Wallis, J.D., 2000. Inhibitory control and affective processing in the prefrontal cortex: neuropsychological studies in the common marmoset. *Cerebral Cortex* 10, 252–262.

Rogers, M.A., Bradshaw, J.L., Pantelis, C. and Phillips, J.G., 1998. Frontostriatal deficits in unipolar major depression. *Brain Research Bulletin* 47, 297–310.

Rueter, L.E., de Montigny, C. and Blier, P., 1998. Electrophysiological characterization of the effect of long-term duloxetine administration on the rat serotonergic and noradrenergic systems. *Journal of Pharmacology and Experimental Therapeutics* 285, 404–412.

Sapolsky, R.M., Krey, L.C. and McEwen, B., 1986. The neuroendocrinology of stress and ageing: the glucocorticoid cascade hypothesis. *Endocrine Reviews* 7, 284–301.

Sato, R., Bryan, R.N. and Fried, L.P., 1999. Neuroanatomic and functional correlates of depressed mood: the Cardiovascular Health Study. *American Journal of Epidemiology* 150, 919–929.

Schneider, F., Gur, R.E., Mozley, L.H., Smith, R.J., Mozley, P.D., Censits, D.M., Alavi, A. and Gur, R.C., 1995. Mood effects on limbic blood flow correlate with emotional self-rating: a PET study with oxygen-15 labeled water. *Psychiatry Research—Neuroimaging* 61, 265–283.

Schneider, F., Grodd, W. and Machulla, H.J., 1996. Behavioral neuroimaging with positron emission tomography and magnetic resonance imaging. *Nervenarzt* 67, 721–729.

Schneider, F., Grodd, W., Weiss, U., Klose, U., Mayer, K.R., Nagele, T. and Gur, R.C., 1997. Functional MRI reveals left amygdala activation during emotion. *Psychiatry Research—Neuroimaging* 76, 75–82.

Schnitzler, A. and Ploner, M., 2000. Neurophysiology and functional neuroanatomy of pain perception. *Journal of Clinical Neurophysiology* 17, 592–603.

Selemon, L.D., Lidow, M.S. and Goldman-Rakic, P.S., 1999. Increased volume and glial density in primate prefrontal cortex associated with chronic antipsychotic drug exposure. *Biological Psychiatry* 46, 161–172.

Selye, H., 1936. A syndrome produced by diverse nocuous agents. *Nature* 138, 32.

Serretti, A., Benedetti, F., Colombo, C., Lilli, R., Lorenzi, C. and Smeraldi, E., 1999. Dopamine receptor D4 is not associated with antidepressant activity of sleep deprivation. *Psychiatry Research* 89, 107–114.

Shah, P. and Ebmeier, K.P., 1998. Structural and functional brain markers of age of onset and chronicity in major depressive disorder. In: Ebert, D. and Ebmeier, K.P. (eds), *New Models for Depression*, vol. 19, pp. 136–152. Karger, Basel.

Shah, P.J., Ogilvie, A., Goodwin, G.M. and Ebmeier, K.P., 1997. Clinical and psychometric correlates of dopamine D2 binding in depression. *Psychological Medicine* 27, 1247–1256.

Shah, P.J., Ebmeier, K.P., Glabus, M.F. and Goodwin, G.M., 1998. Cortical grey matter reductions associated with treatment resistant chronic unipolar depression: a controlled MRI study. *British Journal of Psychiatry* 172, 527–532.

Sheline, Y.I., Gado, M.H. and Price, J.L., 1998. Amygdala core nuclei volumes are decreased in recurrent major depression. *Neuroreport* 9, 2023–2028.

Sheline, Y.I., Sanghavi, M., Mintun, M.A. and Gado, M.H., 1999. Depression duration but not age predicts hippocampal volume loss in medically healthy women with recurrent major depression. *Journal of Neuroscience* 19, 5034–5043.

Shumake, J., Poremba, A., Edwards, E. and Gonzalez-Lima, F., 2000. Congenital helpless rats as a genetic model for cortex metabolism in depression. *Neuroreport* 11, 3793–3798.

Simpson, S., Baldwin, R.C., Jackson, A. and Burns, A.S., 1998. Is subcortical disease associated with a poor response to antidepressants? Neurological, neuropsychological and neuroradiological findings in late-life depression. *Psychological Medicine* 28, 1015–1026.

Simpson, J.R., Drevets, W.C., Snyder, A.Z., Gusnard, D.A. and Raichle, M.E., 2001a. Emotion-induced changes in human medial prefrontal

cortex: II. During anticipatory anxiety. *Proceedings of the National Academy of Sciences of the United States of America* 98, 688–693.

Simpson, J.R., Snyder, A.Z., Gusnard, D.A. and Raichle, M.E., 2001b. Emotion-induced changes in human medial prefrontal cortex: I. During cognitive task performance. *Proceedings of the National Academy of Sciences of the United States of America* 98, 683–687.

Sloane, J.A., Hollander, W., Rosene, D.L., Moss, M.B., Kemper, T. and Abraham, C.R., 2000. Astrocytic hypertrophy and altered GFAP degradation with age in subcortical white matter of the rhesus monkey. *Brain Research* 862, 1–10.

Smith, G.S., Reynolds, C.F., Pollock, B., Derbyshire, S., Nofzinger, E., Dew, M.A., Houck, P.R., Milko, D., Meltzer, C.C. and Kupfer, D.J., 1999a. Cerebral glucose metabolic response to combined total sleep deprivation and antidepressant treatment in geriatric depression. *American Journal of Psychiatry* 156, 683–689.

Smith, K.A., Morris, J.S., Friston, K.J., Cowen, P.J. and Dolan, R.J., 1999b. Brain mechanisms associated with depressive relapse and associated cognitive impairment following acute tryptophan depletion. *British Journal of Psychiatry* 174, 525–529.

Soares, J.C. and Mann, J.J., 1997. The anatomy of mood disorders — review of structural neuroimaging studies. *Biological Psychiatry* 41, 86–106.

Speer, A.M., Kimbrell, T.A., Wassermann, E.M., D'Repella, J., Willis, M.W., Herscovitch, P. and Post, R.M., 2000. Opposite effects of high and low frequency rTMS on regional brain activity in depressed patients. *Biological Psychiatry* 48, 1133–1141.

Steffens, D.C., Tupler, L.A., Ranga, K. and Krishnan, R., 1998. Magnetic resonance imaging signal hypointensity and iron content of putamen nuclei in elderly depressed patients. *Psychiatry Research* 83, 95–103.

Steffens, D.C., Helms, M.J., Krishnan, K.R. and Burke, G.L., 1999. Cerebrovascular disease and depression symptoms in the cardiovascular health study. *Stroke* 30, 2159–2166.

Steingard, R.J., 2000. The neuroscience of depression in adolescence. *Journal of Affective Disorders* 61, 15–21.

Stevens, A. and Price, J., 2000. Disorders of attachment and rank. In: *Evolutionary Psychiatry*, 2nd edn. Routledge, London.

Stoll, A.L., Renshaw, P.F., Yurgelun-Todd, D.A. and Cohen, B.M., 2000. Neuroimaging in bipolar disorder: what have we learned? *Biological Psychiatry* 48, 505–517.

Strakowski, S.M., DelBello, M.P., Sax, K.W., Zimmerman, M.E., Shear, P.K., Hawkins, J.M. and Larson, E.R., 1999. Brain magnetic resonance imaging of structural abnormalities in bipolar disorder. *Archives of General Psychiatry* 56, 254–260.

Swerdlow, N.R. and Koob, G.F., 1987. Dopamine, schizophrenia, mania, and depression: toward a unified hypotheses of cortico-striato-pallido-thalamic function. *Behavioural and Brain Sciences* 10, 197–245.

Teasdale, J.D., Howard, R.J., Cox, S.G., Ha, Y., Brammer, M.J., Williams, S.C.R. and Checkley, S.A., 1999. Functional MRI study of the cognitive generation of affect. *American Journal of Psychiatry* 156, 209–215.

Tebartz van Elst, L., Woermann, F.G., Lemieux, L. and Trimble, M.R., 1999. Amygdala enlargement in dysthymia — a volumetric study of patients with temporal lobe epilepsy. *Biological Psychiatry* 46, 1614–1623.

Tebartz van Elst, L., Woermann, F., Lemieux, L. and Trimble, M.R., 2000. Increased amygdala volumes in female and depressed humans. A quantitative magnetic resonance imaging study. *Neuroscience Letters* 281, 103–106.

Thomas, A.J., Ferrier, I.N., Kalaria, R.N., Perry, R.H., Brown, A. and O'Brien, J.T.O., 2001. A neuropathological study of vascular factors in late-life depression. *Journal of Neurology, Neurosurgery and Psychiatry* 70, 83–87.

Vakili, K., Pillay, S.S., Lafer, B., Fava, M., Renshaw, P.F., Bonello-Cintron, C.M. and Yurgelun-Todd, D.A., 2000. Hippocampal volume in primary unipolar major depression: a magnetic resonance imaging study. *Biological Psychiatry* 47, 1087–1090.

Vasile, R.G., Sachs, G., Anderson, J.L., Lafer, B., Matthews, E. and Hill, T., 1997. Changes in regional cerebral blood flow following light treatment for seasonal affective disorder: responders versus nonresponders. *Biological Psychiatry* 42, 1000–1005.

Videbech, P., 1997. MRI findings in patients with affective disorder: a meta-analysis. *Acta Psychiatrica Scandinavica* 96, 157–168.

Videbech, P., 2000. PET measurements of brain glucose metabolism and blood flow in major depressive disorder: a critical review. *Acta Psychiatrica Scandinavica* 101, 11–20.

Volk, S.A., Kaendler, S.H., Hertel, A., Maul, F.D., Manoocheri, R., Weber, R., Georgi, K., Pflug, B. and Hor, G., 1997. Can response to partial sleep deprivation in depressed patients be predicted by regional changes of cerebral blood flow? *Psychiatry Research ó Neuroimaging* 75, 67–74.

Welberg, L.A., Seckl, J.R. and Holmes, M.C., 2001. Prenatal glucocorticoid programming of brain corticosteroid receptors and corticotrophin-releasing hormone: possible implications for behaviour. *Neuroscience* 104, 71–79.

Whalen, P.J., Bush, G., McNally, R.J., Wilhelm, S., McInerney, S.C., Jenike, M.A. and Rauch, S.L., 1998. The emotional counting Stroop paradigm: a functional magnetic resonance imaging probe of the anterior cingulate affective division. *Biological Psychiatry* 44, 1219–1228.

Willeit, M., Praschak-Rieder, N., Neumeister, A., Pirker, W., Asenbaum, S., Vitouch, O., Tauscher, J., Hilger, E., Stastny, J., Brucke, T. and Kasper, S., 2000. [123I]-beta-CIT SPECT imaging shows reduced brain serotonin transporter availability in drug-free depressed patients with seasonal affective disorder. *Biological Psychiatry* 47, 482–489.

Wu, J., Buchsbaum, M.S., Gillin, J.C., Tang, C., Cadwell, S., Wiegand, M., Najafi, A., Klein, E., Hazen, K. and Bunney, W.E., 1999. Prediction of antidepressant effects of sleep deprivation by metabolic rates in the ventral anterior cingulate and medial prefrontal cortex. *American Journal of Psychiatry* 156, 1149–1158.

Yatham, L.N., Liddle, P.F., Dennie, J., Shiah, I.S., Adam, M.J., Lane, C.J., Lam, R.W. and Ruth, T.J., 1999. Decrease in brain serotonin 2 receptor binding in patients with major depression following desipramine treatment: a positron emission tomography study with fluorine-18-labeled setoperone. *Archives of General Psychiatry* 56, 705–711.

Yatham, L.N., Clark, C.C. and Zis, A.P., 2000. A preliminary study of the effects of electroconvulsive therapy on regional brain glucose metabolism in patients with major depression. *Journal of ECT* 16, 171–176.

Zheng, X.M., 2000. Regional cerebral blood flow changes in drug-resistant depressed patients following treatment with transcranial magnetic stimulation: a statistical parametric mapping analysis. *Psychiatry Research ó Neuroimaging* 100, 75–80.

Zis, A.P. and Goodwin, F.K., 1982. The amine hypothesis. In: Paykel, E.S. (ed.), *Handbook of Affective Disorders*, pp. 175–190. Guildford Press, New York.